

**COPPER NUTRITION AND TRANSPORT MECHANISMS IN PLANKTON
COMMUNITIES IN THE NORTHEAST PACIFIC OCEAN**

by

David Mathew Semeniuk

B.Sc., The University of British Columbia, 2006

A THESIS SUBMITTED IN PARTIAL FULFILLMENT OF
THE REQUIREMENTS FOR THE DEGREE OF

DOCTOR OF PHILOSOPHY

in

THE FACULTY OF GRADUATE AND POSTDOCTORAL STUDIES
(Oceanography)

THE UNIVERSITY OF BRITISH COLUMBIA
(Vancouver)

October 2014

© David Mathew Semeniuk, 2014

Abstract

Copper (Cu) is an essential micronutrient for phytoplankton, particularly during iron limitation, but can also be toxic at relatively low concentrations. While Cu stoichiometry and metabolic functions in marine phytoplankton have been studied, little is known about the substrates for Cu transport and the Cu nutritional state of indigenous phytoplankton communities. The aim of my thesis was two-fold: investigate the bioavailability of organically bound Cu to laboratory and indigenous phytoplankton, and evaluate Cu nutrition of phytoplankton along Line P, a coastal-open ocean transect in the northeast subarctic Pacific Ocean. Organically complexed Cu was bioavailable to four laboratory phytoplankton strains and an Fe-limited phytoplankton community. A laboratory investigation of the substrates for the high-affinity Cu transport system in the model diatom *Thalassiosira pseudonana* confirmed that organically complexed Cu(II) can be acquired, and likely via extracellular reduction and internalization of Cu(I). Cellular uptake rates of the laboratory strains were similar to those estimated for the natural phytoplankton assemblage, and provide additional evidence that some *in situ* Cu ligand complexes are likely bioavailable. Using bottle incubations, I investigated the potential for Cu limitation and toxicity in open ocean Fe-limited phytoplankton communities. In 2010, I provided physiological evidence for an interaction between Fe and Cu metabolisms in an Fe-limited phytoplankton community. In 2011, Cu availability to an Fe-limited community was reduced, using a strong Cu(II)-specific ligand, resulting in slower Cu uptake rates, faster growth rates, and increased cyanobacteria abundance. Despite large variations in macronutrient, light, and iron along Line P in 2011, net primary productivity was negatively correlated with inorganic Cu concentrations, and positively correlated with the strength of the *in situ* ligands. The potential roles of Cu

ligands in the sea are discussed, highlighting that the bioavailability of *in situ* organic Cu complexes is a key determinant for marine primary productivity.

Preface

A version of Chapter 2 is currently under review for publication: D. M. Semeniuk, R. M. Bundy, C. D. Payne, K. A. Barbeau, and M. T. Maldonado, (*accepted with revisions*). Acquisition of organically complexed copper by marine phytoplankton and bacteria in the NE subarctic Pacific Ocean. I designed the experiment, executed the majority of the field sampling and sample analysis, performed the majority of the data analysis, and wrote the manuscript. C. D. Payne assisted in field sampling. R. M. Bundy measured the ligand conditional stability constants, and measured the total dissolved Cu sample. Dr. K. A. Barbeau and Dr. M. T. Maldonado provided editorial assistance and invaluable feedback on data analysis during preparation of the manuscript.

A version of Chapter 3 is currently in preparation for submission to a scientific journal. The co-authors are: D. M. Semeniuk and M. T. Maldonado. Title: Acquisition of organically complexed Cu(II) by a high-affinity Cu transport system in marine phytoplankton. I designed and executed the experiment, and wrote the manuscript. Dr. M. T. Maldonado provided editorial assistance during preparation of the manuscript.

A version of Chapter 4 is currently in preparation for submission to a scientific journal. The co-authors are: D.M. Semeniuk, R. L. Taylor, R. M. Bundy, W. K. Johnson, J. T. Cullen, K. A. Barbeau, and M. T. Maldonado. Title: Iron-copper interactions in HNLC phytoplankton in the northeast subarctic Pacific Ocean. I designed the incubation experiments, executed the majority of the field sampling and sample analysis, performed the majority of the data analysis, and wrote

the manuscript. R. L. Taylor assisted in field sampling, and R. M. Bundy measured the copper speciation sample. W. K. Johnson assisted with field sampling and measured the dissolved Fe samples, and M. Robert organized the field expedition and provided ancillary data. Dr. J. T. Cullen provided expertise and instrumentation to make the dissolved Cu measurements. Dr. K. A. Barbeau and Dr. M. T. Maldonado provided editorial assistance and feedback on data analysis during preparation of the manuscript.

A version of Chapter 5 is currently in preparation for submission to a scientific journal. The co-authors are: D.M. Semeniuk, A. Posacka, R. M. Bundy, M. Robert, K. A. Barbeau, and M. T. Maldonado. Title: The effects of copper speciation on phytoplankton and bacterial rate processes in the northeast subarctic Pacific Ocean. I designed the incubation experiment and transect sampling plan. I performed all of the radioisotope work, and a large portion of the sample collection and processing. A. Posacka assisted with transect and incubation sampling, R. M. Bundy measured the copper speciation samples, and M. Robert provided ancillary data and organized the field expedition. Dr. K. A. Barbeau and Dr. M. T. Maldonado assisted with data interpretation and provided editorial feedback during the preparation of the manuscript.

Table of Contents

Abstract	ii
Preface	iv
Table of Contents	vi
List of Tables	xiv
List of Figures	xix
Acknowledgements	xxv
Dedication	xxvii
Chapter 1: Introduction	1
1.1 Trace Metal Control of Primary Productivity	3
1.1.1 Trace Metal Speciation and Notation	3
1.1.2 Trace Metal Bioavailability to Marine Phytoplankton	5
1.1.3 Case Study of Trace Metal Limitation – Iron	9
1.1.4 Trace Metal Toxicity.....	11
1.2 Copper Physiology in Marine Phytoplankton.....	13
1.2.1 Phytoplankton Metabolic Copper Requirements and Homeostasis.....	13
1.2.2 Copper Detoxification.....	15
1.2.3 The Distribution and Speciation of Copper in Seawater	16
1.2.4 Copper Bioavailability and Transporter Substrates	20
1.2.5 Copper Nutritional Status of Natural Marine Phytoplankton Populations	23
1.3 Oceanography of the Northeast Subarctic Pacific Ocean.....	24
1.3.1 Water Properties and Circulation.....	25

1.3.2	Phytoplankton and Nutrient Dynamics along Line P	26
1.3.3	Copper Concentration and Speciation along Line P	27
1.4	Thesis Organization	27
1.5	Figures.....	33
Chapter 2: Acquisition of Organically Complexed Copper by Marine Phytoplankton and Bacteria in the NE Subarctic Pacific Ocean		37
2.1	Introduction.....	38
2.2	Materials and Methods.....	41
2.2.1	Sampling and Incubation	41
2.2.2	Determination of Initial Chemical and Biological Parameters	42
2.2.3	Determination of Conditional Stability Constants for Cyclam and Cyclen.....	43
2.2.4	Preparation of the Copper-Ligand Complex Additions for Copper Uptake Assay ..	43
2.2.4.1	<i>In Situ</i> Cu Ligands	44
2.2.4.2	Cu(II)-Ligand Complexes (1:10 nM).....	45
2.2.4.3	Weak Cu(I)-Ligand Complexes (1:10 nM).....	45
2.2.5	Copper Uptake Assay	47
2.2.6	Diffusive Boundary Layer Inorganic Cu Flux Calculations	48
2.3	Results.....	51
2.3.1	Station Parameterization	51
2.3.2	Size Fractionated Short-Term (3 to 4 h) Uptake Rates.....	51
2.3.2.1	Artificial Cu(II)-Ligands.....	51
2.3.2.2	<i>In Situ</i> Ligands	52
2.3.2.3	<i>In Situ</i> Ligands in the Presence of 1 nM Cu and 10 nM Weak Ligands.....	53

2.3.3	Diffusive Boundary Layer Cu' Fluxes	53
2.3.4	Long-Term (14 h) Cu Accumulation	54
2.3.4.1	Artificial Cu(II)-Ligands.....	54
2.3.4.2	<i>In Situ</i> Ligands	54
2.3.4.3	<i>In Situ</i> Ligands in the Presence of 1 nM Cu and 10 nM Weak Cu(I) Ligands ..	55
2.4	Discussion	55
2.4.1	Copper Acquisition from Strong Cu(II)Ligand Complexes by Eukaryotic Phytoplankton	56
2.4.2	Copper Acquisition from <i>In Situ</i> CuL Complexes by Eukaryotic Phytoplankton....	59
2.4.2.1	Influence of Light on Cu Uptake from <i>In Situ</i> CuL Complexes.....	62
2.4.3	Marine Prokaryotic Copper Uptake	63
2.4.4	Copper Cycling in Surface Waters	64
2.4.5	Oceanographic Implications	67
2.5	Tables.....	69
Chapter 3: Acquisition of Organically Complexed Cu(II) by a High-Affinity Cu Transport		
System in Marine Phytoplankton		
3.1	Introduction.....	77
3.2	Materials and Methods.....	80
3.2.1	Study Organisms, Media, Growth Conditions and Monitoring.....	80
3.2.2	Cu Uptake Experiments	81
3.2.2.1	Choice of Cu-Ligand Complex.....	81
3.2.2.2	Preparation of ⁶⁴ Cu-Ligand Complexes.....	82
3.2.2.3	<i>Thalassiosira pseudonana</i> HACuTS Competitive Inhibitors.....	84

3.2.2.4	Copper Uptake Assay	85
3.2.3	Statistical Analyses	88
3.3	Results.....	88
3.3.1	Cu Uptake by <i>T. pseudonana</i> Grown in Low Cu.....	88
3.3.2	Competitive Inhibition of the HACuTS in <i>T. pseudonana</i> Grown in Low Cu.....	89
3.3.3	Cu Uptake Rates of Phytoplankton Grown in High Cu Media.....	89
3.3.4	Short-Term Accumulation of Cu and C in <i>T. pseudonana</i>	90
3.4	Discussion	91
3.4.1	Acquisition of Organically Complexed Cu(II) by Marine Phytoplankton	91
3.4.2	Mechanism of Cu Acquisition from Strong Organic Ligands in <i>T. pseudonana</i> Grown in Low Cu Media	93
3.4.2.1	Cell Surface Cu(II) Reduction	93
3.4.2.2	Cu(I) Transport	95
3.4.2.3	Reconciliation with the “Free Ion Model”	96
3.4.3	Influence of Ligands on Cu Availability and Implications for Culture Studies	99
3.5	Tables.....	103
3.6	Figures.....	108

Chapter 4: Iron-Copper Interactions in HNLC Phytoplankton in the Northeast Subarctic Pacific Ocean	115	
4.1	Introduction.....	116
4.2	Materials and Methods.....	118
4.2.1	Plastic Cleaning Protocol.....	118
4.2.2	Station Parameterization and Water Collection.....	119

4.2.3	Incubation Treatments	120
4.2.4	Biological and Chemical Sampling and Analyses	124
4.2.4.1	Sampling, Nutrients, and Chlorophyll <i>a</i>	124
4.2.4.2	Photo-Physiological Measurements	125
4.2.4.3	Dissolved Fe and Cu Sampling	126
4.2.4.4	Dissolved Fe and Cu Analysis	127
4.2.4.5	Iron Uptake Assays from Desferrioxamine B	128
4.2.5	Statistical Analyses	131
4.3	Results	132
4.3.1	Station Parameterization	132
4.3.2	Chl <i>a</i>	133
4.3.2.1	P20GO	133
4.3.2.2	P26GO	133
4.3.3	Photo-Physiological Responses	134
4.3.3.1	P20GO	134
4.3.3.2	P26GO	134
4.3.4	Day 3 HAFeTS Activity	135
4.3.4.1	P20GO	135
4.3.4.2	P26GO	136
4.3.5	Heterotrophic Bacterial Abundance	137
4.3.6	Dissolved Fe in the Incubation Bottles	137
4.4	Discussion	137
4.4.1	Null Cu Limitation at P20	137

4.4.2	Interaction Between Fe and Cu in an Fe-Limited Phytoplankton Community Grown Under Light-Replete Levels at P26.....	141
4.4.3	Fe-Cu Interactions During Light Limitation at P26.....	142
4.4.4	Comparison with Previous Incubations	143
4.4.5	Oceanographic Significance	144
4.5	Tables.....	146
4.6	Figures.....	149

Chapter 5: The Effects of Copper Speciation on Phytoplankton and Bacterial Rate

	Processes in the Northeast Subarctic Pacific Ocean.....	153
5.1	Introduction.....	154
5.2	Materials and Methods.....	158
5.2.1	Plastic Cleaning	158
5.2.2	Experimental Design and Execution.....	158
5.2.2.1	Line P Survey.....	158
5.2.2.2	Incubation at P16	159
5.2.3	Water Collection and Station Parameterization along Line P	161
5.2.3.1	Line P Transect	161
5.2.3.2	P16 Incubation	162
5.2.4	Biological and Chemical Sampling and Analysis.....	163
5.2.5	Dissolved Cu Concentrations and Speciation.....	163
5.2.6	Cu Uptake Rates, Cu:C Assimilation Ratios, and Net Primary Productivity	163
5.3	Results.....	169
5.3.1	Line P Transect	169

5.3.1.1	Descriptions of Depth Profiles.....	169
5.3.1.2	Copper Concentration and Speciation	170
5.3.1.3	Biomass and Productivity	171
5.3.1.4	Transect Correlations	173
5.3.1.5	Cu:C Assimilation Ratios and Cu Uptake Rates.....	173
5.3.2	P16 Incubation	175
5.3.2.1	Biomass and Net Primary Productivity.....	175
5.3.2.2	>1 μm Cu:C Assimilation Ratios and Cu Uptake Rates.....	177
5.4	Discussion	178
5.4.1	Distribution of Total Dissolved Cu in Line P Surface Waters.....	178
5.4.2	Inorganic Cu along Line P	179
5.4.3	Source of Cu Ligands in Surface Waters along Line P	180
5.4.4	Environmental Controls of Cu Acquisition along Line P.....	183
5.4.4.1	Comparing Cu:C Assimilation Ratios with Previous Measurements	183
5.4.4.2	Macronutrient and Light Availability	185
5.4.4.3	Iron-Copper Interactions.....	186
5.4.4.4	Copper Acquisition and Speciation along Line P.....	187
5.4.4.5	Strong Ligands and Bacterial Cu Assimilation.....	188
5.4.4.6	Copper Uptake During the P16 Incubation.....	189
5.4.5	Copper Influences Rate Processes along Line P: Three Lines of Evidence	190
5.4.5.1	NPP _V Covaries with Cu Speciation along Line P.....	190
5.4.5.2	Decreasing Cu Bioavailability Increased NPP _B at P16.....	191
5.4.5.3	Cyanobacteria Abundance Increased as Cu Bioavailability Decreased at P16	192

5.4.6	Reevaluating the Role Of Organic Complexation in Mediating Cu Bioavailability to <i>In Situ</i> Marine Microbial Communities	193
5.5	Tables.....	196
5.6	Figures.....	207
Chapter 6: Conclusion		216
6.1	Major Findings And Contributions.....	217
6.2	Future Directions	220
References		225
Appendices		244
Appendix A.....		244

List of Tables

Table 2.1. Functional groups, equilibrium constants, and conditional stability constants for the ligands used in the Cu uptake assay.....	69
Table 2.2. Average short-term (3 to 4 h) total particulate Cu uptake rates (pmol Cu L ⁻¹ d ⁻¹) measured at P26. Values in parentheses represent half of the range of two replicates.....	70
Table 2.3. Cellular short-term Cu uptake rates and calculated fluxes of inorganic Cu to the cell surface within the diffusive boundary layer for various cell sizes in the Cu(II)L and <i>in situ</i> ligand treatments. Refer to section 2.7 for a detailed description of the calculations.	71
Table 3.1. Species, class, clone, cell diameter (µm), and isolation site of the marine phytoplankton used in this study.....	103
Table 3.2. Competitive inhibitors used to target the components of the proposed high-affinity Cu transport system (HACuTS) in <i>T. pseudonana</i> . Short-term Cu uptake assays were performed with either 1 nM Cu(II) bound to 3 nM Cyclam, or 1 nM Cu bound to 10 nM reduced glutathione (GSH). Due to the weak complex formed between Cu(I) and GSH (see section 3.2.2.1), the Cu species in this treatment is effectively Cu'.....	103
Table 3.3. Short-term Cu uptake rates by <i>T. pseudonana</i> (± 1σ; n=3) of inorganic Cu (Cu'), and Cu from within Cu(I)GSH and Cu(II)Cyclam complexes. Due to the weak complex formed between Cu(I) and GSH (see section 3.2.2.1), the Cu species in this treatment is effectively Cu'. The average growth rate for the triplicate cultures was 2.20 ± 0.05 d ⁻¹ , and cell densities in the uptake assays ranged between 0.55 and 1.91 million cells mL ⁻¹ . The cultures were grown in Aquil containing 0.6 nM total dissolved Cu. A student's t-test (one-way, unequal variances) was	

used to compare uptake rates in the Cu' treatment with the Cu(I)GSH and Cu(II)Cyclam (1:3) treatments. Uptake in the Cu(II)Cyclam (1:3) treatment was also compared with rates in the 1:100 and 1:1000 Cu:Cyclam ratio treatments. Significant differences ($p < 0.05$) are in bold. 104

Table 3.4. Inorganic Cu concentrations ($[Cu']$), calculated Cu' diffusive fluxes (J_D), and the ratio of measured Cu uptake rates (ρCu) and J_D ($\rho Cu:J_D$) for each species and treatment of the Cu(II)Cyclam uptake assays reported in Tables 3.3 and 3.5. 105

Table 3.5. Short-term uptake ($\pm 1\sigma$; $n=3$) of Cu in the Cu(II)Cyclam and Cu(I)GSH treatments by the species grown in Cu-replete media (10.2 nM), and previously published steady-state and short-term Cu uptake rates are included for comparison (see footnotes for details). Average growth rates for the triplicate are reported beneath each species name ($\pm 1\sigma$). Copper(II) was complexed with 3 nM Cyclam, while 10 nM GSH was added. Due to the weak complex formed between Cu(I) and GSH (see section 3.2.2.1), the Cu species in this treatment is effectively Cu'. Short-term rates that were significantly faster in the Cu(I)GSH treatment are in bold (one-way student t-test, unequal variances). Copper uptake rates in both treatments were significantly different between *T. oceanica*, *C. polylepis*, and *P. pouchetii*..... 106

Table 4.1. Initial station parameters for stations P20 and P26 in the subarctic NE Pacific Ocean sampled between August 17 and September 2, 2010. Discrete chemical and biological measurements were made on samples collected from 10 m 146

Table 4.2. Volumetric ($\text{pmol Fe L}^{-1} \text{d}^{-1}$; ρFe_V) and carbon-normalized ($\mu\text{mol Fe mol C}^{-1} \text{d}^{-1}$; ρFe_C) size-fractionated Fe uptake rates (24 h) of $1 \text{ nmol L}^{-1} {}^{55}\text{Fe}$ bound to 1.05 nmol L^{-1} DFB in the P20GO incubation. Uptake rates were measured on Day 3 of the incubation. Carbon-normalized uptake rates were calculated by converting total bacterial abundances and chl *a* to

carbon (20 fg C cell⁻¹, and 50 g C g chl *a*⁻¹, respectively). Values in parentheses are 1σ for triplicates. Values in bold are significantly different from the control treatment (two-tailed t-test, unequal variances, p<0.05). 147

Table 4.3. Volumetric (pmol Fe L⁻¹ d⁻¹; ρFe_v) and carbon-normalized (μmol Fe mol C⁻¹ d⁻¹; ρFe_c) size fractionated Fe uptake rates (24 h) of 1 nmol L⁻¹ ⁵⁵Fe bound to 1.05 nmol L⁻¹ DFB in the P26GO incubation. Uptake rates were measured on Day 3 of the incubation. Carbon-normalized uptake rates were calculated by converting total bacterial abundances and chl *a* to carbon (20 fg C cell⁻¹, and 50 g C g chl *a*⁻¹, respectively). Values in parentheses are 1σ for triplicate measurements. In the *in situ* light treatments, values in bold are significantly different from the control treatment (two-way Student t-test, unequal variances, p<0.05). In the low light (LL) treatments, values in bold are significantly different from all other treatments (ANOVA, p<0.05, Tukey test). 148

Table 5.1. Locations, sampling dates, seafloor depths, mixed layer depths (MLD), and light extinction coefficient (*k_D*) of the stations sampled along Line P in August, 2011. 196

Table 5.2. Light intensities, euphotic zone depth (*Z_{eu}*), and macronutrient concentrations at each sampling depth along Line P. Depths in bold are below the mixed layer. 197

Table 5.3. Total dissolved Cu ([Cu]_d), ligand concentrations ([L] ± 1σ), conditional stability constants (log *K_{CuL,Cu²⁺^{cond}}* ± 1σ), inorganic Cu concentration ([Cu']), and the dissolved [L]:[Cu]_d ratio at each sampling depth along Line P. Depths in bold are below the mixed layer. 198

Table 5.4. Initial total dissolved Cu ([Cu]_d), Cu-binding ligands ([L]), free Cu²⁺ (pCu), and total inorganic Cu concentrations ([Cu']) in the P16 incubation treatments. The initial [Cu]_d and [L]

in the amended treatments were determined by adding the initial $[Cu]_d$ and $[L]$ to the $CuSO_4$ and Cyclam additions, respectively. 199

Table 5.5. Biomass and rate parameters measured at each sampling depth along Line P. Depths in bold are below the mixed layer. Volumetric (NPP) and chl-normalized (NPP_B) net primary productivity (NPP) was measured over 24 h. Volumetric (BP_V) and cell-normalized (BP_B) bacterial productivity was measured over 3-4 h. 200

Table 5.6. Size-fractionated Cu:C assimilation ratios (24 h), short-term Cu uptake rates (2 h), long-term Cu uptake rates (24 h), and the short-term:long-term uptake rate ratio for each sampling depth along Line P in August 2011. Cu:C assimilation ratios were determined using ⁶⁷Cu and ¹⁴C. Carbon-normalized uptake rates were measured using ⁶⁷Cu, and dividing by particulate C concentrations derived from bacterial abundance and chl *a* concentrations (section 5.2.6 for details). The ST:LT ratios were calculated by converting the hourly short-term Cu uptake rates to daily dates, and then dividing by the long-term Cu uptake rates. Values for half the range are reported for the average of duplicate measurements, and values in bold are for the total particulate size fraction. Errors reported are ± half the range of two replicate measurements. 201

Table 5.7. Statistically significant Pearson correlations of biomass, productivity, Cu uptake, and chemical parameters measured along Line P in August 2011. Correlations with r^2 greater than 0.6 are in bold. 204

Table 5.8. Cyanobacteria and picoeukaryote abundance on Day 4 of the P16 incubation determined by flow cytometry. Values in parentheses are standard deviations (n=3) or half the range (n=2). For a description of the treatments, please see section 5.2.3.2. 205

Table 5.9. Literature particulate Cu:C ratios in laboratory grown phytoplankton species (20 species from 5 phyla) and in field samples..... 206

Table A.1. Previously published short-term and steady-state Cu uptake rates (ρ_{Cu}) measured for a suite of phytoplankton, inorganic Cu (Cu') in the uptake media, the ligand used to complex Cu, calculated maximum diffusive supply of Cu' to the cell surface (J_D), and the ratio of $\rho_{Cu}:J_D$.

Italicized values indicate the study measured short-term uptake rates; the other rates are steady-state rates calculated from the cellular Cu quotas ($zmol\ Cu\ cell^{-1}$) and growth rates (h^{-1})..... 244

List of Figures

Figure 1.1. Literature review of phytoplankton growth rates of exponentially growing species in varying inorganic Cu (Cu') concentrations. Rates are expressed as a percent of the maximum growth rate reported (Brand et al. 1986; Croot et al. 2003; Peers et al. 2005; Annett et al. 2008; Guo et al. 2012).....	33
Figure 1.2. Steady-state intracellular Cu concentrations ($\mu\text{mol Cu L}^{-1}$ cell volume) of <i>Thalassiosira pseudonana</i> , <i>T. oceanica</i> , and <i>Emiliania huxleyi</i> grown in different inorganic Cu (Cu') concentrations (pM) (adapted from Sunda and Huntsman 1995b). The inset focuses on intracellular Cu concentrations measured in media containing less than 8 pM Cu'	34
Figure 1.3. Literature review of short-term and steady-state cellular uptake rates performed with laboratory monocultures, and calculated maximum diffusive fluxes ($\text{mol Cu cell}^{-1} \text{h}^{-1}$) expressed as a log of the ratio with respect to the inorganic Cu concentration in the medium. The maximum diffusive flux was calculated using equation (11). All rates and fluxes are reported in Table A.1. Legend references are S&H1995b (Sunda and Huntsman 1995b), Croot2003 (Croot et al. 2003), Quigg2006 (Quigg et al. 2006), Annett2008 (Annett et al. 2008), Guo2010 (Guo et al. 2010), Guo2012 (Guo et al. 2012), This thesis (Chapter 3).	35
Figure 1.4. General locations of major surface currents and stations of the Line P transect in the northeast subarctic Pacific Ocean (NPC = North Pacific Current, AG = Alaska Current, CC = California Current). Station symbol shades indicate the prevalence of Fe limitation; black represents no Fe-limitation, grey represents intermittent or seasonal Fe-limitation, and white represents year-round Fe-limitation.	36

Figure 2.1. Depth profile of seawater density (σ_t ; kg m^{-3}), fluorescence, and dissolved nitrate (μM) in the upper 75 m at P26 on June 9, 2008. 72

Figure 2.2. Short-term (3 to 4 h) volumetric Cu uptake rates ($\text{pmol Cu L}^{-1} \text{h}^{-1}$) in the treatments amended with 1 nM Cu and 10 nM weak Cu(I) ligands (A), 1 nM Cu(II) bound to 10 nM Cu(II) ligands (B), and for trace amounts of ^{67}Cu added to the *in situ* ligands (C) for the 0.22-1 μm and $>1 \mu\text{m}$ size fractions. The bars represent the range of the two replicate assays. 73

Figure 2.3. Short-term (3 to 4 h) chlorophyll-normalized Cu uptake rates ($\text{pmol Cu } \mu\text{g chl } a^{-1} \text{h}^{-1}$) for three size fractions in the treatments amended with 1 nM Cu and 10 nM weak Cu(I) ligands (A), 1 nM Cu(II) bound to 10 nM Cu(II) ligands (B), and for trace amounts of ^{67}Cu added to the *in situ* ligands (C). The bars represent the range of the two replicate assays. 74

Figure 2.4. Size fractionated time course accumulation of Cu (pmol Cu L^{-1}) in the Cu(II)-ligand treatments (a-d), *in situ* treatments (e-h), and treatments amended with 1 nM Cu and 10 nM weak Cu(I) ligands (i-l). The bars represent the range of the two replicate assays. If bars are missing, then they are within the symbol. 75

Figure 3.1. Time-course accumulation of Cu by *T. pseudonana* (replicate A) grown in low Cu (0.6 nM) media. $^{64}\text{Copper}$ (1 nM) was added to the assay as either inorganic Cu(II) (Cu'), Cu(II) complexed with 3 nM Cyclam (Cu(II)Cyc), or Cu(I) with 10 nM GSH (Cu(I)GSH). Due to the weak complex formed between Cu(I) and GSH (see section 3.2.2.1), the Cu species in this treatment is effectively Cu' . Least-squares linear regressions are plotted for the Cu(II)Cyclam (dashed) and Cu(I)GSH (dotted) treatments. Cell concentrations ranged between 0.49 and 0.55 million cells mL^{-1} 108

Figure 3.2. Time-course accumulation of Cu by *T. pseudonana* replicate cultures grown in low Cu (0.6 nM) media. $^{64}\text{Copper}$ (1 nM) was added to the assay complexed with 3 nM Cyclam.

Cell concentrations for replicates A, B, and C were 0.55, 1.22, and 1.80 million cells mL⁻¹, respectively. 109

Figure 3.3. Time-course accumulation of 1 nM Cu bound to 3 nM Cyclam by *T. pseudonana* (replicate A) grown in low Cu (0.6 nM) media, including treatments with competitive inhibitors targeting the components of the proposed high-affinity Cu transport system (100 nM Pt(II), 500 nM FeDFB, and 500 nM Ag(I)). Least-squares linear regressions are plotted for each assay. Cell concentrations ranged between 0.49 and 0.55 million cells mL⁻¹..... 110

Figure 3.4. Average short-term Cu uptake rates ($\pm 1\sigma$; n=3) by *T. pseudonana* grown in low Cu (0.6 nM) media in the presence of competitive inhibitors for components of the proposed high-affinity Cu transport system. (A) 1nM Cu(II) bound to 3 nM Cyclam (Cu(II)Cyc) with additions of 500 nM FeDFB, 100 nM Pt(II), or 500 nM Ag(I); (B) 1nM Cu with 10 nM GSH (Cu(I)GSH) with the addition of 500 nM Ag(I). Due to the weak complex formed between Cu(I) and GSH (see section 3.2.2.1), the Cu species in this treatment is effectively Cu'. Single-tail student's t-tests (unequal variances) were performed to compare uptake rates between the unamended treatments and those with inhibitors. Significant differences ($p < 0.05$) are marked with an asterisk. Cell concentrations for replicates A, B, and C ranged between 0.49-0.55, 0.92-1.28, and 1.37-1.87 million cells mL⁻¹, respectively. 111

Figure 3.5. Carbon fixation rates by *T. pseudonana* grown in low Cu media (0.6 nM) for each treatment and replicate of the competitive inhibition Cu uptake assays..... 112

Figure 3.6. Intracellular Cu (amol Cu cell⁻¹) and carbon (fmol C cell⁻¹) accumulated in *T. pseudonana* at the end of the short-term Cu uptake assays for all treatments and replicates. Least-squares linear regression is plotted ($[\text{Cellular C}] = 121.8 \times [\text{Cellular Cu}] + 15.0$; $R^2 = 0.70$, $p < 0.0001$). Cultures were grown in low Cu (0.6 nM) media..... 113

Figure 3.7. Cyclam chemical structure and coordination with Cu(II).	114
Figure 4.1. Vertical profiles of dissolved nitrate (μM), photosynthetically active radiation (PAR; $\mu\text{mol quanta m}^{-2} \text{s}^{-1}$), density ($\sigma\text{-t}$; kg m^{-3}), and fluorescence in the upper 100 m at stations P20 and P26.	149
Figure 4.2. Chl <i>a</i> concentrations ($\mu\text{g L}^{-1}$) over the course of the P20GO incubation. Asterisks denote a significant difference compared to the control treatment for each respective sampling time, and error bars represent $\pm 1\sigma$ ($p < 0.05$; $n = 3$, two tailed t-test). Note that the right y-axis is for the Fe-amended treatment.	150
Figure 4.3. Chl <i>a</i> concentrations ($\mu\text{g L}^{-1}$) over the course of the P26GO incubation in the <i>in situ</i> (a) and low (b) light treatments. Asterisks denote a significant difference compared to the control treatment for each respective sampling time for the high light ($p < 0.05$; $n = 3$, two-tailed t-test) and low light ($p < 0.05$; $n = 3$, ANOVA, Tukey). Errors bars represent $\pm 1\sigma$. Missing error bars are within the symbols.....	151
Figure 4.4. Measurements of F_v/F_m made over the course of the P20GO (a) and P26GO (b). The mean ($\pm 1\sigma$) initial values (0 h) are marked with solid and dashed lines, respectively. Statistically significant differences between the treatment and control for each sampling time are marked with an asterisk (see text), and errors bars represent $\pm 1\sigma$ ($p < 0.05$; $n = 3$).	152
Figure 5.1. Stations sampled along the Line P transect in the northeast subarctic Pacific Ocean.	207
Figure 5.2. Depth profiles of $\sigma\text{-t}$ (kg m^{-3}), fluorescence (unitless), dissolved oxygen (μM), dissolved nitrate (μM), phosphate (μM), and silicic acid (μM) in surface waters ($< 50 \text{ m}$) of stations sampled along the Line P transect. Only data collected during the same cast were plotted.	208

Figure 5.3. Surface salinity, total dissolved Cu (nM), Cu-binding ligands (nM), and inorganic Cu (nM) concentrations along the Line P transect. Salinity was sampled at 5 m using the ship’s internal seawater pumping system, while the Cu concentration and speciation samples were from the shallowest depths sampled along the transect (7 to 10 m; Table 2)..... 209

Figure 5.4. Volumetric net primary productivity ($\mu\text{g C L}^{-1} \text{d}^{-1}$) (a-c), and chl *a*-normalized net primary productivity 210

Figure 5.5. Chlorophyll *a* concentrations ($\mu\text{g L}^{-1}$) (a,b), volumetric net primary productivity ($\mu\text{g C L}^{-1} \text{d}^{-1}$) (c,d), and chl *a*-normalized net primary productivity ($\mu\text{g C } \mu\text{g chl } a^{-1} \text{d}^{-1}$) (e,f) measured during the P16 incubation. Error bars represent $\pm 1\sigma$ (n=3). Asterisks indicate a statistically significant difference compared to the control on the respective sampling day ($p < 0.05$; two-way t-test). For a description of the treatments, please see section 5.2.3.2. 211

Figure 5.6. Cyanobacteria (closed symbols) and picoeukaryote (open symbols) cell abundance measured on day 4 of the P16 incubation ($10^6 \text{ cells L}^{-1}$) with respect to the estimated inorganic Cu concentrations in the incubation treatments (Table 4). 212

Figure 5.7. Cu:C assimilation ratios ($\mu\text{mol Cu mol C}^{-1}$) (ab), volumetric Cu uptake rates ($\text{pmol Cu L}^{-1} \text{d}^{-1}$) (cd), and long-term biomass normalized Cu uptake rates ($\mu\text{mol Cu mol C}^{-1} \text{d}^{-1}$) (ef) for the $>1 \mu\text{m}$ size fraction on each sampling day of the P16 incubation. Biomass-normalized Cu uptake rates were calculated by dividing volumetric rates by particulate carbon concentrations derived from total [chl *a*] and a C:Chl *a* ratio of $50 \text{ g C g chl } a^{-1}$. For a description of the treatments, please see section 5.2.3.2. 213

Figure 5.8. Biomass-normalized net primary productivity ($\mu\text{g C } \mu\text{g chl } a^{-1} \text{d}^{-1}$) and biomass-normalized Cu uptake rates ($\mu\text{mol Cu } \mu\text{mol C}^{-1} \text{d}^{-1}$) measured during the P16 incubation for the $>1 \mu\text{m}$ size fraction. Biomass-normalized Cu uptake rates were calculated by dividing volumetric

rates by particulate carbon concentrations derived from total [chl *a*] and a C:Chl *a* ratio (50 g C g chl *a*⁻¹). Data from each respective day and all the data were each fit to a logarithmic function ($p < 0.05$)..... 214

Figure 5.9. Satellite derived sea surface height anomalies (cm) along the Line P transect for August 8, 2011. Data were retrieved from the Colorado Centre for Astroynamics Research (CCAR) online database. 215

Acknowledgements

I want to express my sincere gratitude for the guidance and assistance provided by my supervisory committee, Maite Maldonado, Jay Cullen, and Paul Harrison. Their insight and support made this thesis possible. In particular, I want to thank Maite for pushing me further than I thought I could go, and, on occasion, for letting me pursue my other passions.

I want to thank NSERC for funding this thesis, because, otherwise, this prairie kid would never have been able to sail around the North Pacific and Arctic oceans, hold an injured storm petrol in the middle of the night, watch an otter preen itself next to the rosette, witness a school of dolphins play, experience how truly terrifying and awe inspiring the oceans are, or see a polar bear in the wild.

The captains and crew of the CCGS JP Tully, and the scientists at the Institute of Ocean Sciences provided any and all assistance one could require to do oceanographic field work – and with a smile. In particular, I want to thank chief scientist Marie Robert for organizing the Line P cruises, and Keith Johnson for my crash course in trace metal sampling, as well as for having positive attitude at sea that is infectious.

There are many students and staff to thank, past and present, but the camaraderie, advice, and support provided the Tornado lab and friends – Nina, Lizzy, Anna, new Dave, Ania, Rebecca, Carolyn, Kang, Kristina, Chris, Phil, and Maureen – is very much appreciated. Kristina – thanks for lunch. Nina, Ania – thanks for coffee. Kang, new Dave – thanks for the beer. Anna – thanks for letting me know you care by telling me how tired I look. Rebecca, Lizzy – thanks for being amazing office mates, and for reminding me that one person can excel at two things. Chris – thanks for being a great comrade at sea. Maureen – thanks for having an answer to nearly every question. Phil – thanks for your feedback, anecdotes, and impressions.

Lastly, from the bottom of my heart, I want to thank my family and friends for their support over the years. Mom, Dad, Ryan, Baba, Digi, Jeff, Lauren, Jenna, Andrew, Mikhail, Courtney, Alice, Jen – thank you.

For my family.

And in the tractor man there grows the contempt that comes only to a stranger who has little understanding and no relation. For nitrates are not the land, nor phosphates; and the length of fiber in the cotton is not the land. Carbon is not a man, nor salt nor water nor calcium. He is all these, but he is much more, much more; and the land is so much more than its analysis. The man who is more than his chemistry, walking on the earth, turning his plow point for a stone, dropping his handles to slide over an outcropping, kneeling in the earth to eat his lunch; that man who is more than his elements knows the land that is more than its analysis. But the machine man, driving a dead tractor on land he does not know and love, understands only chemistry; and he is contemptuous of the land and of himself. When the corrugated iron doors are shut, he goes home, and his home is not the land.

-John Steinbeck, *Grapes of Wrath* (1939)

*What a filthy job.
Could be worse.
How?
Could be raining.
[it pours]*

-Mel Brooks, *Young Frankenstein* (1974)

Chapter 1: Introduction

Phytoplankton are a fundamental component of marine ecosystems and the global carbon cycle. Through photosynthesis, carbon fixed by marine phytoplankton accounts for half of global net primary productivity (Field et al. 1998), and provides the basal energy source for many marine food webs. Phytoplankton also take part in the “biological pump”. Primary producers convert inorganic carbon into organic matter in surface waters, resulting in a drawdown of dissolved inorganic carbon at the surface. Most of this fixed organic carbon is oxidized back to CO₂ via respiration by marine heterotrophic bacteria in the upper 500 m of the water column. A small amount (1 to 3 %) of fixed carbon sinks to the ocean floor as cell flocculates, ballasted with biogenic and lithogenic mineral phases or in zooplankton fecal pellets, thereby sequestering it from the atmosphere over > 1000 year time scales (e.g. Sigman and Boyle 2000; Buesseler et al. 2007; De La Rocha and Passow 2007). This “pumping” of carbon out of surface waters and into the deep ocean is a significant flux term in the global carbon cycle over 100 to 1000’s of years, and is thought to be partially responsible for the 80 ppm shift in atmospheric CO₂ concentrations during glacial-interglacial periods (Sigman and Boyle 2000; Hain et al. 2014). The processes controlling the rate of primary production and the fate of fixed carbon have a significant impact on marine food webs, the global carbon cycle, and climate.

The availability of macronutrients (nitrate, phosphate, and silicic acid for silicifying organisms) provides a cap for the total biomass that can be supported in a marine environment. However, a suite of mineral nutrients (e.g. iron (Fe), zinc (Zn), manganese (Mn), copper (Cu), nickel (Ni), cobalt (Co), cadmium (Cd), molybdenum (Mo)) is required by phytoplankton in trace amounts

for a variety of metabolic functions. Typically, these metals are incorporated as cofactors into enzymes involved in electron transfer reactions inside the mitochondria and chloroplast (Fe, Cu, Mn), in carbon-concentrating mechanisms within the chloroplast (Zn, Co, Cd), inorganic and organic nitrogen transport and assimilation (Fe, Cu, Ni), diazotrophic nitrogen fixation (Fe, Mo), organic phosphorus assimilation (Zn), vitamin B₁₂ synthesis (Co), chlorophyll synthesis (Fe), sequestering reactive oxygen species (Fe, Mn, Cu, Zn), and water splitting in photosystem II (Mn) (Palenik and Morel 1991; Bowler et al. 1994; Raven et al. 1999). If these mineral nutrients are present in too low concentrations in seawater, or in forms that are not bioavailable to marine phytoplankton, then they could limit marine primary productivity (e.g. Morel and Price 2003).

Indeed, the availability of trace mineral nutrients can mediate phytoplankton rate processes and primary productivity in large areas of the ocean (Morel and Price 2003; Moore et al. 2013). When present in too low or too high availability, trace metals can cause limitation or toxicity, respectively (e.g. Brand et al. 1986; Martin and Fitzwater 1988; Moffett et al. 1997). Many trace metals are present in sparingly low concentrations (sub-nanomolar), due to either low source inputs (e.g. atmospheric deposition, rivers, upwelling, lateral transfer from continental margins, or diffusion) or fast removal rates (e.g. precipitation, scavenging onto particles, or uptake by biota) (reviewed by Bruland and Lohan 2003). As a result, some trace metals, most notably Fe, have been implicated in limiting marine primary productivity (Morel and Price 2003; Boyd et al. 2007). Numerous natural and artificial mesoscale Fe-enrichment experiments have demonstrated that primary productivity in approximately one third of the global surface ocean is limited by Fe (reviewed by Boyd et al. 2007). Therefore, there is considerable interest in fully elucidating the

controls on Fe acquisition and intracellular Fe requirements in marine phytoplankton (see section 1.1.3)

Copper as a trace nutrient is of particular interest because it has the potential to be either limiting or toxic to marine phytoplankton (e.g. Brand et al. 1986; Peers et al. 2005). A limited number of studies have investigated how Cu availability might influence phytoplankton biomass and rate processes in open ocean primary producers (Coale 1991; Mann et al. 2002; Peers et al. 2005). These studies added dissolved Cu to seawater, and observed the response of phytoplankton communities to increased Cu availability. However, the response of open ocean phytoplankton communities to lower Cu availability has not been investigated, and so the Cu nutritional state of phytoplankton populations inhabiting large regions of the ocean is uncertain.

The goal of this thesis was to investigate Cu nutrition in open ocean Fe-limited and Fe-replete phytoplankton communities using a combination of process (e.g. microcosm shipboard incubations) and observational approaches. One laboratory and three field studies were performed to investigate how the concentration and chemical speciation of Cu affects Cu bioavailability to marine microbes, as well as rate processes of natural phytoplankton and bacteria communities in the northeast subarctic Pacific Ocean.

1.1 Trace Metal Control of Primary Productivity

1.1.1 Trace Metal Speciation and Notation

Most transition metals in seawater are referred to as “trace metals” because their dissolved concentrations are <100 nM. Dissolved trace metals (*Me*) in seawater are present as either

inorganic (Me') or organic complexes (MeL). The dissolved Me' pool is made up of the “free”, hydrated species (Me^{n+}), as well as metal complexes with anionic ligands (L_i^{p-}) such as OH^- , CO_3^{2-} , Cl^- , SO_4^{3-} , and F^- . The concentration of Me^{n+} is often reported in the literature, and is related to $[Me']$ by the equations:

$$[Me'] = [Me^{n+}] \alpha_{Me^{n+}} \quad (1)$$

$$\alpha_{Me^{n+}} = \frac{[Me^{n+}] + \sum MeL_i^{(n-p)+}}{[Me^{n+}]} \quad (2)$$

The side reaction coefficient, $\alpha_{Me^{n+}}$, accounts for all inorganic complexes formed by a metal with the major anionic ligands in seawater. Due to the low concentration of $[Me^{n+}]$, a notation is commonly used to refer to free metal concentrations: $pMe = -\log[Me^{n+}]$. Since pMe is a negative log, higher values correspond to lower free metal concentrations.

For many trace metals in seawater, >99% of the total dissolved metal pool is complexed by what are thought to be organic ligands. The structure and origin of these organic ligands are largely unknown, but likely consist of terrestrially derived humic and fulvic acids, as well as autochthonous ligand sources, such as biota and sediments. Often, the concentrations of Me' and MeL , as well as the binding strength of the complex (the conditional stability constant, $K_{MeL,Me'}^{cond}$) are of interest, and can be represented by the following equations:



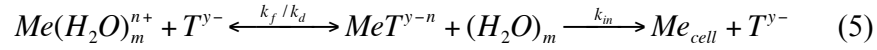
$$K_{MeL,Me'}^{cond} = \frac{[MeL]}{[Me'][L]} \quad (4)$$

Equations (3) and (4) are the simplest representations of trace metal speciation in seawater, and take into account effects of ionic strength as well as metal and ligand side reactions with other dissolved components in seawater. As $K_{MeL,Me'}^{cond}$ can be measured in natural seawater samples containing unknown organic ligands – with unknown ligand side reactions – equations (3) and (4) are primarily used in this thesis.

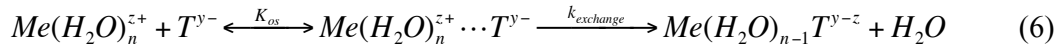
1.1.2 Trace Metal Bioavailability to Marine Phytoplankton

Trace metal bioavailability to marine phytoplankton is controlled by the chemical speciation of metals in seawater (Hudson 1998; Sunda and Huntsman 1998; Morel and Price 2003). For some metals (e.g. Fe, Cu, Zn), the majority of the dissolved forms are bound to strong organic ligands, resulting in scarce inorganic metal concentrations (e.g. van den Berg 1984; Bruland 1989; Rue and Bruland 1995). In laboratory studies, early workers observed that the acquisition of trace metals was closely related to the concentration of “free” hydrated Me^{n+} , and not total dissolved Me , and suggested that Me^{n+} was the sole bioavailable species to marine phytoplankton (e.g. Anderson and Morel 1982; Sunda and Huntsman 1992; 1995b). The “Free Ion Model” (FIM) was thus postulated, whereby the concentration of Me^{n+} controls metal bioavailability to algal surface transporters (reviewed by Campbell 1995; Hudson 1998; Sunda and Huntsman

1998). The transport of a metal by an algal surface membrane transporter (T) can be described by:



Few measurements of the rate of internalization (k_{in}) have been made, but they are dependent on the particular transporter and can vary between $(0.3 \text{ to } 3) \times 10^{-3} \text{ s}^{-1}$ for Fe (Hudson and Morel 1990), and $0.025 \text{ to } 0.33 \text{ s}^{-1}$ for Cu (Croot et al. 2003). The forward reaction between a metal ion and transporter active site undergoes an Eigen-Wilkins reaction mechanism:



Where K_{os} (M^{-1}) is the outer sphere complex formation constant between the ligand and metal, and $k_{exchange}$ (s^{-1}) is the rate constant for the exchange of the first water molecule from within the inner coordination sphere of the metal with a coordinating ligand in the transporter active site (Morel et al. 1991). The loss of the first inner water molecule is the rate limiting step for complexation, and so the overall forward reaction rate constant, k_f , is thus:

$$k_f = K_{OS} k_{exchange} \approx K_{OS} k_{-w} \quad (7)$$

K_{OS} is determined primarily by the product of net charges of the transporter active site and reacting metal species, is highly influenced by ionic strength, and has been estimated to vary

between 0.5 and 8 M⁻¹ in seawater (Morel et al. 1991; Morel and Hering 1993). The rate constant for inner water replacement, $k_{exchange}$, is limited by the water loss rate, k_{-w} , and so an approximation for $k_{exchange}$ is made using k_{-w} . Unlike K_{os} , k_{-w} can vary 16 orders of magnitude between slow (e.g. Cr³⁺) and fast (e.g. CH₃Hg⁺) reacting metals (reviewed by Hudson 1998). Water loss rate constants tend to increase with decreasing charge, such that rates for divalent metals (e.g. $k_{-w} \sim 10^9 \text{ s}^{-1}$ for Cu²⁺) are faster than trivalent metals (e.g. $k_{-w} \sim 10^2 \text{ s}^{-1}$ for Fe³⁺). Complexation of metal ions by inorganic ligands also increases k_{-w} by decreasing the charge of the complexed metal ion (e.g. k_{-w} increases from $\sim 10^2$ to 10^5 s^{-1} when Fe³⁺ is complexed by OH⁻¹).

The FIM has proven to be a powerful tool for predicting transport rates of a variety of metals by marine phytoplankton in laboratory studies (reviewed by Sunda and Huntsman 1998; Hudson 1998), although it has yet to be demonstrated for open ocean phytoplankton communities. The FIM holds true when k_{in} is significantly lower than k_d , and the concentration of MeT depends on the equilibrium concentration of Me^{n+} in the medium, and the subsequent equilibrium established between Me^{n+} and the transporter. Although the FIM was developed for describing the bioavailability of Me^{n+} , it should also describe transport of any metal species – including inorganically and organically complexed Me – for which the apparent forward reaction rate constant for exchange of the metal species and the transporter is significantly faster than k_{in} (Hudson 1998). Thus, a more general “equilibrium paradigm” may describe trace metal bioavailability as long as a rapid pseudoequilibrium is established between the bioavailable metal species and the transporters.

There are a few important exceptions to the FIM or “equilibrium model” that involve kinetic control of metal transport. During Fe limitation in the diatom *Thalassiosira weissflogii*, Fe bound to the transporter is not at equilibrium with the bulk medium (Hudson and Morel 1990). Thus, transport of Fe under these conditions is not controlled by the formation of *MeT* due to the rapid equilibrium established between the transporter and the bioavailable metal species in solution, but rather by the formation of the *MeT* complex itself. Under these conditions, k_{in} is similar to k_f and much greater than k_d . Indeed, k_f for the formation of *FeT* in *T. weissflogii* and *Pleurochrysis carterae* were similar to k_w for the fastest Fe species $\text{Fe}(\text{OH})_2^-$, and were on par with k_f for the strong Fe(III) binding siderophore desferrioxamine B (Hudson and Morel 1990). This indicates that Fe' transport during Fe limitation is under kinetic control, and limited by the inner coordination sphere water loss rate.

Diffusion of the bioavailable metal substrate to the cell surface can also impart kinetic control of metal transport in marine phytoplankton. As phytoplankton transporters internalize trace metals, the concentration of bioavailable metal species near the cell surface is depleted and a concentration gradient is formed within the diffusive boundary layer of the cell. Thus, a metal transporter that is under equilibrium control when the bioavailable metal substrate concentration is high will be under kinetic control if the rate of *MeT* formation is limited by the diffusion of the metal substrate to the cell surface (Jackson and Morgan 1978). For example, Zn transport rates in Zn-limited diatoms and prymnesiophytes can comprise between 28 and 61% of the diffusive flux of Zn^{2+} to the cell surface. Under these conditions, Zn^{2+} concentrations at the cell surface would be significantly lower than the equilibrium concentration of Zn^{2+} in the uptake medium.

More recent work has demonstrated that metals within organic complexes can be bioavailable. For example, Fe bound to strong and weak organic ligands can be accessed by phytoplankton (Maldonado and Price 2001; Maldonado et al. 2002; Shaked et al. 2005; Hassler et al. 2011), and Zn bound within weak organic complexes is also bioavailable (Aristilde et al. 2012). Complexation of metals by weak ligands can decrease the inorganic metal concentration in solution, requiring a re-equilibration between the strong metal-ligand complexes and the inorganic metal pool. Acquisition of metals from the weaker complexes would effectively draw metals from the strong ligands via a weaker metal-ligand intermediate complex (e.g. Aristilde et al. 2012). The acquisition of metals from ligands by phytoplankton transporters may proceed via ternary complex formation between the transporter and *MeL* complex (Aristilde et al. 2012). Forward reaction rates for ternary complex formation between *MeL* and transporters have not been described, and so it is not possible to determine whether acquisition of organically complexed metals is under equilibrium or kinetic control. The mixture of unknown strong and weak metal binding ligands in seawater, and the bioavailability of organically complexed metals to laboratory marine phytoplankton emphasizes the importance of elucidating the bioavailability of *in situ* dissolved metals to marine phytoplankton communities.

1.1.3 Case Study of Trace Metal Limitation – Iron

In three large oceanic regions – the subarctic Pacific, the eastern equatorial Pacific, and the Southern Ocean – macronutrient concentrations are not completely drawn down over a yearly growth period. This indicates that another nutrient ultimately limits primary productivity in these “high nutrient low chlorophyll” (HNLC) regions. Over the last three decades, Fe has been recognized as limiting primary productivity in HNLC waters (as reviewed by Boyd et al. 2007).

Dissolved Fe concentrations in open ocean surface waters are low (~70 pM; Johnson et al. 1997) due to low inputs of Fe, and the low solubility of Fe in seawater. Iron is abundant on land, but is primarily found within oxide and hydroxide mineral phases (e.g. ferrihydrite; Lindsay and Schwab 1982) that are insoluble in seawater (< 0.5 nM at pH 8.2; Liu and Millero 2002). Iron input to open ocean surface waters is dominated by episodic inputs from atmospheric deposition (e.g. Mahowald et al. 2005; Hamme et al. 2010), lateral transfer of Fe-rich coastal waters by mesoscale eddies (Johnson et al. 2005), isopycnal movement of Fe away from Fe-rich continental shelves (Lam et al. 2006), and vertical mixing and entrainment of deep waters that contain higher Fe concentrations (~0.7 nM; Johnson et al. 1997) into the sunlit surface layer. In contrast, coastal waters receive a high input of Fe from rivers and continental shelf sediments (Elrod et al. 2004), and dissolved Fe concentrations in coastal surface waters can be more than an order of magnitude higher than offshore waters (> 1 nM; Johnson et al. 1997; Elrod et al. 2004; Johnson et al. 2005). Thus, coastal waters are less frequently Fe-limited (e.g. Hutchins et al. 1998).

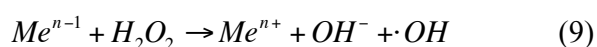
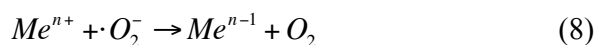
Dissolved Fe speciation in seawater is dominated by complexation with strong organic ligands (reviewed by Gledhill and Buck 2012). Strong Fe binding ligands tend to be in excess of the total dissolved Fe pool, and have high $K_{FeL,Fe}^{cond}$ (10^{10} to 10^{14}). The strong ligands that bind Fe are likely siderophores, strong Fe(III) binding ligands that are produced by marine bacteria (Granger and Price 1999; Gledhill et al. 2004). Strong ligands aid in maintaining dissolved Fe concentrations in seawater that are above the solubility of inorganic Fe, and microbes may produce them to prevent rapid loss of Fe from seawater due to precipitation or scavenging onto particles (e.g. Johnson et al. 1997). Due to the strong complexes formed between Fe(III) and

organic ligands, eukaryotic phytoplankton evolved physiological adaptations to access Fe from organic ligands. In marine diatoms, an extracellular reductase can reduce Fe(III) bound to strong ligands using a high-affinity Fe transport system (HAFETS) (Maldonado and Price 2001; Shaked et al. 2005; Kustka et al. 2007). The Fe(II) produced is then oxidized by a multi-copper containing oxidase (MCO), and subsequently internalized by an Fe(III) permease (Maldonado et al. 2006; Kustka et al. 2007). Interestingly, marine diatoms grown in low Cu containing media have slower Fe(III) oxidation rates, and subsequently slower Fe uptake rates (Peers et al. 2005; Maldonado et al. 2006). Thus, it is possible for Fe-limited marine phytoplankton to become co-limited by Cu availability (Peers et al. 2005; Annett et al. 2008; Guo et al. 2012).

1.1.4 Trace Metal Toxicity

While essential for optimal growth, trace metals are also toxic to microorganisms at elevated concentrations due to their induction of intracellular oxidative stress (reviewed by Pinto et al. 2003; Kawakami et al. 2006). Oxidative stress inside the cell is caused by elevated concentrations of hydrogen peroxide (H_2O_2), as well as superoxide (O_2^-) and hydroxyl (OH^\cdot) free radicals. These reactive oxygen species (ROS) are strong oxidizing and reducing agents, and can react with lipids, DNA, sulfur-containing proteins, and other sulfur compounds such as glutathione. Reactive oxygen species are naturally produced inside the chloroplast and mitochondrion, and enzymes, such as superoxide dismutase and H_2O_2 -degrading catalase, are synthesized to degrade them (reviewed by Noctor and Foyer 1998). However, if cytoplasmic trace metal concentrations are high, they can facilitate the production of ROS that can overwhelm cellular mechanisms for quenching ROS. For example, at physiological pH, Fe and

Cu can exist in oxidized and reduced forms that will react with H₂O₂ and superoxide to produce hydroxyl radicals via the Haber-Weiss cycle (8-9) and Fenton reaction (9), respectively.



The hydroxyl radicals react with intracellular glutathione – a compound integral to maintaining reduced sulfur moieties in amino acids, and for ameliorating intracellular oxidative stress – and deplete its concentration (e.g. Okamoto et al. 2001). Metals that are not redox reactive in physiological conditions (e.g. Zn) can also induce oxidative stress by binding and depleting intracellular reduced glutathione concentrations (Tripathi et al. 2006). As metal toxicity worsens and glutathione can no longer mediate intracellular oxidative stress, oxygen free radicals begin reacting with lipids and proteins. This results in a loss of membrane integrity, followed by membrane depolarization, and finally a disruption of intracellular homeostasis (Pinto et al. 2003).

In addition to causing oxidative stress, excess divalent metals (e.g. Cu, Zn, Cd) can exhibit antagonistic effects on metal metabolism in biological systems. For example, Cu can also cause toxicity by binding non-specifically to thiol-containing proteins and thereby disrupt their optimal functioning (Letelier et al. 2005). In marine phytoplankton, low affinity non-specific divalent metal transporters are responsible for transporting a number of metals into the cell (e.g. Cu(II), Fe(II), Zn(II), Mn(II), and Cd(II)) (Sunda and Huntsman 1983; 2000; Lane et al. 2008). If one metal concentration is significantly higher than another, then transport of the less abundant metal

decreases due to competition at the transporter active site (e.g. Sunda and Huntsman 1983). Indeed, excess Cu may lead to inhibition of phytoplankton growth due to the competition between Cu and Mn and/or Zn for either surface transport sites or intracellular metal enzyme active sites (Sunda and Huntsman 1983). Thus, the speciation of dissolved trace metals – and their bioavailability – may facilitate metal toxicity.

1.2 Copper Physiology in Marine Phytoplankton

1.2.1 Phytoplankton Metabolic Copper Requirements and Homeostasis

Copper is a particularly interesting trace metal because it is a required micronutrient, but can cause toxicity at elevated concentrations in many marine phytoplankton (Figure 1.1). Copper helps to catalyze a number of important electron transfer reactions in marine phytoplankton. These include electron transfer between photosystem II and photosystem I by plastocyanin (Peers and Price 2006), electron transfer within the mitochondria between O₂ and cytochrome *c* oxidase, the conversion of superoxide radicals into hydrogen peroxide by superoxide dismutase (Raven et al. 1999), and the extracellular conversion of primary amines into ammonium (Palenik and Morel 1991). As a result, intracellular Cu quotas – often defined as $\mu\text{mol Cu per mol}$ organic carbon within the cell at steady-state – of phytoplankton grown under non-toxic conditions vary between 0.74 and 9.93 $\mu\text{mol Cu mol C}^{-1}$ (Sunda and Huntsman 1995b; Ho et al. 2003; Annett et al. 2008), and are on par with the minimum Fe requirements of marine phytoplankton (Brand 1991; Sunda et al. 1991; Sunda and Huntsman 1995a; Maldonado and Price 1996). Fewer studies have reported Cu quotas during toxicity, but they have indicated that Cu quotas can vary between 15 and 150 $\mu\text{mol Cu mol C}^{-1}$ (Sunda and Huntsman 1995b; Chang and Reinfelder 2000).

Laboratory evidence suggests that marine phytoplankton can regulate intracellular Cu concentrations. Reanalyzing the intracellular Cu concentrations reported by Sunda and Huntsman (1995b) demonstrated that, at low Cu' concentrations (< 8 pM), cellular Cu increased linearly and reached a plateau in three species (Figure 1.2, see inset). This plateau indicated that the phytoplankton were able to either exclude Cu by decreasing Cu uptake rates, or by transporting Cu out of the cell to maintain a constant intracellular Cu concentration (i.e. efflux). As Cu' concentrations increased above 8 pM, intracellular Cu increased nearly linearly in all three species and began to form a second plateau above 100 pM. The linear increase in cellular Cu above 8 pM indicated that the marine phytoplankton may not have complete control over intracellular Cu accumulation at higher Cu' concentrations. The second plateau may be due to slower metabolic rates as Cu begins to cause intracellular oxidative stress (e.g. Pinto et al. 2003). These data imply that intracellular Cu accumulation by marine phytoplankton is metabolically regulated at lower Cu concentrations, by either down-regulating uptake rates or up-regulating efflux, but Cu may enter the cell accidentally at higher Cu concentrations (e.g. through other divalent metal transporters; Sunda and Huntsman 1983).

Interestingly, Fe can also alter intracellular Cu requirements in 4 of 18 phytoplankton species surveyed thus far (Annett et al. 2008; Guo et al. 2012), and for large phytoplankton (>20 μm diameter) in the subarctic northeast Pacific Ocean (Semeniuk et al. 2009). This may be due to upregulation of the Cu-dependent high-affinity Fe transport system during Fe-limitation (see section 1.1.3) (Maldonado et al. 2006). Cellular Cu requirements are also significantly higher in phytoplankton isolated from the open ocean than those isolated from coastal regions (Annett et al. 2008; Guo et al. 2012). This likely reflects the low Fe concentrations present in open ocean

surface waters (Johnson et al. 1997), and the resulting dependency of phytoplankton on either the HAFeTS, or on Cu to replace Fe-containing enzymes (e.g. plastocyanin can be used in lieu of cytochrome c_6 in at least one diatom species; Peers and Price 2006). While Fe and Cu metabolisms may be linked in some laboratory marine phytoplankton strains, there is no physiological evidence for this occurring in natural marine phytoplankton communities.

1.2.2 Copper Detoxification

At optimal intracellular Cu concentrations, cytoplasmic free Cu concentrations are low (e.g. in yeast, < 1 free atom per cell) due to complexation by chaperone proteins (Rae et al. 1999). Copper not bound to chaperones can induce oxidative stress (see section 1.1.4). Organisms typically employ three methods for detoxifying Cu: intracellular sequestration by organic chelators, exudation of specific chelators that bind Cu' to decrease Cu bioavailability, and the active cellular efflux of heavy metals (either inorganic or chelated) (Pinto et al. 2003).

Evidence for all three detoxification methods has been observed in laboratory marine phytoplankton strains. In some species, thiol-containing phytochelatins are produced within the cell to bind Cu and prevent the formation of ROS (Ahner and Morel 1995; Ahner et al. 1997; 2002). Since Cu' is believed to be the primary substrate for Cu transport, marine cyanobacteria release ligands when exposed to Cu toxicity to complex extracellular Cu and thus decrease Cu' (Moffett and Brand 1996; Wiramanaden et al. 2008). These ligands are nitrogen-rich, contain sulfur, and may bind Cu(I) (Ross et al. 2003). For example, work by Leal et al. (1999) has indicated that *Emiliania huxleyi* grown in natural seawater with Cu amendments produce thiol-containing ligands that ameliorate the effects of Cu toxicity, and allow growth when dissolved

Cu in the medium is high. These authors hypothesized that the thiols released may bind Cu' and make it less available to Cu transporters. The intracellular Cu concentrations of cells inoculated in a medium containing thiol-exudates and Cu increased rapidly after 2 days, and subsequently decreased after 10 days. The authors argued that intracellular Cu concentrations were diluted as a result of cellular division. However, the increased cellular Cu concentrations after 2 days may indicate that Cu bound to the thiols was bioavailable, and other detoxification strategies – e.g. efflux – may explain the decreased cellular Cu concentrations over time. Indeed, recent evidence suggests that *E. huxleyi* can efflux Cu (Walsh and Ahner 2014). Efflux has also been observed in the Cu-sensitive cyanobacterium *Synechococcus sp.* DC2 (Croot et al. 2003). In addition, indirect evidence for efflux has been obtained for a natural phytoplankton community in the northeast subarctic Pacific Ocean; short-term Cu uptake rates were significantly faster than long-term Cu uptake rates (Semeniuk et al. 2009). While Cu efflux may occur in marine phytoplankton species to prevent Cu toxicity, it remains uncertain whether natural marine phytoplankton populations use efflux to maintain optimal intracellular Cu concentrations.

1.2.3 The Distribution and Speciation of Copper in Seawater

The primary natural sources of Cu to seawater are atmospheric deposition, continental shelf sediments, and rivers (Boyle et al. 1977; Boyle et al. 1981; Duce et al. 1991). Both wet and dry deposition events can release Cu into surface waters. Dissolved Cu in rainwater is enriched in Cu relative to open ocean surface seawater (>5 nM), but is complexed by a suite of unidentified organic ligands (Spokes et al. 1996; Kieber et al. 2004; Witt and Jickells 2005). In contrast, dry deposition of natural dust and volcanic ash may be minor sources of Cu to surface waters (Heller and Croot 2011). Copper in rivers is similarly enriched, with an average riverine concentration

of 23 nM (reviewed by Gaillardet et al. 2003), and is either complexed by organic ligands or present in polynuclear sulphide clusters (Rozan and Benoit 1999; Rozan et al. 2000). In coastal surface waters, total dissolved Cu ranges between 2 and 18 nM, and can reach 400 nM if anthropogenic Cu sources are present (Flegal et al. 1991; Donat et al. 1994; Moffett et al. 1997; Croot 2003). In open ocean waters, Cu concentrations are lower (0.25 to 3 nM), and may be due to lower inputs from atmospheric deposition or lateral transport from coastal waters (Jacquot et al. 2013; Thompson et al. 2014). Copper displays a modified nutrient-type depth profile (Boyle et al. 1977, Coale and Bruland 1988; 1990; Jacquot et al. 2013; Thompson et al. 2014). Dissolved Cu is lower at the surface (0.25 to 3 nM) and increases with depth (3 to 4 nM). This is due to biological Cu uptake in surface waters, export and remineralization below the thermocline (Sunda and Huntsman 1995b), scavenging of Cu onto sinking particles (Boyle et al. 1977), or the formation of insoluble Cu sulfide minerals in microanoxic environments in intermediate waters (Janssen et al. 2014).

Copper in seawater can exist in two oxidation states (+1 and +2). While the oxidized form is thermodynamically favoured in oxygenated seawater, significant Cu(I) concentrations may exist in coastal and open ocean waters. Copper is reduced by hydrogen peroxide, superoxide radicals, reduced sulfur compounds, and light-mediated ligand-to-metal electron transfer reactions (Moffett and Zika 1987; Leal and van den Berg 1998; Zafirou et al. 1998; Voelker et al. 2000; Beurge-Weirich and Sulzberger 2004; Heller and Croot 2010; Pérez-Almeida et al. 2013). Reactions with superoxide likely dominates the reduction of inorganic and organically complexed Cu(II), with effective reduction rate constants of $\sim 2 \times 10^9 \text{ M}^{-1} \text{ s}^{-1}$ and $0.3\text{--}1 \times 10^9 \text{ M}^{-1} \text{ s}^{-1}$, respectively (Zafirou et al. 1998; Voelker et al. 2000). In oxygenated surface waters, the

oxidation of inorganic Cu(I) by O₂ has a half-life of ~12 min (González-Dávila et al. 2009), while oxidation by superoxide is considerably faster (half-life ~5 s, assuming a steady-state superoxide concentration of 100 pM found in open ocean surface waters; Zafirou et al. 1998, Heller and Croot 2010). Cu(I) is likely stabilized by Cl⁻ ions (Moffett and Zika 1983; González-Dávila et al. 2009; Pérez-Almeida et al. 2013; Walsh and Ahner 2013). While CuCl_n species dominate inorganic Cu(I) in seawater, the oxidation rates of “free” hydrated Cu⁺, CuCO₃⁻, and CuClOH⁻ are between 10 and 1000 times faster than CuCl_n species (Yuan et al. 2011). Although current analytical methods are unable to accurately differentiate between Cu(I) and Cu(II) at low Cu concentrations found in seawater, a few estimates of Cu(I) concentrations in seawater suggest that between 5 and 80% of the total dissolved Cu may be Cu(I) (Moffett et al. 1985; Moffett and Zika 1988; Beurge-Weirich and Sulzberger 2004). Estimates of steady-state inorganic Cu(I) concentrations (1-63 pM; Heller and Croot 2010) are similar to inorganic Cu concentrations found in surface waters (10-1000 pM; Moffett and Dupont 2007; Buck et al. 2010; Bundy et al. 2013; Jacquot et al. 2013). Thus, Cu(I) may be an important substrate for Cu transport in marine biota.

Between 98-99.9% of dissolved Cu in coastal and open ocean seawater is bound to strong and weak organic ligands with $K_{CuL,Cu^{2+}}^{cond}$ ranging from 10^{8.5} to 10¹⁶ (Coale and Bruland 1988; Moffett and Dupont 2007; Buck et al. 2010; Bundy et al. 2013; Jacquot et al. 2013; Thompson et al. 2014). In electrochemical studies of dissolved CuL complexes in seawater, sometimes two ligand classes are identified (a stronger L₁ class, and a weaker L₂ class) (e.g. Coale and Bruland 1989). The distinction between strong and weak Cu ligands is operationally defined, whereby L₁

ligands have a higher $K_{CuL,Cu^{2+}}^{cond}$ than L₂ ligands (e.g. $\log K_{CuL,Cu^{2+}}^{cond} \geq 13.5$ for L₁, and ≤ 13.5 for L₂; Bundy et al. 2013). Unfortunately, variations in analytical procedures used by different laboratories to measure the strength of Cu binding ligands makes it difficult to compare ligand strengths between studies (Bruland et al. 2000). Furthermore, the identification of strong and weak ligand classes may be due to the application of simplistic data modeling, and there is likely a mixture of ligands with varying strengths, numbers of binding sites, and functional groups (c.f. Hudson et al. 2003). Inter-laboratory calibration of Cu speciation sampling and analysis has only recently been undertaken (Bruland et al. 2000; Buck et al. 2012). In surface waters, the strong ligand class is typically 2 to 3-fold in excess of the total dissolved Cu concentration. As a result, the concentration of Cu' ranges between 10^{-10} and $10^{-14.5}$ mol L⁻¹ (van den Berg 1984; Sunda and Hanson 1987; Coale and Bruland 1988; 1990; Moffett 1995; Moffett and Dupont 2007; Buck et al. 2010; Bundy et al. 2013).

There is strong evidence supporting a biological source for the weak and strong Cu-complexing ligands in seawater. During Cu toxicity, laboratory strains of eukaryotic marine phytoplankton produce weak ligands, while marine prokaryotes produce stronger ligands (Moffett and Brand 1996; Croot et al. 2000; Gordon et al. 2000; Wiramanaden et al. 2008). The $K_{CuL,Cu^{2+}}^{cond}$ of the stronger ligands produced by marine cyanobacteria ($>10^{13}$) is similar to the $K_{CuL,Cu^{2+}}^{cond}$ of strong ligands found in seawater (Moffett and Brand 1996). Since cyanobacteria are more sensitive to high Cu concentrations (Brand et al. 1986), the strong Cu-binding ligands have been hypothesized to detoxify Cu by complexing it outside the cell and thereby make it less bioavailable. However, the bioavailability of *in situ* Cu ligand complexes to marine

phytoplankton has received limited attention (Semeniuk et al. 2009), and warrants further investigation.

The oxidation state of organically complexed Cu has been implicitly assumed to be Cu(II). However, it is possible that a portion of dissolved Cu in seawater could be Cu(I). Due to the soft Lewis acid nature of Cu(I), thiol-containing ligands (e.g. cysteine, glutathione) may complex and stabilize Cu(I) (Leal and van den Berg 1998; Dupont et al. 2006; Walsh and Ahner 2013). Few measurements of dissolved thiols have been made in seawater, but they tend to be similar to total dissolved Cu concentrations (0.1 to 10 nM; Tang et al. 2004; Dupont et al. 2006). Thiols in seawater may also be able to reduce Cu(II) and subsequently complex Cu(I) (Leal and van den Berg 1998). There is also evidence that the strong ligands produced by prokaryotes may complex Cu(I) (Wiramanaden et al. 2008). Given the likelihood of Cu(II) reduction in surface waters, the ability of thiols to stabilize Cu(I), and the concentration of dissolved thiols in seawater, Cu(I)-thiol complexes may make up a portion of the total dissolved Cu pool in marine environments.

1.2.4 Copper Bioavailability and Transporter Substrates

Early laboratory investigations attempted to determine the substrate for Cu transporters in marine phytoplankton by using high concentrations of synthetic ligands (e.g. ethylenediaminetetraacetic acid; EDTA) to complex Cu, effectively buffering the concentration of inorganic Cu(II) in the assay (Sunda and Guillard 1976; Jackson and Morgan 1978; Sunda and Lewis 1978; Sunda and Huntsman 1995b). Steady-state Cu transport rates appeared to co-vary with the inorganic Cu(II) concentrations in the growth medium, and not total dissolved Cu, indicating that inorganic Cu(II)

was the most likely substrate for transport (Sunda and Huntsman 1995b). Like Fe and Zn, recent uptake studies have demonstrated that organically complexed Cu may be bioavailable. This evidence rests largely on comparisons between measured cellular uptake rates and the calculated maximum rates of the diffusion of Cu' to the cell surface (J_D) across the diffusive boundary layer (DBL) surrounding the cell. The diffusive flux of Cu' can be determined using a derivation of Fick's Law for a spherical surface (Wolf-Gladrow and Riebesell 1997):

$$J_D = 4\pi r D_{Cu^{n+}} ([Cu']_{Bulk} - [Cu']_{Cell}) \quad (10)$$

In equation (10), r is the cell radius (cm), $D_{Cu^{n+}}$ is the diffusion coefficient for Cu^{n+} in seawater ($cm^2 h^{-1}$), and $[Cu']_{Bulk}$ and $[Cu']_{Cell}$ are the inorganic Cu concentrations the bulk seawater and at the cell surface, respectively ($mol cm^{-3}$). In order to calculate the maximum diffusive rate, $[Cu']_{Cell}$ is assumed to be zero as diffusion of Cu across the DBL becomes the rate limiting step for transport. Thus, equation (10) simplifies to:

$$J_D = 4\pi r D_{Cu^{n+}} [Cu']_{Bulk} \quad (11)$$

If cellular uptake rates exceed J_D , then Cu' cannot be the only substrate for Cu transport. Uptake rates can exceed J_D by 2 to 610 times in 18 phytoplankton species from five phyla (Figure 1.3). This suggests that the acquisition of organically bound Cu may be a common trait among diverse marine phytoplankton species. However, the mechanism by which organically complexed Cu is acquired by marine phytoplankton remains unknown.

In *Saccharomyces cerevisiae*, the freshwater green alga *Chlamydomonas reinhardtii*, and in most eukaryotes, Cu uptake by a high-affinity Cu transport system (HACuTS) requires an extracellular reduction step prior to the internalization of Cu(I) (Hill et al. 1996; Van Ho et al 2002; Pope et al. 2012; Merchant et al. 2013). In *S. cerevisiae*, the iron reductase encoded by FRE1 gene can also reduce Cu(II) (Hassett and Kosman 1995; Georgatsou et al. 1997). In marine phytoplankton, Fe(III) reduction has also been observed (Jones et al. 1987; Maldonado and Price 2001; Shaked et al. 2005). Two putative FRE genes (FRE1 and FRE2) have been identified in the genome of the centric marine diatom *Thalassiosira pseudonana*, but only the expression of FRE2 is controlled by Cu availability (Kustka et al. 2007; Guo et al. *submitted*). Inorganic Cu(II) can be reduced by marine phytoplankton (Jones et al. 1987), suggesting that the putative FRE2 reductase may also be a Cu(II) reductase. The marine diatoms *T. pseudonana* and *T. oceanica* possess a high-affinity Cu transport system (HACuTS) that is likely capable of acquiring Cu(II) bound to EDTA (Guo et al. 2010). Thus, Cu(II) within organic ligands may be acquired by marine phytoplankton via reduction by FRE2.

In many eukaryotes, Cu(I) is transported intracellularly by members of the CTR gene family, a Cu(I)-specific HACuTS (reviewed by Pope et al. 2012). Amino acid sequences among CTR proteins are variable, but a sulfur-containing Cu(I) binding motif is highly conserved among eukaryotes (Rubino et al. 2010). Two putative CTR genes were identified in *T. pseudonana*, and their expression respond to changes in Cu availability (Guo et al. *submitted*). If the putative FRE2 gene in *T. pseudonana* encodes a Cu(II) reductase, then Cu(I) produced by FRE2 may be taken up by the putative CTR transporters. Preliminary evidence suggests that organically complexed Cu(I) may be acquired by an indigenous phytoplankton community (Semeniuk et al.

2009). Since Cu(I) may be prevalent in seawater, it may be an important substrate for Cu acquisition by natural marine phytoplankton populations.

1.2.5 Copper Nutritional Status of Natural Marine Phytoplankton Populations

While numerous laboratory studies have investigated the effect of Cu on phytoplankton growth, few studies have examined the Cu nutritional status of natural phytoplankton populations. Early work in the equatorial Pacific demonstrated that carbon-fixation rates increased with the addition of the synthetic metal chelator EDTA to recently upwelled surface waters (Barber and Ryther, 1969; Barber 1973). This response could have been due to the chelation of toxic concentrations of Cu' from deeper waters. Early culture studies proposed that Cu' was the sole bioavailable form of Cu to marine phytoplankton monocultures grown under high Cu concentrations (Sunda and Guillard 1976; Jackson and Morgan 1978; Sunda and Lewis 1978), and provided tentative support for the detoxification of Cu' via extracellular chelation. Cyanobacterial isolates grown in culture produce strong Cu binding ligands when exposed to high Cu' concentrations (Moffett and Brand 1996), which suggests that cyanobacteria may often experience Cu toxicity in nature. Indeed, ambient Cu' concentrations may control the distribution and productivity of coastal cyanobacteria (Moffett et al. 1997; Croot 2003). Although dissolved Cu is lower in open ocean surface waters, recent work suggests that the distribution of open ocean cyanobacteria is also controlled by Cu availability. The speciation and concentration of Cu could partially control the distribution of high and low light *Prochlorococcus* ecotypes in the Sargasso Sea (Mann et al. 2002). Light-mediated degradation of strong Cu ligands in the surface water (Laglera and van den Berg 2006; Shank et al. 2006), and elevated Cu concentrations in anthropogenic atmospheric deposition (Kieber et al. 2004; Paytan et al. 2009; Jordi et al. 2012) could all lead to an increased

likelihood of Cu toxicity during short-term water column mixing and atmospheric deposition events in the open ocean.

While Cu-toxicity has been documented in a few field studies, there has been an increased interest recently in Cu as a limiting nutrient, particularly in Fe-limited waters. Some Fe-limited phytoplankton have higher cellular Cu quotas during Fe-limitation (see section 1.2.1). If Cu' is the sole substrate for natural phytoplankton assemblages, then recent Cu' concentration measurements in the Southern Ocean, Northwest Pacific Ocean, and Bering Sea ($10^{-12.5}$ to $10^{-14.5}$ M) are low enough to induce Cu-Fe co-limitation of Fe-limited diatoms (Peers et al. 2005; Maldonado et al. 2006; Moffett and Dupont 2007; Annett et al. 2008; Buck et al. 2010; Bundy et al. 2012; Guo et al. 2012; Jacquot et al. 2013). Bottle incubation studies in the Fe-limited regions of the northeast subarctic Pacific Ocean and Bering Sea observed a large increase in chl *a* concentrations with the addition of Fe, and a modest increase with the addition of 2 to 4 nM CuSO₄, suggesting that the *in situ* Fe-limited phytoplankton could have been co-limited by Cu (Coale 1991; Peers et al. 2005). However, micrograzers are sensitive to elevated Cu' concentrations (Stoecker et al. 1986), so neither study was able to distinguish between changes in grazing pressure and co-limitation. As such, it remains unclear whether HNLC waters are co-limited by Cu availability, or Fe-Cu co-limitation is a transient feature in HNLC waters.

1.3 Oceanography of the Northeast Subarctic Pacific Ocean

The northeast subarctic Pacific was the first verified Fe-limited HNLC region (Martin and Fitzwater 1988). The Line P transect is characterized by three biogeographical domains – a nitrate-limited coastal region, an Fe-limited open ocean region, and a transition zone between

them (Boyd and Harrison 1999) (Figure 1.4). Mixed layer dissolved Fe concentrations are highest at the coastal station P4 (~0.5 nM), then decrease at P12 (~0.2 nM), are lowest at P16 and P20 (< 0.05 nM), and increase slightly at P26 (< 0.1 nM) (Johnson et al. 2005). Given the metabolic dependence of Fe on Cu in some marine phytoplankton, the gradient of dissolved Fe along Line P provides a unique setting to study the effects of Fe limitation on Cu nutrition in marine phytoplankton communities.

1.3.1 Water Properties and Circulation

The dominant atmospheric circulation cell over the region is the cyclonic Aleutian low-pressure system, and this drives the east flowing North Pacific Current (NPC) towards the west coast of North America (Figure 1.4). The NPC bifurcates along the coast, moving southward as the California Current (CC), and northward as the Alaska Current (AC) (Thomson 1981; Whitney and Freeland 1999; Cummins and Freeland 2007). As the AC moves north, Ekman pumping causes downwelling to occur along the coast of BC during the winter (Hsieh 1996). In the spring, the Aleutian low subsides and is pushed northward by the North Pacific high (Cummins and Freeland 2007). This results in a shift of the bifurcation point of the AC and CC northward (Cummins and Freeland 2007), and the beginning of upwelling along Vancouver Island (Foreman et al. 2011).

The northeast subarctic Pacific Ocean has been most intensely studied by the Line P research program (Peña and Bograd 2007). The transect begins in shallow coastal waters (< 150 m depth) near the opening of the Juan de Fuca Strait, and traverses the bifurcation point of the AC and CC along the continental shelf (750-2500 m depth) into open ocean waters (> 2500 m depth).

Surface waters along Line P are characterized by a permanent halocline occurring near 150 m that determines the deepest mixing layer during the winter (Gargett 1991). In spring, winter mixing subsides and a thermocline begins to form that shoals into the early fall to depths <25 m.

1.3.2 Phytoplankton and Nutrient Dynamics along Line P

During the winter, light limits primary productivity near the coast (Whitney and Freeland 1999), while light and Fe limit productivity in the Fe-limited oceanic stations (Maldonado et al. 1999). In the spring, light is no longer limiting as a seasonal thermocline layer forms and shoals, and phytoplankton growth draws down mixed layer nitrate concentrations to below detection in the near coastal stations (P4 and P12) (Boyd and Harrison 1999; Peña and Varela 2007). As a result, biomass is variable at P4, and mixed layer chl *a* concentrations range from $0.55 \pm 0.08 \mu\text{g chl } a \text{ L}^{-1}$ in the winter, $1.31 \pm 0.37 \mu\text{g chl } a \text{ L}^{-1}$ in the spring, and $0.98 \pm 0.27 \mu\text{g chl } a \text{ L}^{-1}$ in the fall (Peña and Varela 2007). In contrast, mixed layer biomass is relatively constant year-round ($\sim 0.35 \mu\text{g chl } a \text{ L}^{-1}$) at the offshore and Fe-limited stations (P12, P16, P20 and P26), resulting in incomplete utilization of surface macronutrients (Peña and Varela 2007). For example, yearly average nitrate concentrations at P26 are drawn down from 14-16 μM in March to 8-10 μM by September (Whitney and Freeland 1999).

Small, photosynthetic flagellates tend to dominate the phytoplankton assemblage along Line P (Varela and Harrison 1999; Peña and Varela 2007). However, during the spring, diatoms can comprise up to 25% of the total chl *a* concentration at station P26 (Booth et al. 1993; Steiner et al. 2012). Dinoflagellates, prymnesiophytes, and cryptomonads make up > 70% of the total chl *a* at P26 year round (Steiner et al. 2012). Stochastic supplies of Fe to the HNLC stations can

cause small diatom blooms (e.g. Marchetti et al. 2006a). These events have been attributed to atmospheric deposition of volcanic ash (Hamme et al. 2010), lateral transport of coastal waters by anticyclonic eddies (Johnson et al. 2005), and isopycnal transport of Fe minerals from shelf waters (Lam et al. 2006). During natural Fe-enrichment events at the Fe-limited stations, chl *a* concentrations can exceed $1 \mu\text{g chl } a \text{ L}^{-1}$ (Hamme et al. 2010).

1.3.3 Copper Concentration and Speciation along Line P

Few measurements of total dissolved Cu concentrations ($[\text{Cu}]_d$) have been made in the northeast subarctic Pacific Ocean. Similar to other oceanic regions, dissolved Cu is high near the coast (1.86 to $5.25 \text{ nmol kg}^{-1}$) (Jones and Murray 1984). At station P26, $[\text{Cu}]_d$ in surface waters is lower ($\sim 1.5 \text{ nM}$) than at depth ($\sim 2.4 \text{ nM}$) (Martin et al. 1989). Copper speciation has not been measured in this region. However, in the NW Pacific and Bering Sea, copper is bound to strong organic ligands that are present in a 2 to 3-fold excess of $[\text{Cu}]_d$ and have $K_{\text{CuL},\text{Cu}^{2+}}^{\text{cond}}$ ranging between $10^{12.7}$ to $10^{14.1}$ (Moffett and Dupont 2007). The resulting pCu ranges between 13 and 14, and is similar to those that may begin to cause Cu limitation in some Fe-limited marine phytoplankton. Thus, Cu availability may influence phytoplankton rate processes in the Fe-limited region of Line P.

1.4 Thesis Organization

Despite growing interest in the speciation of Cu in seawater (e.g. Buck et al. 2012), there remain a number of fundamental questions concerning its bioavailability to marine phytoplankton and its role in mediating biological rate processes in marine ecosystems. Although a few studies have investigated the effect of dissolved Cu amendments on natural phytoplankton communities, the

influence of *in situ* Cu bioavailability on rate processes (e.g. carbon fixation, Fe and Cu uptake rates) in open ocean phytoplankton communities remains unknown. Since Cu availability can co-limit Fe-limited phytoplankton in laboratory cultures (Peers et al. 2005; Annett et al. 2008; Guo et al. 2012), it is possible that *in situ* Cu bioavailability may influence the growth of Fe-limited phytoplankton communities along Line P.

The bioavailability of Cu to marine phytoplankton is determined by its speciation in seawater. The presence of strong Cu binding ligands has previously been hypothesized to be the result of microbially mediated production of Cu(II) detoxifying ligands. However, whether *in situ* Cu binding ligands prevent Cu acquisition by marine phytoplankton has yet to be demonstrated. A preliminary investigation of short-term Cu uptake by a natural phytoplankton community at P26 revealed that organically complexed Cu might be bioavailable (Semeniuk et al. 2009). However, a detailed study of the bioavailability of Cu within *in situ* ligands, as well as Cu within different well-defined ligands, has not been completed. These data will aid in our understanding of how speciation may influence Cu bioavailability – and thus Cu nutrition – in open ocean phytoplankton communities.

Although laboratory studies have demonstrated that organically complexed Cu may be bioavailable, a mechanism for acquiring Cu from strong organic complexes has not been elucidated. Furthermore, nearly all Cu uptake rate measurements performed thus far used Cu and ligand concentrations that are between 10 and 10,000 times higher than those found in open ocean surface waters (Sunda and Huntsman 1995b; Croot et al. 2003; Annett et al. 2008; Guo et al. 2010; 2012). Ligands used in culture studies have binding constants that are up to 10^6 times

lower than *in situ* ligands (e.g. $K_{CuEDTA,Cu^{2+}}^{cond} = 10^{10.6}$; Coale and Bruland 1988). Therefore, the results of earlier Cu uptake studies may not accurately represent *in situ* Cu speciation or Cu bioavailability.

This thesis attempts to address these uncertainties by using the short-lived gamma-emitting radioisotopes ^{64}Cu (half-life = 12.7 h) and ^{67}Cu (half-life = 61.8 h) in a combination of laboratory and field studies, respectively. The ^{67}Cu isotope used in the field studies is the by-product of medical ^{67}Ga production, and has a very high specific activity (>1000 GBq mol $^{-1}$). Therefore, a small amount of radioisotope can be added to natural seawater without changing the ambient Cu concentration by more than 1 to 2%. Thus, the ^{67}Cu additions made in this thesis were effectively “carrier free”, allowing measurements of *in situ* rate process (e.g. uptake rates) that, until now, had not been quantified for any trace metal in seawater. The thesis consists of four data chapters:

Chapter 2: Acquisition of organically complexed copper by marine phytoplankton and bacteria in the northeast subarctic Pacific Ocean

In this chapter, I used ^{67}Cu to measure short-term and long-term accumulation of Cu from *in situ* ligands and three Cu(II)-chelates in order to determine the bioavailability of potential Cu-ligand complexes present in seawater. I also determined the role that weak ligands may play in the bioavailability of *in situ* dissolved Cu. Uptake rates were significantly faster for the *in situ* ligands than the Cu(II)-ligand treatments, and the addition of weak ligands enhanced Cu uptake from the *in situ* ligands. Estimates of the

maximum flux of Cu' to the phytoplankton population indicate that Cu bound to strong *in situ* organic ligands was bioavailable. Particulate Cu concentrations reached a plateau over time, and decreased in a number of treatments, indicating that either Cu efflux by plankton or particulate Cu remineralization by micrograzers was occurring.

Chapter 3: Acquisition of organically complexed Cu(II) by a high-affinity Cu transport system in marine phytoplankton

Using ⁶⁴Cu, I investigated the substrate of the high-affinity Cu transport system in two model diatom species, and two prymnesiophytes previously isolated along Line P. In order to compare the laboratory uptake rates with those measured at P26, uptake experiments were performed with a strong Cu(II) ligand complex present in concentrations similar to open ocean surface waters. All four species were able to acquire Cu from the complex. Cellular uptake rates were on par with those measured in chapter 2, and support the conclusion that Cu within the *in situ* ligands was bioavailable. The uptake mechanism of the HACuTS in *Thalassiosira pseudonana* was investigated using competitive uptake inhibitors, and confirmed the involvement of a reductase and Cu(I) permease. My results also demonstrate that the addition of excess Cu(II)-specific ligands appears to slow Cu uptake via competition for Cu between the ligands and the HACuTS components, and not by lowering Cu'. Previous laboratory growth rate studies of Cu limitation and toxicity used high ligand concentrations, and so competition between the ligands and transporters for Cu would result in artificially lower Cu uptake rates, as well as lower intracellular Cu concentrations. Thus, the concentrations of Cu

that have previously been reported in laboratory studies to cause Cu limitation or toxicity are likely overestimates. These results imply that previous laboratory culture studies of Cu limitation and toxicity likely do not reflect *in situ* processes, and underscore the importance of mimicking *in situ* Cu speciation in future laboratory studies.

Chapter 4: Iron-copper interactions in HNLC phytoplankton in the northeast subarctic Pacific Ocean

Incubations were performed at two Fe-limited stations along Line P (stations P20 and P26) to investigate how Fe-limited phytoplankton respond to increases in Cu availability. At P20, dissolved Cu concentrations and speciation were manipulated, while at station P26, light availability and Cu concentrations were changed. The community at P20 and the Fe-light limited community at P26 were not affected by Cu additions. However, in the high light treatment Fe uptake rates by the >5 μm phytoplankton and the maximum variable fluorescence (F_v/F_m) – both proxies for Fe-limitation – increased with a 1 nM Cu amendment, suggesting that there was an interaction between Fe and Cu physiology in large phytoplankton.

Chapter 5: The effects of copper speciation on phytoplankton and bacteria rate processes in the northeast subarctic Pacific Ocean

In my last chapter, I surveyed Cu uptake rates and Cu:C assimilation ratios in surface waters along the Line P transect using ^{67}Cu . In addition, various rate measurements (e.g.

primary productivity), biomass indicators (e.g. chlorophyll *a*, cyanobacteria and heterotrophic bacterial abundance), macronutrient availability, and Cu speciation were measured concomitantly in order to determine which environmental variables might control phytoplankton Cu:C assimilation ratios. Along the transect, Cu uptake rates and Cu:C assimilation ratios were not related to any measured phytoplankton parameters, and likely reflect different phytoplankton species compositions. Primary productivity was negatively correlated with Cu' concentrations, and positively correlated with $K_{CuL,Cu^{2+}}^{cond}$. This indicates that Cu speciation along Line P may influence rate processes in marine phytoplankton. An incubation performed at station P16 demonstrated that small additions (5 and 30 nM) of a strong Cu(II)-chelator caused Cu uptake to decrease, and cyanobacteria abundance and primary productivity to increase. These results suggest that some members of the phytoplankton community sampled at P16 may have been experiencing Cu toxicity.

1.5 Figures

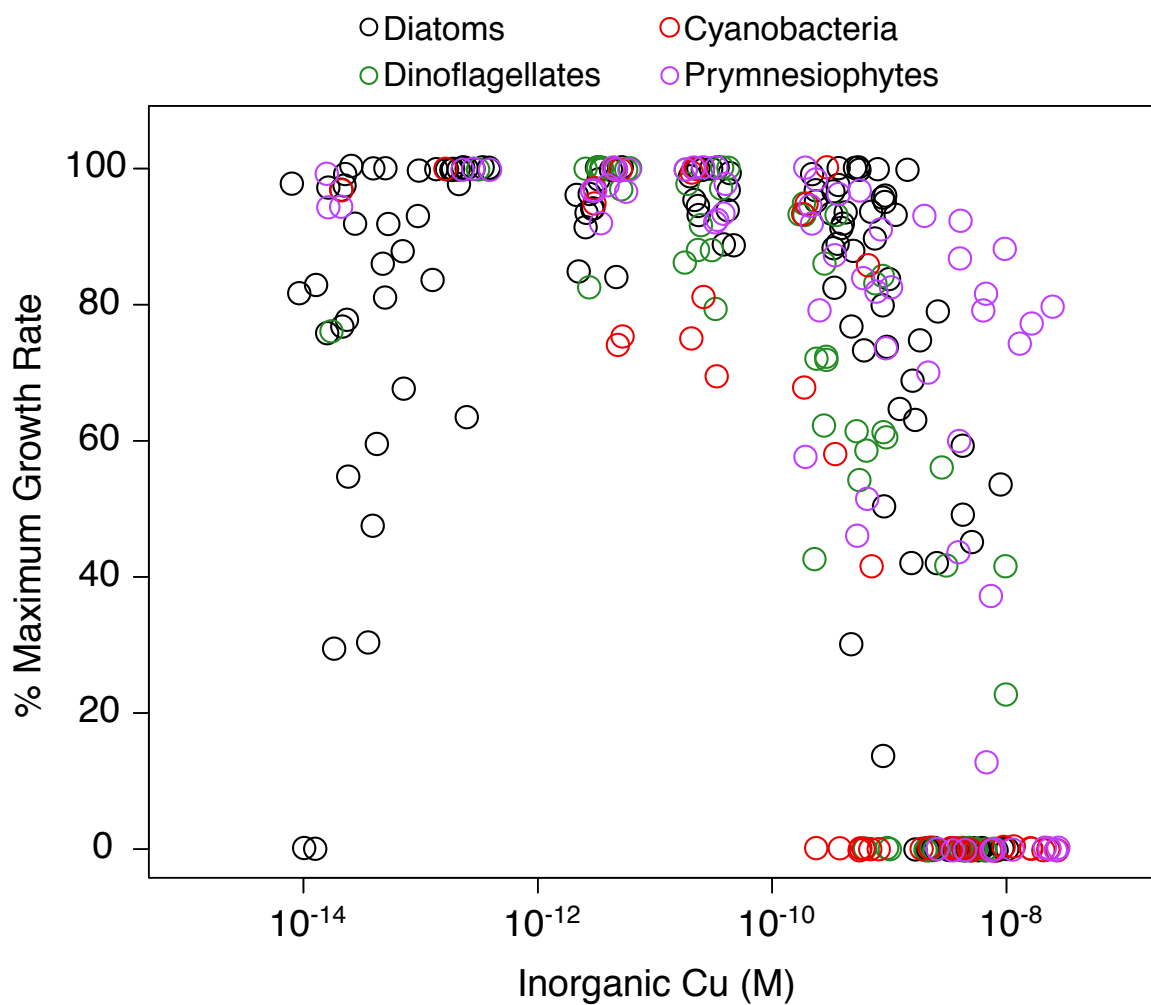


Figure 1.1. Literature review of phytoplankton growth rates of exponentially growing species in varying inorganic Cu (Cu') concentrations. Rates are expressed as a percent of the maximum growth rate reported (Brand et al. 1986; Croot et al. 2003; Peers et al. 2005; Annett et al. 2008; Guo et al. 2012).

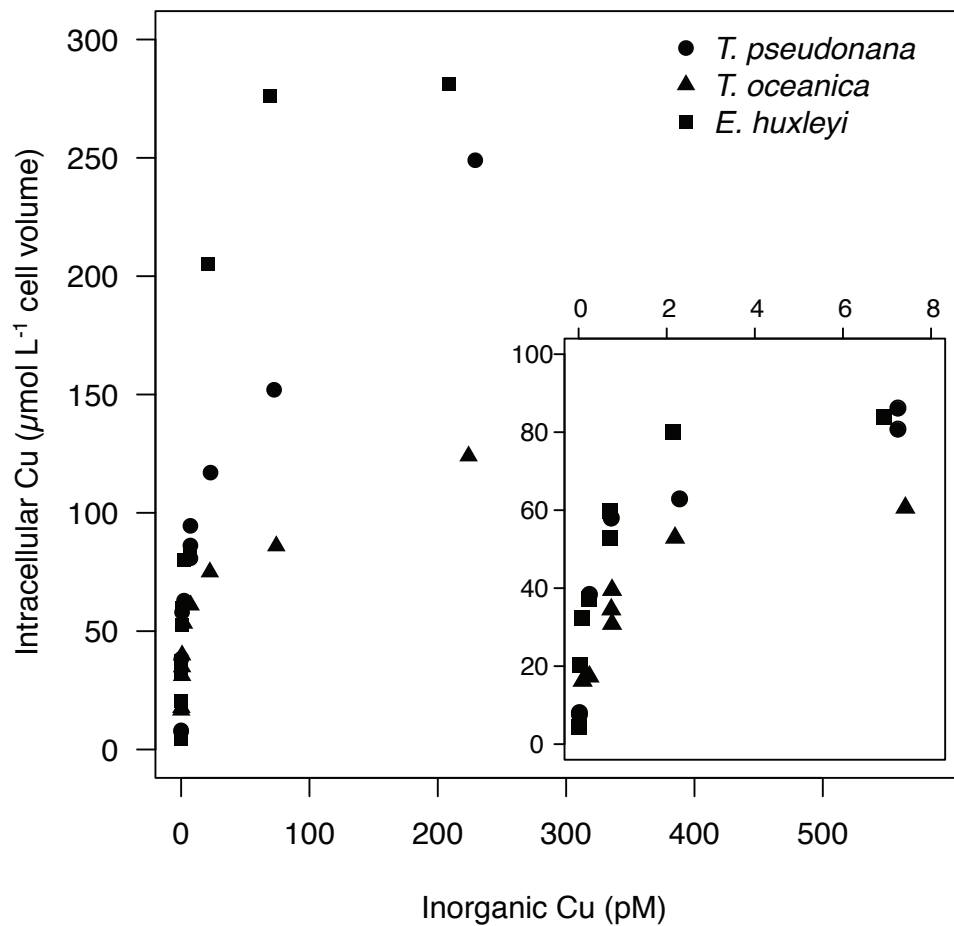


Figure 1.2. Steady-state intracellular Cu concentrations ($\mu\text{mol Cu L}^{-1}$ cell volume) of *Thalassiosira pseudonana*, *T. oceanica*, and *Emiliana huxleyi* grown in different inorganic Cu (Cu') concentrations (pM) (adapted from Sunda and Huntsman 1995b). The inset focuses on intracellular Cu concentrations measured in media containing less than 8 pM Cu' .

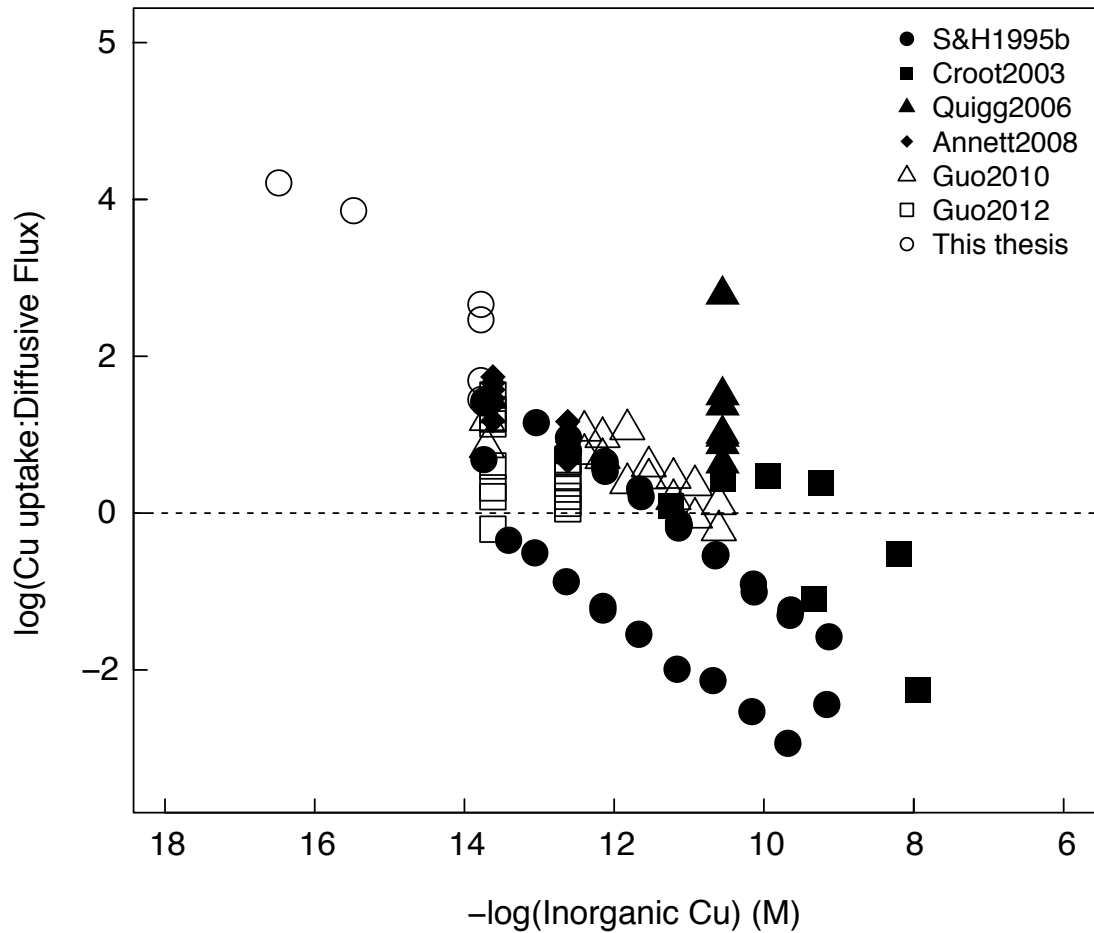


Figure 1.3. Literature review of short-term and steady-state cellular uptake rates performed with laboratory monocultures, and calculated maximum diffusive fluxes ($\text{mol Cu cell}^{-1} \text{h}^{-1}$) expressed as a log of the ratio with respect to the inorganic Cu concentration in the medium. The maximum diffusive flux was calculated using equation (11). All rates and fluxes are reported in Table A.1. Legend references are S&H1995b (Sunda and Huntsman 1995b), Croot2003 (Croot et al. 2003), Quigg2006 (Quigg et al. 2006), Annett2008 (Annett et al. 2008), Guo2010 (Guo et al. 2010), Guo2012 (Guo et al. 2012), This thesis (Chapter 3).

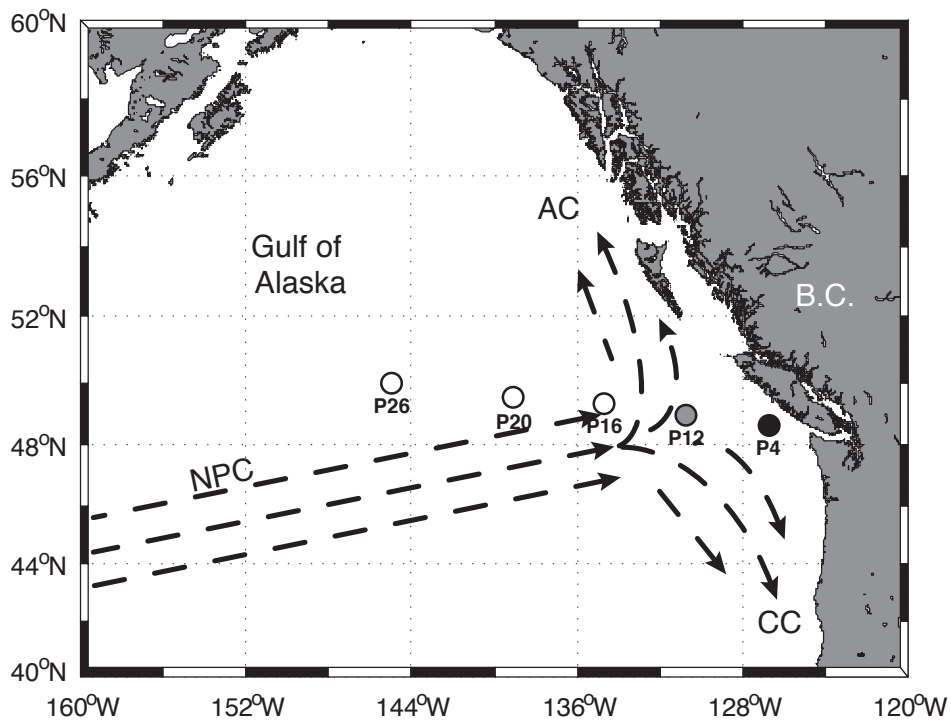


Figure 1.4. General locations of major surface currents and stations of the Line P transect in the northeast subarctic Pacific Ocean (NPC = North Pacific Current, AG = Alaska Current, CC = California Current). Station symbol shades indicate the prevalence of Fe limitation; black represents no Fe-limitation, grey represents intermittent or seasonal Fe-limitation, and white represents year-round Fe-limitation.

Chapter 2: Acquisition of Organically Complexed Copper by Marine Phytoplankton and Bacteria in the NE Subarctic Pacific Ocean

Copper (Cu) is an essential micronutrient for marine phytoplankton, but can cause toxicity at elevated intracellular concentrations. The majority of Cu (>99.9%) in oceanic surface waters is bound to strong organic ligands, presumably produced by prokaryotes to detoxify Cu. Although laboratory studies have demonstrated that organically complexed Cu may be bioavailable to marine eukaryotic phytoplankton, the bioavailability of Cu organic complexes to indigenous marine phytoplankton has not been examined in detail. Using the carrier free radioisotope ^{67}Cu at an iron limited station in the northeast subarctic Pacific Ocean, we performed size fractionated short-term Cu uptake assays with three Cu(II)-chelates, and ^{67}Cu bound to the strong *in situ* ligands, with or without additions of weak Cu(I) ligands. Estimates of the maximum supply of inorganic Cu (Cu') to the cell surface of eukaryotic phytoplankton were unable to account for the observed Cu uptake rates from the *in situ* ligands and two of the three added Cu(II)-chelates. Addition of 10 nM weak organic Cu(I) ligands enhanced uptake of Cu bound to the *in situ* ligands. Thus, Cu within the *in situ* and strong artificial Cu(II) organic ligands was accessible to the phytoplankton community via various possible Cu uptake strategies, including: cell surface enzymatically mediated reduction extracellular reduction of Cu(II) to Cu(I), the substrate of the high-affinity Cu transport system in eukaryotes; or ligand exchange between weak Cu-binding ligands and the cellular Cu transporters. During a 14-hour uptake assay, particulate Cu concentrations reached a plateau in most treatments. Losses were observed in some treatments, especially in the small size fractions (< 5 μm), corresponding with

faster initial Cu uptake rates. This may indicate that Cu cycling is rapid between particulate and dissolved phases due to cellular efflux or remineralization by micrograzers. The acquisition of Cu from the strong *in situ* ligands puts into question the historic role attributed to Cu binding ligands of reducing Cu bioavailability.

2.1 Introduction

Copper (Cu) is a metabolically essential micronutrient for marine phytoplankton, and is involved in a number of important electron transfer reactions, including iron (Fe) uptake via the high-affinity Fe transport system (Peers et al. 2005; Wells 2005; Maldonado et al. 2006), electron transfer between photosystem II and photosystem I via plastocyanin (Peers and Price 2006), extracellular amine oxidation (Palenik and Morel 1991), quenching of reactive oxygen species via superoxide dismutase (Raven et al. 1999), and respiration via cytochrome *c* oxidase. Indeed, intracellular Cu requirements are on par with those of other essential micronutrients like Fe and zinc (Sunda and Huntsman 1992; Maldonado and Price 1996), and limitation of growth rates by Cu has been observed in 4 of 18 laboratory phytoplankton strains examined thus far (Annett et al. 2008; Guo et al. 2012). However, Cu is also toxic to marine phytoplankton at nanomolar concentrations (Brand et al. 1986), and growth rates decrease as intracellular Cu increases (Sunda and Guillard 1976). Some phytoplankton groups are more susceptible to Cu toxicity (e.g. cyanobacteria; Brand et al. 1986) and Cu limitation (e.g. oceanic diatoms; Peers et al. 2005), and so elucidating the bioavailability of *in situ* Cu to marine phytoplankton communities would provide a first order approximation of the Cu nutritional status of natural phytoplankton populations.

Total dissolved Cu concentrations ($[\text{Cu}]_d$) in open ocean surface waters vary between 0.5 to 3 nM (Coale and Bruland 1988; Moffett and Dupont 2007; Bundy et al. 2013; Jacquot et al. 2013), and the speciation of Cu is dominated by strong organic complexes that comprise >99% of total dissolved Cu (van den Berg 1984). A strong ligand class has been identified with conditional stability constants ($\log K_{\text{CuL.Cu}^{2+}}^{\text{cond}}$) ranging $10^{11.5}$ to 10^{16} , that is present in concentrations ranging from 1 to 10 nM (van den Berg 1984; Coale and Bruland 1988; Moffett et al. 2007; Buck et al. 2010; Bundy et al. 2013; Jacquot et al. 2013). The resulting calculated “free” cupric ion concentrations are between $10^{-13.5}$ and $10^{-16.3}$ M in surface waters, and are within the range that can cause Cu-limitation in diatoms and prymnesiophytes (10^{-15} M; Peers et al. 2005; Annett et al. 2008; Guo et al. 2012). There is evidence that the strongest ligands found in seawater are produced by cyanobacteria and heterotrophic bacteria to alleviate Cu toxicity by complexing Cu extracellularly (Moffett et al. 1996; Gordon et al. 2000), while eukaryotes produce weaker ligands (Croot et al. 2000). Indeed, in the absence of strong organic chelators, Cu concentrations in surface waters (0.5 to 3 nM) would cause growth rates to decrease in many marine phytoplankton groups (Brand et al. 1986). Although the structures of the strong *in situ* Cu binding ligands remain unknown, the ligands may contain thiol and amine functional groups (Ross et al. 2003), and could be phytochelatin, phytochelatin precursors (e.g. glutathione and cysteine), humic and fulvic acids, or other low molecular weight compounds (Leal and van den Berg 1998; Laglera and van den Berg 2003; Tang et al. 2004; Dupont et al. 2006; Dryden et al. 2007; Yang and van den Berg 2009).

To date, the substrate for Cu transport by *in situ* marine phytoplankton communities has yet to be fully elucidated. Early laboratory studies suggested that inorganic Cu (Cu') was the sole substrate

for Cu transport in isolated marine phytoplankton strains (Sunda and Guillard 1976). Various studies supported the hypothesis that prokaryotes produce strong ligands to detoxify Cu via extracellular complexation, thereby lowering the [Cu'] in the growth media and decreasing the potential for Cu toxicity (Moffett and Brand 1996; Gordon et al. 2000). However, subsequent work has demonstrated that organically complexed Cu appears to be bioavailable to many marine phytoplankton phyla. Copper uptake rates by phytoplankton can exceed the diffusive supply of inorganic Cu to the cell surface by 2 to 1000-fold when Cu is complexed by the artificial chelators ethylenediamine tetraacetic acid (EDTA) (Hudson 1998; Quigg et al. 2006; Annett et al. 2008; Guo et al. 2010; Guo et al. 2012) or nitrilotriacetic acid (NTA) (Croot et al. 2003). A preliminary study in the subarctic Northeast Pacific Ocean demonstrated that Cu was acquired ~5 times faster from strong *in situ* ligands than from a strong artificial Cu(II) ligand of comparable strength (Semeniuk et al. 2009). Thus, the bioavailability of strongly complexed *in situ* Cu does not appear to be mediated solely by Cu' availability.

Although the mechanism allowing eukaryotic marine phytoplankton to acquire Cu from within strong ligands has not been described, the mechanisms of Cu transport have been elucidated for other eukaryotes. In *Saccharomyces cerevisiae*, *Chlamydomonas reinhardtii*, and most eukaryotes, Cu(II) is reduced to Cu(I) by a FRE-encoded surface reductase, and the Cu(I) produced is subsequently internalized by the CTR-encoded high-affinity Cu transport system (reviewed by Pope et al. 2012). The FRE reductases in diatoms are capable of reducing strongly complexed Fe(III) (Maldonado and Price 2001; Shaked et al. 2005; Kustka et al. 2007), and so strongly complexed Cu(II) may also be reduced by these reductases prior to internalization.

Weak ligands may also play an important role in metal acquisition. A ligand shuttle mechanism has recently been described for Zn uptake in marine diatoms (Aristilde et al. 2012).

Complexation of Zn' by weak ligands draws down the concentration of Zn', and pushes the equilibrium of strongly bound Zn towards dissociation. Thus, the total concentration of Zn' remains relatively constant while weakly complexed Zn species increase in concentration. Both inorganic and weak organic complexes of Zn and Fe appear to be bioavailable (Maldonado et al. 2002; Hassler et al. 2011; Aristilde et al. 2012), so weak Cu binding ligands may similarly facilitate transport in marine phytoplankton.

Given the uncertain role of organic complexation in determining the bioavailability of Cu to marine phytoplankton, and the potential for Cu limitation and toxicity in surface waters, the aim of the present study was to expand on our preliminary work examining the substrates for Cu transport in phytoplankton and bacteria at an Fe-limited station in the northeast subarctic Pacific Ocean (Semeniuk et al. 2009). We monitored Cu uptake from three Cu(II)-ligand complexes and Cu bound to the *in situ* strong ligands using the carrier free gamma emitting radionuclide ⁶⁷Cu. We also investigated how additions of weaker ligands influenced *in situ* Cu bioavailability.

2.2 Materials and Methods

2.2.1 Sampling and Incubation

Seawater was sampled from Station P26 (50°N 145°W) during the September 2008 Line P Cruise (2008-26) aboard the C.C.G.S. J.P. Tully. Station P26 is a perennially Fe-limited station along the Line P transect. Approximately 3 h before sunrise on June 10, 2008, seawater was pumped from the mixed layer (10 m depth) into trace metal clean 2 L polycarbonate bottles (Nalgene)

using a trace metal clean pumping system and class 100 laminar flow hood (Johnson et al. 2005; Semeniuk et al 2009). To remove large grazers, the water was filtered through a 250 μm trace metal cleaned nylon mesh. The average light intensity was calculated for the mixed layer (56 m), and this corresponded to 14% of the surface irradiance (I_0). Thus, the bottles were immediately placed into an on-deck Plexiglas shipboard incubator, and the light intensity (10% I_0) and temperature were maintained using neutral density screening and continuously pumped seawater from 5 m depth.

2.2.2 Determination of Initial Chemical and Biological Parameters

Size-fractionated chlorophyll *a* concentrations ([chl *a*]) were sampled by filtering 500 mL onto stacked 20, 5, 1 and 0.22 μm polycarbonate filters (AMD) separated by nylon drain disks (Millipore) (Semeniuk et al. 2009). Filters were archived at -20°C until analysis in the lab. The chl *a* was extracted in 90% acetone at 4°C overnight, and [chl *a*] was determined using a Turner Designs Model 10 fluorometer (Parsons et al. 1984). Nutrients (nitrate, phosphate, and silicic acid) were analyzed on board using freshly collected samples (Barwell-Clarke and Whitney 1996). A sample for total dissolved Cu (0.22 μm Opticap® cartridge filter) was collected in trace metal clean low-density polyethylene bottles using a Teflon pump and laminar flow hood as previously described (Johnson et al. 2005). The sample bottles were rinsed three times before being filled and acidified to pH 1.7 using ultraclean HCl (Seastar) in a Class 100 laminar flow hood. Total dissolved Cu was measured after UV-oxidation by adsorptive cathodic stripping voltammetry (ACSV) with salicylaldoxime (SA) (Buck and Bruland 2005).

2.2.3 Determination of Conditional Stability Constants for Cyclam and Cyclen

Ten milliliter subsamples of open ocean surface seawater were UV-irradiated for 8 h and chelexed prior to being aliquoted into acid cleaned Teflon cups. Cyclam or cyclen (10 nM) was then added to each cup, followed by boric acid buffer (pH 8.2), and CuSO₄ additions ranging from 0-100 nM. Subsamples were allowed to equilibrate for 2 h before adding 25 μM SA. After equilibrating for 15 minutes with SA, samples were then analyzed by competitive ligand-exchange adsorptive cathodic stripping voltammetry (CLE-ACSV) according to Bundy et al. (2013). The total dissolved copper concentration in the chelexed, UV-irradiated seawater (0.1 nM) was determined via ACSV with SA (Buck and Bruland 2005)

2.2.4 Preparation of the Copper-Ligand Complex Additions for Copper Uptake Assay

Using the carrier free radioisotope ⁶⁷Cu (courtesy of TRIUMF), we measured the time-course accumulation of Cu by microorganisms at Station P26. Three strong Cu(II)-ligands and three weak Cu(I)-ligands were chosen with differing Cu-binding functional groups and conditional stability constants (Table 1). Ligand solutions were prepared as described elsewhere (Wiramanaden 2006; Semeniuk et al. 2009). Briefly, Cyclam and Cyclen powders were dissolved in a few drops of HPLC grade methanol, and subsequently diluted to 12.5 mM in ultrapure water (Millipore). Ethylenediamine tetraacetic acid disodium salt (EDTA; Sigma), reduced glutathione (GSH; Sigma), cysteine (Sigma), and bathocuproinedisulfonic acid disodium salt hydrate (BCDS; Sigma) were dissolved in water immediately prior to complexation to Cu to ensure oxidation of the sulfhydryl groups by O₂ did not occur.

All of the uptake treatments were performed in duplicate, and the average and range of the

replicate data are reported. Once the ^{67}Cu -ligand complex additions were prepared, the bottles were removed from the incubator and the additions were made just after sunrise (06:31 local time). The bottles were then closed, the caps were sealed with parafilm, and the bottles were immediately returned to the incubator.

2.2.4.1 *In Situ* Cu Ligands

Copper uptake was monitored with ^{67}Cu bound to the *in situ* ligands in the light and dark (dark bottles were covered in multiple layers of electrical tape). A spike of ^{67}Cu was added to 10 mL of 0.22 μm filtered seawater (0.22 μm Opticap[®] cartridge filter) collected at station. We did not measure the background [Cu] in the stock provided for this cruise. However, using a Quadrupole ICP-MS, we regularly measure [Cu] in the ^{67}Cu shipments received by our laboratory, and it does not exceed 50 nM. During pre-complexation, we added approximately 200 μL of the ^{67}Cu stock to 10 mL of filtered seawater, diluting the 50 nM ^{67}Cu stock to 1 nM. The total dissolved Cu concentration measured at station was 2.1 nM (see section 3.1), and so the dilution of the 10 mL solution of 1 nM ^{67}Cu into the 2 L assay seawater resulted in a final ^{67}Cu concentration of 5 pM (0.2% of the total dissolved Cu concentration). Strong Cu-binding ligands are 3-4 times in excess of the total dissolved Cu concentrations in surface waters along the Line P transect (R. Bundy, unpub. data), and so the 5 pM ^{67}Cu addition would have been completely bound to the resulting 6 to 8 nM excess strong ligands. The ^{67}Cu spike was allowed to equilibrate with the *in situ* ligands for 2 hours before being added to the 2 L uptake assay seawater. A 2 hour equilibration time was chosen as it is commonly employed in Cu speciation measurements (Moffett and Dupont 2007; Buck et al. 2010; Bundy et al. 2013). The strong Cu binding ligands in seawater bind Cu rapidly (<10 min; Coale and Bruland 1988; Campos and van den Berg

1994), and so the added ^{67}Cu tracer would have been strongly complexed by the excess strong Cu ligand pool. Thus, we must assume that the uncomplexed strong ligands and complexed strong ligands are chemically similar. This is prudent, as cyanobacteria produce strong ligands that are 1.5 to 2-fold in excess of the total dissolved Cu to buffer toxic Cu concentrations (Moffett and Brand 1996).

2.2.4.2 Cu(II)-Ligand Complexes (1:10 nM)

To prepare the Cu(II)-ligand complexes (Cyclam, Cyclen, EDTA), a solution of $^{67}\text{Cu(II)}$ and unlabeled Cu(II) was added to each Cu(II) ligand solution (1:10 molar ratio) and allowed to equilibrate for at least two hours at $\text{pH} > 4$. The resulting $^{67}\text{Cu(II)}$ -ligand solutions were then equilibrated in filtered seawater for 2 h. Additions of the equilibrated $^{67}\text{Cu(II)}$ -ligand solutions were made to each 2 L assay bottle at a final ^{67}Cu concentration of 1 nM.

We assumed that the ^{67}Cu bound to the Cu(II)-ligands did not appreciably exchange with the *in situ* ligands. For the stronger ligand complexes, this is likely a good first order assumption. Given the inorganic Cu concentration in the EDTA treatment was the highest for all the treatments ($10^{-10.17}$ M; Table 2.1), a portion of the ^{67}Cu tracer may have been complexed by the *in situ* strong ligands. However, the observed uptake rates in the EDTA treatment were much slower than the *in situ* ligand treatment (see section 3.2), so it is unlikely that an appreciable amount of ^{67}Cu in the EDTA complex exchanged with the *in situ* ligands.

2.2.4.3 Weak Cu(I)-Ligand Complexes (1:10 nM)

The weak ligands used in this study (GSH, Cysteine, BCDS) bind Cu(I), and so a solution of

$^{67}\text{Cu}(\text{II})$ and unlabeled $\text{Cu}(\text{II})$ was reduced with 0.22 μm filtered SO_2 gas. Although this protocol was developed for reducing $\text{Fe}(\text{III})$ (Anderson and Morel 1982), we determined that it also reduces 100% of $\text{Cu}(\text{II})$ within 10 minutes (determined using BCDS and a UV/vis spectrophotometer; Moffett et al. 1985; Walsh and Ahner 2013). The $^{67}\text{Cu}(\text{I})$ solution was bubbled with 0.22 μm filtered N_2 gas for 10 minutes to remove any excess SO_2 . Under mildly acidic conditions (pH 4), the oxidative half life of $\text{Cu}(\text{I})$ (>30 hours) is much longer than the time required for GSH and Cys to completely bind $\text{Cu}(\text{I})$ (2 to 40 min) (Leal and van den Berg 1998; González-Dávila et al. 2009). Aliquots of the $^{67}\text{Cu}(\text{I})$ solution were added to solutions containing each weak $\text{Cu}(\text{I})$ ligand (1:10 molar ratio) and allowed to equilibrate for 2 hours. The resulting $\text{Cu}(\text{I})$ -ligand solutions were equilibrated for 2 h with filtered seawater before being added to the 2 L uptake assay bottles.

This work was initially carried out under the assumption that GSH and cysteine strongly bind $\text{Cu}(\text{I})$ in seawater (Leal and van den Berg 1998). However, more recent data indicates that these ligands form much weaker complexes than previously reported (Table 1; Walsh and Ahner 2013). For example, when the $\log K_{\text{Cu}(\text{I})\text{GSH},\text{Cu}^+}^{\text{cond}}$ (11.9) is converted to $\log K_{\text{Cu}(\text{I})\text{GSH},\text{Cu}^+}^{\text{cond}}$, (6.6; assuming a side reaction coefficient for Cu^+ of $10^{4.95}$; Walsh and Ahner 2013), it is clear that the 6-8 nM excess strong *in situ* ligands would rapidly complex the 1 nM ^{67}Cu once added to the filtered seawater to equilibrate for 2 h (see 2.2.4.1). Thus, the 10 nM weak Cu ligand additions may act as weak ligand shuttles as observed for Zn (Aristilde et al. 2012), and increase the bioavailability of the *in situ* strongly complexed Cu.

2.2.5 Copper Uptake Assay

Every 3 to 5 h, between 250 and 750 mL were removed from each 2 L bottle over 14 h in a class 100 laminar flow hood. The water was filtered onto a series of 20, 5, 1, and a 0.22 μm polycarbonate filters in series (47 mm diameter; separated by nylon drain disks). The filters were soaked in 1 mM DTPA wash solution for 5 min to remove extracellular Cu (Croot et al. 2003), and were subsequently rinsed with 10 mL filtered (0.22 μm) seawater to remove any loosely associated tracer. The filters were then placed into 7 mL glass scintillation vials and the disintegrations per minute (dpm) for each filter were measured using a ship-board gamma counter (Semeniuk et al. 2009).

The specific activity of ^{67}Cu (mol per dpm) in the Cu(II)-ligand amended treatments was determined for each bottle by dividing the added Cu concentration (1 nM) by the ^{67}Cu activity (dpm per L; measured in 1 mL of labeled seawater). For the *in situ* ligand treatments, the specific activity was calculated by dividing the total dissolved Cu concentration (2.1 nM) by the ^{67}Cu activity. For the weak Cu(I)-ligand treatments, the specific activity was calculated by dividing the total dissolved Cu concentration (1 nM ^{67}Cu + 2.1 nM *in situ* Cu) by the ^{67}Cu activity. Total particulate Cu per filter (mol Cu per filter) was calculated by multiplying the filter activity (dpm per filter) by the specific activity of the seawater that was filtered.

The short-term uptake rates reported in Table 2.2 and Figure 2.2 & 2.3 were calculated for the first sampling time point (~ 3 to 4 h) because in many treatments, particulate Cu concentrations reached a plateau or decreased after 5 to 9 h (refer to Figure 2.4). Although the plateau could be due to rapid adsorption of the Cu-chelates to the cell surface (and subsequent saturation of

adsorption sites), adsorption is normally observed within the first few minutes (~ 15 min) of uptake experiments using laboratory phytoplankton cultures (Croot et al. 2003; Quigg et al. 2006), and would not be discerned by our first sampling time (3 to 4 h). Furthermore, in culture studies performed in our laboratory, Cu uptake from Cu(II)EDTA was linear for at least 4 h (J. Guo, unpub. data). Abiotic surface adsorption of the *in situ* Cu ligand complexes to the filters and particles was not determined in this study, but was measured in August 2011 and it accounted for <20% of the total particulate ⁶⁷Cu signal (Chapter 5). Therefore, the plateau in particulate Cu concentrations observed for some treatments and size fractions is unlikely due to abiotic adsorption of the Cu-chelates to particle surfaces.

2.2.6 Diffusive Boundary Layer Inorganic Cu Flux Calculations

To determine if the phytoplankton at P26 were directly accessing Cu from within the Cu(II)L or *in situ* CuL complexes, we compared the observed Cu uptake rates with a calculated maximum supply of Cu' (J_T) to cell surface transporters by: a) diffusion of Cu' from the bulk medium across the diffusive boundary layer (DBL) (J_D); and b) dissociation of the CuL complexes within the DBL (J_k) (Table 3). If the observed uptake rates exceeded the total maximum supply of Cu' to cell surface transporters, then Cu' cannot be the sole substrate for transport and phytoplankton must be directly accessing Cu from CuL complexes.

To calculate the supply rate of Cu' to the cell surface via diffusion across the DBL, we assume that the phytoplankton phyla sampled at P26 were dominated by prymnesiophytes, cryptophytes, and prasinophytes (representing 90% of the total [chl *a*] at the time of sampling; Steiner et al. 2012), and abundant phytoplankton species in these groups tend to be spherical. Thus, the rate at

which Cu' diffuses to the surface of an individual cell can be estimated using Fick's Law, expanded for the surface area of a spherical cell: $J_D = 4\pi r D_{Cu'} ([Cu']_{Bulk} - [Cu']_{Cell})$ where r is the cell radius (cm), $D_{Cu'}$ is the diffusion coefficient for Cu' in seawater ($2.12 \times 10^{-2} \text{ cm}^2 \text{ h}^{-1}$; Li and Gregory 1974), and $[Cu']_{Bulk}$ and $[Cu']_{Cell}$ are the inorganic Cu concentrations the bulk seawater and at the cell surface, respectively (mol cm^{-3}) (Wolf-Gladrow and Riebesell 1997). Three cell radius sizes (0.5, 2.5, and 10 μm) were used in the calculations to account for a large possible range of cell sizes captured by the $\geq 1 \mu\text{m}$ filters. The maximum diffusive rate of Cu' across the DBL can be calculated by assuming the Cu transporters are capable of drawing down $[Cu']_{Cell}$ to zero, thus simplifying the diffusive flux calculation to: $J_D = 4\pi r D_{Cu^{m+}} [Cu']_{Bulk}$. For each ligand treatment, equilibrium $[Cu']$ were calculated using the $\log K_{CuL_n, Cu^{m+}}^{cond}$ of each ligand, and the added Cu (1 nM) and ligand (10 nM) concentrations (Table 1). For the *in situ* ligand treatment, an average $[Cu']$ (49.3 fM) was calculated based on recent measurements along the Line P transect (18.7 to 94.0 fM) (R. Bundy unpub. data).

To calculate the supply rate of Cu' to the cell surface via dissociation of CuL within the DBL

(J_K), we first calculated the $J_K:J_D$ ratio following Jackson and Morgan (1978):

$J_K : J_D = (k_d [Cu^{n+} L_m]) r^2 / (D_{Cu'} [Cu'])$, where k_d is the pseudo-first order dissociation rate constant for the CuL complex (s^{-1}). J_K was then calculated from this ratio and the calculated J_D . The k_d of the complexes were calculated from the relationship $K_{CuL, Cu'}^{cond} = k_f / k_d$, where $K_{CuL, Cu'}^{cond}$ is the conditional stability constant of each ligand with respect to Cu', and k_f is the forward rate constant for the CuL complex (Hudson et al. 1992). The forward rate constant is approximated by $k_f \approx K_{OS} k_{-w}$, where K_{OS} is the outer sphere stability constant (M^{-1}), and k_{-w} is the inner sphere

first water loss rate constant (10^9 s^{-1} for Cu^{2+} ; Hudson 1998). The outer sphere stability constant likely varies between 0.3 and 8 M^{-1} for metals in seawater (Morel et al. 1991), where values increase as the charge difference between the metal ion and ligand increases (Morel and Hering 1993). We chose a mid-range value of 4 for all ligand treatments in order to calculate k_f . Since $\log K_{\text{CuL,Cu}'}^{\text{cond}}$ was not determined for the seawater sampled for the Cu uptake assay, we used an average $\log K_{\text{CuL,Cu}'}^{\text{cond}}$ calculated from previous speciation measurements along Line P ($\log K_{\text{CuL,Cu}'}^{\text{cond}} = 12.82 \pm 0.22$, $n = 10$; R. Bundy unpub. data).

The J_D calculation assumes that the concentration of Cu' at the cell surface is zero, thereby producing a maximum possible diffusive flux of Cu' to the cell. Similarly, the calculated dissociative flux assumes that the cells acquire all the Cu' produced within the DBL, and not complexed by excess strong ligands in solution. Thus, J_T provides a maximum possible upper limit to the supply of Cu' to the cell surface. In order to compare the calculated cellular Cu' fluxes with the measured Cu uptake rates, volumetric short-term uptake rates ($\text{pmol Cu L}^{-1} \text{ h}^{-1}$) in the $>1 \mu\text{m}$ size fraction were normalized to the total photosynthetic eukaryotic cell abundance determined by flow cytometry ($21.1 \text{ million cells L}^{-1}$; F. Ribulet, pers. comm.).

2.3 Results

2.3.1 Station Parameterization

The upper 75 m at P26 were characterized by a deep mixed layer (59 m) that extended below the euphotic zone ($Z_{\text{eu}} = 43$ m) (Figure 1). The noise in density in the upper 18 m was due to an inconsistent descent rate (M. Robert, pers. comm.). Station P26 experiences chronic Fe-limitation throughout most of the year (Harrison et al. 2004), and elevated nitrate concentrations in the mixed layer during sampling ($15.3 \mu\text{M}$) suggest that the phytoplankton community sampled was Fe-limited (Figure 1). A broad subsurface chlorophyll maximum occurred between 20 and 50 m. At 10 m, total [chl a] ($0.37 \mu\text{g L}^{-1}$) was primarily found within the 1-5 μm ($0.09 \mu\text{g L}^{-1}$), 5-20 μm ($0.15 \mu\text{g L}^{-1}$) and >20 μm ($0.11 \mu\text{g L}^{-1}$) size fractions. Less than 5% was in the 0.22-1 μm size fraction ($0.02 \mu\text{g L}^{-1}$). Although phytoplankton composition samples were not taken at 10 m, the phytoplankton assemblage at 5 m depth was dominated by prymnesiophytes (60%), cryptophytes (21%), and prasinophytes (10%), with minor contributions from diatoms (6%) and dinoflagellates (3%) (Steiner et al. 2012). The total dissolved Cu concentration was 2.1 nM at 10 m.

2.3.2 Size Fractionated Short-Term (3 to 4 h) Uptake Rates

2.3.2.1 Artificial Cu(II)-Ligands

Total particulate ρCu_V ranged between 0.46 ± 0.04 and $1.06 \pm 0.14 \text{ pmol Cu L}^{-1} \text{ h}^{-1}$ among Cu(II)L treatments (Table 2), and were similar to rates previously measured at P26 (0.7 to 5.2 $\text{pmol Cu L}^{-1} \text{ h}^{-1}$; Semeniuk et al. 2009). In order to compare partitioning of Cu between the prokaryotes and eukaryotes, we calculated ρCu_V for the 0.22-1 μm and >1 μm size fractions

(Figure 2). The 0.22-1 and >1 μm size fractions made up $22 \pm 1\%$ and $77 \pm 1\%$ of the total particulate Cu uptake rates, respectively.

Chlorophyll-normalized Cu uptake rates ranged between 0.59 ± 0.04 and 6.9 ± 0.4 $\text{pmol Cu } \mu\text{g chl a}^{-1} \text{h}^{-1}$ among the Cu(II)L treatments (Figure 3). Average $\rho\text{Cu}_{\text{chl}}$ in the 1-5 μm size fraction (3.6 ± 3.0 $\text{pmol Cu } \mu\text{g chl a}^{-1} \text{h}^{-1}$) was 4.6 and 4.2 times faster than the 5-20 μm (0.78 ± 0.18 $\text{pmol Cu } \mu\text{g chl a}^{-1} \text{h}^{-1}$) and >20 μm (0.85 ± 0.33 $\text{pmol Cu } \mu\text{g chl a}^{-1} \text{h}^{-1}$) size fractions, respectively. Uptake rates in the 1-5 μm size fraction varied 6.7-times between Cu(II)-ligand treatments, while uptake rates by the 5-20 and >20 μm size fractions only varied 1.6 and 1.9-times, respectively. Interestingly, while uptake of Cu(II) bound to Cyclam was fastest for the 1-5 and 5-20 μm size fractions, it was the slowest for the >20 μm size fraction. In contrast, uptake rates were slowest for Cu(II)EDTA in the 1-5 μm size fraction, but fastest for the >20 μm size fraction.

2.3.2.2 *In Situ* Ligands

The illuminated ρCu_V in the 0.22-1 μm (11 ± 1 $\text{pmol Cu L}^{-1} \text{h}^{-1}$) and >1 μm (6.9 ± 1.3 $\text{pmol Cu L}^{-1} \text{h}^{-1}$) size fractions in the *in situ* ligand treatment were 71 and 13-times faster than the average uptake rates in the Cu(II)L treatments, respectively (Figure 2). Rates were similarly faster for $\rho\text{Cu}_{\text{chl}}$ in the 1-5 μm (13-times), 5-20 μm (14-times), and >20 μm (10-times) size fractions (Figure 3). The $\rho\text{Cu}_{\text{chl}}$ were similar for the 5-20 μm and >20 μm size fractions, and was 5.9 times faster in the 1-5 μm size fraction. Light affected *in situ* Cu uptake rates in the 0.22-1 μm , 5-20 μm , and >20 μm size fractions, but not the 1-5 μm size fraction. In the 0.22-1 μm size fraction, ρCu_V was 4.7 times faster in the light than in the dark (Figure 2). In contrast, $\rho\text{Cu}_{\text{chl}}$ in

the dark treatment increased 94% and 61% in the 5-20 μm and $> 20 \mu\text{m}$ size fractions, respectively (Figure 3).

2.3.2.3 *In Situ* Ligands in the Presence of 1 nM Cu and 10 nM Weak Ligands

Total particulate volumetric Cu uptake rates in the 1nM Cu and 10 nM weak ligand amended treatments ranged between 34.1 ± 1.2 and $46.8 \pm 6.2 \text{ pmol Cu L}^{-1} \text{ h}^{-1}$, and were between 1.9 and 2.6 times faster than the illuminated *in situ* treatment (Table 2). Average ρCu_v in the 0.22-1 μm and $>1 \mu\text{m}$ size fractions were 1.9 and 3.1 times faster than uptake in the illuminated *in situ* treatment (Figure 2). Similarly, average size fractionated ρCu_{chl} for the 1-5 μm ($160 \pm 33 \text{ pmol Cu } \mu\text{g chl } a^{-1} \text{ h}^{-1}$), 5-20 μm ($29.2 \pm 0.2 \text{ pmol Cu } \mu\text{g chl } a^{-1} \text{ h}^{-1}$), and $>20 \mu\text{m}$ ($23.1 \pm 1.9 \text{ pmol Cu } \mu\text{g chl } a^{-1} \text{ h}^{-1}$) size fractions were 3.3, 2.6, and 2.9 times faster than the illuminated *in situ* treatment (Figure 3). In contrast, total dissolved Cu concentrations in these 1 nM Cu / 10 nM weak ligand treatments increased 1.5 times relative to those in the illuminated *in situ* treatment.

2.3.3 Diffusive Boundary Layer Cu' Fluxes

In the Cyclam and Cyclen treatments, cell-normalized Cu uptake rates by the $\geq 1 \mu\text{m}$ size fraction were 2050 and 118 times faster than the calculated combined diffusive and dissociative Cu' fluxes (J_T) for a cell diameter of 1 μm , respectively (Table 3). For mid-sized cells (diameter = 5 μm), uptake rates were between 12 and 220 times faster than J_T for the Cyclam and Cyclen treatments, respectively. In the illuminated *in situ* treatment, uptake rates exceeded J_T by 393 and 13 times for cell diameters of 1 and 5 μm , respectively. Copper uptake rates for the largest cell size (diameter = 20 μm) were faster than J_T only for the Cyclam treatment (6.7 times).

Uptake rates in the EDTA treatment were always slower than the calculated J_T , regardless of cell size.

Phytoplankton in the 1-5 μm size range account for between 56 and 80% the total cellular carbon along Line P (Booth 1988). Similarly, small prymnesiophytes, cryptophytes, and prasinophytes made up 90% of the total chl *a* at the time of sampling (Steiner et al. 2012). This is in accord with observations that small cells are numerically dominant in oligotrophic waters. Thus, calculations of J_T for the 1 and 5 μm cell diameters are most representative of the phytoplankton community sampled.

2.3.4 Long-Term (14 h) Cu Accumulation

2.3.4.1 Artificial Cu(II)-Ligands

There was a rapid accumulation of Cu in nearly all ligands and size classes in the first 4 hours (Figure 4 A-D). After 4 to 8 hours in the 0.22-1 μm , 5-20 μm , and >20 μm size fractions, particulate Cu remained nearly constant in the Cyclam and Cyclen treatments, but decreased between 37% and 63% in the EDTA treatment. In contrast, particulate Cu in the 1-5 μm size fraction remained constant in the EDTA treatment, and decreased in the Cyclam and Cyclen treatments. The only treatment and size fraction to display nearly linear Cu accumulation was the >20 μm size fraction in the Cyclam treatment.

2.3.4.2 *In Situ* Ligands

Similar to the Cu(II)L treatments, in the illuminated *in situ* ligand treatment, Cu accumulated rapidly in all size fractions within the first 4 hours, and stayed relatively constant for nearly all

the size fractions (Figure 4 E-H). In the 0.22-1 μm size fraction, there was a rapid loss (74%) of particulate Cu between 4 and 8 hours in the illuminated treatment, and by the end of the assay, particulate Cu concentrations were similar in the illuminated and dark treatments in the 0.22-1 μm size fraction. Light availability had a different effect on the accumulation of Cu in the > 5 μm size fractions where particulate Cu concentrations in the dark were higher (15 to 111%) than in the illuminated treatment.

2.3.4.3 *In Situ* Ligands in the Presence of 1 nM Cu and 10 nM Weak Cu(I) Ligands

Maximal particulate Cu concentrations were reached in nearly every ligand treatment and size fraction within 4 hours (Figure 4 I-L). After 14 hours, between 22 and 41% of the particulate Cu was lost in the < 5 μm size fractions. In contrast, after 4 hours particulate Cu in the > 5 μm size fractions was nearly constant within the measurement error of the assay, and may show minor Cu losses at the end of the assay.

2.4 Discussion

Previous studies on Cu nutrition in eukaryotic phytoplankton determined that intracellular Cu concentrations co-varied with changes to dissolved $[\text{Cu}']$ (0.01 to 3 nM) - not total dissolved Cu (40 nM to 1 mM) - in the growth media (Sunda and Guillard 1976). Copper toxicity to phytoplankton can be mitigated by the addition of artificial Cu(II) chelators, suggesting that organically complexed Cu is not bioavailable (Sunda and Guillard 1976; Anderson and Morel 1978; Brand et al. 1986). However when $[\text{Cu}']$ is low (1 to 10 fM), Cu uptake rates by phytoplankton cultures cannot be sustained by the maximum diffusive supply of Cu' to the cell

surface (J_D) (Hudson 1998; Quigg et al. 2006; Annett et al. 2008; Guo et al. 2010; Guo et al. 2012). Copper bound within organic complexes was hypothesized to be either directly accessed by Cu transporters or undergo rapid dissociation inside the cellular diffusive boundary layer (c.f. Hudson 1998).

We present evidence that, under subsaturating Cu concentrations, Cu within strong artificial Cu(II)-ligand complexes is bioavailable to a community of indigenous marine phytoplankton, and is likely accessed by cell surface reductases. Furthermore, Cu within *in situ* strong Cu ligands was also acquired—directly via cell surface reduction or indirectly via a weak ligand shuttle mechanism. These data suggest that a portion of the strong *in situ* Cu binding ligands might be bioavailable.

2.4.1 Copper Acquisition from Strong Cu(II)Ligand Complexes by Eukaryotic Phytoplankton

The Cu uptake rates reported in this study were performed with sub-saturating Cu concentrations (1nM total dissolved Cu concentration vs. half-saturation constant for the high-affinity Cu transport system (K_{pCu}) = 7-373 nM; Guo et al. 2010), thus the rates of uptake should be directly proportional to the concentration of labile Cu ([labile Cu]) and the rate constant for Cu uptake (k_{in} ; $\rho_{Cu} = [\text{labile Cu}] * k_{in}$). Assuming that k_{in} is similar among phytoplankton (as shown for Fe, Hagar et al. 2014), at subsaturating Cu concentrations, the rates of Cu uptake should be directly proportional to [labile Cu]. The short-term particulate Cu uptake rates by the $\geq 1 \mu\text{m}$ size fraction were similar for the cyclam and cyclen treatments despite the 10-fold range in [Cu'] in these treatments, suggesting that [Cu'] does not determine Cu uptake rates. Furthermore, the

short-term cellular Cu uptake rates were at least an order of magnitude faster than the calculated combined diffusive and dissociative Cu' fluxes (J_T) for the 1 and 5 μm cell diameters (Table 1.3) — the diameters that are most representative of the phytoplankton community sampled at P26 (see section 2.3.3). Therefore, neither the diffusive flux of Cu' across the DBL nor the dissociative flux of Cu(II)L within the DBL can provide enough Cu' to the cell surfaces to account for the observed Cu uptake rates. Thus, the phytoplankton community sampled at P26 was accessing the largest pool of dissolved Cu, organically complexed Cu. There are two possible mechanisms to account for the bioavailability of Cu(II) within these strong complexes: reduction of Cu(II) and subsequent internalization of Cu(I), or shuttling of Cu(II) from the strong ligands by an intermediate weak Cu-ligand pool.

The substrate of the HACuTS in *Saccharomyces cerevisiae*, the freshwater green algae *Chlamydomonas reinhardtii*, and most eukaryotes is Cu(I), whereby Cu(II) reduction by cupri/ferrireductase FRE1/2 precedes transport by a Cu(I) specific CTR transporter (Dancis et al. 1994; Hassett and Kosman 1995; Hill et al. 1996; Xiao et al. 2002; Page et al. 2009; Pope et al. 2012). Two putative CTR genes (*TpCTR|24275* and *TpCTR|9391*) and a FRE2 homologue have been identified in the model centric diatom *Thalassiosira pseudonana*, and they are downregulated (~2-fold) with short-term increases in Cu availability (Guo et al. *in press*). A HACuTS has been identified in the centric diatoms *T. oceanica* and *T. pseudonana*, and their half saturation constants are 7 nM and 350 nM, respectively (Guo et al. 2010). The ubiquity of the high-affinity CTR transporter in eukaryotes as diverse as *S. cerevisiae*, *C. reinhardtii*, *T. pseudonana*, rice (Yuan et al. 2011), *Drosophila* (Zhou et al. 2003), and humans (Zhou and Gitschier 1997), indicates that the FRE2 and putative CTR genes identified in *T. pseudonana* are

likely involved in a HACuTS. Since the total dissolved Cu concentration in open ocean surface waters (0.5-3 nM; Coale and Bruland 1988; Moffett and Dupont 2007; Jacquot et al. 2013) is below the half saturation constant with respect to the HACuTS in diatoms (Guo et al. 2010), Cu(I) uptake via the HACuTS could be the primary Cu acquisition pathway in marine eukaryotic phytoplankton.

Reduction of Cu(II) within the strong ligands is likely facilitated via the formation of a ternary complex between the Cu(II)-ligand complex and the reductase (similar to Fe(III)L reduction; Albrecht-Gary and Crumbliss 1998; Mies et al. 2006). The formation of a ternary complex could reduce the reduction potential of strongly bound Cu(II)L (half-wave reduction potentials < -680 mV; Croot et al. 1999) to within the range of the surface reductase (-250 mV for the ferrireductase in *S. cerevisiae*; Shatwell et al. 1996). Cyclam does not form a stable complex with Cu(I) (Zanello et al. 1982), and so the Cu(I) could be stripped away from the ligand and internalized by the putative CTR transporter. Thus, while cyclam and cyclen form stable complexes with Cu(II), cell surface transporters could still acquire Cu(II) via a reductive mechanism. Laboratory work investigating the reduction of organically complexed Cu(II) would help support this mechanism.

Recent work has demonstrated that weak organic iron (Fe) and zinc (Zn) complexes can enhance metal uptake rates in marine eukaryotic phytoplankton (Maldonado et al. 2002; Hassler et al. 2011; Aristilde et al. 2012). Weak Zn-binding ligands like cysteine can enhance Zn uptake rates in laboratory phytoplankton cultures above the calculated J_D by ~2-fold (Aristilde et al. 2012). The small pool of ZnCys appears to be bioavailable via a ligand-exchange mechanism with the

surface Zn transporter, while strongly complexed ZnEDTA is not bioavailable. Thus, weak ligands can act to “shuttle” metals from less bioavailable strong ligands to more bioavailable weak ligands. Similarly, weak *in situ* Cu-binding ligands may enhance Cu uptake from the cyclam and cyclen complexes by decreasing the Cu' pool, thereby pushing the Cu(II)-ligand equilibria towards dissociation. Weak Cu ligands are likely common in seawater, and may be humic and fulvic acids or low molecular weight thiols (Leal and van den Berg 1998; Yang and van den Berg 2009; Walsh and Ahner 2013). Although we are unable to determine if weak Cu ligands are responsible for the uptake rates in the strong Cu(II)-ligand treatments, they may increase the bioavailability of *in situ* Cu-ligands (see section 2.4.2).

Copper uptake rates in the EDTA treatment were similar to the cyclam and cyclen treatments despite $10^{4.2}$ times lower [Cu']. In contrast to the stronger ligands, calculated J_T in the EDTA treatment could provide enough Cu' to account for the cellular uptake rates. The $^{67}\text{Cu(II)EDTA}$ would have slowly dissociated when added to the seawater, and the $^{67}\text{Cu(II)'}$ would have been complexed by the 6-8 nM excess strong *in situ* ligands. Since Cu uptake rates in the *in situ* ligand treatment were significantly faster than in the Cu(II)L treatments, we expected the uptake rates in the EDTA treatment to be faster than the cyclam and cyclen treatments. We are unable to account for this discrepancy at this time.

2.4.2 Copper Acquisition from *In Situ* CuL Complexes by Eukaryotic Phytoplankton

Dissolved Cu in open ocean surface waters is complexed to an excess of strong organic ligands with $\log K_{\text{CuL,Cu}^{2+}}^{\text{cond}}$ that range between 13.5 and 16, resulting in low inorganic Cu concentrations (1-

750 fM, or $10^{-13.5}$ to $10^{-16.3}$ M “free” Cu; Moffett and Dupont 2007; Buck et al. 2010; Jacquot et al. 2013). The source and chemical nature of the strong *in situ* ligands are largely unknown, but they may be produced by prokaryotes to detoxify Cu via extracellular complexation (Moffett and Brand 1996; Gordon et al. 2000). Early laboratory studies determined that intracellular Cu concentrations and growth rates co-varied with inorganic Cu concentrations – not total dissolved Cu – and so Cu bound to *in situ* strong ligands has not been considered bioavailable to marine phytoplankton (Sunda and Guillard 1976; Anderson and Morel 1978; Brand et al. 1986; Sunda and Huntsman 1995b).

Like the cyclam and cyclen ligand treatments, estimated cellular Cu uptake rates in the illuminated *in situ* treatment were at least 10-times faster than the calculated J_T for the 1 and 5 μm cell diameters (Table 1.3)— the diameters that are most representative of the phytoplankton community sampled at P26 (see section 2.3.3). This suggests that the phytoplankton at P26 likely had access to Cu within the strong *in situ* ligands. Thus, a pool of the strong *in situ* organically complexed Cu appears to be bioavailable.

We are unable to determine whether cell surface reduction or the weak ligand shuttle is responsible for the cellular Cu uptake rates in the presence of *in situ* ligands. As discussed above, reduction of organically bound Cu at the cell surface might account for the Cu uptake rates we measured in the presence of *in situ* ligands. In addition, weak ligands may facilitate Cu transport from the strong *in situ* ligands. The addition of 10 nM weak Cu(I) ligands (cysteine, GSH, and BCDS) with the addition of 1 nM Cu caused $p\text{Cu}_{\text{chl}}$ to increase between 2.6 and 3.3-times for the $>1 \mu\text{m}$ size fractions. In contrast, total dissolved Cu increased only 1.5-times (from

2.1 nM to 3.1 nM). Since the 1 nM Cu addition would have been rapidly complexed to the 6 to 8 nM excess strong ligands (see section 2.2.4.3), this indicates that weak ligands caused Cu uptake rates to increase more than would be predicted by increases in total dissolved Cu. Thus, weak ligands may facilitate Cu transport from the *in situ* ligands via a shuttle mechanism (Aristilde et al. 2012).

Given the likely role of a surface cuprireductase and Cu(I)-specific CTR transporter in the HACuTS in marine eukaryotic phytoplankton, reduced sulfur containing ligands may also facilitate Cu acquisition by reducing inorganic or weakly complexed Cu(II) to Cu(I). The rate-limiting step for Fe uptake by marine phytoplankton is reduction (Shaked et al. 2005). Thus, the added thiols may have increased Cu uptake rates by reducing extracellular Cu(II) to Cu(I), thereby bypassing reduction by the surface cuprireductase.

Unfortunately, given the analytical challenge to distinguish Cu(II) from Cu(I) in seawater at environmentally relevant concentrations of Cu, there is a dearth of research on the oxidation state of Cu in surface waters. Preliminary work using BCDS to detect Cu(I) found that 5% to 80% of dissolved Cu could be Cu(I) (Moffett and Zika 1988; Beurge-Weirich and Sulzberger 2004).

Many potential reducing processes in seawater could impart a kinetic control on Cu redox speciation in surface water, including reduction by hydrogen peroxide (Moffett and Zika 1987), by superoxide radicals (Zafiriou et al. 1998; Voelker et al. 2000; Heller and Croot 2010), and by thiol-containing ligands (Leal and van den Berg 1998), as well as light-mediated ligand-to-metal electron transfer reactions. Superoxide can reduce inorganic and organically complexed Cu at similar rates (Zafiriou et al. 1998; Voelker et al. 2000), and estimates of steady state Cu(I)

concentrations in surface waters (1-63 pM; Heller and Croot 2010) are higher than the total inorganic Cu concentrations measured by voltametry (1-750 fM; Moffett and Dupont 2007; Buck et al 2010; Jacquot et al. 2013). Thus, a significant portion of the dissolved Cu pool at P26 could be Cu(I). Given the relatively short half-life of Cu(I) in oxygenated seawater (~12 min; González-Dávila et al. 2009), Cu(I) is likely stabilized by either Cl⁻ (Moffett and Zika 1983; González-Dávila et al. 2009) or sulfhydryl-containing organic ligands (Leal and van den Berg 1998; Walsh and Ahner 2013). Since thiols like GSH and cysteine are present in open ocean surface seawater at concentrations similar to those of dissolved Cu (0.2-2 nM; Dupont et al. 2006), they may play an important role in stabilizing Cu(I) and influencing the bioavailability of *in situ* Cu to marine eukaryotic phytoplankton.

2.4.2.1 Influence of Light on Cu Uptake from *In Situ* CuL Complexes

Both short-term Cu uptake rates and particulate Cu during the assay were surprisingly higher in the dark than in the light for the 5-20 μm and >20 μm size fractions. This could be due to either a change in Cu bioavailability in the dark or in the physiology of dark-adapted phytoplankton. Low light in the dark treatments would cause the degradation of Cu-binding organic ligands to decrease (Lagler and van den Berg 2006), and presumably make the *in situ* Cu less (not more) bioavailable. Alternatively, metabolic Cu requirements could be higher during light limitation due to an increase in metabolic Fe requirements associated with the synthesis of chl *a* and/or photosynthetic reaction centres (Raven 1990; Sunda and Huntsman 1997). Given that the high-affinity Fe transport system in diatoms requires a multi-copper containing oxidase (Maldonado et al. 2006; Kustka et al. 2007), it is more likely the increase in particulate Cu in the dark for the >5

μm size fractions could be due to higher Cu demands associated with co-limitation by light and Fe.

2.4.3 Marine Prokaryotic Copper Uptake

Since the microorganisms in the 0.22-1 μm size fraction made up more than half of the total particulate Cu uptake rate in the *in situ* ligand treatment, Cu may be an important micronutrient to photosynthetic and heterotrophic bacteria at P26. Little is known about the metabolic requirements of heterotrophic bacteria inhabiting oxygenated seawater. Around half of the global marine heterotrophic bacteria is made up of members of bacteroides, alpha and gamma proteobacteria (Pommier et al. 2007). A genomic analysis surveyed potential copper transporters and Cu-containing proteins in 450 sequenced non-marine bacteria, and found that 94% of gamma-proteobacteria, 99% of alpha-proteobacteria, and 53% of bacteroides strains contained sequences for copper-containing proteins (Ridge et al. 2008). The majority of these bacteria (83%) possessed cytochrome *c* oxidase, a protein involved in organic carbon respiration. Thus, heterotrophic marine bacteria likely have a basal metabolic Cu requirement. In addition, 12 species of cyanobacteria surveyed possessed protein sequences for cytochrome *c* oxidase, and 11 of the species has plastocyanin sequences, a component of the electron transport chain in photosynthesis (Ridge et al. 2008). In support of these genetic data, growth of the cyanobacterium *Synechococcus sp.* WH7803 can become limited by Cu availability (Guo et al. 2012).

The substrate for Cu acquisition by marine cyanobacteria and heterotrophic bacteria is unknown. Due to the similarity in sizes between cyanobacteria and many marine heterotrophic bacteria, the

0.22-1 μm size fraction includes photosynthetic and heterotrophic bacteria. Cyanobacteria are typically 100-1000 times less abundant than heterotrophic bacteria along Line P (D. Semeniuk. unpub.), and so they may not make up a significant portion of the observed uptake rates. However, a survey of known Cu importer enzymes in bacteroides, proteobacteria, and cyanobacteria demonstrated that only cyanobacteria contained the Cu(I)-specific importer CopA while the heterotrophic bacteria contained no known Cu import systems (Ridge et al. 2008). Thus, heterotrophic bacteria may internalize Cu(II) via non-specific divalent metal transporters (Ridge et al. 2008; Rensing and McDevitt 2013). Interestingly, while the addition of weak ligands caused uptake rates in the $>1 \mu\text{m}$ size fractions to increase between 2.6 and 3.3 times, uptake rates in the 0.22-1 μm size fraction increased less with the addition of 1 nM Cu (1.9 times on average). This may indicate that weaker ligands may be less important for facilitating Cu transport in prokaryotes. Thus, marine prokaryotes and eukaryotic phytoplankton likely have different Cu uptake mechanisms.

2.4.4 Copper Cycling in Surface Waters

The increase and subsequent decrease in particulate Cu concentrations over the course of the assay (14 h) in many treatments indicates that Cu cycling between dissolved and particulate phases may be rapid in open ocean surface waters. A plateau in particulate Cu concentrations over time was observed in all size classes and for many of the ligand treatments, while a loss of particulate Cu was more common in the $<5 \mu\text{m}$ size fractions. The particulate Cu plateau and losses could be due to: a) cessation of Cu uptake over the course of the assay; b) loss of particulate Cu via efflux; and/or c) loss of particulate Cu via remineralization by micrograzers.

Efflux is widely used by plants and bacteria to maintain intracellular metal homeostasis (Silver 1996; Hall 2002; Ridge et al. 2008), but direct evidence for Cu efflux in eukaryotic phytoplankton is limited. Copper resistant *Chlorella vulgaris* and *Ectocarpus siliculosus* may survive in high Cu concentrations by effluxing intracellular Cu or down-regulating Cu uptake (Foster 1977; Hall et al. 1979). A decrease in total cellular Cu has been observed over time after exposure to toxic Cu concentrations (Anderson and Morel 1978; Lage et al. 1996). Short-term Cu uptake rates in cultured phytoplankton and in an open ocean phytoplankton community were faster than long-term uptake rates, and could be due to either efflux or the cessation of Cu acquisition (Quigg et al. 2006; Semeniuk et al. 2009). Copper efflux has only been directly observed for a marine cyanobacterium, *Synechococcus* (WH7803), and the haptophyte *Emiliania huxleyi* (Croot et al. 2003; Walsh et al. 2014).

The prevalence of heavy metal P1B-type ATPase export pumps in photosynthetic and heterotrophic bacteria (Kanamaru et al. 1994; Ridge et al. 2008) may indicate that efflux occurred in the 0.22-1 μm size fraction. Particulate Cu in the 0.22-1 μm size fraction accumulated rapidly within 4 hours in the illuminated *in situ* ligand treatment, while particulate Cu increased to a much lesser extent and reached a plateau in the dark treatment. We are unable to account for the rapid influx within 4 hours in the illuminated *in situ* ligand treatment. Given the prevalence of efflux systems in bacteria and efflux observed in the Cu-chelate amended treatments, this likely indicates that both influx and efflux were occurring at equal rates. Furthermore, the particulate [Cu] in the illuminated *in situ* treatment was the same as the dark treatment after 8 hours, indicating that the bacteria were able to maintain the same intracellular [Cu] in the light despite the rapid short-term influx at the beginning of the assay. Efflux in the

freshwater cyanobacterium *Nostoc calciola* is light dependent (Verma and Singh 1991). A similar light-dependency on efflux could account for the rapid loss of particulate Cu in the light treatment, but not the initial rapid influx. Further work on the role of light in mediating Cu bioavailability to marine bacteria is warranted.

Eukaryotic phytoplankton are well known for detoxifying heavy metals by storing them within the cell bound to phytochelatins (Ahner et al. 1997; Ahner et al. 2002). Phytoplankton from multiple phyla produce phytochelatins regardless of whether Cu concentrations in the growth medium are toxic (Ahner et al. 2002). Thus, loss of particulate Cu by the 1-5 μm size fraction may reflect rapid remineralization of Cu by micrograzers. Further inquiry into the role of efflux, intracellular storage, and Cu remineralization by micrograzers would elucidate the importance of these processes in regulating particulate and dissolved Cu concentrations in open ocean surface waters.

Interestingly, particulate Cu in the 1-5 μm size fraction decreased in all amended ligand treatments except for EDTA. In contrast, particulate Cu in the >5 μm size fractions only decreased significantly in the EDTA treatment. Since Cu uptake rates in three Cu(II)L treatments were similar, the loss of particulate Cu in the EDTA treatments is unlikely due to higher intracellular Cu. Instead, if micrograzing caused the loss of particulate Cu in the larger size fractions, then the decreased Cu bioavailability in the Cyclam and Cyclen treatments may have altered grazing rates. Further work on the influence of specific chelators on grazers is necessary to resolve this.

2.4.5 Oceanographic Implications

Until now, Cu' was thought to be the only dissolved Cu species to be available for transport by indigenous marine phytoplankton communities. Total dissolved Cu concentrations in open ocean surface waters (0.5-3 nM) would be toxic to many prokaryotic and eukaryotic phytoplankton if Cu was not complexed by organic ligands (Brand et al. 1986). The production and exudation of strong Cu-binding ligands by marine prokaryotes has primarily been attributed to the mitigation of Cu toxicity in seawater, whereby organic complexation decreases Cu' to non-toxic levels (Moffett and Brand 1996). This paradigm implies that organically complexed Cu is unavailable for transport. However, the data presented herein provide evidence that artificially complexed Cu(II) and *in situ* organically bound Cu was bioavailable to the phytoplankton community at P26. This is could be due to extracellular reduction by cell surface reductases prior to uptake of Cu(I) by a HACuTS. Weak thiols also appear to enhance transport of Cu bound to the strong *in situ* ligands, either via a weak shuttle or by extracellular reduction of inorganic or weak Cu(II)-ligand complexes Cu(II). Thus, organic complexation of Cu may reduce its bioavailability to some Cu-sensitive phytoplankton (e.g. cyanobacteria), but it may not decrease its bioavailability to all eukaryotic marine phytoplankton.

Recent measurements of Cu' concentrations in surface waters (<250 fM) are similar to those that can co-limit Fe-limited phytoplankton cultures – assuming only Cu' is bioavailable – and has led a few authors to suggest that Cu' availability could control phytoplankton growth in HNLC waters (Peers et al. 2005; Moffett and Dupont 2007; Annett et al. 2008; Buck et al. 2010; Guo et al. 2012; Bundy et al. 2013; Jacquot et al. 2013). However, this is unlikely since Cu bound to strong *in situ* ligands was bioavailable to the phytoplankton community sampled in the HNLC

waters at P26. In support of this, calculations of J_D in Cu-limited phytoplankton species grown in Aquil are slower than the cellular uptake rates (calculations not shown; data from Annett et al. 2008; Guo et al. 2012), and indicate that Cu-limited laboratory cultures also access Cu within organic ligands. Further investigations of the chemical nature and source of strong and weak Cu ligands in seawater, and the role of *in situ* ligands in determining the nutritional state of Cu in phytoplankton are necessary to determine how Cu speciation may influence rate processes in natural marine phytoplankton communities.

2.5 Tables

Table 2.1. Functional groups, equilibrium constants, and conditional stability constants for the ligands used in the Cu uptake assay.

Ligand	Functional Groups	Cu^{n+}L_m	Reported $\log K$	Reported ^a $\log K_{\text{CuL}_m, \text{Cu}^{n+}}^{\text{cond}}$	Added $[\text{Cu}']^b$ (mol L ⁻¹)	Reference
Glutathione	-SH	Cu^{1+}L		11.9	^c	Walsh and Ahner (2013)
Cysteine	-SH	Cu^{1+}L		11.4	^c	Walsh and Ahner (2013)
	-SH	$\text{Cu}^{1+}(\text{L})_2$		15.8	^c	Walsh and Ahner (2013)
2-9-dimethyl-4,7-diphenyl-1,10-phenanthroline (BCDS)	-SH	$\text{Cu}^{1+}(\text{L})_2$				
Ethylenediamine tetraacetic acid (EDTA)	-NH ₂ -COOH	Cu^{2+}L	17.9			Croot et al. (1999)
				10.6	$10^{-10.17}$	Coale and Bruland (1988)
1,4,7,10-tetraazacyclododecane (Cyclen)	-NH	Cu^{2+}L	23.3			Croot et al. (1999)
				14.34 ± 0.04	$10^{-13.91}$	This study
1,4,8,11-tetraazacyclotetradecane (Cyclam)	-NH	Cu^{2+}L	26.5			Croot et al. (1999)
				15.29 ± 0.04	$10^{-14.86}$	This Study

^aConditional stability constants are reported using $K_{\text{CuL}_m, \text{Cu}^{n+}}^{\text{cond}} = [\text{CuL}]/[\text{Cu}^{n+}][\text{L}]^m$

^bInorganic Cu concentrations ($[\text{Cu}']$) were calculated for the added 1 nM Cu bound to 10 nM ligand using $K_{\text{CuL}_m, \text{Cu}^{n+}}^{\text{cond}} = [\text{CuL}]/[\text{Cu}^{n+}][\text{L}]^m$ where $[\text{Cu}^{n+}] = [\text{Cu}']/\alpha_{\text{Cu}^{n+}}$, and $\alpha_{\text{Cu}^{n+}}$ is the side reaction coefficient for either Cu(I) (10^5 ; Leal and van den berg 1998) or Cu(II) (24; Coale and Bruland 1988).

^cSince the initial *in situ* Cu speciation was not measured, we are unable to determine how the addition of 1 nM Cu of weakly complexed Cu in these treatment would have increased the $[\text{Cu}']$ (see section 2.2.4.3).

Table 2.2. Average short-term (3 to 4 h) total particulate Cu uptake rates ($\text{pmol Cu L}^{-1} \text{d}^{-1}$) measured at P26. Values in parentheses represent half of the range of two replicates.

Ligand Treatment	Cu Uptake Rate ($\text{pmol Cu L}^{-1} \text{h}^{-1}$)
GSH	46.8 (6.2)
Cys	45.0 (2.2)
BCDS	34.1 (1.2)
Cyclam	1.06 (0.14)
Cyclen	0.55 (0.02)
EDTA	0.46 (0.04)
<i>In situ</i>	17.9 (2.2)
<i>In situ</i> (dark)	11.5 (1.6)

Table 2.3. Cellular short-term Cu uptake rates and calculated fluxes of inorganic Cu to the cell surface within the diffusive boundary layer for various cell sizes in the Cu(II)L and *in situ* ligand treatments. Refer to section 2.7 for a detailed description of the calculations.

Cell Diameter	Ligand	Cellular Uptake ^a (ρ_{Cu}) ($\text{zmol Cu cell}^{-1} \text{ h}^{-1}$)	Dissociative Flux (J_K) ($\text{zmol Cu cell}^{-1} \text{ h}^{-1}$)	Diffusive Flux (J_D) ($\text{zmol Cu cell}^{-1} \text{ h}^{-1}$)	$J_K:J_D$	Total Flux ^b (J_T) ($\text{zmol Cu cell}^{-1} \text{ h}^{-1}$)	$\rho_{Cu}:J_T$
1 μm	EDTA	17	14	917	0.04	930	0.02
	Cyclen	20	0.003	0.17	0.04	0.17	118
	Cyclam	40	0.0003	0.02	0.04	0.02	2050
	<i>In situ</i> ^c	331	0.17	0.67	0.26	0.84	393
5 μm	EDTA	17	1705	4590	0.93	6295	0.002
	Cyclen	20	0.31	0.83	0.93	1.1	12
	Cyclam	40	0.03	0.09	0.93	0.12	220
	<i>In situ</i> ^c	331	22	3.3	6.5	25	13
20 μm	EDTA	17	108785	18300	15	127085	0.0001
	Cyclen	20	20	3.3	15	23	0.39
	Cyclam	40	2.2	0.37	15	2.6	6.7
	<i>In situ</i> ^c	331	1389	13	103	1402	0.24

^aCellular uptake rates for the $>1 \mu\text{m}$ size fraction were calculated from volumetric rates ($\text{pmol Cu L}^{-1} \text{ h}^{-1}$) and total photosynthetic eukaryotic cell abundance ($21.1 \text{ million cells L}^{-1}$)

^bSum of J_K and J_D

^cDissociative and diffusive fluxes for the *in situ* treatment were calculated using an average $[\text{Cu}']$ (49.3 fM) and $\log K_{CuL,Cu'}^{cond}$ (12.82) measured along the Line P transect in August, 2011, and an average (R. Bundy, unpub. data).

Figures

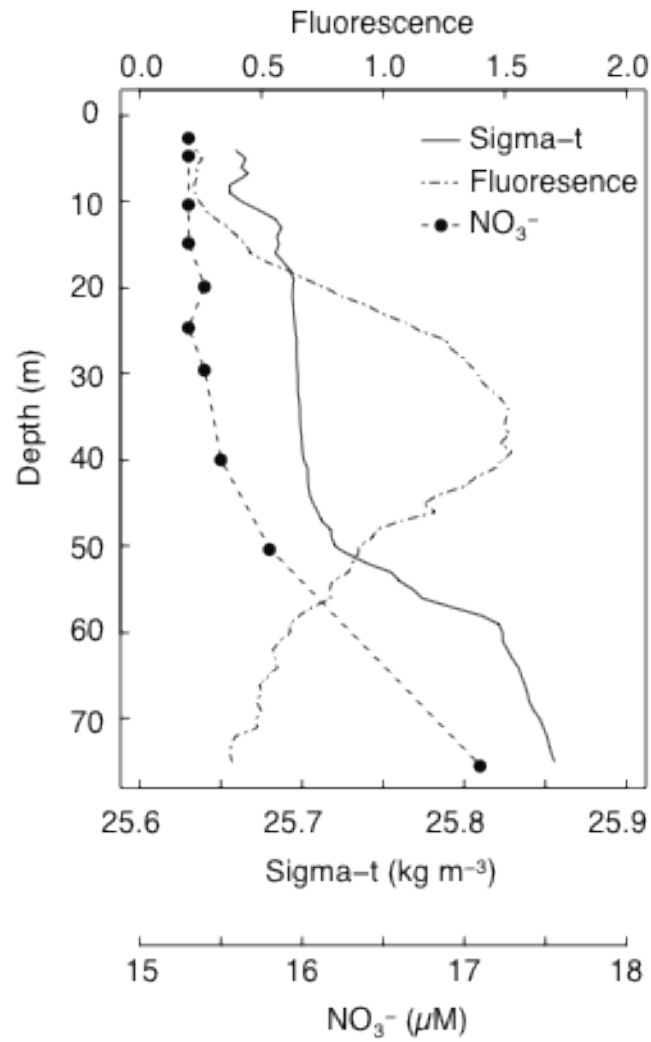


Figure 2.1. Depth profile of seawater density (sigma-t; kg m⁻³), fluorescence, and dissolved nitrate (μM) in the upper 75 m at P26 on June 9, 2008.

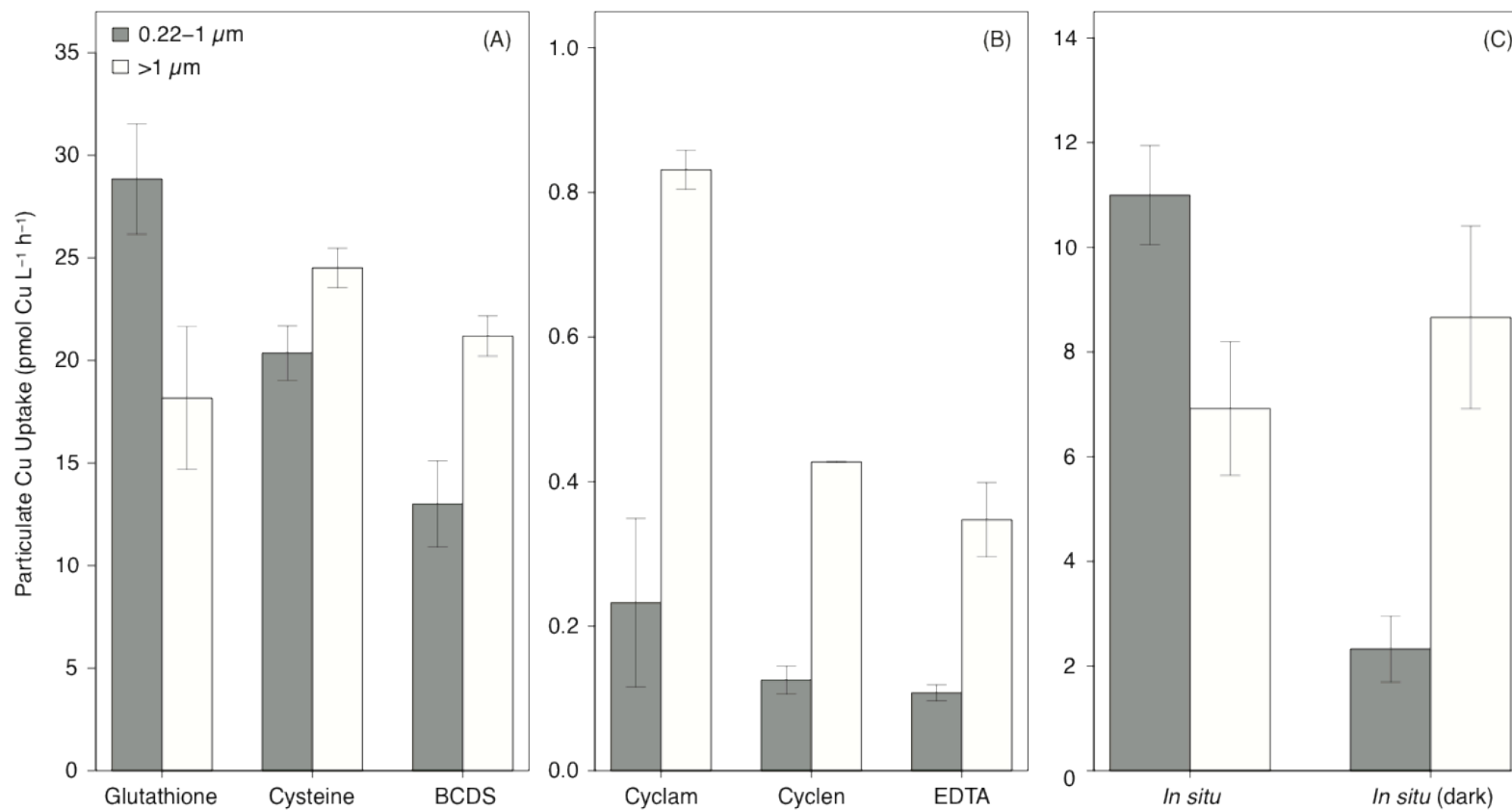


Figure 2.2. Short-term (3 to 4 h) volumetric Cu uptake rates (pmol Cu L⁻¹ h⁻¹) in the treatments amended with 1 nM Cu and 10 nM weak Cu(I) ligands (A), 1 nM Cu(II) bound to 10 nM Cu(II) ligands (B), and for trace amounts of ⁶⁷Cu added to the *in situ* ligands (C) for the 0.22–1 μm and >1 μm size fractions. The bars represent the range of the two replicate assays.

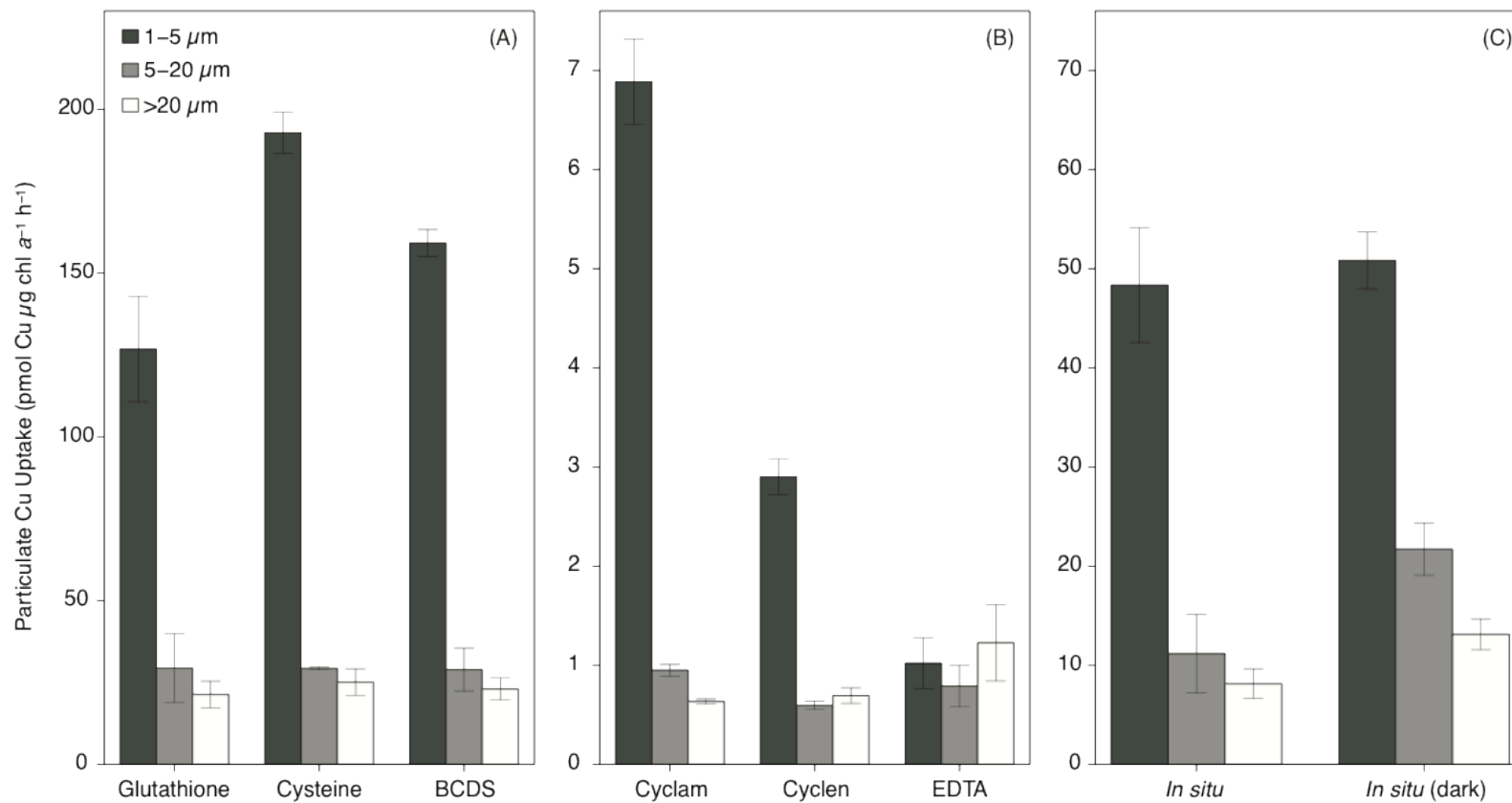


Figure 2.3. Short-term (3 to 4 h) chlorophyll-normalized Cu uptake rates (pmol Cu $\mu\text{g chl } a^{-1} h^{-1}$) for three size fractions in the treatments amended with 1 nM Cu and 10 nM weak Cu(I) ligands (A), 1 nM Cu(II) bound to 10 nM Cu(II) ligands (B), and for trace amounts of ^{67}Cu added to the *in situ* ligands (C). The bars represent the range of the two replicate assays.

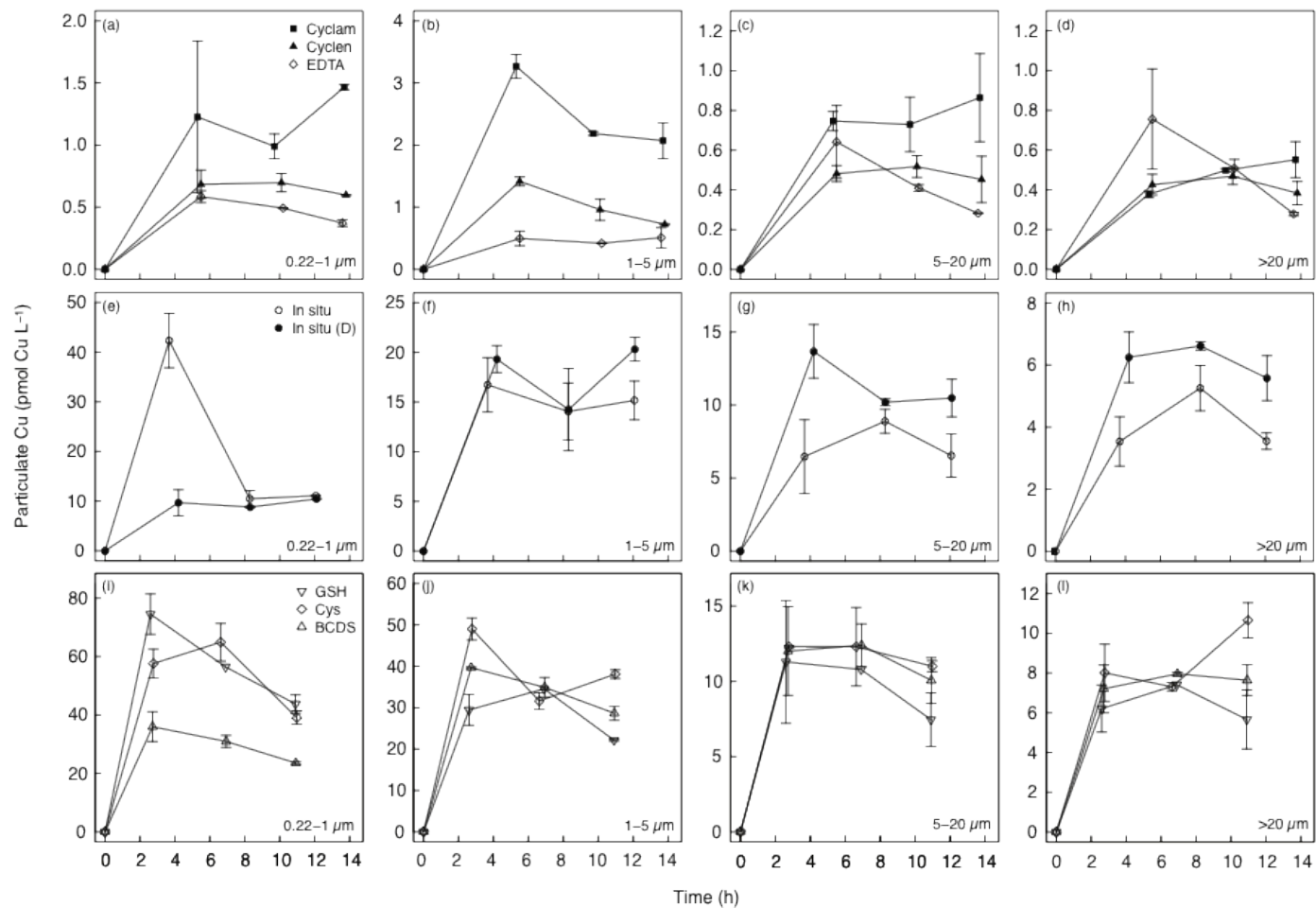


Figure 2.4. Size fractionated time course accumulation of Cu (pmol Cu L⁻¹) in the Cu(II)-ligand treatments (a-d), *in situ* treatments (e-h), and treatments amended with 1 nM Cu and 10 nM weak Cu(I) ligands (i-l). The bars represent the range of the two replicate assays. If bars are missing, then they are within the symbol.

Chapter 3: Acquisition of Organically Complexed Cu(II) by a High-Affinity Cu Transport System in Marine Phytoplankton

There is growing evidence that organically complexed copper (Cu) is bioavailable to marine phytoplankton. However, laboratory Cu uptake experiments performed thus far used dissolved Cu and organic ligand concentrations that are 10 to 10,000 times higher than those found in open ocean surface waters. We measured Cu uptake rates in two diatoms and two prymnesiophytes using Cu concentrations and organic ligands that mimic *in situ* Cu speciation in surface seawater. Acquisition of 1 nM Cu bound to 3 nM of the strong Cu(II) chelator 1,4,8,11-tetraazacyclotetradecane (Cyclam) greatly exceeded the maximum diffusive flux of inorganic Cu to the cell surface for all four phytoplankton species. The cellular Cu uptake rates were similar to uptake rates from *in situ* Cu ligands by a natural phytoplankton community. This indicates that Cu acquisition from organic complexes is likely common in eukaryotic phytoplankton. Copper uptake assays performed with competitive inhibitors suggest that Cu(II) is reduced prior to internalization as Cu(I) by the high-affinity Cu transport system (HACuTS) in *Thalassiosira pseudonana*. These data support the recent identification of putative genes in *T. pseudonana* encoding a Cu(II) reductase and a Cu(I) permease. Copper uptake rates from Cu(II)Cyclam were marginally slower than uptake rates of inorganic Cu. However, excess Cyclam concentrations caused Cu uptake rates to decrease, and may be due to competition for Cu between Cyclam and extracellular components of the HACuTS. In support of this, previously reported short-term Cu uptake rates performed with high concentrations of ethylenediaminetetraacetic acid (EDTA) were significantly slower than uptake from Cu(II)Cyclam. All laboratory phytoplankton growth rate studies investigating Cu limitation and toxicity have used high (micromolar) concentrations

of excess ligands. Thus, competition for Cu between excess ligands and the transporters would result in lower intercellular Cu and an overestimation of the Cu concentrations that induce limitation or toxicity in marine phytoplankton.

3.1 Introduction

Copper (Cu) is an important micronutrient in marine phytoplankton. It catalyzes a number of electron transfer reactions involved in respiration, photosynthesis, nitrogen assimilation, and reactive oxygen species quenching (reviewed by Raven et al. 1999). In addition, recent work has demonstrated that iron (Fe) and Cu nutrition are linked in marine diatoms and freshwater green algae (Maldonado et al. 2006; Merchant et al. 2006; Annett et al. 2008; Guo et al. 2012). During Fe-limitation, a Cu-dependent high-affinity Fe transport system is upregulated (Peers et al. 2005; Maldonado et al. 2006; Kustka et al. 2007). As a result, some Fe-limited phytoplankton have higher cellular Cu quotas (Annett et al. 2008; Guo et al. 2012), and phytoplankton communities in Fe-limited waters increase their intracellular Cu requirements (Chapter 4). Since ~30% of marine surface waters are Fe-limited (Moore et al. 2004), Cu availability could influence the growth of phytoplankton in HNLC waters.

Total dissolved Cu concentrations in unpolluted open ocean surface waters vary between 0.5 and 3 nM (Coale and Bruland 1988; Moffett and Dupont 2007; Buck et al. 2010; Bundy et al. 2013; Jacquot et al. 2013; Thompson et al. 2014). Copper can be toxic to marine phytoplankton at these concentrations if it is not organically complexed (Brand et al. 1986). However, dissolved Cu speciation in surface seawater is dominated by complexation to strong organic ligands that are present in ~3-fold excess of the total dissolved Cu, and have conditional stability constants

($K_{CuL,Cu^{2+}}^{cond}$) between $10^{11.5}$ to 10^{16} (van den Berg 1984; Coale and Bruland 1988; Buck et al. 2010; Bundy et al. 2013; Jacquot et al. 2013). The resulting inorganic Cu (Cu') concentrations in open ocean surface waters range between 10^{-12} and $10^{-14.5}$ M, and correspond to free Cu^{2+} concentrations of $10^{-13.5}$ to $10^{-16.3}$ M (Moffett et al. 2007; Buck et al. 2010; Bundy et al. 2013; Jacquot et al. 2013). The source of the strong ligands is likely biogenic. When experiencing toxicity, laboratory prokaryote cultures produce strong Cu-binding ligands to decrease Cu' concentrations, and thus prevent toxicity (Sunda and Guillard 1976; Anderson and Morel 1978; Moffett and Brand 1996; Gordon et al. 2000).

Interestingly, recent work has demonstrated that organically complexed Cu is likely bioavailable (Hudson 1998; Croot et al. 2003; Quigg et al. 2006; Guo et al. 2010). Steady-state Cu uptake rates (ρCu_{SS}) of growing phytoplankton can be between 2 and 30 times faster than the calculated maximum diffusive supply of Cu' to the cell surface (J_D) (Hudson 1998; Guo et al. 2012).

Similarly, short-term Cu uptake rates (ρCu_{ST}) from the artificial Cu(II) binding ligands ethylenediaminetetraacetic acid (EDTA) and nitrilotriacetic acid (NTA) were between 2 and 15 times faster than J_D in *Synechococcus* DC2 and two marine diatoms (Croot et al. 2003; Guo et al. 2010). Short-term uptake rates of Cu bound to natural ligands in coastal seawater were also faster than J_D (2 to 600 times) for a suite of phytoplankton species (Quigg et al. 2006).

Subsequent work demonstrated that a natural phytoplankton assemblage was able to access Cu from within the *in situ* ligands in open ocean surface waters (Chapter 2). This indicates that organic complexation of Cu lowers Cu' concentrations, but *in situ* organically bound Cu is bioavailable to some marine phytoplankton.

The mechanism by which marine phytoplankton access organically bound Cu remains unknown. The high-affinity Cu transport system (HACuTS) in *Chlamydomonas reinhardtii*, *Saccharomyces cerevisiae*, and nearly all eukaryotes, is encoded by the CTR gene family (reviewed by Pope et al. 2012). Copper(II) must be reduced by an extracellular reductase – often, a reductase that also reduces Fe(III) – prior to internalization of Cu(I) by CTR. A recent uptake kinetics study identified a HACuTS in two marine diatoms that is upregulated during Cu limitation (Guo et al. 2010). The expression of one putative FRE gene (*TpFRE2*) and two putative CTR genes (*TpCTR|24275* and *TpCTR|9391*) in *Thalassiosira pseudonana* is controlled by Cu availability (Guo et al. *submitted*), and suggests that Cu(I) may be the substrate for Cu transport in marine phytoplankton. Indeed, there is putative evidence that Cu(II)' may be reduced by marine phytoplankton (Jones et al. 1987). Thus, reduction of Cu(II) may be a prerequisite step prior to internalization of Cu(I) by a HACuTS in marine phytoplankton.

Early laboratory Cu uptake investigations in marine phytoplankton hypothesized that Cu' was the substrate for transport (e.g. Sunda and Guillard 1976). Most studies have used artificial Cu(II)-binding ligands that are weaker than ligands naturally found in seawater (e.g. NTA, EDTA). As a result, Cu and ligand concentrations employed were often up to 100 and 10,000 times higher, respectively, than those naturally found in open ocean surface waters (Croot et al. 2003; Guo et al. 2010; Walsh and Ahner 2014). Interestingly, a natural phytoplankton assemblage was capable of accessing Cu from within strong artificial and *in situ* ligand complexes (Semeniuk et al. 2009; Chapter 2). Thus, previous laboratory investigations of Cu uptake using artificial Cu(II) binding ligands in large excess of the total dissolved Cu do not adequately represent *in situ* Cu speciation.

Using the gamma emitting and carrier free radioisotope ^{64}Cu , we investigated Cu uptake in marine phytoplankton using Cu concentrations and ligands that closely mimic *in situ* Cu speciation in seawater. Uptake of Cu from the strong Cu(II) chelator 1,4,8,11-tetraazacyclotetradecane (Cyclam) was measured in two model centric diatom species and two prymnesiophytes isolated from the northeast subarctic Pacific Ocean, and compared with uptake of inorganic Cu. In addition, the mechanism of transport in *T. pseudonana* was investigated using competitive inhibitors that target components of the proposed HACuTS – an extracellular reductase and a Cu(I) permease.

3.2 Materials and Methods

3.2.1 Study Organisms, Media, Growth Conditions and Monitoring

Copper uptake was measured in two centric diatoms, *Thalassiosira pseudonana* and *T. oceanica*, and two prymnesiophytes, *Phaeocystis pouchetti* and *Chrysochromulina polylepis* (Table 3.1). The strains were acquired from the Bigelow Laboratory for Ocean Sciences (CCMP strains), West Boothbay Harbor, Maine, USA, and the Canadian Center for the Culture of Microorganisms (NEPCC strains), Vancouver, British Columbia, Canada. The prymnesiophytes were isolated in 1976 along the Line P transect in the northeast subarctic Pacific Ocean, the region of our previous Cu uptake studies (Chapter 2). This permits the comparison of cellular uptake rates by an indigenous phytoplankton community with isolates from the same region.

Cultures were grown in semi-continuous batch cultures in acid cleaned 28 mL polycarbonate tubes using the chemically defined trace metal medium Aquil (Price et al. 1989). The prymnesiophytes and *T. oceanica* were grown in the Cu-replete media described in Maldonado et

al. (2006), and contained 10.2 nM total dissolved Cu. *Thalassiosira pseudonana* was grown in media with no added Cu, and the background dissolved Cu concentration (0.6 nM) was determined in UV-oxidized media via flow injection analysis and chemiluminescence detection (Zamzow et al. 1998; Chapter 4). Trace-metal clean and sterile techniques were employed for all media and culture manipulations.

The phytoplankton were grown in 24 h continuous light ($130 \mu\text{mol quanta m}^{-2} \text{s}^{-1}$) using cool white fluorescent bulbs, and kept at $19 \pm 1 \text{ }^\circ\text{C}$. Cultures were kept in exponential growth phase and acclimated for at least 30 generations prior to performing the uptake experiments. Growth was monitored via *in vivo* fluorescence measurements made at least once a day using a Turner 10-AU fluorometer (Turner Designs, Sunnyvale, CA, USA). Growth rates (d^{-1}) were calculated from the slope of the natural logarithm of fluorescence versus time. Cell diameters were measured using a Coulter Z2 Particle Count and Size Analyzer (Beckman Coulter Inc., Brea, CA, USA). Cell surface area was calculated using the cell diameter and assuming a spherical cell shape.

3.2.2 Cu Uptake Experiments

3.2.2.1 Choice of Cu-Ligand Complex

Copper uptake in each species was monitored from the strong Cu(II)-ligand Cyclam (1,4,8,11-tetraazacyclotetradecane), and from the Cu(I) binding ligand reduced glutathione (GSH) using the gamma emitting radioisotope ^{64}Cu (half-life = 12.7 hours, carrier free; Washington University, St. Louis, Missouri, USA). Cyclam forms a strong Cu(II) complex with a $K_{\text{CuL,Cu}^{2+}}^{\text{cond}}$ ($10^{15.29}$; Chapter 2) that is similar to the stronger natural ligands found in seawater ($10^{13.5}$ to

10^{16}). Thus, Cyclam was chosen as a model for a strong Cu(II) binding ligand, similar to the use of siderophores in studies of Fe(III) reduction by marine phytoplankton (Maldonado and Price 2000; 2001). Reduced glutathione was chosen as a model strong Cu(I) binding ligand using on an early determination of its strength ($\log K_{Cu(I)GSH_2, Cu^+}^{cond} = 32.1$; Leal and van den Berg 1998).

However, more recent data indicates that GSH forms a weak complex with Cu(I) ($\log K_{Cu(I)GSH, Cu^+}^{cond} = 11.9$; Walsh and Ahner 2013), and would have only bound ~5% of the 1 nM Cu' in the uptake assay (using a side reaction coefficient of $10^{4.95}$; Walsh and Ahner 2013). Thus, the GSH treatments are effectively inorganic Cu treatments.

Uptake rate measurements with either Cu-ligand complex were performed with 1 nM Cu. This concentration is within the range of total dissolved Cu concentrations in surface waters (0.5 to 3 nM). The Cu(II)Cyclam complex was prepared in a 1:3 Cu:L ratio in order ensure complete complexation of Cu(II), and to mimic the 3 to 5-fold excess concentration of strong Cu ligands in surface waters (Coale and Bruland 1989; Moffett and Dupont 2007; Bundy et al. 2013). GSH was added in a 10:1 ratio (see below).

3.2.2.2 Preparation of ^{64}Cu -Ligand Complexes

The ^{64}Cu (37 MBq) was delivered in 10 μL of 0.1 M HCl. This was diluted 100-fold with a solution of CuSO_4 prepared in ultrapure water ($18 \text{ M}\Omega \text{ cm}^{-1}$ Milli-Q water; Millipore), resulting in a total Cu concentration of 50 μM (hereafter referred to as the ^{64}Cu stock). A 12.5 mM primary Cyclam stock was prepared as previously described (Semeniuk et al. 2009) and stored in the dark at 4 $^\circ\text{C}$ until used. An aliquot of the ^{64}Cu stock was mixed with a three-fold molar

excess of Cyclam in a 3 mL polypropylene vial and allowed to complex for 1 hour at pH ~5. Given the high thermodynamic equilibrium constant for Cu(II)Cyclam ($10^{26.5}$; Martell and Smith 2004), the complex would have formed rapidly in the absence of competing divalent metals such as Ca^{2+} and Mg^{2+} that are present in seawater. An aliquot of the resulting $^{64}\text{Cu(II)Cyclam}$ complex was added to 50 mL of the uptake assay media (chelexed synthetic ocean water containing 100 μM silicic acid, 10 μM phosphate, and 300 μM nitrate) at a final ^{64}Cu concentration of 1 nM, and allowed to equilibrate for two hours.

Reduced glutathione is oxidized by Cu(II) spontaneously due to the standard reduction potentials of Cu(II)/Cu(I) (0.15 V) and reduced/oxidized glutathione (0.232 V) (Mills et al. 1993). Glutathione forms a weak 1:1 complex with Cu(I) in seawater (Walsh and Ahner 2013). This complex is stable for at least 5 hours in oxygenated water if the initial GSH:Cu(II) ratio is greater than 3:1 (Ciriolo et al. 1990). Thus, we chose a 10:1 ratio of GSH:Cu for the $^{64}\text{Cu(I)GSH}$ complex to ensure the complex remained stable during the assay. A fresh 5 μM GSH stock was made 30 minutes prior to preparing the $^{64}\text{Cu(I)GSH}$ complex. GSH is stable in oxygenated water for at least 60 minutes (Speisky et al. 2011). An aliquot of the ^{64}Cu stock was mixed with a ten-fold molar excess of GSH and allowed to react for one hour at pH ~5. After 15 minutes, the Cu(II) should have been reduced and the Cu(I) completely complexed (Speisky et al. 2008). An aliquot of the resulting $^{64}\text{Cu(I)GSH}$ solution was added to 50 mL SOW and allowed to equilibrate for 2 hours.

The background Cu contamination in our chelexed SOW is less than 0.1 nM (R. Bundy, *pers. comm.*). Thus, the specific activity of the added Cu would not have been significantly changed

by background Cu contamination in the assay media. Furthermore, the addition of excess ligand in each assay would have ensured the complete complexation of the background Cu.

3.2.2.3 *Thalassiosira pseudonana* HACuTS Competitive Inhibitors

The substrate for the HACuTS in *T. pseudonana* was determined using selective competitive inhibitors for Cu uptake (Table 3.2). *Thalassiosira pseudonana* was grown in low Cu containing media (0.6 nM total dissolved Cu) to ensure the HACuTS was up-regulated (Guo et al. 2010). Platinum(II) competes with the ferrireductase in yeast (Eide et al. 1992) and *T. oceanica* (Maldonado and Price 2001). The ferrireductase involved in the HAFETS in *C. reinhardtii* can also reduce Cu(II) (Hill et al. 1996). Thus, to determine whether Cu(II) bound to Cyclam is reduced prior to being internalized as Cu(I), uptake assays were performed with 100 nM Pt(II) additions. Due to the low solubility of Pt(II), a stock solution of 5 mM of Pt(II)Cl₂ was dissolved in 0.1 M HCl for 2 weeks prior to the uptake experiments. The solution was filtered through a 0.22 μm filter (Acrodisc; Pall) to remove any particulate Pt(II)Cl₂ before being added to the uptake assay. The 100 nM Pt(II) addition is similar to that used previously (70 nM; Maldonado and Price 2001). The addition of Pt(II) had no effect on the pH of the uptake assay (8.1).

Organically complexed Fe(III) is reduced by the FRE surface ferrireductase in marine diatoms (Maldonado and Price 2001). If Cu(II) is also reduced by FRE, then the addition of Fe(III)-ligand would compete with the reductase active site and inhibit Cu uptake. Thus, Cu uptake from Cyclam was measured in the presence of 500 nM Fe(III) bound to the siderophore desferrioxamine B (DFB). Iron was bound to 5% excess DFB (i.e. 525 nM) to ensure it was completely complexed, and the FeDFB complex was prepared as previously described

(Maldonado and Price 2001). The 5% excess DFB (25 nM) addition would have little effect on Cu speciation in the uptake assay due to the relatively weak complex it would form with Cu(II) in seawater. Although the conditional stability constant of Cu(II)DFB is unknown, the thermodynamic stability constant is lower ($10^{14.1}$) than the $K_{CuL,Cu^{2+}}^{cond}$ for Cu(II)Cyclam ($10^{15.29}$) (Liu and Hider 2002; Chapter 2). Thus, the $K_{CuL,Cu^{2+}}^{cond}$ for Cu(II)DFB would be considerably lower than $10^{14.1}$, and the Cu(II)Cyclam complex would be the dominant species in the uptake assay.

The sulfur-containing binding sites in the active site of CTR can also bind and transport Ag(I) (Lee et al. 2002; Bertinato et al. 2010). To determine whether Cu(I) was the substrate of transport from Cu(II)Cyclam, 500 nM Ag(I) was added. To confirm that the substrate of Cu uptake in the GSH treatment was also Cu(I), we measured Cu uptake in the presence of 500 nM Ag(I). A 500 μ M Ag(I)NO₃ stock was prepared 24 h before the uptake experiments in MQ water. The addition of Ag(I) has no effect on the pH of the final uptake assay solution.

Lastly, the effect of increasing excess Cyclam on Cu acquisition in *T. pseudonana* was determined by comparing uptake rates of 1 nM Cu' with three concentrations of Cyclam (3, 100, and 1000 nM).

3.2.2.4 Copper Uptake Assay

All uptake experiments were performed in biological triplicates. Manipulations to the cultures and uptake assay solutions were performed inside a class 100 laminar flow hood. For *T. pseudonana*, 2 L cultures were grown to mid-exponential phase. Using trace metal clean

techniques, between 150 and 250 mL of culture was gently vacuum filtered (< 100 mm Hg) onto acid cleaned (1 week in 0.1 M HNO₃ and rinsed with MQ) 2 µm porosity polycarbonate filters (47 mm diameter; Sterlitech) using an acid-cleaned polypropylene filtration stand (Nalgene). The filtered cells were rinsed with 50 mL of chelexed SOW to remove loosely associated metals from the culture media. The filters were immediately resuspended in the 50 mL uptake assay media, resulting in cell concentrations ranging between 0.55 and 1.9 million cells mL⁻¹. For up to 110 minutes, every 15 to 20 minutes, a 5 to 10 mL sample was taken from each assay bottle and gently vacuum filtered onto a 25 mm 2 µm porosity polycarbonate filter. The cells were soaked in a 10 mM DTPA wash for 5 minutes (Croot et al. 2003), and subsequently rinsed with 5 mL chelexed SOW to remove any loosely associated tracer. The filters were removed and placed inside a sample vial, and the ⁶⁴Cu activity was measured with a PerkinElmer 1480 WIZARD 3'' Gamma Counter (PerkinElmer Inc., Waltham, MA, USA). The specific activity of Cu (DPM mol⁻¹) added to each uptake assay bottle was determined by measuring ⁶⁴Cu activity in duplicate 1 mL samples of the assay media, and this value was used to calculate cellular Cu concentrations at each time point. Uptake assay experiments lasted between 85 and 115 minutes. For *T. oceanica*, *P. pouchettii*, and *C. polylepis*, triplicate 250 mL cultures were grown to mid-exponential phase, and the same protocol was followed for measuring Cu uptake from Cu(II)Cyclam and Cu(I)GSH as described for *T. pseudonana*.

In order to determine the contribution of non-specific adsorption of ⁶⁴Cu to the cells surfaces and polycarbonate filters, a 5 mL subsample of each assay was taken after 1-2 minutes exposure to the isotope, filtered, and processed as described above. Non-specific adsorption accounted for

between 3 and 15% of the particulate ^{64}Cu measured during the first time point (with higher values for the inorganic Cu treatment), and was subtracted from each subsequent sample.

Accumulation of Cu from Cu(II)Cyclam and Cu(I)GSH by *T. oceanica*, *P. pouchettii*, and *C. polylepis* was linear over time (1 to 1.5 hours; data not shown), and uptake rates ($\text{zmol Cu cell}^{-1} \text{h}^{-1}$) were determined from the slope of cellular Cu versus time. Similarly, Cu accumulation from the Cu-ligand complexes in the first *T. pseudonana* replicate (replicate A) was also linear over time (Figure 3.1). However, accumulation of Cu' in replicate A was linear for the first 30 minutes, and then decreased to a plateau. This also occurred for uptake from Cu(II)Cyclam in replicates B and C (Figure 3.2). Replicates B and C had 2-3 times more cells than replicate A. Using the Cu uptake rate from the Cu(II)Cyclam complex in replicate A, we calculated that half of the total dissolved ^{64}Cu would be acquired by *T. pseudonana* after 45 and 30 minutes in replicates B and C, respectively. Similarly, drawdown of unchelated Cu' would have occurred via uptake and adsorption to the cell surface. Thus, removal of Cu from the assay media resulted in slower observed accumulation of intracellular Cu. As a result, uptake rates for the Cu' treatments, and for all treatments in replicates B and C were determined using the first sampling time, assuming Cu accumulation was linear during the first 20-30 minutes of the assay (c.f. Guo et al. 2010).

It is possible that the addition of the competitive inhibitors could have a short-term acute toxic effect on the physiology of *T. pseudonana*. Thus, carbon fixation from $\text{H}^{14}\text{CO}_3^-$ was monitored in each assay. Approximately 75 kBq of $\text{H}^{14}\text{CO}_3^-$ was added to each assay bottle. Intracellular fixed carbon concentrations were determined at the end of each assay via filtration onto 25 mm

GFF filters (AMD). Filters were acidified with 6 N HCl, allowed to degas for 48 h, and immersed in scintillation cocktail (Scintisafe 50%, Fisher). The activity of fixed ^{14}C was determined using a Beckman LS65005514 scintillation counter with an internal ^{14}C quench curve.

3.2.3 Statistical Analyses

We hypothesized that complexation of Cu(II) by Cyclam will cause uptake rates to decrease compared to the Cu' or Cu(I)GSH treatments (effectively, a Cu' treatment; see section 3.2.2.1). Furthermore, we hypothesized that the addition of the competitive inhibitors targeting the HACuTS and increasing Cyclam concentration would cause uptake rates to decrease. Thus, each hypothesis was tested using a one-way student's t-test (unequal variances), and statistically significant differences ($p < 0.05$) are reported. Cell surface area normalized uptake rates for each complex were compared among the three species grown in high Cu media (one-way ANOVA, Tukey test).

3.3 Results

3.3.1 Cu Uptake by *T. pseudonana* Grown in Low Cu

Copper uptake rates ranged between 0.43 ± 0.10 and 8.79 ± 0.79 $\text{zmol Cu } \mu\text{m}^{-2} \text{ h}^{-1}$ (Table 3.3). Uptake was fastest for the Cu' treatment, and was 21% ($p = 0.0144$) and 32% ($p = 0.0380$) slower in the Cu(I)GSH and Cu(II)Cyclam treatments, respectively. Increasing the Cyclam concentration from 3 to 100 and 1000 nM caused uptake rates to decrease 69% ($p = 0.0038$) and 93% ($p = 0.0027$), respectively. Uptake rates exceeded the maximum diffusive supply of Cu' to

the cell surface by 459 to 16261 times in the Cu(II)Cyclam treatments (Table 3.4). Uptake rates in the 1 nM Cu' treatment did not exceed J_D .

3.3.2 Competitive Inhibition of the HACuTS in *T. pseudonana* Grown in Low Cu

The addition of all three competitive inhibitors resulted in decreased uptake rates in *T. pseudonana* (Figures 3.3 and 3.4). Uptake from Cu(II)Cyclam decreased 13% and 30% in the Pt(II) and FeDFB treatments compared to the control, respectively, but only the latter was statistically significant ($p = 0.0494$). The Ag(I) addition caused uptake from Cu(II)Cyclam and Cu(I)GSH to decrease 68% ($p = 0.0068$) and 66% ($p = 0.0027$).

3.3.3 Cu Uptake Rates of Phytoplankton Grown in High Cu Media

Copper uptake rates varied an order of magnitude between the three species grown in media containing 10.2 nM total dissolved Cu, and were similar for the Cu(II)Cyclam (0.38 ± 0.13 to 3.13 ± 0.55 $\text{zmol Cu } \mu\text{m}^{-2} \text{ h}^{-1}$) and Cu(I)GSH (0.47 ± 0.18 to 3.92 ± 0.29 $\text{zmol Cu } \mu\text{m}^{-2} \text{ h}^{-1}$) treatments (Table 3.5). Copper uptake rates in both treatments in *T. oceanica* were significantly faster than the two prymnesiophytes, and uptake rates by *C. polylepis* were significantly faster than *P. pouchetii* ($p < 0.001$; ANOVA, Tukey-test). Uptake rates exceeded the supply of Cu' to the cell surface (J_D) in all species for Cu(II)Cyclam (Table 3.4). Uptake from Cu(II)Cyclam in *P. pouchetii* and *C. polylepis* were 28 and 49 times faster than J_D , respectively, while uptake rates exceeded J_D by 292 times in *T. oceanica*.

3.3.4 Short-Term Accumulation of Cu and C in *T. pseudonana*

Carbon fixation varied 20-fold among all treatments and replicates (0.08 to 1.67 fmol C cell⁻¹ min⁻¹) (Figure 3.5). The fastest rates are similar to an estimated steady-state C-fixation rate (~1.4 fmol C cell⁻¹ min⁻¹) that was calculated using published intracellular C concentrations (11 M; Maldonado and Price 1996), the cell volume (~87 fL cell⁻¹) and the average growth rate measured for the three replicate cultures (2.2 d⁻¹). Carbon fixation was faster in treatments with faster Cu uptake rates (e.g. Cu(II)Cyclam and Cu' treatments), and slowest in treatments with the slowest Cu uptake rates (e.g. Cu(II) with 100 and 1000 nM excess Cyclam). For all treatments, C-fixation was fastest for replicate A, and tended to decrease with each subsequent replicate.

Average assay cell concentrations were lowest in replicate A (~0.5 million cells mL⁻¹), and were higher in replicates B (~1 million cells mL⁻¹) and C (~1.6 million cells mL⁻¹). This corresponded with a significant drawdown of the total dissolved Cu added to each assay bottle in replicates B and C (Figure 3.2). Since there were 50% more cells in replicate C than B, drawdown of the total added dissolved Cu occurred faster (~50% drawdown after 30 minutes in replicate C compared to 45 minutes in replicate B). In turn, this resulted in a smaller accumulation of intracellular cellular C during the uptake assay. For example, at the end of the Cu(II)Cyclam treatment assay, approximately 50% less Cu accumulated in the cells in replicate C (342 fmol Cu cell⁻¹) than in B (703 fmol Cu cell⁻¹) (Figure 3.2). This corresponded with ~50% less cellular fixed carbon in replicate B (129 fmol C cell⁻¹) than C (63 fmol C cell⁻¹). There was a positive correlation between the final accumulated cellular C and Cu concentrations for all treatments and replicates (Figure 3.6; R² = 0.70; p < 0.0001). This suggests that individual amendments to the uptake assay treatments were not uniquely causing C-fixation to decrease. Rather, the presence

of Cu transporter competitive inhibitors, and thus decreased cellular Cu accumulation during the uptake assay, caused C-fixation rates to decrease. In support of this, the accumulation of intracellular Cu by the end of the uptake assays in replicates B and C of the Cu(II)Cyclam (1:3 ratio) treatment decreased sequentially due to higher cell abundances and complete drawdown of the total dissolved Cu provided in the assay. Similarly, the accumulation of fixed carbon was also lower in replicates B and C, and was similar to the decrease in Cu accumulation. This suggests that carbon fixation by *T. pseudonana* grown in low Cu media is metabolically dependent on intracellular Cu. Further research is warranted to elucidate a physiological mechanism for this effect.

3.4 Discussion

3.4.1 Acquisition of Organically Complexed Cu(II) by Marine Phytoplankton

Here we present the first Cu uptake rate measurements in marine phytoplankton cultures using Cu concentrations and speciation that mimic open ocean surface waters and show that Cu within a strong organic complex was bioavailable. Copper uptake from Cu(II)Cyclam exceeded J_D of Cu' in all four phytoplankton species surveyed, and was up to 16000 times faster than the J_D in *T. pseudonana* (Table 3.4). Furthermore, the Cu uptake rates in the Cu(II)Cyclam treatment measured for *P. pouchetti* (28 ± 10 zmol Cu cell⁻¹ h⁻¹) and *C. polylepis* (57 ± 9 zmol Cu cell⁻¹ h⁻¹) – both strains isolated near station P26 (50°N 145°W) – are similar to uptake by an indigenous phytoplankton community sampled at P26 (39 zmol Cu cell⁻¹ h⁻¹) that was dominated by prymnesiophytes (60% of the total chl *a*). Thus, acquisition of Cu(II) from within strong organic Cu complexes may be common among eukaryotic marine phytoplankton.

Uptake of Cu from Cyclam was significantly faster for *T. oceanica* than the prymnesiophytes, despite similar growth rates (Table 3.5). Previous steady-state Cu uptake rate measurements were also faster (~2-4 times) in *T. oceanica* than the two prymnesiophytes (Annett et al. 2008; Guo et al. 2012). The intracellular Cu quota of *T. oceanica* ($2.93 \mu\text{mol Cu mol C}^{-1}$) grown under the same culture conditions as in this study was 2.1 and 2.5 times higher than the quotas of *P. pouchetii* ($1.38 \mu\text{mol Cu mol C}^{-1}$) and *C. polylepis* ($1.15 \mu\text{mol Cu mol C}^{-1}$), respectively (Annett et al. 2008; Guo et al. 2012). Thus, the faster short-term uptake rates measured in *T. oceanica* likely reflect its higher intracellular Cu requirements, and may be due to a higher abundance of Cu transport proteins at the cell membrane.

Since GSH is a relatively weak Cu(I) chelator, the GSH treatment is effectively an inorganic Cu treatment (see section 3.2.2.1). Compared to the Cu(II)Cyclam treatment, the Cu uptake rates in the CuGSH treatment were only marginally reduced in *T. pseudonana* (32%), *T. oceanica* (20%), and *C. polylepis* (45%), and were not significantly reduced in *P. pouchetti*. Thus, despite its high Cu binding strength, ligands like Cyclam do not appear to make Cu significantly less bioavailable. Although this appears to be counterintuitive, the similarity between uptake rates of inorganic and organically complexed Cu can be reconciled if reduction of Cu(II) is the rate-limiting step for transport (see below).

3.4.2 Mechanism of Cu Acquisition from Strong Organic Ligands in *T. pseudonana*

Grown in Low Cu Media

3.4.2.1 Cell Surface Cu(II) Reduction

In most eukaryotes, Cu(II) can be reduced at the cell surface by a FRE-encoded transition metal reductase that is capable of reducing both Fe(III) and Cu(II) (e.g. Hassett and Kosman 1996; Hill et al. 1996; Georgatsou et al. 1997). After reduction, Cu(I) is internalized by a high-affinity Cu transporter in the CTR family (reviewed by Pope et al. 2012). Cuprireductase activity has been observed in the photosynthetic eukaryotes *C. reinhardtii*, *Dunaliella tertiolecta*, and *T. weissflogii* (Jones et al. 1987; Hill et al. 1996), and putative *TpFRE1* and *TpFRE2* genes are upregulated during Fe-limitation in *T. pseudonana* (Kustka et al. 2007). Since Cu(II) inhibits Fe uptake in Fe-limited *T. pseudonana* (Hudson et al. 1990; Kustka et al. 2007), this may indicate that Cu(II) and Fe(III) are reduced by a shared reductase. When *T. pseudonana* was grown in low Cu media and exposed to a short-term supply of 500 nM Cu', only *TpFRE2* expression was downregulated (Guo et al. *submitted*). Thus, we hypothesized that, in *T. pseudonana*, Cu(II)Cyclam is reduced by the putative *TpFRE2* before Cu(I) is transported into the cell.

Thalassiosira pseudonana was grown in low Cu-containing media to ensure the HACuTS was upregulated. Uptake from Cu(II)Cyclam by *T. pseudonana* was 30% slower in the presence of Fe(III)DFB. Although the 25 nM uncomplexed DFB would not have impacted dissolved Cu speciation in the uptake assay (see section 3.2.2.3), the DFB could have competed with the transporter active sites for Cu (see section 3.4.4). However, the conditional stability constant of the Cu(II)DFB complex would likely be at least 4 to 5 orders of magnitude lower than its thermodynamic stability constant ($\log K = 14.1$) due to side reactions with major cations in

seawater. Since the addition of 99 nM uncomplexed Cyclam ($\log K = 26.5$) only caused a 59% decrease in Cu uptake rates, it is unlikely that an addition of 25 nM of uncomplexed DFB, a much weaker ligand, would cause uptake rates to decrease by 30%. Thus, the effect of the Fe(III)DFB treatment on Cu uptake from Cyclam likely reflects competition between Cu(II)Cyclam and Fe(III)DFB at the reductase site.

Even though the reduction potential of Cu(II)Cyclam is theoretically too negative (half-wave reduction potential = -820 mV; Croot et al. 1999) to be reduced by a typical reductase, ternary complex formation could reduce its reduction potential (Albrecht-Gary and Crumbliss 1998). Cyclam forms a square planar complex with Cu(II) (Figure 7), whereby the four equatorial coordination sites are bound to nitrogen, and the two remaining axial coordination sites are coordinated by H₂O. These two axial sites would provide an opportunity for a putative reductase to form a ternary complex with Cu(II) bound to cyclam, thereby reducing the reduction potential of the Cu(II)Cyclam to within the range of the reductase (-250 mV for yeast; Shatwell et al. 1996). Reduction of Cu(II) likely proceeds via an outer sphere electron transfer reaction. Copper(I) does not form a stable complex with cyclam (Zanello et al. 1982), and thus would quickly be stripped from the ligand by the reductase or CTR active site. This mechanism has been demonstrated for the reduction of strongly complexed Fe(III) (Mies et al. 2006), and likely accounts for the observed uptake rates presented herein. Thus, the coordination of Cu(II)-ligand complexes may play an important role in determining the bioavailability of CuL complexes. Further work exploring uptake rates of Cu(II) bound to ligands of varying Cu(II) binding strength and coordination geometries is warranted.

3.4.2.2 Cu(I) Transport

Following reduction of Cu(II) by eukaryotes, Cu(I) is then internalized by a CTR Cu transporter (reviewed by Pope et al. 2012). Although amino acid sequences differ among CTR genes in eukaryotes, a Cu(I) binding motif made up of histidine, methionine, and cysteine residues is highly conserved (Rubino et al. 2010). This motif was found in two putative CTR genes in *T. pseudonana* (*TpCTR|24275* and *TpCTR|9391*) (Guo et al. *submitted*). Like *TpFRE2*, both *TpCTR* genes were downregulated (~2-fold) when *T. pseudonana* was amended with 500 nM Cu' (Guo et al. *submitted*), suggesting that these genes are involved in Cu transport. Thus, we hypothesized that Cu(I) was the substrate of the HACuTS in *T. pseudonana*. The 68% reduction of Cu uptake from Cu(II)Cyclam by *T. pseudonana* in the presence of 500 nM Ag(I) suggests Cu(I) is internalized following the reduction of Cu(II). Similarly, uptake rates in the Cu(I)GSH treatment, where Cu is primarily present as Cu(II)', decreased 66% with the addition of 500 nM Ag(I). The similar inhibition in uptake rates by the addition of Ag(I) in the Cu(II)Cyclam and Cu(II)' treatments suggests that both inorganic and organically complexed Cu are substrates for the HACuTS in *T. pseudonana*, and that Cu(II) has to be reduced prior to internalization as Cu(I).

The oxidative half-life of Cu(I)' in seawater is ~12 min at pH 8.11 and 25°C (González-Dávila et al. 2009) due to stabilization of Cu(I) by chloride ions. The turnover time of the Cu transporter in the cyanobacterium *Synechococcus* sp. DC2 is considerably faster (3 to 40 s) than Cu(I) oxidation (Croot et al. 2003). Assuming the Cu(I) transporter in *T. pseudonana* has a similar turnover time, Cu(I) produced by a reductase would be present in the extracellular milieu long enough to be acquired. The Cu(I) binding motifs in the putative *TpCTR* active sites are enriched

in cysteine compared to methionine (Guo et al. *submitted*). Although cysteine is more susceptible to oxidation in oxic environments, it has a higher affinity for Cu(I) than methionine in slightly basic solutions (pH 7.5) (Rubino et al. 2011). Therefore, cysteine-rich motifs are more suitable for CTRs in organisms that inhabit oceanic surface waters (pH = 8.1) with low Cu concentrations.

3.4.2.3 Reconciliation with the “Free Ion Model”

The Free Ion Model (FIM) was developed to account for early laboratory observations that phytoplankton growth rates and intracellular metal quotas co-varied with the “free” hydrated Me^{n+} concentration in the growth medium or uptake assay (reviewed by Campbell 1995; Hudson 1998; Sunda and Huntsman 1998). For metal substrates that abide the FIM, the turnover rate constant of the metal transporter (k_{in}) must be significantly lower than the dissociation (k_d) rate constant of the metal-transporter complex (MeT) at the cell surface (Hudson 1998; see section 1.1.2). An equilibrium is then established between Me^{n+} and the transporter (T), whereby $[MeT]$ at the cell surface is determined by $[Me^{n+}]$ in solution. Laboratory studies that support the FIM use a constant $[Me^{n+}]$ in the medium by buffering high total dissolved metal concentrations with high organic chelator concentrations. This ensures that $[Me^{n+}]$ does not decrease during the experiment, and thus cell surface $[MeT]$ remains constant. Although the FIM was developed to describe the acquisition of Me^{n+} , it should apply to any metal species (e.g. inorganic or organically complexed metals) for which $k_{in} \ll k_d$ (c.f. Hudson 1998). Thus, a more general equilibrium model can be employed that does not presume that Me^{n+} is the substrate for transport, but transport is still determined by a rapid equilibrium established by the transportable metal species and the transporter.

There are two important kinetic exceptions to the FIM. First, for metals that are transported at rates that are faster than the diffusive supply of the bioavailable metal species to the cell surface, a diffusive gradient forms between the bulk medium and the cell surface (the diffusive boundary layer; DBL). If dissociation of MeL within the DBL and diffusion of the transported metal substrate across the DBL is the rate-limiting step to transport, then a transport system that is normally under equilibrium control appears to be under kinetic control (e.g. Zn transport; Hudson 1998). The second exception occurs when $k_{in} \gg k_d$. Under this condition, $[MeT]$ is not determined by the equilibrium concentration of $[MeT]$ established by $[T]$ and $[Me^{n+}]$, but rather by the steady-state formation rate of MeT . For example, Fe bound to the high-affinity Fe transport system in *T. weissflogii* is not at equilibrium with the seawater medium (Hudson and Morel 1990). Indeed, k_f for Fe(III)' binding with surface Fe transporters ($\sim 1 \times 10^6 \text{ M}^{-1} \text{ s}^{-1}$) was between the first inner water loss rate from the inner solvent coordination sphere (k_w) of $\text{Fe}(\text{OH})^{2+}$ ($\sim 1 \times 10^5 \text{ M}^{-1} \text{ s}^{-1}$) and $\text{Fe}(\text{OH})_2^+$ ($\sim 1 \times 10^7 \text{ M}^{-1} \text{ s}^{-1}$), the Fe(III) species in seawater with the fastest water loss kinetics (Hudson and Morel 1990). This indicates that complexation of inorganic metal species by surface transporters, like strong organic ligands in solution, follows an Eigen-Wilkins mechanism. Thus, the upper limit for Fe' uptake is determined by kinetic constraints (i.e. k_w).

It is difficult to experimentally determine whether a metal transporter is under equilibrium or kinetic control. The latter kinetic exception (when $k_{in} \gg k_d$) of a transport system has only been demonstrated for one metal (Fe) based on pulse-chase experiments using ^{59}Fe , and assuming that all surface-associated Fe in the experiment was transporter bound (Hudson and Morel 1990). Although we did not perform similar pulse-chase experiments, using the data presented herein

we can infer that Cu uptake in *T. pseudonana* is under kinetic control, and the rate-limiting step of transport is reduction. Assuming that reduction of Cu(II) bound to Cyclam is the sole route of access for strongly complexed organic Cu(II) by surface transporters, it is prudent to assume that a single transport system is responsible for reducing Cu(II)' and Cu(II)Cyclam.

The first step in reduction of Cu(II) would involve the formation of an outer sphere electrostatic complex between the Cu(II) species and the surface reductase (*R*), followed by formation of a ternary complex between Cu(II)L_X and *R*, in which X denotes either organic or inorganic ligands, including coordinating water molecules of “free” Cu. For inorganic Cu(II) complexes, complexation by organic ligands (or the reductase Cu binding site) follows an Eigen-Wilkins mechanism, and the rate limiting step for complex formation is determined by inner coordination sphere water loss kinetics (Morel and Hering 1993). The forward reaction rate constant for complex formation is approximately $k_f \approx K_{OS} \times k_{-w}$, in which K_{OS} is the outer sphere electrostatic complex formation constant. K_{OS} varies between 0.3 and 8 M⁻¹ for metals in seawater (Morel et al. 1991), while k_{-w} is $\sim 10^9$ s⁻¹ for Cu²⁺ (Hudson 1998), and so k_f for Cu(II)-ligand complex formation would vary between 10^{8.5} and 10^{9.4} M⁻¹ s⁻¹. To our knowledge, the forward reaction rate constants of formation of the ternary complex between Cu(II)Cyclam and other ligands has not been reported. For other metals, such as Fe, the forward reaction rate for the formation of a ternary complex between a strong Fe(III) ligand (e.g. Fe(III)DFB) and a strong Fe(II) ligand is orders of magnitude lower than the k_f of Fe(III)L complex formation (Hudson et al. 1990; Mies et al. 2006). Therefore, under the worse case scenario, if the forward rate constant for ternary complex formation between the Cu(II)Cyclam and the reductase is only an order of magnitude lower than k_f for complexation of Cu(II)' by the reductase, then uptake of Cu(II) from Cyclam

would have been significantly slower than uptake of Cu(II)'. However, uptake rates were marginally slower in the Cu(II)Cyclam treatment (32%), indicating that ternary complex formation was unlikely the rate limiting step during Cu transport.

Instead, we propose that reduction of Cu(II)L_x by the putative reductase is the rate-limiting step for transport, and Cu uptake is determined by the steady-state production of Cu(I) at the cell surface (similar to the Fe(II)s model; Maldonado and Price 2001; Shaked et al. 2005).

Interestingly, reduction of Fe(III)L by the diatom *T. oceanica* is inversely correlated to the log of the ratio of $K_{Fe^{3+}} / K_{Fe^{2+}}$, and varies ~2-fold as the log of the ratios ranged between 7.3 and 16.3 for the weakest and strongest ligands, respectively (Maldonado and Price 2001). This is because the reduction rate constant is related to the reduction potential of the metal complex, which is in turn related to $\log(K_{Me^{n+}} / K_{Me^{n-1}})$ (Heyrovsky and Kuta 1966 in Maldonado and Price 2001). If Cu(II) reduction is the rate limiting step for uptake, then uptake rates should inversely vary with $\log(K_{Cu(II)L} / K_{Cu(I)L})$. Unfortunately, we are unaware of thermodynamic $\log K_{Cu(II)L}$ and $\log K_{Cu(I)L}$ data for Cyclam (see Zanello et al. 1982), and so we are unable to make this comparison.

3.4.3 Influence of Ligands on Cu Availability and Implications for Culture Studies

These results have important implications for interpreting previous laboratory investigations of Cu limitation and toxicity. Previous laboratory Cu uptake studies used much higher Cu(II)-binding ligand concentrations than the work presented here. The effect of excess Cyclam on Cu uptake by *T. pseudonana* was investigated in order to compare the rates reported herein with those previously published. Although a small addition (3 nM) of Cyclam had a small effect on

Cu uptake compared to the Cu' treatment, increasing Cyclam concentrations to 1000 nM caused Cu uptake rates to decrease 93% compared to the 3 nM Cyclam treatment. These slower uptake rates are not due to changes in the Cu speciation in the assay (i.e. lower Cu') since uptake rates were at least 459 times faster than J_D in the three treatments. Thus, excess Cyclam was inhibiting Cu transport in *T. pseudonana* that was not due to its effect on Cu speciation in the medium.

In order to determine how excess Cyclam might cause Cu uptake rates to decrease, we looked to similar investigations of Fe uptake in marine phytoplankton. Excess ligands can compete with components of the HAFETS, whereby high concentrations of strong or weak Fe(II) ligands can compete with Fe(II) produced at the cell by the ferrireductase (Maldonado and Price 2001; Shaked et al. 2005). While dissolved Fe concentrations are kept the same, increased ligand concentrations cause Fe uptake rates to decrease as ligand concentrations increase (Maldonado and Price 2001; Shaked et al. 2005). Uptake of 45 nM Fe bound to 10% excess DFB decreases significantly when 1 μ M additional DFB is present (Shaked et al. 2005). This is likely due to competition between DFB and components of the HAFETS. Weaker ligands, like EDTA, can also compete with the HAFETS when present in very high concentrations (100 to 1000 μ M) (Shaked et al. 2005). Similarly, short-term uptake rates of 2 nM Cu(II) bound to 100 μ M EDTA were between 33 and 100-times slower (13 ± 4 and 5.5 ± 2.5 $\text{zmol Cu cell}^{-1} \text{h}^{-1}$, accounting for the differences in Cu concentrations used in the two uptake assays; refer to Table 3.5) than uptake of 1 nM Cu(II) bound to 3 nM Cyclam in *T. pseudonana* and *T. oceanica*, respectively (Guo et al. 2010). Steady-state uptake rates of cultures grown with 100 μ M EDTA were also slower – between 5 and 48 times – than Cu(II)Cyclam uptake by the four species surveyed

(Table 3.5). As observed for Fe, we suggest that reduction of Cu uptake rates in the presence of excess Cyclam or high EDTA concentrations is due to competition for Cu(I) between the ligands and components of the proposed HACuTS.

Ultimately, the FIM is a model that can predict the Cu nutritional state of a phytoplankton community in natural waters. Laboratory studies used high concentrations (100 μM) of either NTA or EDTA to maintain constant Cu' concentrations in culture media, and monitored phytoplankton growth rates in order to determine when phytoplankton experienced Cu limitation and toxicity (e.g. Anderson and Morel 1978; Brand et al. 1986; Sunda and Huntsman 1995b; Annett et al. 2008; Guo et al. 2010). This work effectively produced a calibration for phytoplankton health and Cu', a parameter that could be measured in natural waters. However, the high ligand concentrations in previous work would compete with Cu transporters, resulting in artificially slower Cu uptake rates. Thus, the concentration of total dissolved Cu or Cu' at which phytoplankton begin to experience toxicity would be lower if there was no competing ligand. Since uptake of 1 nM Cu(II)Cyclam (1:3 ratio) by *T. oceanica* and *T. pseudonana* was up to 100-times faster than uptake of Cu bound to 100 μM EDTA, Cu concentrations reported to cause toxicity in lab studies may be overestimates. Similarly, investigations of Cu-limitation would also be affected by high ligand concentrations. High excess ligand concentration would be competing with cell surface transporters for Cu, resulting in slower uptake rates. Phytoplankton would experience Cu-limitation at higher Cu concentrations than if the excess ligands were not present. This would result in an overestimate of the Cu concentrations reported to cause limitation.

Copper binding ligand concentrations in surface waters are much lower (3 to 10 nM; Coale and Bruland 1988; Moffett and Dupont 2007; Buck et al. 2010; Bundy et al. 2013; Jacquot et al. 2013; Chapter 5) than the ligand concentrations typically used in laboratory studies. Thus, previous laboratory growth rate data in response to varying Cu' concentrations are likely unrepresentative of how *in situ* phytoplankton communities would respond to the same Cu' concentrations. Recent measurements of low inorganic Cu concentrations ($<10^{-13.5}$ M) in surface waters are similar to those that limit phytoplankton growth in laboratory studies, and have led a few authors to suggest that Cu could limit *in situ* phytoplankton community growth (e.g. Moffett and Dupont 2007; Jacquot et al. 2013). However, since strongly complexed Cu(II) is as bioavailable as Cu(II)', and *in situ* organically complexed Cu is bioavailable (Chapter 2), limitation of phytoplankton growth by Cu seems unlikely (see chapter 4). The results presented herein emphasize the importance of carefully choosing Cu and ligand concentrations when investigating Cu uptake. Future laboratory studies of phytoplankton growth responses to Cu availability would benefit from using Cu and ligand concentrations that are typical of oceanic surface waters.

3.5 Tables

Table 3.1. Species, class, clone, cell diameter (μm), and isolation site of the marine phytoplankton used in this study.

Species	Class	Clone	Diameter	Isolation Site
<i>Thalassiosira pseudonana</i> Hasle et Heimdal	Bacillariophyceae	3H, NEPCC 58	5.5 μm	Moriches Bay, NY
<i>Thalassiosira oceanica</i> Hasle	Bacillariophyceae	CCMP 1003	6.7 μm	Sargasso Sea
<i>Chrysochromulina polylepis</i> Manton et Parke	Prymnesiophyceae	NEPCC 242	5.2 μm	49°36' N, 140°37' W
<i>Phaeocystis pouchetti</i> (Har.) Lagerh.	Prymnesiophyceae	CCMP 2495	4.8 μm	49°52' N, 142°40' W

Table 3.2. Competitive inhibitors used to target the components of the proposed high-affinity Cu transport system (HACuTS) in *T. pseudonana*. Short-term Cu uptake assays were performed with either 1 nM Cu(II) bound to 3 nM Cyclam, or 1 nM Cu bound to 10 nM reduced glutathione (GSH). Due to the weak complex formed between Cu(I) and GSH (see section 3.2.2.1), the Cu species in this treatment is effectively Cu'.

CuL Substrate	HACuTS Target	Competitive Inhibitor
Cu(II)Cyclam	Reductase	500 nM FeDFB
	Reductase	100 nM Pt(II)
	Cu(I) Permease	500 nM Ag(I)
		100-1000 nM Cyclam
Cu(I)GSH	Cu(I) Permease	500 nM Ag(I)

Table 3.3. Short-term Cu uptake rates by *T. pseudonana* ($\pm 1\sigma$; n=3) of inorganic Cu (Cu'), and Cu from within Cu(I)GSH and Cu(II)Cyclam complexes. Due to the weak complex formed between Cu(I) and GSH (see section 3.2.2.1), the Cu species in this treatment is effectively Cu'. The average growth rate for the triplicate cultures was $2.20 \pm 0.05 \text{ d}^{-1}$, and cell densities in the uptake assays ranged between 0.55 and 1.91 million cells mL^{-1} . The cultures were grown in Aquil containing 0.6 nM total dissolved Cu. A student's t-test (one-way, unequal variances) was used to compare uptake rates in the Cu' treatment with the Cu(I)GSH and Cu(II)Cyclam (1:3) treatments. Uptake in the Cu(II)Cyclam (1:3) treatment was also compared with rates in the 1:100 and 1:1000 Cu:Cyclam ratio treatments. Significant differences ($p < 0.05$) are in bold.

Treatment	Cu:L Ratio (nM)	-log[Cu'] (M) ^a	Cu Uptake Rate		p-value
			(zmol Cu cell ⁻¹ h ⁻¹)	(zmol Cu μm^{-2} h ⁻¹)	
Cu'	-	9	786 \pm 47	8.79 \pm 0.79	
Cu(I)GSH	1:10	9.05	618 \pm 97	6.38 \pm 1.03	0.0144
Cu(II)Cyclam	1:3	13.78	536 \pm 96	5.71 \pm 1.14	0.0380
	1:100	15.48	168 \pm 78	2.33 \pm 0.90	0.0038
	1:1000	16.48	38 \pm 15	0.43 \pm 0.10	0.0027

^aInorganic Cu concentrations were calculated for each treatment using $K_{CuL,Cu^{n+}}^{cond} = [CuL]/[Cu^{n+}][L]$ where $[Cu^{n+}] = [Cu']/\alpha_{Cu^{n+}}$, and $\alpha_{Cu^{n+}}$ is the side reaction coefficient for either Cu(II) (24; Coale and Bruland 1988) or Cu⁺ ($10^{4.95}$; Walsh and Ahner 2013). The $K_{CuL,Cu^{2+}}^{cond}$ used for Cyclam is $10^{15.29}$ (Chapter 2), and the K_{CuL,Cu^+}^{cond} used for GSH is 11.9 (Wash and Ahner 2013).

Table 3.4. Inorganic Cu concentrations ($[Cu']$), calculated Cu' diffusive fluxes (J_D), and the ratio of measured Cu uptake rates (ρCu) and J_D ($\rho Cu:J_D$) for each species and treatment of the Cu(II)Cyclam uptake assays reported in Tables 3.3 and 3.5.

Species	Media [Cu] (nM)	Cu:L Ratio (nM)	$-\log[Cu']$ (M) ^a	Cu' Diffusive Flux (J_D) (zmol Cu cell ⁻¹ h ⁻¹) ^b	$\rho Cu:J_D$
<i>C. polylepis</i>	10.2	Cu(II)Cyclam (1:3)	13.78	1.16	49
<i>P. pouchettii</i>	10.2	Cu(II)Cyclam (1:3)	13.78	1.01	28
<i>T. oceanica</i>	10.2	Cu(II)Cyclam (1:3)	13.78	1.50	292
<i>T. pseudonana</i>	0.6	Cu' (1:0)	9.00	10 ^{4.85}	0.010
		Cu(II)Cyclam (1:3)	13.78	1.17	459
		Cu(II)Cyclam (1:100)	15.48	10 ^{-1.63}	7189
		Cu(II)Cyclam (1:1000)	16.48	10 ^{-2.63}	16261

^aInorganic Cu concentrations were calculated for each treatment using $K_{CuL,Cu^{2+}}^{cond} = [CuL]/[Cu^{2+}][L]$ where $[Cu^{2+}] = [Cu']/\alpha_{Cu^{2+}}$, and $\alpha_{Cu^{2+}}$ is the side reaction coefficient for Cu(II) (24; Coale and Bruland 1988). The $K_{CuL,Cu^{2+}}^{cond}$ used for Cyclam was 10^{15.29} (Chapter 2).

^bMaximum diffusive fluxes (J_D) were determined using $J_D = 4\pi r D_{Cu^{2+}} [Cu']$, where r is the cell radius (μm), $D_{Cu^{2+}}$ is the diffusion coefficient for Cu²⁺ ($D_{Cu^{2+}} = 2.12 \times 10^{-10} \mu m^2 h^{-1}$; Gregory 1974), and $[Cu']$ is the inorganic Cu concentration (mol l^{-1}) in each assay (Wolf-Gladrow and Riebesell 1997). Dissociation of Cu(II)Cyclam is not a significant source of Cu' within the diffusive boundary layer for small cells ($<5 \mu m$; Chapter 2), so it was not calculated.

Table 3.5. Short-term uptake ($\pm 1\sigma$; n=3) of Cu in the Cu(II)Cyclam and Cu(I)GSH treatments by the species grown in Cu-replete media (10.2 nM), and previously published steady-state and short-term Cu uptake rates are included for comparison (see footnotes for details). Average growth rates for the triplicate are reported beneath each species name ($\pm 1\sigma$). Copper(II) was complexed with 3 nM Cyclam, while 10 nM GSH was added. Due to the weak complex formed between Cu(I) and GSH (see section 3.2.2.1), the Cu species in this treatment is effectively Cu^I. Short-term rates that were significantly faster in the Cu(I)GSH treatment are in bold (one-way student t-test, unequal variances). Copper uptake rates in both treatments were significantly different between *T. oceanica*, *C. polylepis*, and *P. pouchetii*.

Species	Uptake Type	CuL	Cu Uptake Rate ^c		p-value
			(zmol Cu cell ⁻¹ h ⁻¹)	(zmol Cu μm ⁻² h ⁻¹)	
<i>T. oceanica</i> (1.07 ± 0.04 d ⁻¹)	Short-term	Cu(I)GSH	546 ± 31	3.92 ± 0.29	0.0497
	Short-term	Cu(II)Cyclam	437 ± 83	3.13 ± 0.55	
<i>C. polylepis</i> (1.15 ± 0.03 d ⁻¹)	Short-term	Cu(I)GSH	104 ± 13	1.24 ± 0.16	0.0003
	Short-term	Cu(II)Cyclam	57 ± 9	0.67 ± 0.11	
<i>P. pouchetii</i> (1.18 ± 0.02 d ⁻¹)	Short-term	Cu(I)GSH	34 ± 13	0.47 ± 0.18	0.265
	Short-term	Cu(II)Cyclam	28 ± 10	0.38 ± 0.13	
<i>T. oceanica</i> ^a	Steady-state	Cu(II)EDTA		0.190 ± 0.011	
<i>T. pseudonana</i> ^b	Steady-state	Cu(II)EDTA		0.119 ± 0.012	
<i>C. polylepis</i> ^a	Steady-state	Cu(II)EDTA		0.046 ± 0.002	
<i>P. pouchetii</i> ^a	Steady-state	Cu(II)EDTA		0.076 ± 0.032	
<i>T. oceanica</i> ^c	Short-term	Cu(II)EDTA	13 ± 4		
<i>T. pseudonana</i> ^c	Short-term	Cu(II)EDTA	5.5 ± 2.5		
NE Pacific ^d	Short-term	Cu(II)Cyclam	39		
	Short-term	<i>In situ</i> CuL	331		

^aSteady-state Cu uptake rates reported elsewhere (Annett et al. 2008; Guo et al 2012). The rates were calculated from cellular Cu quotas (zmol Cu cell^{-1}) and growth rates (h^{-1}) measured in exponentially growing cells in Aquil containing 10.2 nM Cu and 100 μM EDTA. The rates presented were divided by 10.2 to account for the lower Cu concentration used in this study (1 nM).

^bSteady-state Cu uptake rate measured in exponentially growing cells in Aquil containing 2 nM Cu and 100 μM EDTA. The rates presented were divided by 2 to account for the lower Cu concentration used in this study (1 nM).

^cShort-term Cu uptake of 2 nM bound to 100 μM EDTA. Cultures were grown in Aquil containing 10.2 nM Cu (Guo et al. 2010). The rates presented were divided by 2 to account for the lower Cu concentration used in this study (1 nM).

^dAverage cellular Cu uptake rates reported for a natural phytoplankton assemblage in the northeast subarctic Pacific Ocean (Semeniuk et al. *submitted*). The assemblage was dominated by prymnesiophytes (60% of the total chl *a* concentration). For the Cu(II)Cyclam treatment, 1 nM Cu was complexed to 10 nM ligand. For the *in situ* treatment, a carrier free ⁶⁷Cu tracer was allowed to equilibrate with the *in situ* Cu-complexes (2.1 nM).

^eAverage cell densities ($\pm 1\sigma$) in the uptake assays were 39000 ± 2500 cells mL^{-1} for *T. oceanica*, 510000 ± 26000 cells mL^{-1} for *C. polylepis*, and 350000 ± 31000 cells mL^{-1} for *P. pouchetii*.

3.6 Figures

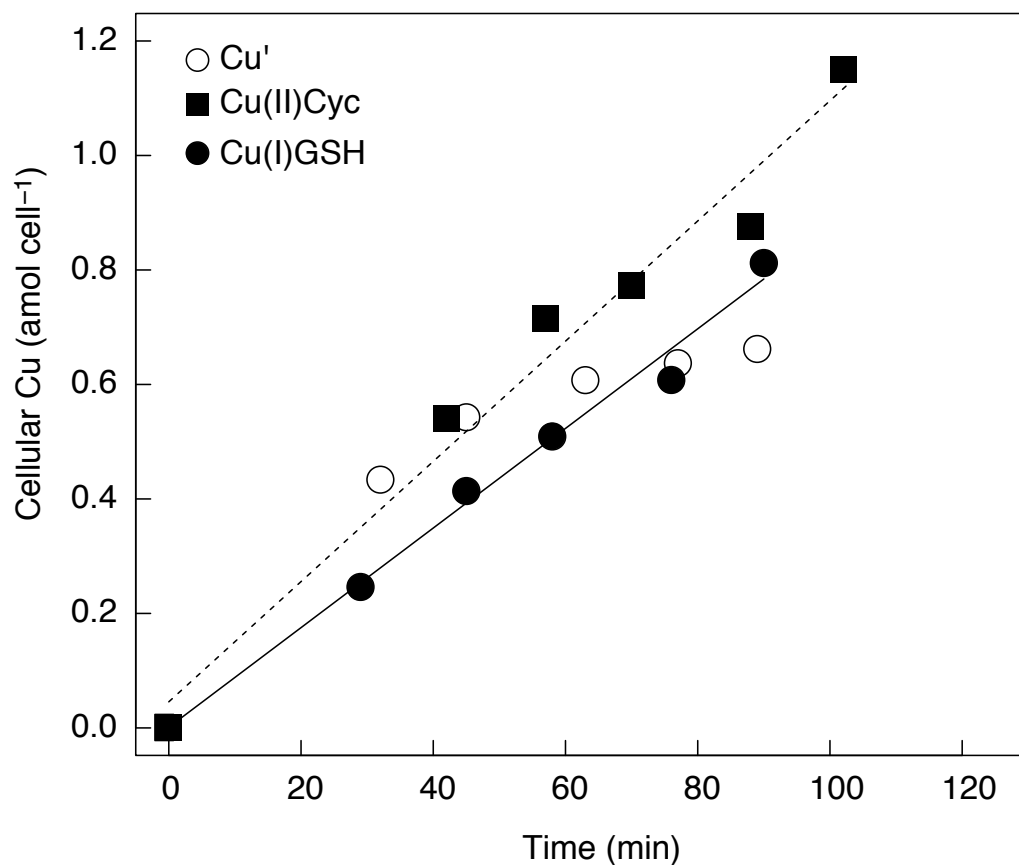


Figure 3.1. Time-course accumulation of Cu by *T. pseudonana* (replicate A) grown in low Cu (0.6 nM) media. ⁶⁴Copper (1 nM) was added to the assay as either inorganic Cu(II) (Cu'), Cu(II) complexed with 3 nM Cyclam (Cu(II)Cyc), or Cu(I) with 10 nM GSH (Cu(I)GSH). Due to the weak complex formed between Cu(I) and GSH (see section 3.2.2.1), the Cu species in this treatment is effectively Cu'. Least-squares linear regressions are plotted for the Cu(II)Cyclam (dashed) and Cu(I)GSH (dotted) treatments. Cell concentrations ranged between 0.49 and 0.55 million cells mL⁻¹.

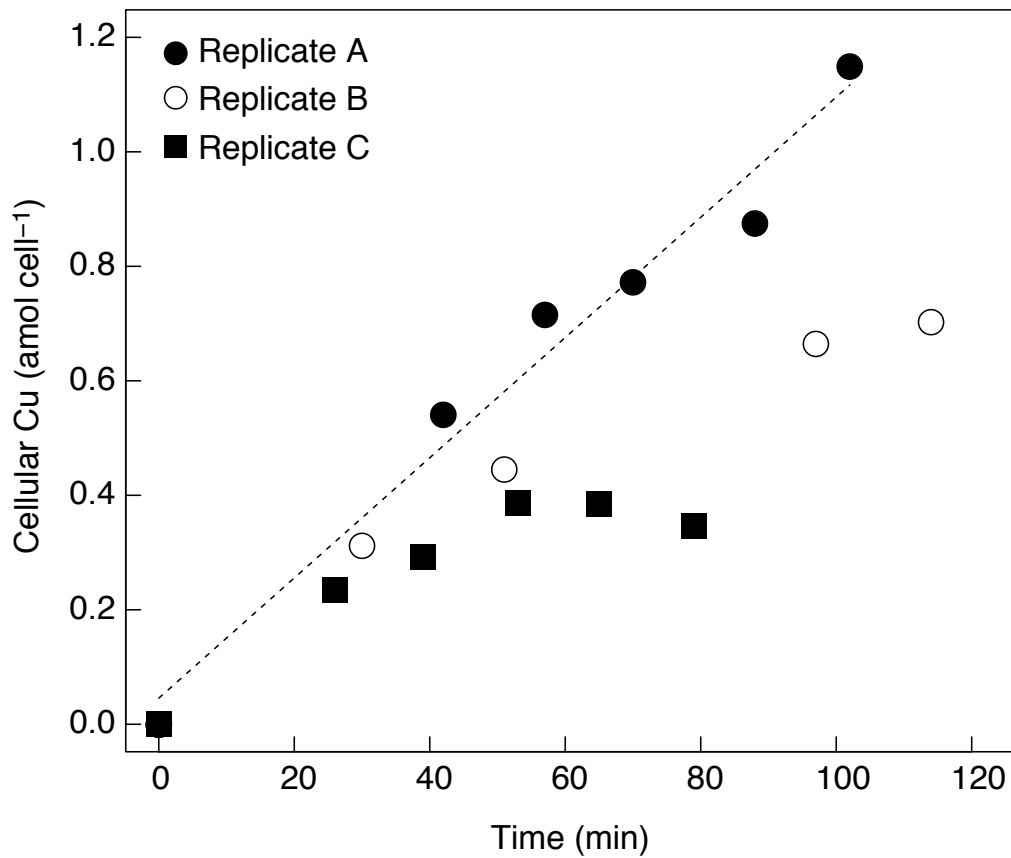


Figure 3.2. Time-course accumulation of Cu by *T. pseudonana* replicate cultures grown in low Cu (0.6 nM) media. ⁶⁴Copper (1 nM) was added to the assay complexed with 3 nM Cyclam. Cell concentrations for replicates A, B, and C were 0.55, 1.22, and 1.80 million cells mL⁻¹, respectively.

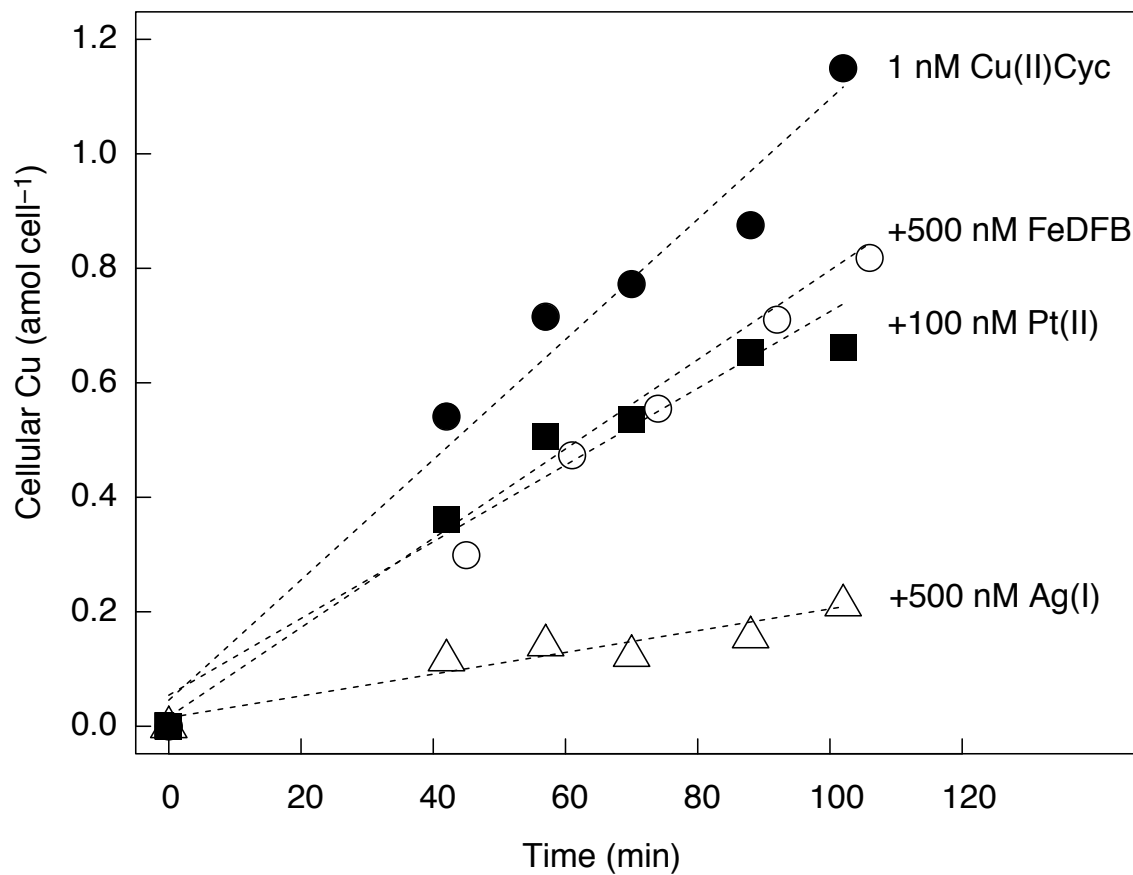


Figure 3.3. Time-course accumulation of 1 nM Cu bound to 3 nM Cyclam by *T. pseudonana* (replicate A) grown in low Cu (0.6 nM) media, including treatments with competitive inhibitors targeting the components of the proposed high-affinity Cu transport system (100 nM Pt(II), 500 nM FeDFB, and 500 nM Ag(I)). Least-squares linear regressions are plotted for each assay. Cell concentrations ranged between 0.49 and 0.55 million cells mL⁻¹.

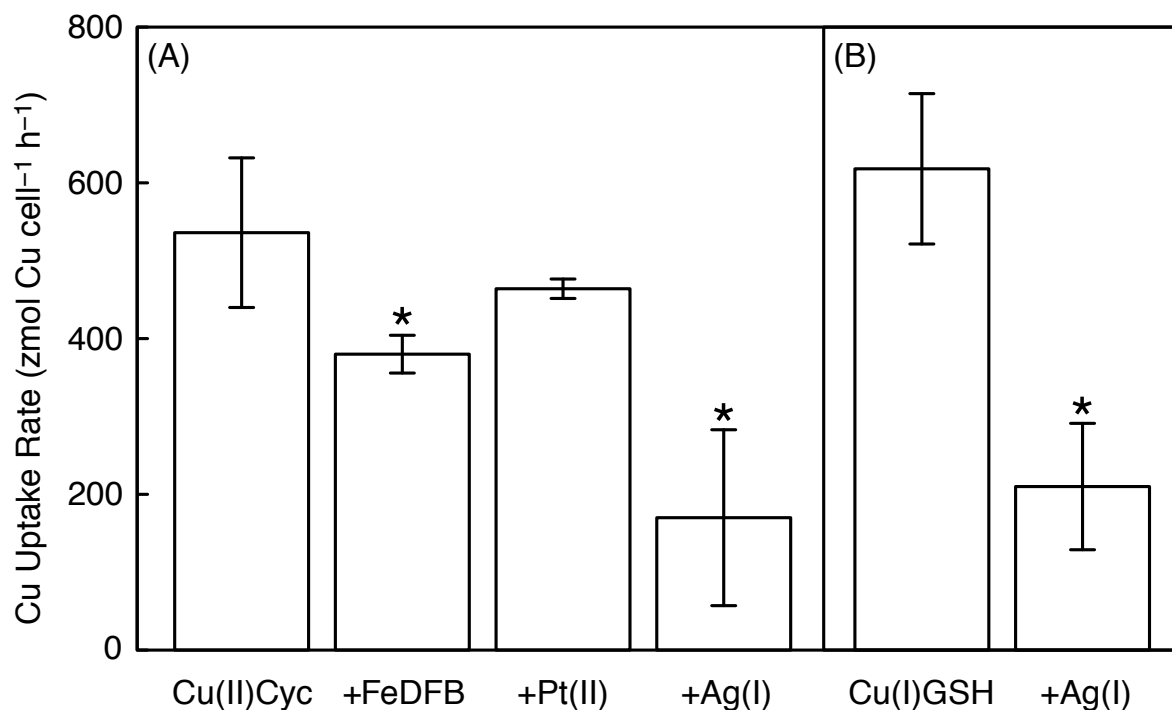


Figure 3.4. Average short-term Cu uptake rates ($\pm 1\sigma$; $n=3$) by *T. pseudonana* grown in low Cu (0.6 nM) media in the presence of competitive inhibitors for components of the proposed high-affinity Cu transport system. (A) 1nM Cu(II) bound to 3 nM Cyclam (Cu(II)Cyc) with additions of 500 nM FeDFB, 100 nM Pt(II), or 500 nM Ag(I); (B) 1nM Cu with 10 nM GSH (Cu(I)GSH) with the addition of 500 nM Ag(I). Due to the weak complex formed between Cu(I) and GSH (see section 3.2.2.1), the Cu species in this treatment is effectively Cu'. Single-tail student's t-tests (unequal variances) were performed to compare uptake rates between the unamended treatments and those with inhibitors. Significant differences ($p < 0.05$) are marked with an asterisk. Cell concentrations for replicates A, B, and C ranged between 0.49-0.55, 0.92-1.28, and 1.37-1.87 million cells mL⁻¹, respectively.

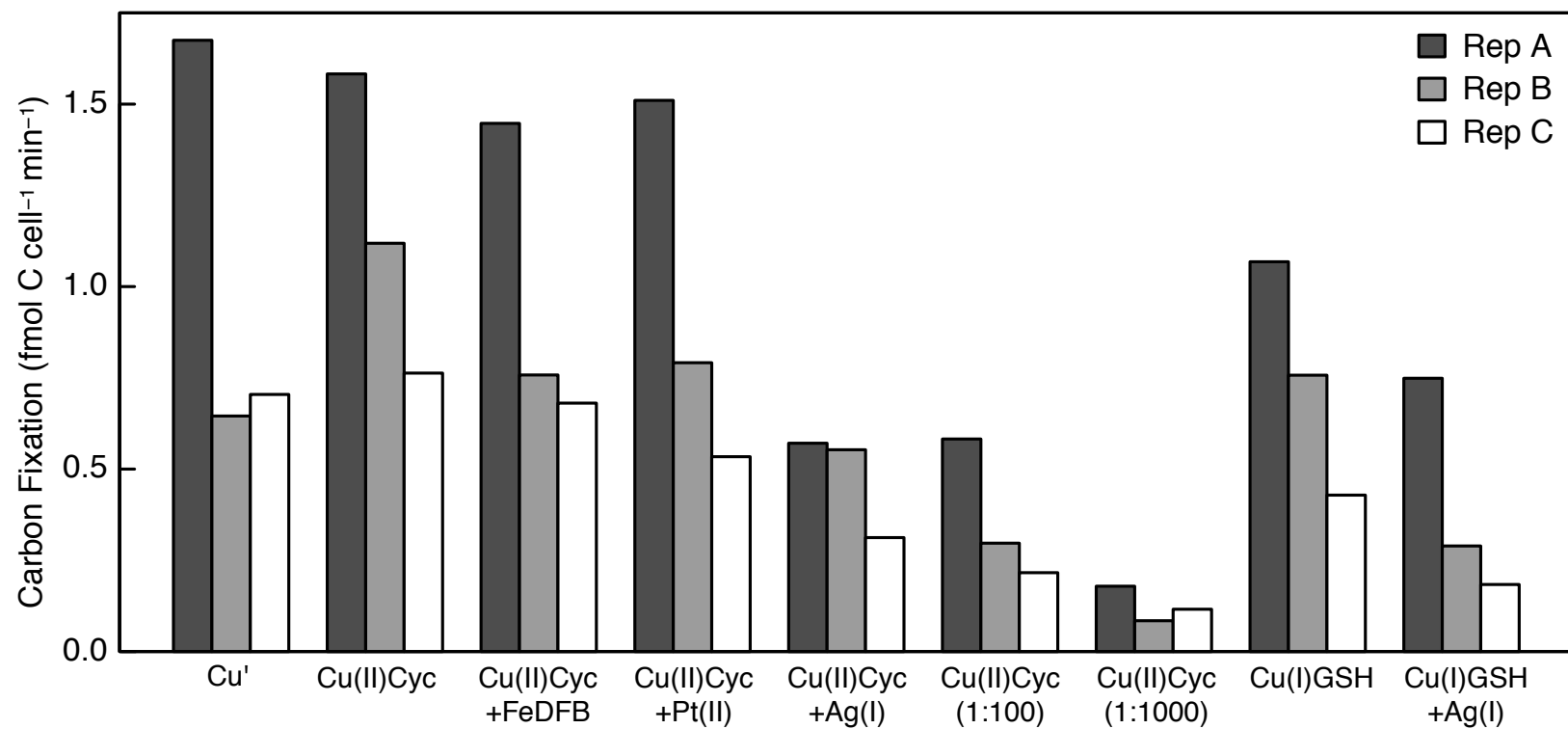


Figure 3.5. Carbon fixation rates by *T. pseudonana* grown in low Cu media (0.6 nM) for each treatment and replicate of the competitive inhibition Cu uptake assays.

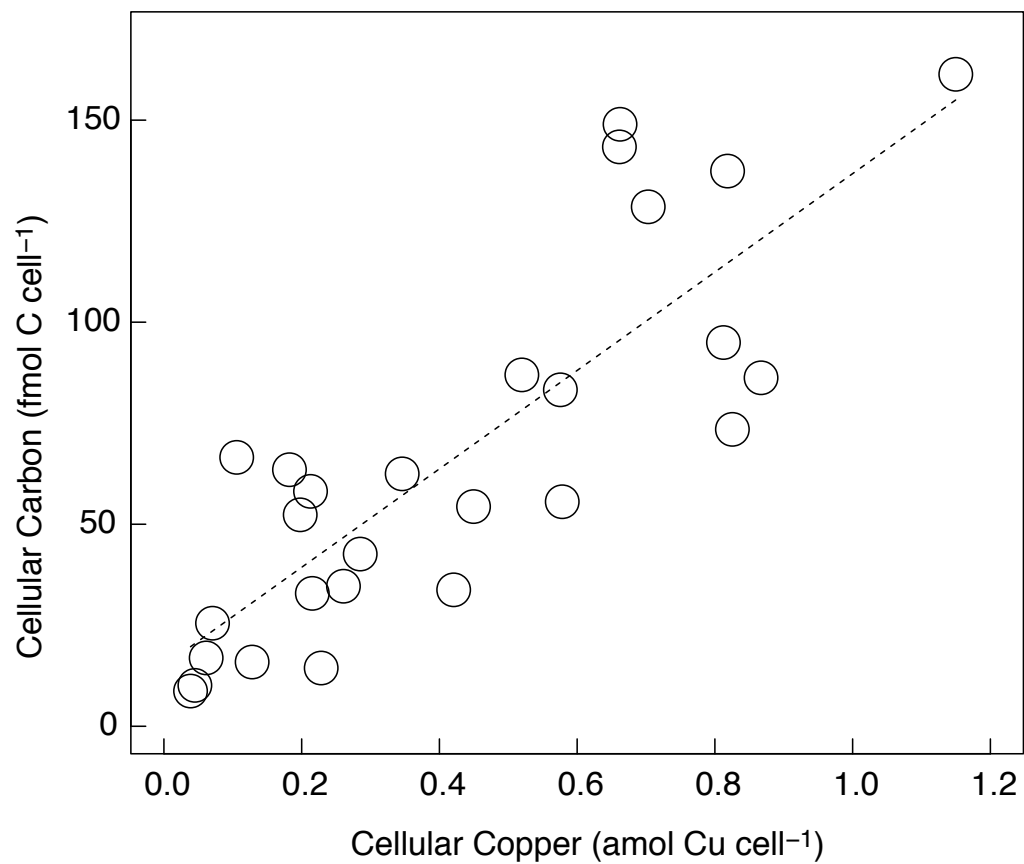


Figure 3.6. Intracellular Cu (amol Cu cell^{-1}) and carbon (fmol C cell^{-1}) accumulated in *T. pseudonana* at the end of the short-term Cu uptake assays for all treatments and replicates. Least-squares linear regression is plotted ($[\text{Cellular C}] = 121.8 \times [\text{Cellular Cu}] + 15.0$; $R^2 = 0.70$, $p < 0.0001$). Cultures were grown in low Cu (0.6 nM) media.

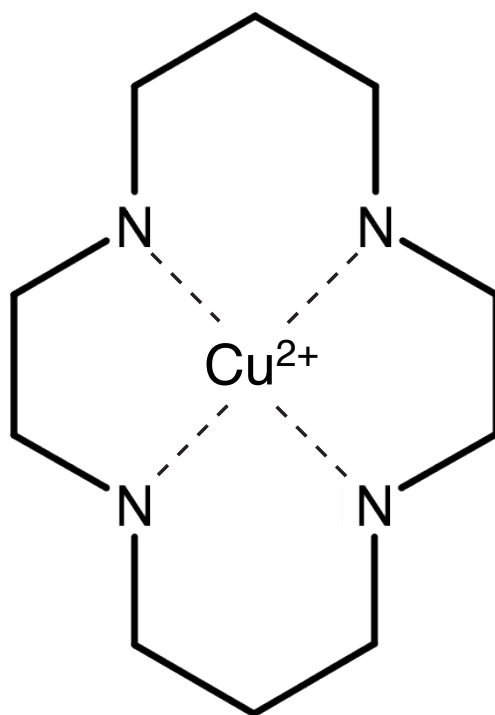


Figure 3.7. Cyclam chemical structure and coordination with $\text{Cu}(\text{II})$.

Chapter 4: Iron-Copper Interactions in HNLC Phytoplankton in the Northeast Subarctic Pacific Ocean

In August 2010, Fe and Fe/Cu addition incubation experiments were conducted at two low iron (Fe) stations (P20 and P26) along Line P, a 1450 km long coastal-oceanic transect off the western coast of British Columbia, to investigate copper (Cu) physiology in Fe- and Fe-light co-limited phytoplankton. Chlorophyll *a* concentrations ([chl *a*]), maximum variable fluorescence yield (F_v/F_m), and Fe uptake rates by the Cu-dependent high-affinity Fe transport system (HAFETS) were measured. Additions of Fe resulted in an increase in [chl *a*] and F_v/F_m at both stations compared to the controls, regardless of light availability, and confirmed that the phytoplankton communities were Fe-limited. Uptake of Fe by the HAFETS in both incubations increased with the addition of Fe, and likely reflects luxury Fe uptake and storage. While the *in situ* inorganic Cu concentrations were similar to those that can induce Cu-limitation in laboratory cultures, increasing Cu availability had no effect on biomass accumulation during both incubations, regardless of Fe availability or light regime. At P26, additions of 1 nM CuSO₄ resulted in a short-term increase in F_v/F_m of the phytoplankton community, and an increase in Fe uptake rates by large phytoplankton (>5 μm), but only when light was not limiting. These data confirm a complex interaction between Fe and Cu physiology in indigenous phytoplankton communities, and suggest that these interactions may be spatially heterogeneous for different phytoplankton size classes.

4.1 Introduction

Low dissolved Fe concentrations limit primary productivity in up to 40% of the global surface oceans (Moore et al. 2004; Falkowski et al. 2012). To survive with sparingly little Fe, marine phytoplankton have numerous physiological adaptations, including: increased cellular surface area:volume ratios to enhance nutrient uptake while decreasing intracellular Fe requirements (Sunda & Huntsman, 1995a; Maldonado & Price, 1996); the replacement of Fe-containing enzymes with Fe-free alternatives (e.g. metal-free flavodoxin replaces ferredoxin; Cu-containing plastocyanin replaces cytochrome c_6) (La Roche et al. 1996; Peers et al. 2006); reduced Fe-rich photosystem I abundance and altered photosynthetic protein stoichiometry (Strzepek and Harrison 2004); and up-regulation of a high-affinity Fe transport system (HAFETS) containing a coupled ferrereductase and multiple-Cu containing ferroxidase (Maldonado and Price, 2001; Shaked et al. 2005; Wells et al. 2005; Maldonado et al. 2006; Kustka et al. 2007). Copper is required for two of these adaptations and so there may exist a physiological link between intracellular Fe and Cu requirements in Fe-limited marine phytoplankton. Monoclonal phytoplankton culture studies have demonstrated that 4 of 18 species surveyed significantly increased their intracellular Cu quotas (defined as the ratio of cellular Cu:C) in response to Fe-limitation (Annett et al. 2008; Guo et al. 2012). The Cu:C assimilation ratios and HAFETS activity were positively correlated for large phytoplankton cells (>20 μm) in the mixed layer along a high-low Fe gradient in the subarctic NE Pacific, indicating that the intracellular Cu requirements of natural phytoplankton can also be modulated by the degree of *in situ* Fe limitation (Semeniuk et al. 2009). Furthermore, oceanic phytoplankton isolates have significantly higher Cu quotas and are more susceptible to Cu limitation than their coastal

counterparts, suggesting oceanic phytoplankton may rely on Cu in order to inhabit waters with chronically low Fe (Peers et al. 2005; Annett et al. 2008; Guo et al. 2012).

While the role of Fe in limiting marine primary productivity is well established (Boyd et al. 2007), the role of Cu remains contentious. Early field studies demonstrated that the addition of the metal chelator ethylenediamine tetraacetic acid (EDTA) to recently upwelled seawater caused an increase in phytoplankton growth, and could possibly have been due to the chelation and subsequent detoxification of inorganic metals such as Cu (Barber and Ryther, 1969; Barber 1973). Subsequent laboratory work demonstrated that inorganic Cu (Cu') was the sole bioavailable source of Cu (Sunda and Guillard 1976; Jackson and Morgan 1978; Sunda and Lewis 1978), and [Cu'] in surface waters were on par with those that induced Cu toxicity in cyanobacteria (Brand et al. 1986). Interestingly, recent measurements of surface water [Cu'] in the Bering Sea, Northwest Pacific Ocean (Moffett and Dupont 2007), and Southern Ocean (Buck et al. 2010) are similar to those that can induce Cu limitation in Fe-limited monocultures (Peers et al. 2005; Maldonado et al. 2006; Annett et al. 2008; Guo et al. 2012), thereby demonstrating that low Cu availability in high-nutrient, low chlorophyll (HNLC) waters could induce Fe-Cu co-limitation.

To date, two bottle incubation studies, one in the Northeast subarctic Pacific Ocean (Coale 1991) and another in the Bering Sea (Peers et al. 2005), have amended Fe-limited waters with Cu. Each Cu addition elicited an increase in chl *a* levels compared to the control, indicating the phytoplankton community may have been Cu limited. Unfortunately, with the data presented in these two studies, it is not possible to distinguish between alleviating Cu-limitation in

phytoplankton or decreasing grazing pressure due to Cu toxicity in Cu-sensitive micrograzers (Stoecker et al. 1986). Therefore, the presence and possible prevalence of Cu limitation in HNLC waters remains unknown.

Along the Line P transect in the NE subarctic Pacific Ocean, we performed two bottle incubation experiments (4 to 5 days), one with varying Cu availability and another manipulating Cu and light levels at two Fe limited stations. In addition to chl *a* accumulation, we measured Fe uptake rates from FeDFB and maximum variable fluorescence (F_v/F_m), two physiological variables that reflect the degree of Fe limitation experienced by phytoplankton. At P26, we present evidence for Fe-Cu metabolic interactions in a light replete, Fe-limited phytoplankton community.

4.2 Materials and Methods

4.2.1 Plastic Cleaning Protocol

The incubation cubitainers (LDPE) and other plastics were soaked sequentially in 3% Extran detergent for 1 week, 50% HCl for 1 week, 2% HNO₃ for 1 week, and were thoroughly rinsed with ultrapure water (18M Ω resistance; Millipore) after each soak. Before filling the cubitainers, they were emptied and rinsed four times on station with seawater collected from 10m depth.

Low-density polyethylene bottles (LDPE, 125 mL) used for collecting samples for total dissolved Fe and Cu were cleaned following GEOTRACES cleaning protocols (Cutter et al. 2010). All cleaning occurred in class 100 conditions. The cubitainers and LDPE bottles were stored with 0.01 N ultrapure HCl (Seastar) before sampling, and triple bagged for transportation to and from the ship.

4.2.2 Station Parameterization and Water Collection

Incubations were performed aboard the CCGS John P. Tully between August 17-September 2, 2010 (cruise 2010-14). Water was collected before dawn at two stations in the HNLC waters along Line P, P20 (49°33.92 N, 138°40.04 W) and P26 (50°00.04 N, 145°00.03 W). The Fe-limited status of phytoplankton in these waters was confirmed in incubations presented here (see section 3.3). Trace metal clean cubitainers (4 L and 10 L for the P20 and P26 incubations, respectively) were rinsed and filled with water pumped from the mixed layer (10m depth) using a trace metal clean pumping system and an on-deck class 100 laminar flow hood (c.f. Johnson et al. 2005). Until the treatment additions could be made, each full cubitainer was stored in an on-deck incubator with flowing seawater pumped from 5 m depth. Over the course of filling the cubitainers, water samples were collected at three discrete times for the initial biological and chemical parameters.

Vertical profiles of various parameters were obtained with a CTD (SeaBird Electronics, model SBE 911) fitted with a dissolved oxygen sensor (SBE 43), fluorometer (Seapoint), and an underwater photosynthetically active radiation (PAR) sensor (Biospherical QSP-400). CTD data collected at the surface for each station were used to calculate the mixed layer depths (MLD) using the $\Delta\sigma_t$ criterion of 0.125 kg m^{-3} (Levitus 1982). Light extinction coefficients (k_d) were determined from PAR data via exponential curve fitting software (MS Excel), and the incident irradiance at 0 m (I_0) was determined by extrapolating the curve fitted to the PAR data. The euphotic zone was determined at each station as $Z_{eu} = \ln(100)/k_d$. Surface PAR (SPAR) was collected hourly during daylight hours over the course of the incubations using a LI-COR LI-1000 radiation sensor located 2 m above the deck level where the incubations took place. The

average mixed layer irradiance ($\bar{I}_D = [I_0/k_d \times \text{MLD}] \times [1 - \exp(-k_d \times \text{MLD})]$) for each station was calculated as a fraction of the incident surface irradiance to allow for a comparison between the average *in situ* mixed layer light intensity and the chosen incubation light intensities.

4.2.3 Incubation Treatments

All treatments for both incubations were performed in triplicate, and cubitainers filled at each station were randomly assigned a treatment. The incubation at Station P20 (hereafter referred to as P20 grow-out, or P20GO) aimed to determine whether: a) Cu was co-limiting the Fe-limited phytoplankton community; and b) whether the speciation of Cu mediated co-limitation. All of the P20GO treatments were incubated at 10% surface light intensity (I_0) to avoid light limitation or stress due to high irradiance. The average light intensity experienced by the P20 incubation was $33.5 \pm 28.6 \mu\text{mol quanta m}^{-2} \text{ s}^{-1}$, with a maximum of $118.9 \mu\text{mol quanta m}^{-2} \text{ s}^{-1}$. The average maximum light intensity on each day during the incubation was $82 \pm 29 \mu\text{mol m}^{-2} \text{ s}^{-1}$. Although this light intensity may begin to cause light limitation, the rapid response in chl *a* to the Fe amendment and the high final chl *a* concentration indicates the community was not limited by light availability (see section 4.3.2.1).

In both incubations, a positive control treatment for Fe limitation included that was amended with 1 nM FeCl_3 (in 0.001 M HCl; Sigma) bound to 1.5 nM ethylenediaminetetraacetic acid (EDTA; Sigma). Iron was added pre-complexed to EDTA to ensure it did not immediately precipitate out of solution upon addition to the seawater (Coale 1991). Given the high affinity of EDTA for Ca and Mg in seawater (Hering and Morel 1988), it is unlikely that the 1.5 nM

addition significantly impacted the bioavailability of bioactive trace metals for the sampled phytoplankton community.

Four Cu treatments were chosen to investigate how altering the total dissolved Cu concentration and speciation of dissolved Cu would impact the indigenous phytoplankton community at Station P20. In the first treatment, Cu was added as 1 nM CuSO₄ to verify whether the indigenous phytoplankton community was Cu-limited. The 1 nM Cu addition was chosen to mimic how surface water Cu concentrations may increase during a natural mixing event, whereby water below the mixed layer with a Cu concentration ranging from 1.8 to 2.2 nM would be mixed with surface waters (D. Semeniuk *unpub. data*). The excess strong Cu binding ligands present (6.79 ± 0.61 nM; see section 4.3.1) would have completely bound the 1 nM CuSO₄ addition, resulting in a 2.5-fold increase in inorganic Cu from 27.6 to 69.2 fM.

The presence of weak organic ligands may influence the bioavailability of strongly organically complexed *in situ* trace metals. Weaker ligand may be more labile near the cell surface, and a pool of weakly complexed trace metals can effectively shuttle metals away from the strong organic ligand complexes to the cell surface (e.g. Aristilde et al. 2012). Preliminary field evidence suggests that weak Cu binding ligands may enhance Cu transport in marine phytoplankton from *in situ* strong ligands (Chapter 2). Thus, we included a second treatment of 10 nM of reduced glutathione (GSH) to potentially increase the bioavailability of the *in situ* Cu without changing the concentration of total dissolved Cu. Although we added 10 nM GSH to our incubation bottle, it was likely oxidized to 5 nM oxidized glutathione (GSSG) by any number of possible oxidizing agents in seawater (e.g. O₂, superoxide, Cu(II), Fe(III)) over the course of the

incubation. Reduced glutathione binds Cu(I) very weakly in seawater and has a $\log K_{CuL,Cu^+}^{cond} = 11.9$ (Walsh and Ahner 2013). Similarly, GSSG binds Cu(II) weakly, with an estimated $\log K_{CuL,Cu^{2+}}^{cond} = 11.4$ (Leal and van den Berg 1998). Since the strong *in situ* Cu binding ligands at P20 have a significantly higher $\log K_{CuL,Cu^{2+}}^{cond}$ (14.23; see section 4.3.1) than GSH or GSSG, the glutathione addition would have complexed only a small portion of the inorganic Cu as a more labile CuL species, thus promoting dissociation of the strong *in situ* CuL complexes to maintain an equilibrium inorganic Cu concentration. Thus, the glutathione addition would have caused the Cu' concentration to decrease slightly, while increasing the combined concentrations of inorganic and weakly complexed Cu(II). Unfortunately, without more information about the nature of weak Cu binding ligands (e.g. strengths, concentrations, and Cu:L binding stoichiometry) in oceanic surface waters, we are unable to predict the degree to which GSSG would lower the *in situ* Cu' concentration. In addition to the 1 nM CuSO₄ and 10 nM GSH treatments, a third treatment included 1 nM CuSO₄ + 10 nM GSH. The final P20GO treatment consisted of a 10 nM CuSO₄ addition. Previous workers who observed an increase in primary productivity with the addition of Cu to Fe-limited phytoplankton argued that grazing pressure might have decreased as a result of Cu-induced toxicity to micrograzers (Coale 1991). This treatment was a positive control for this scenario, whereby the 10 nM Cu addition would have saturated the *in situ* Cu ligands, resulting in a large increase in inorganic Cu and a pCu of 9.9 (see section 4.3.1).

The P26 incubation (hereafter referred to as P26GO) aimed to determine whether Fe, light, or Fe-light co-limited phytoplankton could be co-limited by Cu. When light availability is low,

phytoplankton increase the number of Fe-rich reaction centres and electron transport chain components, thereby increasing intracellular Fe demands (Raven 1990; Sunda and Huntsman 1997). Previous work at Station P26 has demonstrated that intracellular Cu uptake by $>5\mu\text{m}$ phytoplankton increased 20-100% in low light (Chapter 2). This could be due to the up-regulation of the Cu-dependent HAFETS in order to satisfy increased intracellular Fe demands in low light, or some other hitherto unknown cellular Cu requirement for photosynthesis. As such, low light conditions provide the most likely scenario for Fe-limited phytoplankton to become co-limited by Cu.

Two light levels were chosen for the P26GO incubation: 50 and 1% I_0 , representing light replete (*in situ* light) and limiting (low light) conditions, respectively. In the *in situ* and low light treatments, average light intensities experienced were $170 \pm 135 \mu\text{mol quanta m}^{-2} \text{ s}^{-1}$ and $3.4 \pm 2.7 \mu\text{mol quanta m}^{-2} \text{ s}^{-1}$, the maximum light intensities experienced were $521 \mu\text{mol quanta m}^{-2} \text{ s}^{-1}$ and $10.4 \mu\text{mol quanta m}^{-2} \text{ s}^{-1}$, and the average maximum light intensities each day were $402 \pm 91 \mu\text{mol quanta m}^{-2} \text{ s}^{-1}$ and $8.0 \pm 1.8 \mu\text{mol quanta m}^{-2} \text{ s}^{-1}$, respectively. The *in situ* treatment light intensity (50% I_0) was slightly lower than the calculated average light intensity experienced by a phytoplankton cell in the mixed layer (70% I_0 ; Table 4.1). The 1% I_0 light intensity was confirmed to induce light limitation (see section 4.2). Iron (1 nM bound to 1.5 nM EDTA) and Cu (1 nM CuSO_4) were added to both high and low light treatments. In low light, both Fe and Cu were added to an additional treatment to test for Fe-Cu co-limitation under low light.

Both incubations were kept at the mixed layer temperature in an on-deck incubator supplied continuously with seawater pumped from 5 m depth, and light levels were maintained using

neutral density screening. Temperatures in the incubators did not exceed the *in situ* temperature by more than 1°C throughout the incubations. Copper, Fe, EDTA, and GSH additions were made using fresh stocks stored in the dark at 4°C. To ensure complete metal-ligand complexation, the Cu(I)GSH₂ and FeEDTA complexes were allowed to complex in MQ for 2 h prior to being added to the incubation bottles (Leal and van den Berg, 1998; Taylor et al. 2013).

4.2.4 Biological and Chemical Sampling and Analyses

4.2.4.1 Sampling, Nutrients, and Chlorophyll *a*

The P20GO incubation was sampled on Days 1, 3, and 5, while the P26GO incubation was sampled on Days 2, 3, and 4. In order to avoid contaminating the incubation cubitainers, the cubitainers were filled and sub-sampled within a Class 100 laminar flow hood. Analysis of total dissolved Fe, [chl *a*], and F_v/F_m at the end of the incubations confirmed that the cubitainers were not contaminated (see section 3). Samples (200mL) for total [chl *a*] were filtered onto 25 mm glass fiber filters (GFF) using a low vacuum pressure and archived at -20°C in 15 mL polypropylene Falcon tubes. On the last day of each incubation, size fractionated [chl *a*] was collected by filtering onto 0.22, 1, and 5µm polycarbonate filters (AMD) separated by nylon drain discs. Within 4 weeks of collection, chl *a* samples were soaked in 10 mL of chilled 90% acetone, placed in a -20°C freezer overnight for extraction, and the chl *a* concentrations were determined using a Turner Designs Model 10 fluorometer (Parsons et al. 1984). Dissolved macronutrients (nitrate+nitrite, phosphate, and silicic acid) were sampled by filtering 15mL with a syringe through a 0.45µm polysulfone filter, and samples were immediately frozen and archived at -20°C. Within 6 months of collection, samples were thawed and immediately analyzed with a Bran and Luebbe AutoAnalyzer 3 using air-segmented continuous flow analysis.

Triplicate samples for counting heterotrophic bacteria by flow cytometry were dispensed into cryovials and fixed with glutaraldehyde to a final concentration of 0.1%. Samples were incubated in the dark for 15 minutes before being frozen in liquid nitrogen, and archived at -80°C. In the laboratory, samples were enumerated with a FACSCalibur flow cytometer (Becton-Dickinson FACSCalibur) that was equipped with a 488 nm, 15 mW laser. Samples were thawed at ~1 °C, diluted 10-fold with 0.22 μm filtered 10% TE buffer (10 mM-Tris HCl, 1 mM EDTA, pH 8), and stained with SYBR Green I (0.5 x 10⁻⁴ dilution of the commercial stock; Invitrogen) for 15 minutes in the dark prior to analysis (Taylor et al. 2013). Triplicate samples of 0.22 μm filtered 10% TE buffer were stained using the same methods as the other samples, and used to blank-subtract the samples. The data files produced were analyzed using Cytowin software version 4.31 (Vaulot, 1989), and blank-subtracted cell counts derived from the software scatterplots were used to calculate cell abundances using the analysis time and instrument flow rate.

4.2.4.2 Photo-Physiological Measurements

Maximum variable fluorescence yield (F_v/F_m ; unitless) is low (0.2-0.3) in Fe-limited phytoplankton, and increases following the alleviation of Fe-limitation (Greene et al. 1991; Boyd and Abraham 2001). If Fe-limited phytoplankton are co-limited by Cu due to an insufficient number of Cu-dependent HAFETS, then the addition of Cu may result in an increase in F_v/F_m as the cellular internalization of Fe increases and Fe-limitation is partially relieved. Copper nutrition can also affect the photophysiology of marine phytoplankton. Both Cu limitation and toxicity can damage photosystem II reaction centres and decrease F_v/F_m (Lombardi and Maldonado 2011). Using a fluorescence induction and relaxation (FIRE) system (Satlantic,

Halifax NS Canada), F_v/F_m was derived for dark-adapted samples on each sampling day. Discrete samples were taken from each cubitainer between 10:00-15:00 local time, and dark acclimated for at least 30 minutes in a water bath set to the incubation temperature to ensure all P680 reaction centers were reduced prior to excitation (Moore et al. 2006). A high intensity saturating light pulse (1 W m^{-2}) of 100 μs at 450 and 540 nm wavelengths was applied to each sample to oxidize all P680 reaction centres and reduce all Q_A . Minimum fluorescence measured before the pulse (F_o) and the maximum fluorescence measured immediately after the pulse (F_m) were used to derive the variable fluorescence ($F_v = F_m - F_o$). Data from the 20 pulses were averaged, and F_m and F_o were determined from the best-fit using the Matlab® script Fireworx (A. Barnett, pers. comm.) after correcting for the blank fluorescence (0.22 μm filtered sample).

4.2.4.3 Dissolved Fe and Cu Sampling

Samples for total dissolved Fe and Cu were collected using trace metal clean (TMC) sampling protocols as previously described (Johnson et al. 2005). Briefly, water samples were collected using a Teflon double-bellows air-driven pump (Asti) and Teflon-lined sampling tube attached to a Kevlar wire. Water was pumped into a PVC ULPA (ultra low penetration air filter) clean hood where it was sampled. Samples collected from depths greater than 40 m were taken using TMC 10 L GO-FLO samplers (Ocean Optics) on an 800 m Kevlar line, and solid Teflon messengers were used to trip the bottles. All samples were filtered through a 0.22 μm Opticap cartridge filter. The cartridge filter was rinsed with at least 2 L of seawater from each depth before sampling into 125 mL TMC LDPE bottles. Each LDPE sample bottle was emptied and rinsed three times with fresh sample before being filled.

Samples for total dissolved Fe in the incubation bottles without added Fe were taken on the final day of the incubations to confirm whether any Fe contamination had occurred. Approximately 250 mL of water were sampled from each cubitainer into TMC LDPE bottles inside a Class 100 laminar flow hood. These samples were then filtered with acid-cleaned 0.22 μm filters (Supor) in a 47 mm Teflon filter tower (Savillex) attached to the top of a cylindrical polycarbonate vacuum chamber. A short piece of Teflon tubing extended from the outlet of the filter manifold into a TMC 125 mL LDPE sample bottle placed within the vacuum chamber. A small vacuum pressure was then applied (<5 mm Hg), thereby allowing the sample bottle inside the vacuum chamber to collect the filtrate. The filter and sample bottles were rinsed with 30 mL of fresh sample three times before the sample bottles were filled. Within 12 h of sampling, the samples were acidified to pH 1.7 in the ULPA clean hood using 6M ultrapure HCl (Seastar).

4.2.4.4 Dissolved Fe and Cu Analysis

Total dissolved Fe was determined as previously described (Johnson et al. 2005). Six months after the samples were collected, total dissolved Cu was determined via the reaction between Cu and 1,10-phenanthroline using flow injection analysis and chemiluminescence detection (Zamzow et al. 1998). Samples for total dissolved Cu were UV oxidized before analysis (Achterberg et al. 2001). At the start of each analytical session, samples were surveyed to determine which had the lowest chemiluminescence signal, and this sample was used to produce a standard curve via standard additions using a fresh CuNO_3 stock solution made from a 1000 ppm atomic adsorption standard solution. The standard curve produced was then used to determine the sample concentrations run during that analytical session. One standard was run at multiple times to account for signal drift over the course of the session. Each sample was measured at least four

times, and the standard errors are reported. A procedural blank was estimated via standard additions during each analytical session using MQ acidified to pH 1.7 with ultrapure HCl, and was subtracted from each sample measured during that session. SAFe-D2 (K. Bruland) or NASS-5 (National Research Council of Canada) reference materials were run during each analytical session to ensure data credibility, and our values were within the reported accepted range (SAFe-D2: 2.35 ± 0.03 nM vs. reported range 2.35 ± 0.19 nM; NASS-5: 4.58 ± 0.06 nM vs. reported range 4.71 ± 0.73 nM; errors in our measurements represent the standard error of the intercept of 5 standard additions, and at least 4 replicate measurements for each addition). The concentration and strength of the strong Cu binding ligands in the initial water sampled at P20 were determined as previously described (Bundy et al. 2013).

4.2.4.5 Iron Uptake Assays from Desferrioxamine B

On Day 3 for both incubations, uptake rates of Fe bound to the siderophore desferrioxamine B (DFB) were assayed. DFB is a siderophore, a strong Fe(III)-specific ligand, derived from the terrestrial fungus *Streptomyces pilosus*, and has conditional stability constant of $10^{16.5}$ (Hudson et al. 1992). Acquisition of Fe from the FeDFB complex by the HAFeTS requires the reduction of Fe(III), followed by the dissociation of the Fe(II) and DFB complex, the oxidation of Fe(II) by an extracellular multi-Cu containing ferroxidase, and subsequent internalization of Fe(III) (Maldonado and Price 2001; Maldonado et al. 2006; Kustka et al. 2007). Uptake rates of Fe bound to DFB increase with Fe-limitation (Maldonado and Price 2000; Taylor et al. 2013), and decrease with Cu limitation (Peers et al. 2005; Maldonado et al. 2006), so Fe uptake from FeDFB (hereafter referred to as HAFeTS activity) of the phytoplankton community could reflect the degree of Fe and Cu limitation experienced in the incubations.

HAFETS activity was assayed using $^{55}\text{FeCl}_3$ (PerkinElmer). The $^{55}\text{FeDFB}$ complex was prepared by complexing 5% excess DFB (Sigma Aldrich) with ^{55}Fe in MQ for 1h at a pH of 3.5, thereby ensuring that ^{55}Fe was completely coordinated and stabilized by the DFB (Monzyk and Crumbliss, 1982). The resulting complex was equilibrated for at least 2 h at pH 8 in 0.22 μm -filtered seawater collected immediately before filling the incubation bottles at each station. It has previously been demonstrated that there is no detectable inorganic Fe in solution after 30 min under these conditions (Maldonado and Price, 1999).

Before dawn on Day 3 of the incubations, 250 mL of seawater were sampled from each cubitainer into trace metal clean polycarbonate bottles. The bottles were spiked with 1 nM of the $^{55}\text{FeDFB}$ mixture and placed in the on-deck incubators alongside the incubated cubitainers.

After 24 h, the contents of each bottle were filtered onto a series of Poretics polycarbonate filters (5, 1, and 0.22 μm porosities) separated by nylon drain discs (Millipore) under low vacuum pressure (<5 mm Hg). The filters were then washed in a Ti-citrate-EDTA solution for 5 min to remove any extracellular Fe (Hudson et al. 1989), and subsequently rinsed with 10 mL of filtered seawater to remove any loosely associated tracer. The filters were removed and placed in 7 mL scintillation vials, immersed in scintillation cocktail (Scintisafe 50%, Fisher), and archived. A 1 mL aliquot was taken from each HAFETS assay bottle to determine the concentrations of the tracer added.

The activity of ^{55}Fe was determined in each sample using a Beckman LS65005514 scintillation counter with an internal ^{55}Fe quench curve. The activity-per-L was determined from 1 mL subsamples of each 250 mL assay bottle. The specific activity (DPM mol^{-1}) of ^{55}Fe on the

date of the assay was calculated from the specific activity provided by the manufacturer (after accounting for decay), and was used to convert the nuclide activity on each filter (DPM per filter) to mol Fe per filter. Uptake rates of Fe from DFB were assumed to be linear over 24 h as previously demonstrated along Line P (Maldonado and Price, 1999). Volume-normalized uptake rates (ρFe_V) for each size fraction were calculated by dividing the intracellular Fe that accumulated over 24h by the volume filtered ($\text{pmol Fe L}^{-1} \text{d}^{-1}$). Carbon-normalized HAFETS activities (ρFe_C) were calculated by dividing volumetric uptake rates by particulate carbon concentrations derived from [chl *a*] and bacterial abundance. Volumetric rates in the 0.22-1 μm size fraction were normalized to total (autotrophic and heterotrophic) bacterial carbon that was calculated from cell abundance converted to particulate carbon (20 fg C cell⁻¹; Lee and Fuhrman, 1987). Volumetric rates in the 1-5 and >5 μm fractions were normalized to particulate carbon that was calculated from [chl *a*] in each size fraction (50 g C g chl *a*⁻¹; Booth et al. 1993). Although size fractionated [chl *a*] was not sampled on Day 3, the relative contribution of each size fraction to total [chl *a*] was not significantly different between treatments on the final day of each incubation (see section 3.2). As such, we assumed the contribution of each size class to total [chl *a*] was the same on Day 3 and the final days of the incubations.

The background dissolved Fe concentration for treatments without added Fe was not included in the calculation of the ⁵⁵Fe specific activity because it is negligible (<0.1 nM) compared to the added ⁵⁵Fe (1 nM). For treatments with a 1 nM Fe amendment, it is likely that an insignificant portion of the ⁵⁵Fe bound to DFB would have exchanged with the unlabeled Fe in solution over 24 h. In artificial seawater at pH 8 and room temperature, the conditional stability constant ($K_{\text{FeL,Fe}'}^{\text{cond}}$) of inorganic Fe complexation by DFB is $10^{16.5}$, and the forward reaction rate constant

(k_f) is $\sim 2 \times 10^6 \text{ L mol}^{-1} \text{ s}^{-1}$ (Hudson et al. 1992). Using the relationship between the forward rate constant, the dissociation rate constant (k_d), and the conditional stability constant ($K_{FeL,Fe'}^{cond} = k_f / k_d$), k_d was estimated to be $10^{-10.22} \text{ s}^{-1}$ (assuming dissociation follows first-order reaction kinetics). The time required for the ^{55}Fe and unlabeled Fe in solution to re-equilibrate with DFB, estimated using the half-life of the dissociation (1.3×10^5 days), is much longer (> 250 years) than the time of our HAFETS incubation (24 h). While FeDFB is not photolabile (Albrecht-Gary and Crumbliss 1998), it is possible that the dissociation of $^{55}\text{FeDFB}$ could be facilitated by the presence of natural ligands capable of forming a ternary complex with $^{55}\text{FeDFB}$, whereby ^{55}Fe bound could be shuttled from DFB into weaker complexes. The dissociation of the Fe mineral goethite by DFB increases more than an order of magnitude in the presence of oxalate (Cheah et al. 2003). While it is not possible to estimate how the unknown *in situ* ligands might affect FeDFB dissociation, they would have to increase dissociation by five orders of magnitude in order for a significant portion of the ^{55}Fe bound to DFB to be replaced by unlabelled Fe.

4.2.5 Statistical Analyses

We were concerned whether each treatment was significantly different from the respective control treatment in both incubations. For P20GO, amended treatments were compared with the control using a two-way Student's t-test (unequal variances, $n=3$, $\alpha=0.05$). For the P26GO, we analyzed the high and low light treatments separately. The control treatments in the *in situ* light regime were compared with the respective control using a two-way Student's t-test (unequal variances, $n=3$, $\alpha=0.05$). The low light treatments were compared with each other using a one-way ANOVA ($n=3$, $\alpha=0.05$) and a Tukey-Kramer post-hoc test to test for differences between treatments. For some variables measured, we were interested in comparing

the initial response of a specific treatment to the initial values measured prior to making our amendments, and so a two-way Student's t-test was employed. All statistical analyses were carried out using JMP version 10 statistical software (SAS).

4.3 Results

4.3.1 Station Parameterization

Each station had well defined mixed layers (P20 = 29 m; P26 = 18 m) that extended below the 10 m sampling depth (Figure 4.1, Table 4.1). The euphotic zones at P20 (124 m) and P26 (110 m) extended well beyond the mixed layers of each station. The average dissolved nitrate, phosphate, and silicic acid concentrations in the mixed layer were elevated at both stations compared to the N-deficient surface waters near the coast ($\sim 0 \mu\text{M}$), and confirmed that we had sampled the eastern side of the subarctic Pacific high nutrient low chlorophyll (HNLC) region. This was corroborated by low dissolved Fe (P20 = $0.01 \pm \text{nM}$ and P26 = 0.04 nM) and F_v/F_m values (P20 = 0.22 ± 0.02 and P26 = 0.27 ± 0.02) at each station, and confirmed by large increases in the net accumulation of chl *a* after the additions of Fe to the incubations compared to the control treatments (see section 3.3). The [chl *a*] at 10 m at each station were similar (0.38 ± 0.07 and $0.44 \pm 0.03 \mu\text{g L}^{-1}$ at P20 and P26, respectively). At P20, the total dissolved Cu concentration at 10 m (1.11 nM) was complexed by a pool of excess strong Cu ligands ($6.79 \pm 0.61 \text{ nM}$) with a high-affinity for Cu ($\log K_{\text{CuL},\text{Cu}^{2+}}^{\text{cond}} = 14.23$). This resulted in a free Cu^{2+} concentration of 1.15 fM ($\text{pCu} = 14.94$). The total inorganic Cu concentration (27.6 fM) was calculated using the side reaction coefficient ($\alpha_{\text{Cu}^{2+}}$) for Cu^{2+} (24; Coale and Bruland, 1988) and the relationship $[\text{Cu}'] = \alpha_{\text{Cu}^{2+}} [\text{Cu}^{2+}]$.

4.3.2 Chl *a*

4.3.2.1 P20GO

The [chl *a*] in the control treatment increased 15% after five days ($0.44 \pm 0.14 \mu\text{g L}^{-1}$) compared to the initial [chl *a*] ($0.38 \pm 0.09 \mu\text{g L}^{-1}$) (Figure 4.2). The addition of 1 nM Fe resulted in a 4-fold increase in [chl *a*] ($1.73 \pm 0.08 \mu\text{g L}^{-1}$) compared to the control treatment by Day 5 ($p < 0.05$). There were no significant differences between the control and any of the Cu amended treatments on each sampling day. The relative contribution of the 0.22-1 μm , 1-5 μm , and $>5 \mu\text{m}$ size fractions to the total particulate [chl *a*] in all treatments was $5 \pm 1\%$, $55 \pm 3\%$, and $40 \pm 2\%$, respectively on Day 5 (data not shown). Their relative contribution of each size class to the total [chl *a*] was not significantly different between treatments.

4.3.2.2 P26GO

In the *in situ* light control, [chl *a*] increased 66% ($0.73 \pm 0.04 \mu\text{g L}^{-1}$) compared to the initial [chl *a*] ($0.44 \pm 0.03 \mu\text{g L}^{-1}$), and the addition of 1 nM Fe resulted in a 6-fold increase in [chl *a*] ($2.66 \pm 1.40 \mu\text{g L}^{-1}$) after four days compared to the initial (Figure 4.3a). Under high light, the 1 nM CuSO_4 amendment had no significant effect on [chl *a*] compared to the control on all sampling days. At the end of the incubation, [chl *a*] in the low-light control increased 13% ($0.48 \pm 0.14 \mu\text{g L}^{-1}$) compared to the initial [chl *a*], and was 34% lower than the high-light control (Figure 4.3b). In low light, Fe additions caused a significant increase in [chl *a*], with or without added Cu, compared to the low light control on Days 2 and 3 ($p < 0.05$, Tukey), and was 33 and 22% higher, respectively, by the end of the incubation compared to the control. The addition of 1 nM Cu had no significant effect on [chl *a*] under low light. The 0.22-1 μm , 1-5 μm , and $>5 \mu\text{m}$ size fractions consisted of 3 ± 1.5 , 38 ± 6 , and $59 \pm 6\%$ of the total [chl *a*] in all treatments (data not

shown), and there were no significant differences between the relative contribution of each size class to the total [chl *a*] for all treatments.

4.3.3 Photo-Physiological Responses

4.3.3.1 P20GO

F_v/F_m ranged between 0.20 and 0.44 for all treatments over the course of the incubation, and only the Fe-amended treatment was consistently higher (0.36 to 0.44) than the control (0.20 to 0.24) (Figure 4.4a). Indeed, the F_v/F_m measured in the control did not differ appreciably from the F_v/F_m of the water initially sampled (0.22 ± 0.02). Sporadic increases in F_v/F_m were observed in some of the Cu treatments. For example, compared with the controls (~ 0.2), F_v/F_m was significantly higher in the 1 nM Cu (0.28 ± 0.01) and 10 nM Cu treatments (0.28 ± 0.04) on Day 3 (0.20 ± 0.03), and in the 10 nM GSH treatment (0.29 ± 0.03) on Day 5 ($p < 0.05$). Otherwise, the addition of Cu had no effect on F_v/F_m on each sampling day.

4.3.3.2 P26GO

The range of F_v/F_m values measured during the P26GO incubation was higher than the P20GO incubation (0.27 to 0.53) (Figure 4.4b). The F_v/F_m in the *in situ* light control treatment was indistinguishable from the initial F_v/F_m (0.27 ± 0.02) on Day 2, and increased to 0.30 ± 0.04 by Day 4. In the low light control, F_v/F_m increased 41% (0.38 ± 0.03) on Day 2 compared to the initial ($p < 0.05$; t-test), and remained elevated until Day 4 (0.37 ± 0.03). The addition of Fe was the only treatment that elicited a sustained and significant increase in F_v/F_m throughout the experiment, in both the high-light (~ 0.53) and low-light incubations (~ 0.38). The Cu amendments had only an ephemeral effect on F_v/F_m . For example, the addition of 1 nM CuSO₄ in *in situ* light

resulted in a transient 37% increase in F_v/F_m (0.37 ± 0.03) on Day 2 compared to the control. F_v/F_m was significantly higher in the Fe-Cu-amended low light treatments compared to the low light control on Day 4 ($p < 0.05$, ANOVA, Tukey).

4.3.4 Day 3 HAFETS Activity

4.3.4.1 P20GO

Volumetric uptake rates (ρFe_v) ranged between 0.45 ± 0.03 and 11.43 ± 1.70 $\mu\text{mol Fe L}^{-1} \text{d}^{-1}$ for all size fractions (Table 4.2), and are within the range previously reported for this region (0.22 ± 0.01 to 12.55 ± 2.17 $\mu\text{mol Fe L}^{-1} \text{d}^{-1}$; Semeniuk et al. 2009). The average uptake rates calculated for all five treatments for the 0.22-1 μm , 1-5 μm , and >5 μm size fractions made up 14 ± 3 , 45 ± 2 , and $40 \pm 5\%$ of the total particulate ρFe_v . ρFe_v were significantly faster in the Fe-amended treatment for all size fractions ($p < 0.05$), and increased 76, 227, 338, and 245% for the 0.22-1 μm , 1-5 μm , >5 μm , and total particulate size fractions, respectively. The Cu amendments had no significant effect on ρFe_v .

Carbon-normalized Fe uptake rates (ρFe_c) ranged between 0.17 ± 0.10 and 4.53 ± 0.29 $\mu\text{mol Fe mol C}^{-1} \text{d}^{-1}$ for all size fractions, and are similar to previously measured rates along Line P (0.32 ± 0.06 to 2.93 ± 0.39 $\mu\text{mol Fe mol C}^{-1} \text{d}^{-1}$; Semeniuk et al. 2009). Similar to the volumetric rates, Cu amendments had no effect on ρFe_c ($p > 0.05$). ρFe_c increased in the Fe-amended treatment compared to the control by 114, 44, and 33% for the 0.22-1 μm , >5 μm , and total size fractions, respectively ($p < 0.05$).

4.3.4.2 P26GO

Total particulate ρFe_V in the *in situ* light treatments varied between 13.37 ± 3.29 and 37.98 ± 2.03 $\mu\text{mol Fe L}^{-1} \text{d}^{-1}$, while uptake rates were approximately an order of magnitude lower in the low light treatments (1.93 ± 0.17 to 2.65 ± 0.24 $\mu\text{mol Fe L}^{-1} \text{d}^{-1}$) (Table 4.3). Similar to the P20GO incubation, the 0.22-1 μm , 1-5 μm , and >5 μm size fractions made up 16 ± 6 , 43 ± 5 , and $41 \pm 11\%$ of the total particulate ρFe_V , respectively. ρFe_V was 2.3, 3.5, and 2.3-fold faster in the *in situ* light Fe-amended treatment compared to the *in situ* light control for the 1-5 μm , $>5\mu\text{m}$, and total size fraction, respectively. ρFe_V decreased 68%, 81%, 88%, and 83% in the low light control compared to the *in situ* light control for the 0.22-1 μm , 1-5 μm , >5 μm and total particulate size fractions, respectively. There were no significant changes in ρFe_V among the low light treatments.

Carbon-normalized HAFETS activity ranged between 0.50 ± 0.16 and 11.33 ± 0.48 $\mu\text{mol Fe mol C}^{-1} \text{d}^{-1}$ for the *in situ* light treatments, and 0.12 ± 0.07 and 2.07 ± 0.11 $\mu\text{mol Fe mol C}^{-1} \text{d}^{-1}$ for the low light treatments. In *in situ* light, the Fe amendment caused ρFe_C to significantly increase 147, 460, and 271% in the 1-5 μm , >5 μm , and total particulate size fractions, respectively ($p < 0.05$). ρFe_C also significantly increased 86 and 57% for the >5 μm and total size fractions, respectively, in the Cu-amended *in situ* light treatment ($p < 0.05$). In low light, ρFe_C decreased 64, 62, 71, and 63% for the 0.22-1 μm , 1-5 μm , >5 μm , and total particulate size fractions, respectively, compared to the *in situ* light control ($p < 0.05$; t-test). Compared to the low light control, ρFe_C was 33% slower in the $> 5\mu\text{m}$, and the total particulate size fractions in the Fe-Cu amended treatment. Statistical analysis by one-way ANOVA indicated no significant differences between treatments ($p = 0.1073$).

4.3.5 Heterotrophic Bacterial Abundance

Heterotrophic bacterial cell abundance over the course of the P20 and P26 incubations varied between $1.13 \pm 0.38 \times 10^6$ and $2.35 \pm 1.68 \times 10^6$ cells mL⁻¹, and $1.55 \pm 0.03 \times 10^6$ and $1.95 \pm 0.19 \times 10^6$ cells mL⁻¹, respectively (data not shown). There were no significant differences between the treatments in the P20GO or P26GO treatments on each sampling day ($p > 0.05$).

Bacterial abundances were similar to previous observations along Line P (0.80 to 1.35×10^6 cells mL⁻¹; Sherry et al. 1999).

4.3.6 Dissolved Fe in the Incubation Bottles

Samples for total dissolved Fe were taken from treatments without added Fe at the end of the P20GO and P26GO incubations to verify Fe contamination did not occur. The final average dissolved Fe concentration for the P20GO treatments was 0.014 ± 0.006 nM, ranging between 0.01 and 0.03 nM (data not shown), and was very similar to the initial dissolved Fe concentration (0.01 nM). The final dissolved Fe concentrations in the P26GO incubation ranged between 0.03 and 0.07 nM, with an average of 0.05 ± 0.02 nM (data not shown), and were similar to the initial dissolved Fe concentration (0.04 nM).

4.4 Discussion

4.4.1 Null Cu Limitation at P20

Dissolved nitrate (2.2 μ M), low dissolved Fe (0.01 nM), and low F_v/F_m (0.22 ± 0.02) of the waters sampled indicate that the phytoplankton community sampled at P20 was likely Fe-limited. Indeed, after 24 h of exposure to 1 nM Fe, [chl *a*] and F_v/F_m were 62 and 83% higher than in the control, respectively. As a result, we considered the *in situ* phytoplankton at P20 to

be Fe-limited. If Cu' is the sole bioavailable source of Cu to phytoplankton (c.f. Sunda and Guillard 1976; Moffett and Dupont 2007), then the pCu of the water sampled (pCu = 14.96) was on par with the pCu found to co-limit Fe-limited phytoplankton laboratory cultures (pCu = 15; Annett et al. 2008; Guo et al. 2012). The addition of 1 nM CuSO₄ should have increased the inorganic Cu concentration 2.5 fold (pCu from 14.94 to 14.67), and could have potentially relieved Cu limitation.

Unlike the previous two Cu amended incubations in HNLC waters (Coale 1991; Peers et al. 2005), net biomass accumulation did not respond to either increased total dissolved Cu concentration (i.e. 1 nM CuSO₄, 1 nM Cu CuSO₄ +10 nM GSH, and 10 nM CuSO₄ treatments), or increased labile dissolved Cu (10 nM GSH treatment) in the P20GO incubation. These results were unexpected, particularly for the treatment amended with 10 nM CuSO₄. Coale (1991) argued that Cu toxicity incurred by micrograzers was responsible for the increase in [chl *a*] in their Cu-amended treatment (see section 4.5). Our addition of 10 nM CuSO₄ should have saturated the pool of free Cu ligands present (6.79 ± 0.60 nM), resulting in an increase of 3.3 nM of inorganic Cu and a corresponding pCu of 9.86. At least two species of ciliates are known to be unable to grow at pCu 10, so micrograzing should have been greatly reduced in our 10 nM Cu treatment (Stoecker et al. 1986). Previous laboratory studies of phytoplankton have demonstrated that inorganic Cu concentrations become toxic to many species below a pCu of 10 (Brand 1986). It is possible that net biomass accumulation did not change in the 10 nM Cu treatment due to simultaneous decrease in grazing pressure and Cu-induced toxicity to phytoplankton. Interestingly, a previous incubation of coastal phytoplankton re-suspended in deep water collected from 800 m demonstrated a 4-6 day lag phase in community growth in

treatments with CuSO_4 additions between 10 and 100 nM (Sunda et al. 1981). The null response of [chl *a*] to our 10 nM Cu addition could also be due to a similar lag period. More Cu-sensitive species would have died, leaving a niche open for more Cu-resistant species to grow. Since Fe was the primary limiting nutrient at this station, the low Fe concentration (0.01 nM) would have placed a cap on the amount of biomass that could be eventually sustained, regardless of the Cu nutritional state of the phytoplankton community.

Changes in phytoplankton biomass due to Cu additions cannot discern between alterations to primary productivity or micrograzing rates. We monitored two physiological variables of the phytoplankton community – high-affinity Fe transport activity and F_v/F_m – that would allow us to determine if the physiology of the primary producers responded to Cu additions. The HAFETS in diatoms involves reduction of Fe(III) to Fe(II) by a ferrireductase, oxidation by a multi-Cu containing ferroxidase, and eventual internalization by a Fe(III) permease (Peers et al. 2005; Maldonado et al. 2006; Kustka et al. 2007). Cellular Fe uptake and Fe(II) oxidation rates decrease under Cu-limitation, but partially recover with the addition of Cu (Maldonado et al. 2006). If the Fe-limited phytoplankton sampled at P20 were also limited by Cu, then it is likely that HAFETS activity would increase with the alleviation of Cu limitation.

The Cu amendments in the P20GO had no effect on ρFe_v or ρFe_c for all size fractions, indicating that increasing Cu availability did not enhance the ability of the phytoplankton community to access Fe. In the Fe-amended treatment, ρFe_c was between 76 and 245% faster compared to the control for all size fractions. These results are counter-intuitive since previous work has demonstrated that severely Fe-limited phytoplankton communities take up Fe

complexed to siderophores faster than when Fe-replete. Iron uptake rates from the FeDFB complex increased an order of magnitude when DFB was added to an Arctic phytoplankton community to artificially induce Fe-limitation (Taylor et al. 2013). Uptake rates of Fe bound to desferrioxamine E and EDTA decreased shortly after the SOIREE mesoscale Fe addition (Maldonado et al. 2001b). However, Taylor et al. (2013) also observed a doubling in Fe uptake rates by the >5 μm size class of a Fe-light co-limited phytoplankton community when Fe was added, suggesting that uptake rates from FeDFB may not solely reflect the degree of Fe limitation experienced by the phytoplankton community. When Fe is replete, phytoplankton can take up Fe beyond their metabolic requirements, a process called “luxury uptake” (Iwade et al. 2006; Marchetti et al. 2006b). Pennate diatoms of the genus *Pseudo-nitzschia* contain ferritin, an Fe-storage protein capable of storing up to 600 atoms of Fe (Marchetti et al. 2009). During a period of Fe limitation following Fe-replete conditions, storage of Fe by ferritin allows *Pseudo-nitzschia* to undergo several more divisions than phytoplankton that do not possess ferritin. Pennate diatoms like *Pseudo-nitzschia* tend to bloom during Fe-enrichment events in the northeastern subarctic Pacific HNLC region (Marchetti et al. 2006a; Boyd et al. 2007), and light microscopic analysis of our Fe-amended treatment confirmed that pennate diatoms were abundant. We suspect that the phytoplankton that bloomed in our Fe-amended treatment up-regulated their HAFETS as part of a luxury uptake strategy. Indeed, an Fe-enrichment bottle incubation previously undertaken at P26 observed a 50-fold increase in intracellular Fe quotas compared to the Fe-limited control when Fe was first added (Lohan et al. 2005). Luxury uptake and storage may account for the success of pennate diatoms during intermittent Fe-enrichment events in remote HNLC surface waters (Marchetti et al. 2009).

4.4.2 Interaction Between Fe and Cu in an Fe-Limited Phytoplankton Community Grown Under Light-Replete Levels at P26

The high nitrate (8.27 μM), low dissolved Fe (0.04 nM), and low F_v/F_m (0.27 ± 0.02) observed at P26 suggest the phytoplankton community was Fe-limited. This was confirmed in the Fe-amended *in situ* light treatment, whereby net biomass accumulation and F_v/F_m doubled by Day 2 compared to the *in situ* light control treatment. The 52% increase in biomass in the *in situ* light control compared to the low light control at the end of the incubation indicates that 1% light intensity caused light limitation. The modest 33% increase in [chl *a*] in the Fe-amended low light control treatment by Day 4 was much smaller than the 263% increase [chl *a*] in the Fe-amended *in situ* light treatment compared to the *in situ* light control (Figure 4.3). Therefore, the phytoplankton community in the low light control treatment was co-limited by Fe and light availability. Unfortunately, samples for Cu speciation and total dissolved Cu were not collected at P26, so it is not possible to determine the pCu at the beginning of the incubation. However, the pCu at 10 m depth at P26 in August 2011 was 15.11 (Chapter 5), suggesting that low inorganic Cu concentrations are common in surface waters in this region. For the subsequent argument, we assume the inorganic Cu concentration at P26 is similar to that measured at P20, and within the range reported to induce Cu limitation in laboratory phytoplankton cultures.

Similar to the P20GO, ρFe_c was significantly faster in the Fe-amended treatment for the $>5 \mu\text{m}$ and total size fractions in the *in situ* light Fe-amended treatment compared to the control, and this is likely due to luxury Fe uptake. The 1 nM Cu addition had no effect on net biomass accumulation in *in situ* light, but F_v/F_m increased 37% on Day 2 compared to the control before decreasing on Day 3 back near the initial value. In this treatment, we also observed an 89 and

61% increase in ρFe_C in the $>5\ \mu\text{m}$ and total size fractions, respectively, compared to the control treatment on Day 3. Thus, the 1 nM CuSO_4 addition may have supplied Cu to multi-copper oxidase apo-proteins of the HAFeTS in the large size fraction, resulting in a short-term increase in cellular Fe uptake (Maldonado et al. 2006). This would have resulted in a short-term increase in intracellular Fe and corresponding increase in F_v/F_m as Fe-limitation briefly subsided. The increase in ρFe_C of the $>5\ \mu\text{m}$ size fraction in response to the Cu addition indicates that larger Fe-limited phytoplankton may be more susceptible to Cu limitation. Indeed, previous work demonstrated that intracellular Cu:C assimilation ratios were positively correlated with ρFe_C for only the $>20\ \mu\text{m}$ size fraction along the Line P transect (Semeniuk et al. 2009). These data imply that Fe transport and intracellular Cu levels may be metabolically linked in larger cells.

4.4.3 Fe-Cu Interactions During Light Limitation at P26

Light-limited phytoplankton have higher intracellular Fe demands due to the increased number of Fe-rich photosynthetic reaction centres and electron transport chain components (Falkowski et al. 1981; Raven 1990; Sunda and Huntsman 1997; Strzepek and Harrison, 2004). We hypothesized that Fe-Cu co-limitation would be more severe in the low light treatment, and ρFe_C would increase as cells up-regulated their HAFeTS to access Fe. Previous work at P26 has demonstrated that the $>5\ \mu\text{m}$ phytoplankton have 20-80% higher intracellular Cu requirements under low light (Chapter 2), and may indicate that light-limited phytoplankton increase their Cu demands for Fe acquisition via the HAFeTS. Although Fe and Cu physiologies appear to be linked in the *in situ* light treatment, the addition of Cu alone had no significant effect on ρFe_C , net [chl *a*] accumulation, or F_v/F_m in the Fe-light co-limited treatments. Indeed, ρFe_C decreased

in the low light control compared to the *in situ* light control. This is likely due to a decrease in available cellular NADH during light limitation, resulting in Fe uptake by the HAFETS to be limited by a supply of reducing agent. If true, then light limitation may impart a greater control on Fe-limited phytoplankton growth than Cu availability, whereby uptake of Fe may become co-limited by the availability of reducing agent, and not Cu.

4.4.4 Comparison with Previous Incubations

Two previous incubations demonstrated a net accumulation of biomass following the addition of Cu to HNLC surface waters, and imply that Fe-limited phytoplankton may be co-limited by Cu (Coale 1991; Peers et al. 2005). Coale (1991) observed an increase in net [chl *a*] accumulation and volumetric carbon-fixation rates at P26 with the addition of 3.9 nM CuSO₄. This Cu amendment increased the ambient dissolved Cu concentration by 4-fold (from 1.3 to 5.2 nM), resulting in nearly a 1000-fold increase in [Cu²⁺] (from 10^{-13.4} to 10^{-10.6} mol L⁻¹). By Day 6 of the incubation, [chl *a*] and in the Cu amended treatment had increased 180%. However, carbon-normalized primary productivity rates decreased in the Cu amended treatment compared to the control, indicating that the phytoplankton community was less efficient at fixing carbon and may be the result of Cu-induced intracellular oxidative stress. Coale (1991) argued that a decrease in grazing pressure by Cu-sensitive ciliates (Stoecker et al. 1986) was likely responsible for the increases in biomass since ciliate abundance decreased in the Cu amended treatment compared to the control.

Peers et al. (2005) amended water collected from Fe-limited surface waters in the Bering Sea with 2 nM CuSO₄. They did not report total dissolved Cu concentration or Cu speciation of the

water sampled. Total dissolved Cu concentrations in this region are between 1.5 and 2 nM in surface waters, and strong ligands are usually in excess of Cu in a 2:1 ratio (Moffett and Dupont 2007). The 2 nM addition of CuSO₄ may have saturated the free excess strong Cu ligands, resulting in an elevated inorganic Cu concentration. Similar to Coale (1991), at the end of the incubation, net [chl *a*] accumulation increased in the Cu amended treatment by approximately 30% compared to the control. Unfortunately, micrograzing data were not reported, and so it is not possible to discount alterations to grazing in this treatment. In the Fe and Cu amended treatment, the rate of [chl *a*] accumulation seemed faster than that in the treatment only amended with Fe, but the slopes were not statistically compared. A reanalysis of these data, where the initial [chl *a*] datum is included, demonstrates that a log fit produces indistinguishable slopes for the Fe ($\log[\text{chl } a] = -1.04(\pm 0.16) + 0.57(\pm 0.05) \cdot \text{Day}$) and Fe/Cu ($\log[\text{chl } a] = -1.57(\pm 0.27) + 0.66(\pm 0.08) \cdot \text{Day}$) amended treatments. As such, it is unlikely that Fe-Cu co-limitation was occurring.

4.4.5 Oceanographic Significance

The results herein provide evidence of an interaction between Fe and Cu physiology in phytoplankton communities in the NE Pacific HNLC region. Increasing Cu availability at P20 did not measurably influence the physiology of the phytoplankton community, and suggests Cu bioavailability is not limiting phytoplankton growth at this station despite low Cu'. In contrast, amending P26 surface waters with Cu caused a transient increase in Fe acquisition rates in >5 μm phytoplankton, as well as an increase in F_v/F_m on Day 2, but only when light was not limiting. Winter phytoplankton populations at P26 can be co-limited by Fe and light (Maldonado et al. 1999). As light availability increases, a small annual spring diatom bloom

occurs at P26 each year, resulting in drawdown of half of the dissolved silicic acid between June and July (Whitney and Freeland, 1999). Once light is no longer limiting, and access to Fe becomes scarce, Cu availability may play a role in mediating phytoplankton growth. Given the different responses of the P20 and P26 phytoplankton communities to an increase in Cu concentrations, Cu bioavailability may vary with depth (i.e. light availability) and across this Fe-limited region.

The faster pFe_C of the $>5 \mu\text{m}$ size fraction phytoplankton – but not the $< 5 \mu\text{m}$ size fractions – when Cu was added under *in situ* light at P26 indicates that natural Cu additions to Fe-limited surface waters by atmospheric deposition or vertical mixing may have different effects on large and small phytoplankton. Small phytoplankton cells have a higher surface area to volume ratio and a thinner diffusive boundary layer than large cells. This provides smaller cells with an advantage over larger cells in encountering limiting micronutrients such as Fe (Sunda and Huntsman 1997). However, smaller cells may be also more susceptible to metal toxicity. The encounter rate between Cu and the transporter active sites would increase as the thickness of the diffusive boundary layer decreases, resulting in an increased potential rate of Cu internalization. During episodic atmospheric deposition events in Fe-limited surface waters, larger cells may preferentially grow as Fe and Cu bioavailability might be enhanced. However, smaller cells may be selected against as the Cu concentration, and potential for toxicity, increases. A switch to larger cells could decrease microzooplanton grazing rates, increase sinking rates, and possibly increase carbon export without significantly affecting primary production.

4.5 Tables

Table 4.1. Initial station parameters for stations P20 and P26 in the subarctic NE Pacific Ocean sampled between August 17 and September 2, 2010. Discrete chemical and biological measurements were made on samples collected from 10 m

Parameter	P20	P26
Latitude (N)	49°33.92	50°00.04
Longitude (W)	138°40.04	145°00.03
Mixed layer depth (m)	29	18
Light Extinction coefficient (k_d ; m^{-1})	0.037	0.042
Euphotic Zone (m)	124	110
I_D (% I_0) ^a	61%	70%
Nitrate (μM)	2.2	8.2
Phosphate (μM)	0.56	0.86
Silicic Acid (μM)	3.9	13.6
Chl <i>a</i> ($\mu g L^{-1}$)	0.38 ± 0.09	0.44 ± 0.03
F_v/F_m	0.22 ± 0.02	0.27 ± 0.02
Total dissolved Fe (nM)	0.01	0.04
Total dissolved Cu (nM)	1.11	ND ^b
[L'] (nM)	6.79 ± 0.61	ND
$\log K_{CuL,Cu^{2+}}^{cond}$	14.23	ND
$-\log[Cu^{2+}]$ (M)	14.94	ND

^aThe average light intensity experienced by a single phytoplankton cell mixing throughout the water column (I_D) was expressed as a percentage of the surface irradiance (I_0)

^bND: not determined

Table 4.2. Volumetric ($\text{pmol Fe L}^{-1} \text{d}^{-1}$; ρFe_V) and carbon-normalized ($\mu\text{mol Fe mol C}^{-1} \text{d}^{-1}$; ρFe_C) size-fractionated Fe uptake rates (24 h) of $1 \text{ nmol L}^{-1} {}^{55}\text{Fe}$ bound to 1.05 nmol L^{-1} DFB in the P20GO incubation. Uptake rates were measured on Day 3 of the incubation. Carbon-normalized uptake rates were calculated by converting total bacterial abundances and chl *a* to carbon ($20 \text{ fg C cell}^{-1}$, and $50 \text{ g C g chl } a^{-1}$, respectively). Values in parentheses are 1σ for triplicates. Values in bold are significantly different from the control treatment (two-tailed t-test, unequal variances, $p < 0.05$).

Volumetric FeDFB Uptake Rates ($\text{pmol Fe L}^{-1} \text{d}^{-1}$)												
Size (μm)	Control		1 nM Cu		1 nM CuGSH		10 nM GSH		1 nM Fe		10 nM Cu	
0.22-1	0.55	(0.08)	0.47	(0.06)	0.45	(0.03)	0.54	(0.18)	0.97	(0.15)	0.51	(0.12)
1-5	1.47	(0.32)	1.49	(0.16)	1.28	(0.10)	1.61	(0.51)	4.81	(0.82)	1.50	(0.15)
>5	1.29	(0.25)	1.35	(0.06)	0.97	(0.11)	1.45	(0.42)	5.65	(0.73)	1.14	(0.04)
Total	3.31	(0.43)	3.30	(0.23)	2.69	(0.15)	3.60	(1.08)	11.43	(1.70)	3.14	(0.19)

Carbon-normalized FeDFB Uptake Rates ($\mu\text{mol Fe mol C}^{-1} \text{d}^{-1}$)												
Size (μm)	Control		1 nM Cu		1 nM CuGSH		10 nM GSH		1 nM Fe		10 nM Cu	
0.22-1	0.22	(0.08)	0.21	(0.02)	0.25	(0.13)	0.17	(0.10)	0.47	(0.09)	0.29	(0.11)
1-5	1.44	(0.42)	1.42	(0.11)	1.28	(0.08)	1.48	(0.51)	1.55	(0.12)	1.61	(0.14)
>5	1.74	(0.43)	1.78	(0.11)	1.34	(0.13)	1.83	(0.60)	2.51	(0.09)	1.68	(0.03)
Total	3.39	(0.51)	3.41	(0.12)	2.87	(0.25)	3.48	(1.11)	4.53	(0.29)	3.58	(0.28)

Table 4.3. Volumetric ($\text{pmol Fe L}^{-1} \text{d}^{-1}$; ρFe_v) and carbon-normalized ($\mu\text{mol Fe mol C}^{-1} \text{d}^{-1}$; ρFe_c) size fractionated Fe uptake rates (24 h) of $1 \text{ nmol L}^{-1} {}^{55}\text{Fe}$ bound to 1.05 nmol L^{-1} DFB in the P26GO incubation. Uptake rates were measured on Day 3 of the incubation. Carbon-normalized uptake rates were calculated by converting total bacterial abundances and chl *a* to carbon ($20 \text{ fg C cell}^{-1}$, and $50 \text{ g C g chl } a^{-1}$, respectively). Values in parentheses are 1σ for triplicate measurements. In the *in situ* light treatments, values in bold are significantly different from the control treatment (two-way Student t-test, unequal variances, $p < 0.05$). In the low light (LL) treatments, values in bold are significantly different from all other treatments (ANOVA, $p < 0.05$, Tukey test).

Volumetric FeDFB Uptake Rates ($\text{pmol Fe L}^{-1} \text{d}^{-1}$)														
Size (μm)	<i>In situ</i> Light Control		<i>In situ</i> Light 1 nM Fe		<i>In situ</i> Light 1 nM Cu		LL							
							LL Control	LL 1 nM Fe	LL 1 nM Cu	1nM FeCu				
0.22-1	1.41	(0.42)	2.25	(0.46)	1.62	(0.06)	0.45	(0.04)	0.53	(0.06)	0.46	(0.20)	0.39	(0.17)
1-5	5.31	(1.44)	12.33	(1.40)	5.80	(1.13)	1.03	(0.27)	1.29	(0.16)	0.90	(0.34)	0.87	(0.09)
>5	6.65	(1.51)	23.40	(2.39)	6.31	(1.44)	0.81	(0.17)	0.83	(0.04)	0.60	(0.19)	0.68	(0.14)
Total	13.37	(3.29)	37.98	(2.03)	13.74	(2.58)	2.30	(0.18)	2.65	(0.24)	1.96	(0.61)	1.93	(0.17)

Carbon-normalized FeDFB Uptake Rates ($\mu\text{mol Fe mol C}^{-1} \text{d}^{-1}$)														
Size (μm)	<i>In situ</i> Light Control		<i>In situ</i> Light 1 nM Fe		<i>In situ</i> Light 1 nM Cu		LL							
							LL Control	LL 1 nM Fe	LL 1 nM Cu	1nM FeCu				
0.22-1	0.50	(0.16)	0.81	(0.15)	0.56	(0.16)	0.18	(0.01)	0.19	(0.02)	0.14	(0.07)	0.12	(0.07)
1-5	2.37	(0.89)	2.92	(0.34)	3.40	(0.30)	0.91	(0.24)	0.89	(0.01)	0.76	(0.32)	0.61	(0.07)
>5	2.72	(0.67)	7.61	(0.68)	5.07	(0.63)	0.98	(0.20)	0.80	(0.09)	0.70	(0.25)	0.66	(0.14)
Total	5.59	(1.29)	11.33	(0.48)	9.02	(0.84)	2.07	(0.11)	1.88	(0.10)	1.60	(0.58)	1.39	(0.16)

4.6 Figures

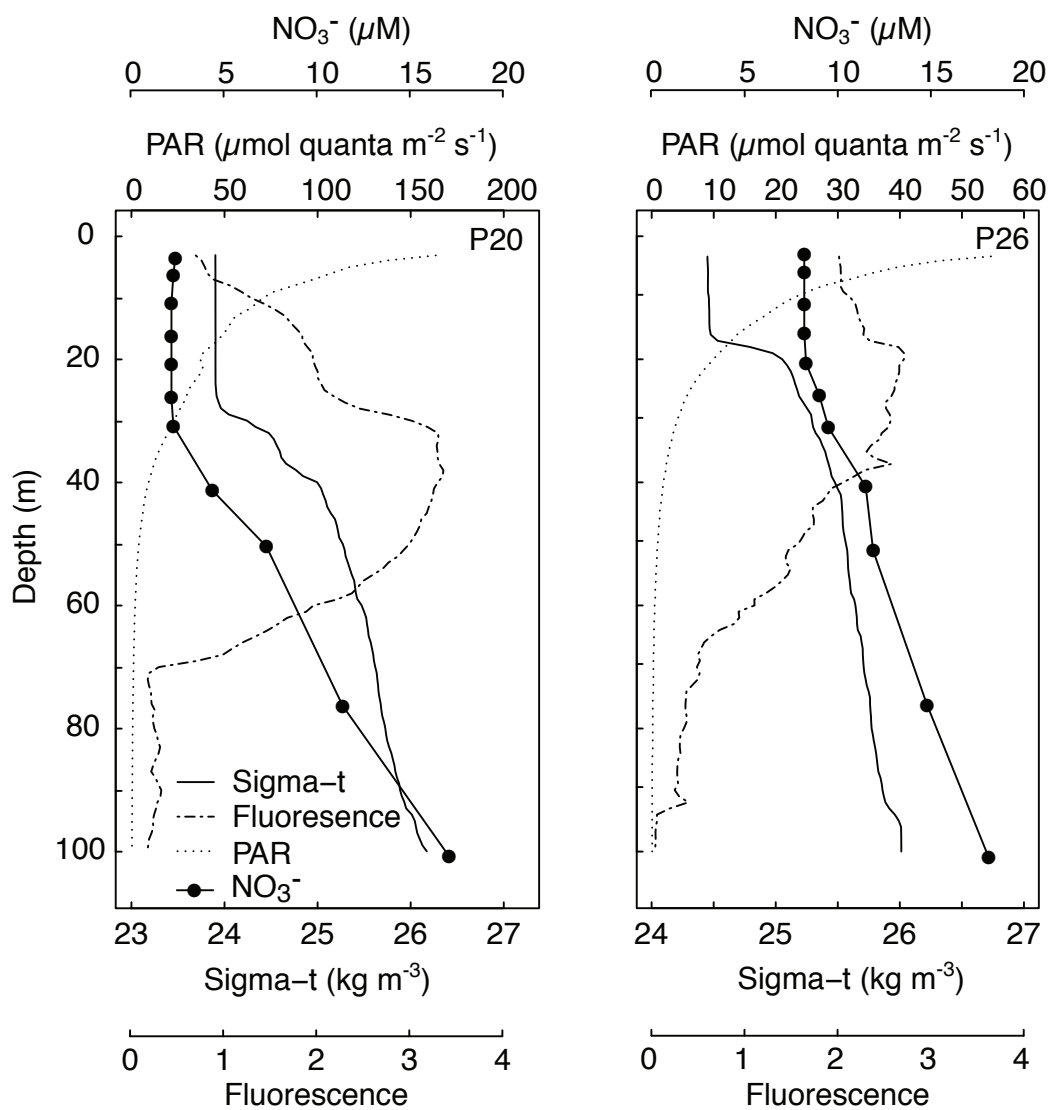


Figure 4.1. Vertical profiles of dissolved nitrate (μM), photosynthetically active radiation (PAR; $\mu\text{mol quanta m}^{-2} \text{s}^{-1}$), density ($\sigma\text{-t}$; kg m^{-3}), and fluorescence in the upper 100 m at stations P20 and P26.

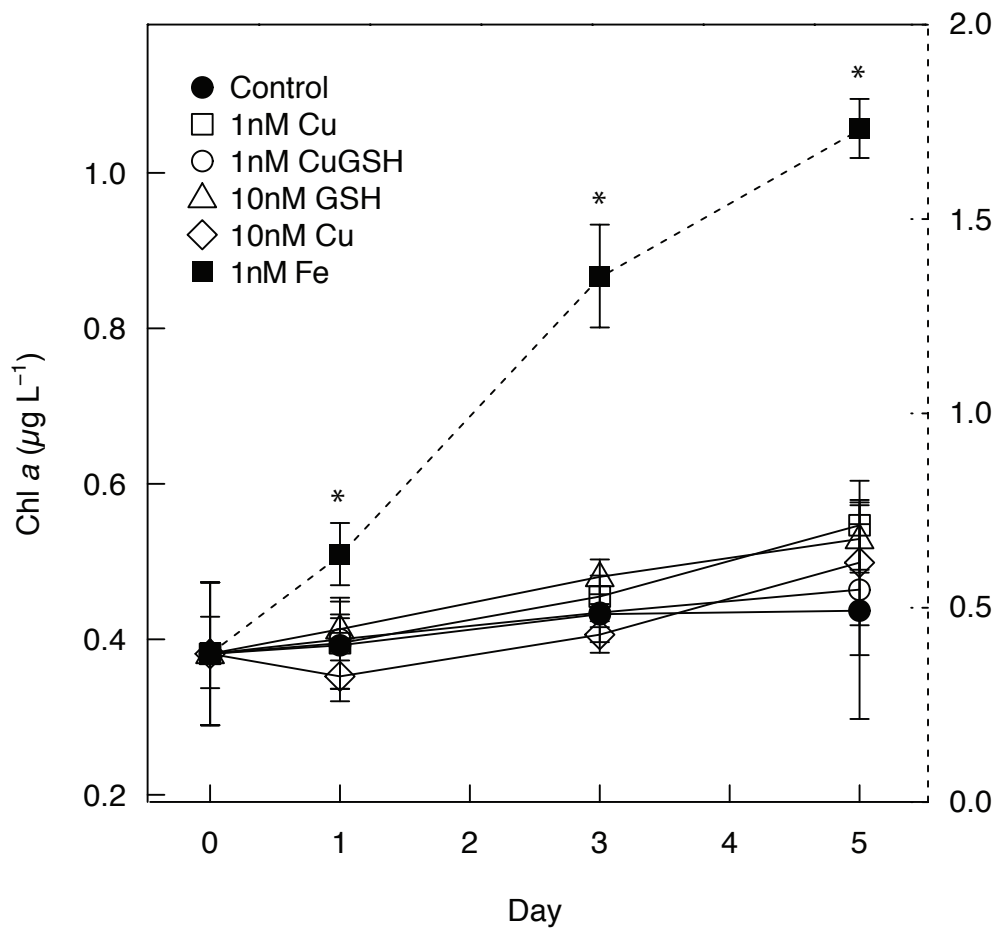


Figure 4.2. Chl *a* concentrations (µg L⁻¹) over the course of the P20GO incubation. Asterisks denote a significant difference compared to the control treatment for each respective sampling time, and error bars represent ± 1σ (p < 0.05; n = 3, two-tailed t-test). Note that the right y-axis is for the Fe-amended treatment.

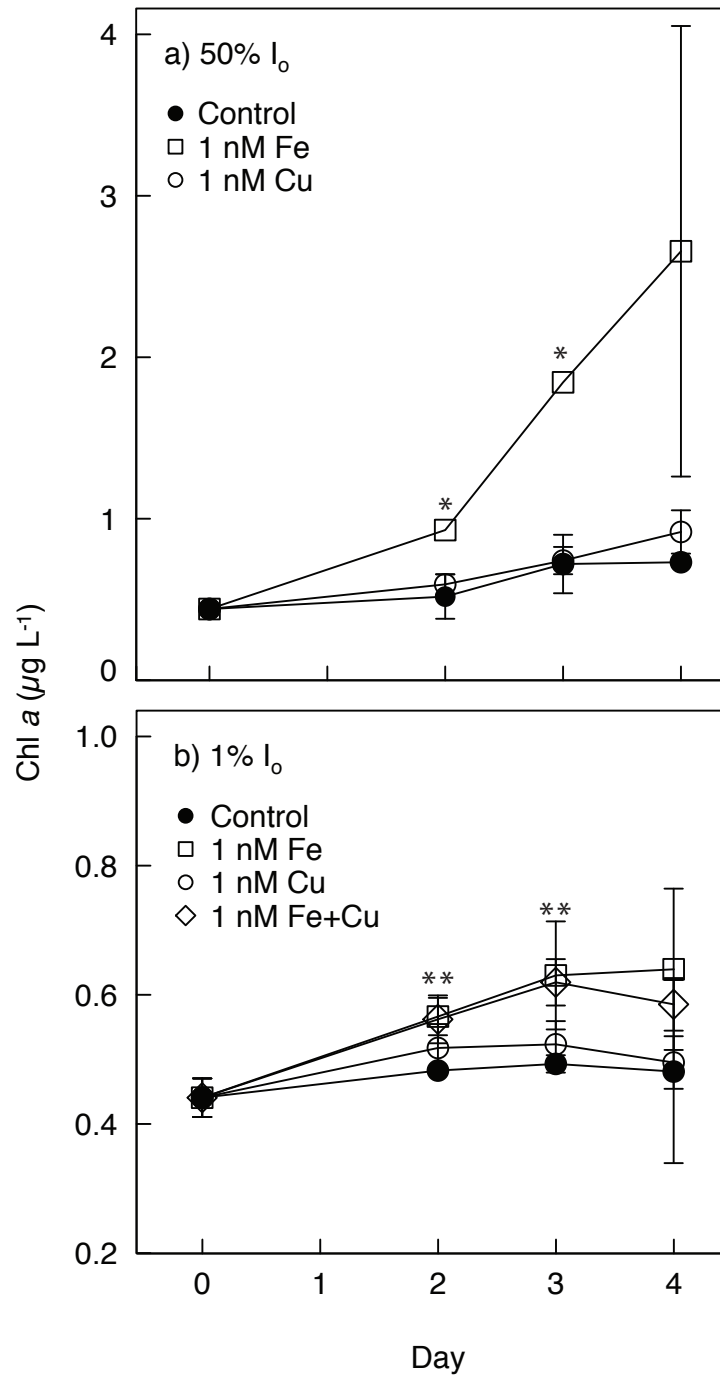


Figure 4.3. Chl *a* concentrations ($\mu\text{g L}^{-1}$) over the course of the P26GO incubation in the *in situ* (a) and low (b) light treatments. Asterisks denote a significant difference compared to the control treatment for each respective sampling time for the high light ($p < 0.05$; $n = 3$, two-tailed t-test) and low light ($p < 0.05$; $n = 3$, ANOVA, Tukey). Error bars represent $\pm 1\sigma$. Missing error bars are within the symbols.

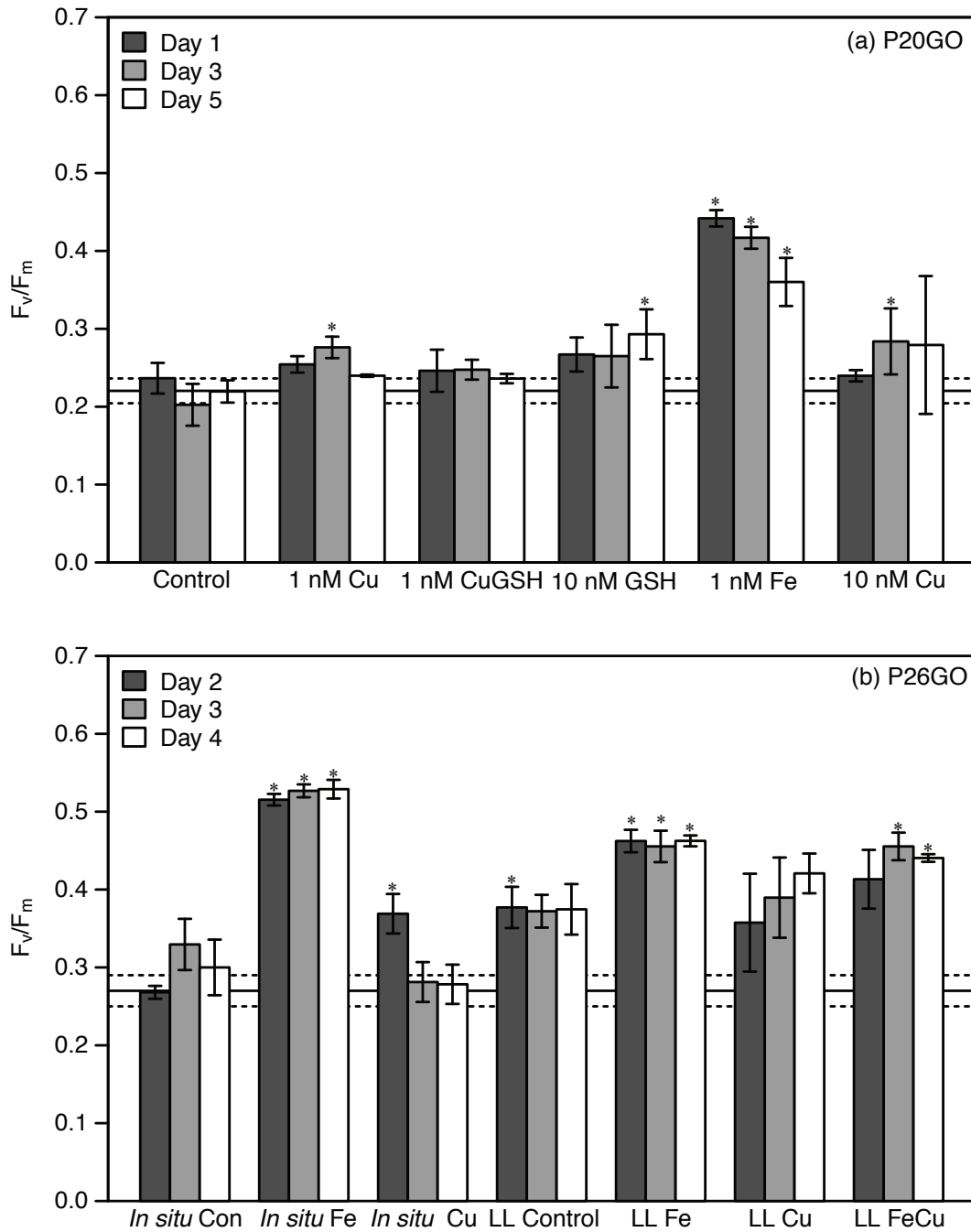


Figure 4.4. Measurements of F_v/F_m made over the course of the P20GO (a) and P26GO (b). The mean ($\pm 1\sigma$) initial values (0 h) are marked with solid and dashed lines, respectively. Statistically significant differences between the treatment and control for each sampling time are marked with an asterisk (see text), and errors bars represent $\pm 1\sigma$ ($p < 0.05$; $n = 3$).

Chapter 5: The Effects of Copper Speciation on Phytoplankton and Bacterial Rate Processes in the Northeast Subarctic Pacific Ocean

In August 2011, we surveyed microbial Cu nutrition along Line P, a coastal-open ocean transect that extends from the coast of British Columbia, Canada to the HNLC zone of the northeast subarctic Pacific Ocean. Size fractionated Cu uptake rates, Cu:C assimilation ratios, net primary productivity, bacterial abundance and productivity, total dissolved Cu, Cu speciation, and a suite of other chemical and biological parameters were measured at multiple depths along the transect. The size fractionated Cu:C assimilation ratios at all stations (0.4 to 80 $\mu\text{mol Cu mol C}^{-1}$) overlap the range of Cu quotas in laboratory marine phytoplankton experiencing Cu limitation or toxicity. Free Cu^{2+} concentrations were low (pCu 14.41 to 15.11), yet net primary productivity ($\mu\text{g C L}^{-1} \text{d}^{-1}$) was negatively correlated with inorganic Cu concentrations and positively correlated with the conditional stability constants of the *in situ* ligands. These data suggest that Cu speciation may influence phytoplankton rate processes along Line P. In addition to the transect study, a four day incubation was performed at an Fe-limited oceanic station (P16) to determine the Cu nutritional state of an indigenous phytoplankton community. Copper availability was increased with 1.5 nM or 10 nM CuSO_4 additions, and decreased with 5 nM or 30 nM additions of Cyclam (1,4,8,11-tetraazacyclotetradecane), a strong Cu(II) chelator. Copper acquisition increased nearly linearly with increasing total dissolved Cu despite being strongly complexed to *in situ* ligands, and suggests that not all *in situ* organic ligands prevent Cu uptake by marine phytoplankton. Cu:C assimilation ratios and Cu uptake rates decreased with increasing Cyclam concentrations, while picoeukaryotes and Cu-sensitive cyanobacteria

abundance, as well as chl *a*-normalized net primary productivity increased. These results provide the first evidence for *in situ* Cu availability influencing phytoplankton rate processes in the open ocean. Since strong Cu ligands have historically been thought to detoxify inorganic Cu in seawater, we reexamine the role of organic complexation in mediating the bioavailability of Cu to marine microorganisms.

5.1 Introduction

The availability of trace mineral nutrients can control marine primary productivity in some areas of the ocean. While it is well established that Fe availability limits primary productivity in up to 40% of the global surface oceans (Moore et al. 2004; Boyd et al. 2007), other trace elements may control phytoplankton community composition and growth. Copper is of particular interest because it is a required micronutrient and can also be toxic to marine phytoplankton (Brand et al. 1986; Levy et al. 2007).

Copper is involved in a number of electron transfer reactions in marine phytoplankton, including respiration, photosynthesis, reactive oxygen quenching, and nitrogen and Fe assimilation. Copper is a cofactor in cytochrome *c* oxidase in the respiratory electron transport chain inside mitochondria. Plastocyanin shuttles electrons in the light reactions of photosynthesis in an oceanic diatom (Peers and Price 2005). The intracellular production of superoxide is ameliorated by Cu/Zn superoxide dismutase in marine cyanobacteria (Chadd et al. 1996). Extracellular oxidation of primary amines to ammonium involves a Cu-containing amine oxidase (Paelenik and Morel 1991). The high-affinity Fe transport system (HAFETS) in diatoms involves the reduction of Fe(III) by a ferrireductase, followed by the oxidation of Fe(II) by a multi-Cu

containing ferroxidase and internalization by a transmembrane permease (Maldonado et al. 2006). The metabolic dependency on Cu by these processes results in intracellular Cu requirements that are equivalent to other bioactive trace metals such as Fe and Zn (Sunda and Huntsman 1992; Maldonado and Price 1996; Ho et al. 2003; Annett et al. 2008; Guo et al. 2012).

Although marine phytoplankton have a basal metabolic Cu requirement, Cu is toxic at relatively low concentrations. Growth rates for a variety of phytoplankton phyla are impeded when inorganic Cu (Cu') concentrations exceed 0.1 nM (Brand et al. 1986). Copper catalyzes the production of hydroxyl radicals via the Fenton reaction, and can cause a depletion of intracellular glutathione – a compound involved in ameliorating intracellular oxidative stress (Pinto et al. 2003). In addition, excess Cu can compete with divalent metals such as Mn at the transporter site or other enzymatic active sites inside the cell (Sunda and Huntsman 1983). Thus, competitive interactions between Cu and other metals may interrupt optimal metabolic functioning.

The concentration and bioavailability of a metal will determine whether it is a limiting or toxic nutrient in a phytoplankton community (Hudson 1998; Sunda 2012). Copper is bound to strong organic ligands in seawater, resulting in >99.9% of the dissolved Cu being complexed and free Cu^{2+} concentrations of $10^{-13.5}$ to $10^{-16.3}$ M (van den Berg 1984; Coale and Bruland 1988; Moffett and Dupont 2007; Buck et al. 2010; Bundy et al. 2013; Jacquot et al. 2013). Free Cu^{2+} makes up approximately 4% of the total inorganic Cu pool, with the remainder dominated by CuCO_3 and CuOH^- (Turner et al. 1981). Early work demonstrated that inorganic Cu (Cu') was the substrate for transport when $[\text{Cu}']$ was high (Sunda and Guillard 1976). However, laboratory

phytoplankton strains are capable of accessing organically complexed Cu when [Cu'] is low (Hudson 1998; Quigg et al. 2006; Annett et al. 2008; Guo et al. 2010; 2012; Chapter 3). Total dissolved Cu concentrations in oceanic surface waters (0.5-2.5 nM) are similar to [Cu'] that can cause toxicity in marine phytoplankton (Brand et al. 1986). Since *in situ* Cu-ligand complexes are bioavailable to indigenous phytoplankton (Chapter 2), it is possible that organic complexation of Cu in surface waters may increase Cu acquisition and thus the likelihood of Cu-induced oxidative stress inside cells.

Few studies have examined the role of Cu in controlling the growth and distribution of marine phytoplankton in the open ocean. There is preliminary evidence that Cu limits growth of phytoplankton in Fe-limited regions. Addition of inorganic Cu to HNLC phytoplankton communities in the subarctic Pacific Ocean and Bering Sea caused an increase in biomass, and may indicate that the dependence of the HAFETS on Cu may co-limit phytoplankton growth in Fe-limited waters (Coale 1991; Peers et al. 2005). More recently, dissolved Cu drawdown has been shown to be higher in Fe-limited than Fe-replete phytoplankton when amended with 1 nM Cu, and HAFETS activity increased in Fe-limited phytoplankton (Chapter 4). Low Cu availability may thus partially affect phytoplankton growth in Fe-limited regions.

Excess Cu availability has also been shown to control the growth and distribution of phytoplankton in unpolluted marine waters. The addition of the ethylenediaminetetraacetic acid (EDTA), a Cu(II)-specific organic chelator, to recently upwelled water in the equatorial Pacific caused an increase in primary productivity (Barber and Ryther 1969). Similarly, phytoplankton inoculated into deep coastal water grew faster when amended with EDTA (Sunda et al. 1981).

The observed increased phytoplankton growth may be due to the chelation of inorganic Cu(II) and concomitant decrease in Cu bioavailability. Atmospheric deposition of Cu-containing aerosols can also inhibit phytoplankton growth in the Gulf of Aqaba and Mediterranean Sea (Paytan et al. 2009; Jordi et al. 2012). While the concentration and speciation of Cu may partially inhibit primary productivity in coastal waters, it remains unclear what role Cu plays in controlling primary productivity in the open ocean.

Here we aim to determine the Cu nutritional status of microbial communities along the Line P transect in the northeast subarctic Pacific Ocean using the carrier free radioisotope ^{67}Cu . A combination of observational and process studies of phytoplankton and bacterial physiology in response to varying Cu availability was performed. We hypothesized that if the microbial communities along the transect are affected by the *in situ* bioavailability of Cu, then phytoplankton growth and Cu requirements would covary with total dissolved [Cu] or some measure of Cu speciation. In addition, we set up a bottle incubation conducted approximately 700 km offshore where we manipulated *in situ* Cu bioavailability in order to assess whether Cu was limiting or toxic to this offshore phytoplankton community. While the transect data provide an opportunity to determine how phytoplankton growth responds to varying Cu concentration and speciation over a large geographical region, the incubation allowed us to determine how a single phytoplankton population along the transect responded to varying Cu availability.

5.2 Materials and Methods

5.2.1 Plastic Cleaning

All plastics were rigorously cleaned in Class 100 conditions before the cruise. The cubitainers used for the incubation at P16, and the polycarbonate bottles used for the Cu uptake assays, Cu:C assimilation ratios, and primary productivity measurements were cleaned for 1 week with 3% Extran, 6M HCl, and 1M HNO₃, and were rinsed thoroughly with ultra pure water (18M Ω resistance; Millipore) between each cleaning step. Sample bottles for dissolved metals (250 mL low-density polyethylene; LDPE) and Cu ligands (500 mL LDPE) were cleaned according to GEOTRACES protocols. Dissolved metal sampling bottles were filled with 0.01 M ultrapure HCl (Seastar) for storage before sampling, and ligand bottles were filled with ultra pure water and left for at least a month before use. All bottles were rinsed three times with sample seawater before they were filled.

5.2.2 Experimental Design and Execution

5.2.2.1 Line P Survey

Net primary productivity, phytoplankton biomass, total dissolved Cu concentrations, Cu speciation, Cu:C assimilation ratios, Cu uptake rates, and a suite of other variables were surveyed at multiple depths along the transect (Tables 5.1 to 5.3). The depths sampled were in the mixed layer and subsurface chlorophyll maximum at each station, with light intensities spanning an order of magnitude (Table 5.2; Figure 5.2). The depths and stations sampled represent waters that may be influenced by coastal processes (P3), macronutrient limited coastal (P4) and oceanic (P12) waters, as well as Fe-limited oceanic waters (P16 and P26). The diverse

light and nutrient regimes in surface waters along Line P provide a range of physical and chemical variation that may influence Cu nutrition in marine phytoplankton.

5.2.2.2 Incubation at P16

Previous workers have induced Fe limitation in natural phytoplankton communities using the strong Fe(III) chelating siderophore desferrioxamine B (DFB) (Eldridge et al. 2004; Wells 2005; Taylor et al. 2013). DFB is a tenacious chelator with a high conditional stability constant ($\log K_{FeL,Fe}^{cond} = 10^{16.5}$; Hudson et al. 1992) that is higher than that of *in situ* Fe ligands (e.g. 10^{13} ; Rue and Bruland 1995). A small addition of DFB can reduce the bioavailability of *in situ* dissolved Fe to cause Fe-limitation (Wells 2005; Taylor et al. 2013). We adopted a similar approach to reduce the bioavailability of *in situ* dissolved Cu at P16, and oceanic Fe-limited station located midway along the transect (Figure 5.1). Copper(II) bound to the artificial macrocyclic ligand Cyclam (1,4,8,11-tetraazacyclotetradecane) is significantly less bioavailable than *in situ* Cu-ligand complexes (Chapter 2). The conditional stability constant of Cyclam ($\log K_{CuL,Cu^{2+}}^{cond} = 15.29 \pm 0.04$; Chapter 2) is higher than the conditional stability constants of the ligands found along the transect ($\log K_{CuL,Cu^{2+}}^{cond} = 13.69$ to 14.53 ; Table 5.3). Two amendments of Cyclam were made: 5 nM and 30 nM additions. These additions are similar to the *in situ* ligand concentration of the water sampled at P16 (7.75 nM, Table 5.3), and should effectively compete with the *in situ* ligands for dissolved Cu. As such, the 5 nM and 30 nM Cyclam additions made the *in situ* dissolved Cu increasingly more difficult to acquire, and thus decreased the bioavailability of the *in situ* Cu. To increase the *in situ* bioavailability of Cu, treatments with 1.5

nM and 10 nM CuSO₄ amendments were included. The Cyclam and CuSO₄ amended treatments were compared with an unamended control treatment.

It is possible that the addition of Cyclam may affect the speciation – and thus the bioavailability – of other mineral nutrients. Cyclam has a high-affinity for Cu ($\log K = 26.5$) compared to other divalent trace metal nutrients ($\log K$ of 22 and 15 for Ni and Zn, respectively) (Martell and Smith 2004). The conditional stability constants of Ni and Zn bound to Cyclam in seawater are unknown. However, assuming the $\log K$ of these complexes decreases in seawater to a similar extent as for Cu due to side reactions with Ca²⁺ and Mg²⁺, then the estimated $\log K_{MeL,Me^{2+}}^{cond}$ for Ni and Zn would be 11 and 4, respectively. Dissolved Zn along Line P is already strongly complexed to ligands with much higher $\log K_{ZnL,Zn^{2+}}^{cond}$ (9 to 11; Lohan et al. 2005), and so the addition of Cyclam would have little influence on Zn speciation.

Nickel speciation has not been measured in the North Pacific, but strong organic complexes ($\log K_{NiL,Ni^{2+}}^{cond} \sim 18$) comprise between 10 to 40% of the total dissolved Ni concentrations in coastal waters and in the western Mediterranean (Nimmo et al. 1989; Achterberg and van den Berg 1997). It is unclear whether the remaining Ni is inorganic or complexed to weak organic ligands (c.f. Achterberg and van den Berg 1997). Nickel toxicity in marine phytoplankton occurs at concentrations that are >100 times higher than those found in unpolluted surface waters (Debelius et al. 2011). As such, it is unlikely that Ni complexation by Cyclam would relieve Ni toxicity at P16. Cyclam could also cause Ni-limitation by complexing labile Ni, and decrease its bioavailability. Nickel is used by eukaryotic phytoplankton primarily to assimilate urea as a

nitrogen source when nitrogen is limiting (Price and Morel, 1991; Egleston and Morel, 2008; Dupont et al. 2010). Cyanobacteria also use Ni in superoxide dismutase to detoxify superoxide radicals (Palenik et al. 2003). Given net primary productivity and cyanobacteria abundance increased in the Cyclam-amended treatments compared to the control (see section 5.3.2), the addition of Cyclam did not cause Ni limitation at P16.

Due to the low mixed layer fluorescence at P16, for the incubation we collected water from 37 m, in the subsurface chlorophyll maximum (SCM) below the thermocline (Figure 5.2). This depth was chosen because it corresponded with the peak of the O₂ maximum and was within the SCM. The *in situ* light intensity at this depth (3% I₀) was increased to 26% I₀ in the incubation to relieve light limitation of the community and increase phytoplankton growth.

5.2.3 Water Collection and Station Parameterization along Line P

5.2.3.1 Line P Transect

Between August 17 and 26, 2011, surface waters were sampled on board the C.C.G.S. John P. Tully (Cruise 2011-27) at five stations along the Line P transect (Figure 5.1). Low nitrate concentrations at stations P3, P4, and P12, and high unutilized nitrate concentrations at P16 and P26 confirm that the first three stations were nitrate-limited, while the latter two stations were Fe-limited (Table 5.2). A few hours before dawn on each sampling day, water was pumped from between 7 and 40 m depth using a trace metal clean Teflon® diaphragm pump and Teflon® lined tubing attached to a Kevlar® wire (Johnson et al. 2005). Water was pumped directly into a Class 100 laminar flow hood where it was sampled. Around noon on each sampling day, physical water profile data were collected at each station as described in Chapter 4.

Samples collected for Cu uptake rates, Cu:C assimilation ratios, and net primary productivity were immediately placed in on-deck incubators supplied with water continuously pumped from 5 m depth until radiotracer additions could be made. The depths that were sampled were inside and below the mixed layer, and spanned a range of light intensities from 3 to 39% of I_0 (Table 5.2). The *in situ* light intensities for each depth were maintained ($\pm 4\%$) using neutral density screening.

5.2.3.2 P16 Incubation

On August 23, 2011, water was collected from 37 m depth at station P16. Just after 01:00, the cubitainers were rinsed three times with unfiltered water, filled, and immediately placed in the on-deck incubators. Cubitainers were randomly assigned to treatments, and treatments were performed in triplicate. Initial samples (day 0) were taken from each cubitainer before the CuSO_4 and Cyclam amendments were made. The cubitainers were filled the day after the P16 depth profile samples were collected, and so differences between the initial variables measured in cubitainers and those measured the previous day at 37 m depth likely reflect temporal and spatial patchiness. The Cyclam and CuSO_4 stocks used to amend the cubitainers were prepared one week in advance. A 1 mM Cyclam stock was prepared as previously described (Semeniuk et al. 2009). A 0.1 mM stock of CuSO_4 was prepared as described in Chapter 4. The stocks were stored in the dark at 4°C until needed. Cyclam and CuSO_4 amendments were made directly to the cubitainers.

5.2.4 Biological and Chemical Sampling and Analysis

Samples for total and size fractionated chl *a* concentrations, macronutrient concentrations, maximum variable fluorescence yield (F_v/F_m), and total bacterial abundance (determined by flow cytometry) were collected and analyzed as previously described (Chapter 4). Cyanobacteria and picoeukaryotes were sampled and enumerated by flow cytometry according to Taylor et al. (2013).

5.2.5 Dissolved Cu Concentrations and Speciation

Total dissolved Cu ($[Cu]_d$) samples were collected and analyzed as described in Chapter 4. Dissolved Cu speciation samples were collected using the same procedure as that for total dissolved Cu samples, but the sample bottles were not acidified, and instead they were immediately frozen and stored at -20°C until further analysis. The Cu speciation measurements – conditional stability constant ($\log K_{CuL,Cu^{2+}}^{cond}$), ligand concentration, and free Cu^{2+} concentration – were determined via competitive ligand exchange-adsorptive cathodic stripping voltametry. A single analytical window was employed using 5 μ M of the competing ligand salicylaldehyde. A detailed description of the methodology is provided in Bundy et al. (2013).

5.2.6 Cu Uptake Rates, Cu:C Assimilation Ratios, and Net Primary Productivity

Copper uptake rates and Cu:C assimilation ratios were measured using the gamma emitting radioisotope ^{67}Cu (half-life = 62 h; provided by TRIUMF, UBC) and $H^{14}CO_3^-$ (Perkin Elmer). The 37 MBq ^{67}Cu stock was kept in 0.005 M HCl, and diluted at least 2500-fold in the assay bottles to prevent significant pH changes in the assay bottle. Approximately 10 mL of seawater from each assay bottle were filtered through acid-cleaned 0.22 μ m porosity Acrodisc filters

(Pall) using an acid-cleaned rubberless syringe. The filtrate was collected in a trace metal clean 15 mL falcon tube. Approximately 5 kBq of ^{67}Cu was added to 10 mL filtrate, and allowed to complex with the excess strong Cu ligands for at least 2 h before being added to the assay bottles. A 2 h reaction time is commonly used for titrating Cu ligands with CuSO_4 for speciation analysis by electrochemical techniques (Moffett and Dupont 2007; Buck et al. 2010; Bundy et al. 2013), and so there was adequate time for the excess strong ligands to complex the tracer in our assays.

The Cu concentration was not measured in the ^{67}Cu stock that we took to sea. However, the background Cu contamination in isotope stocks received by our laboratory is routinely monitored via quadrupole ICP-MS, and the Cu concentration is always <50 nM. At most, 100 μL of the ^{67}Cu stock was added to 250 mL of collected seawater, resulting in at most a 0.02 nM Cu addition. This corresponds to a maximum possible increase in dissolved Cu of 1.4% in our assays. Given the excess Cu ligand concentrations along the transect were between 6.30 nM and 17.36 nM, there would have been sufficient excess Cu ligands to complex the 0.02 nM ^{67}Cu addition. Since the ^{67}Cu tracer would have been completely complexed by the excess *in situ* Cu ligands, and the total dissolved Cu concentration changed negligibly, then the Cu uptake rates and Cu:C assimilation ratios are representative of *in situ* values.

Previous work along Line P has demonstrated that short-term uptake rates are significantly faster than long-term uptake rates due to either cellular efflux or remineralization of particulate Cu by micrograzers (Semeniuk et al. 2009; Chapter 2). For the transect samples, both short-term (2 h incubation) and long-term (24 h incubation) uptake rates were measured. Only 24 h uptake rates

and Cu:C assimilation ratios were measured in the P16 incubation. Two hours before dawn on each sampling day, 250 mL of seawater were sampled from either the cubitainers or the Teflon pumping system into trace metal clean 250 mL polycarbonate bottles. Sampling occurred inside a Class 100 laminar flow hood. A 10 mL sub-sample was taken from each assay bottle for the ^{67}Cu and *in situ* ligand pre-complexation step (see above), and the bottles were immediately placed inside the on-deck incubators at the appropriate light levels. Once the ^{67}Cu tracer complexation was complete, the assay bottles were retrieved, and the 10 mL ^{67}Cu tracer was added. For the Cu:C assimilation ratio assays, 185 kBq of $\text{H}^{14}\text{CO}_3^-$ were also added to each sample bottle. The bottle lids were sealed with parafilm, and the bottles were immediately returned to the on-deck incubators. Duplicate bottles were prepared for transect measurements of Cu uptake and Cu:C assimilation ratios, while single bottles were sampled from each replicate cubitainer for the P16 incubation (triplicate cubitainers per treatment).

After the specified incubation time, the assay bottles were retrieved from the incubators, and a 1 mL “initial” subsample was taken from each bottle in order to determine the total activity of ^{14}C and/or ^{67}Cu added to each bottle. To each $\text{H}^{14}\text{CO}_3^-$ initial sample, 500 μL of 6 M NaOH was added to prevent degassing of $^{14}\text{CO}_2$. The volume of each bottle was recorded, and the seawater was gently vacuum-filtered onto a series of 47 mm diameter 5, 1, and 0.22 μm polycarbonate filters (AMD) separated by nylon drain discs (Millipore). Just before the filters went dry, 20 mL of 1 mM diethylene triamine pentaacetic acid (DTPA) in seawater adjusted to pH 8 were added to the filters to remove any surface-associated tracer (Croot et al. 2003). The filters were completely immersed in the wash for 10 min, the wash was then drained, and 20 mL of filtered seawater (FSW) was applied to rinse away loosely associated tracer. The filters were vacuumed

dry to prevent transfer of filtered cells between the filters and drain discs. Each filter was carefully folded and placed inside a 7 mL borosilicate scintillation vial. To each scintillation vial, 1 mL of FSW was added, and the vials were vortexed for 30 s to remove filter-bound cells. Filters collected from the Cu:C assimilation ratio assays were immediately acidified with 100 μ L of 6 M HCl to degas inorganic ^{14}C for 24 h before 1 mL of FSW was added. The activity of ^{67}Cu in each vial was determined using a sea-going gamma counter (Semeniuk et al. 2009). Background ^{67}Cu counts were performed on analysis days and subtracted from the sample counts. After ^{67}Cu counting, samples containing ^{14}C were immersed in 50% ScintiSafe scintillation cocktail (Fisher) and archived until further analysis in the laboratory two weeks later. Once the ^{67}Cu had decayed, the activity of ^{14}C was determined with a Beckman LS65005514 scintillation counter with an internal ^{14}C quench curve.

Filter blanks were performed in triplicate in order to account for abiotic adsorption of ^{67}Cu to the polycarbonate filters and particles that was not removed by the DTPA wash. Unfiltered seawater was spiked for two minutes with pre-complexed ^{67}Cu , the seawater was filtered, and the filters were processed as in the Cu uptake assays. The average activity for each filter blank was subtracted from the assay filters.

The specific activity of ^{67}Cu (DPM per mol) in the assays conducted along the transect was calculated by dividing the activity measured in 1 mL of unfiltered sample (DPM per mL) by the total dissolved Cu concentration measured in UV-digested samples (mol per mL; see section 2.5). The specific activity of ^{14}C was calculated in the same way, but we assumed a dissolved inorganic carbon concentration of 2.1 mM (Semeniuk et al. 2009). The total amount of Cu

and/or C on each polycarbonate filter was determined by dividing the activity on each filter (DPM per filter) by the specific activity of the isotope (DPM per mol). The same was done for the day 0 measurements in the P16 incubation. We chose to calculate the specific activity of ^{67}Cu on days 2 and 4 by assuming that the dissolved Cu concentration in each treatment remained constant. However, drawdown of Cu in each cubitainer would have decreased the total dissolved Cu concentration, and thus increased the specific activity in the Cu uptake and Cu:C assimilation ratio assays over the course of the incubation. Unfortunately, samples for total dissolved Cu were not taken from the P16 incubation on days 2 and 4, thus preventing a precise determination of the ^{67}Cu specific activity in each treatment on those days. An estimate of total Cu drawdown in the control treatment was calculated by assuming the initial total particulate uptake rates remained nearly constant during the incubation. After 4 days, 10% of the total dissolved Cu would have been transferred from the dissolved into the particulate phase, and so the specific activity would have changed negligibly compared to the variation observed in the data. Since [chl *a*] in the control and the Cu amended treatments were not significantly different, the relative drawdown in these three treatments was likely similar if drawdown increased linearly as previously observed (Chapter 4). As such, the uptake rates and Cu:C assimilation ratios measured on days 2 and 4 of the incubation overestimated the actual values by <10%.

Volumetric Cu uptake rates (ρCu_V ; mol Cu L⁻¹ h⁻¹) were determined by dividing mol of Cu on each filter by the sample volume filtered and the incubation time. In order to calculate biomass-normalized Cu uptake rates (ρCu_B ; $\mu\text{mol Cu mol C}^{-1} \text{ h}^{-1}$), conversion factors were used for converting bacterial abundance and [chl *a*] into particulate carbon concentrations (20 fg C cell⁻¹ and 50 g C g chl *a*⁻¹, respectively) (Booth et al. 1993; Lee and Fuhrman, 1987). The 0.22-1 μm ,

1-5 μm , and $>5 \mu\text{m}$ ρCu_B along the transect were calculated using the particulate carbon concentrations derived from bacterial abundance, and $[\text{chl } a]$ for the 1-5 μm and $>5\mu\text{m}$ size fractions, respectively. Size-fractionated $[\text{chl } a]$ was not sampled from the P16 incubation, and so ρCu_B in the phytoplankton was calculated for the $>1 \mu\text{m}$ size fraction using particulate C derived from total $[\text{chl } a]$, since $<5\%$ of the total $[\text{chl } a]$ was in the 0.22-1 μm size fraction at P16. Total ρCu_B was determined by the sum of volumetric Cu uptake rates divided by total particulate carbon concentrations derived from bacterial abundance and total $[\text{chl } a]$. Cu:C assimilation ratios ($\mu\text{mol Cu mol C}^{-1}$) were calculated for each size fraction by dividing the filtered Cu by the filtered C values measured for each size fraction. Total particulate Cu:C assimilation ratios were calculated by dividing the sum of size-fractionated particulate Cu by sum of size-fractionated particulate C. The Cu:C assimilation ratios for the 0.22-1 μm size fraction include both photosynthetic and non-photosynthetic bacteria. Non-photosynthetic bacteria will acquire Cu without fixing ^{14}C , and will result in an overestimate of the Cu:C assimilation ratios for this size fraction.

The Cu:C assimilation ratios presented herein are not equivalent to steady-state Cu quotas. Our field Cu:C assimilation ratio assays were performed for 24 h under a day-night cycle, and are subject to non-steady-state conditions. Copper uptake could have occurred during the night while C-fixation did not occur. As such, the Cu:C assimilation ratios may overestimate the true Cu quotas of the phytoplankton communities sampled along Line P.

Net primary productivity in the incubation and along the transect was determined using $\text{H}^{14}\text{CO}_3^-$. Just before dawn on each sampling day, four 60 mL TMC polycarbonate bottles were rinsed and

filled with sample water and spiked with 185 kBq of $\text{H}^{14}\text{CO}_3^-$. A 0.5 mL subsample was taken from each bottle in order to determine the total activity of ^{14}C added, and 0.5 mL of 6 M NaOH was added to prevent off-gassing of $^{14}\text{CO}_2$. One bottle was immediately wrapped in tinfoil and placed in an opaque black plastic bag as a “dark” bottle to account for non-photosynthetic carbon fixation and non-specific ^{14}C binding. Bottles were incubated at *in situ* light and temperature for 24 h in the on-deck incubators. After the incubation, the volume of each bottle was recorded and the contents were gently filtered onto 25 mm GFF filters. The filters were then placed into 7 mL scintillation vials, and 100 μL of 6M HCl was added to off-gas inorganic ^{14}C for 24 h. The filters were then immersed in scintillation cocktail and archived until they could be analyzed in the laboratory.

5.3 Results

5.3.1 Line P Transect

5.3.1.1 Descriptions of Depth Profiles

Mixed layer seawater density was highest at P26 (24.50 kg m^{-3}), decreased along the transect towards P4 (23.54 kg m^{-3}), and increased slightly at P3 (23.70 kg m^{-3}) (Figure 5.2). Mixed layer depths ranged 2-fold (15 to 31 m), and were deepest at the farthest offshore stations (P16 and P26) (Table 5.1). Light attenuation was greatest at P3 ($k_D = 0.211 \text{ m}^{-1}$), and the euphotic zone depth (Z_{eu}) was shallowest at this station (22 m) (Table 5.2). At stations P4 to P26, light attenuation ($k_D = 0.093$ to 0.096) and the euphotic zones (48 to 49 m) were similar.

Mixed layer nitrate concentrations were below detection at P3, P4, and P12 (Table 5.2).

However, they were elevated at P16 ($5.20 \mu\text{M}$) and P26 ($11.2 \mu\text{M}$), which is characteristic of

HNLC waters. Phosphate and silicic acid concentrations were not limiting across the transect.

At P3, a broad fluorescence peak was present from 5 to 30 m depth. Dissolved oxygen (DO) was elevated above the mixed layer at this station (293 to 298 μM), showed a large dip between 12 and 17 m (280 μM), and increased again below the thermocline (300 μM) (Figure 5.2).

Subsurface chlorophyll maxima (SCM) were most pronounced below the thermocline at P4 (~45 m) and P12 (~35 m), and corresponded with increased nitrate concentrations, increased DO, and low light levels ($< 5\%$ of the incident irradiation; I_0) (Figure 5.2). Smaller SCM were present at P16 and P26 and corresponded to subsurface DO maxima. The discrete depths sampled across the transect corresponded to a range of irradiances between 3 to 39% of I_0 (Table 5.2)

5.3.1.2 Copper Concentration and Speciation

Total dissolved Cu concentrations ranged between 1.46 nM and 2.79 nM along the transect (Table 2). Dissolved Cu was highest near the coast at P3 (2.42-2.79 nM). Mixed layer $[\text{Cu}]_d$ decreased along the transect towards P20 (1.70 nM), and increased at P26 (2.09 nM). Dissolved ligand concentrations were highest at P3 (14.74 and 17.36 nM at 7 and 12 m depth, respectively). Ligands were between 3 and 7-fold in excess of $[\text{Cu}]_d$ with high $\log K_{\text{CuL},\text{Cu}^{2+}}^{\text{cond}}$ (13.69 to 14.53), and the average $[\text{L}]:[\text{Cu}]_d$ ratio was 4.8 ± 1.2 ($n=12$) (Table 5.3). The $[\text{L}]:[\text{Cu}]_d$ ratio at P3 was higher at both depth (6.1 to 6.2) compared to the remaining 10 depths sampled along the transect (4.6 ± 1.1 ; $n=10$). Ligand concentrations were positively correlated with $[\text{Cu}]_d$ (slope = 5.9; $r^2 = 0.44$, $p = 0.0184$).

The excess strong [L] resulted in inorganic Cu concentrations ($[\text{Cu}']$) between 18.7 and 94 fM and coincident pCu values ($-\log[\text{Cu}^{2+}]$) ranging between 15.11 and 14.41 along the transect

(Table 5.3). At each station, [Cu'] tended to be lowest at the shallowest depth and increase with depth. Notably, the lowest [Cu'] measured along the transect corresponded with the highest NPP_V at P26 (10 m depth) (see section 5.3.1.3). The [Cu]_d, [L], and [Cu'] at the shallowest depth sampled at each station were compared with surface salinities along the transect sampled at 5 m depth (Figure 5.3). [Cu]_d and [L] were highest at the lowest salinities near the coast, and decreased offshore. [Cu'] was more variable, and did not show an obvious trend with salinity.

The CuSO₄ amendments at P16 would have been complexed by the 7.75 nM strong Cu binding ligands within 5 min (Coale and Bruland 1988). The 1.5 nM CuSO₄ addition increased the total dissolved Cu concentration by 77% and increased the inorganic Cu concentration by an estimated 109% (Table 5.4). A previous incubation using surface water collected at P26 demonstrated that a 1.5 nM CuSO₄ addition caused large phytoplankton to increase Fe uptake rates (Chapter 4). The 10 nM addition would have saturated the *in situ* strong Cu ligands (7.75 nM), resulting in an estimated inorganic Cu concentration of 10^{-8.65} M (pCu = 10.03). Given the saturation of the *in situ* strong Cu ligand pool and high resultant inorganic Cu concentration with the 10 nM CuSO₄ addition, the phytoplankton in this treatment may have been experiencing Cu-toxicity (Brand et al. 1986).

5.3.1.3 Biomass and Productivity

Total [chl *a*] varied more than 20-fold along Line P – ranging between 0.04 and 0.96 μg chl *a* L⁻¹ – with highest concentrations at P3, and lowest in the mixed layer at P4 (Table 5.5). The 0.22-1 μm, 1-5 μm, and >5 μm size fractions made up 7±8, 48±15, and 45±12% of the total [chl *a*] across the transect, respectively (Table 5.6). The 0.22-1 μm size fraction made up <10% of the

total [chl *a*] at all sampling depths except for 12 m at P3 (31%). Cyanobacteria and picoeukaryote abundance varied between 0.77 and 200×10^6 cells L⁻¹, and 0.55-16.3 $\times 10^6$ cells L⁻¹, respectively (Table 5.5). They were most abundant at P3 and tended to be more prevalent at deeper depths at all stations (e.g. P4, P12, and P16). The maximum fluorescence yield (F_v/F_m) was highest near the coast (0.23-0.64), lowest at P16 (0.19-0.29), and decreased towards the HNLC waters (Table 5.5)

Volume-normalized rates of net primary productivity ranged between 10.8 and 110.4 $\mu\text{g C L}^{-1} \text{d}^{-1}$. NPP_V was highest in the mixed layer at P26 (110.4 $\mu\text{g C L}^{-1} \text{d}^{-1}$), and co-occurred with a higher F_v/F_m (0.29) compared to the mixed layer at P16 (40.8 $\mu\text{g C L}^{-1} \text{d}^{-1}$; $F_v/F_m = 0.19$) (Table 5.5). These rates are within the range previously reported for the upper 40 m along Line P in the summer (10 to 100 $\mu\text{g C L}^{-1} \text{d}^{-1}$) (Boyd and Harrison, 1999). NPP_B ranged between 74.4 and 583.2 $\mu\text{g C } \mu\text{g chl } a^{-1} \text{d}^{-1}$, with the fastest rate (583.2 $\mu\text{g C } \mu\text{g chl } a^{-1} \text{d}^{-1}$) in the mixed layer at P4.

Total bacterial abundance between stations P4 and P26 varied between 0.82 and 3.66×10^9 cells L⁻¹, and was an order of magnitude higher at P3 (32.0 to 32.2×10^9 cells L⁻¹) (Table 5.5).

Volumetric and cell-normalized rates of bacterial productivity varied between 0.98 and 4.78 $\mu\text{g C L}^{-1} \text{d}^{-1}$, and 0.41 and 4.85 $\text{fg C cell}^{-1} \text{d}^{-1}$, respectively. Both volumetric and carbon-normalized rates of bacterial productivity were fastest at P16 and P26. Bacterial abundance and productivity were within the range previously reported for summer months along Line P (0.80 to 1.35 billion cells L⁻¹ and 2 to 6 $\mu\text{g C L}^{-1} \text{d}^{-1}$, respectively) (Sherry et al. 1999).

5.3.1.4 Transect Correlations

The concomitant sampling of total dissolved Cu, Cu speciation, and various measures of biological biomass and productivity allow us to determine how Cu might influence microorganisms along Line P. There were a number of statistically significant correlations along the transect (for p-values, see Table 5.7). Most strikingly, total particulate NPP_V, as well as 1-5 μm and >5 μm NPP_V, were negatively correlated with [Cu'] ($r^2 = -0.63$ to -0.86) and positively correlated with $\log K_{CuL,Cu^{2+}}^{cond}$ ($r^2 = 0.63$ to 0.74) (Figure 5.4a,c). There were no significant correlations between NPP_B and either [Cu'] or $\log K_{CuL,Cu^{2+}}^{cond}$, with or without the inclusion of the P4 outlier sampled at 10 m (Figure 5.4b,d). These correlations are stronger than those between NPP_V and nitrate ($r^2 = 0.54$), phosphate ($r^2 = 0.56$), or silicic acid ($r^2 = 0.54$). Total chl *a*, as well as >5 μm chl *a*, were weakly correlated with NPP_V ($r^2 = 0.41$ and 0.51 , respectively), while chl *a* in the 1-5 μm size fraction was not correlated with NPP_V ($p > 0.05$). This indicates that the correlations between [Cu'], $\log K_{CuL,Cu^{2+}}^{cond}$, and NPP_V were not solely driven by changes in biomass. Ligand concentrations were positively correlated with total particulate [chl *a*] ($r^2 = 0.39$), >5 μm [chl *a*] ($r^2 = 0.46$), and bacterial abundance ($r^2 = 0.65$).

5.3.1.5 Cu:C Assimilation Ratios and Cu Uptake Rates

The Cu:C assimilation ratios ranged between 0.4 and 80.2, μmol Cu mol C⁻¹ across the transect (Table 5.6). The average Cu:C assimilation ratios were similar across the transect for all size fractions (27.7 ± 20.1 , 26.6 ± 16.4 , 30.3 ± 21.0 , and 26.8 ± 10.7 for the 0.22-1 μm, 1-5 μm, >5 μm, and total particulate size fractions, respectively). The Cu:C assimilation ratios were not correlated with [Cu]_d, [Cu'], [L], or $\log K_{CuL,Cu^{2+}}^{cond}$.

Average short-term volumetric Cu uptake rates ($\rho\text{Cu}_{\text{ST,V}}$) along the transect were similar for the 0.22-1 μm ($5.4 \pm 3.0 \text{ pmol Cu L}^{-1} \text{ h}^{-1}$), 1-5 μm ($5.8 \pm 1.4 \text{ pmol Cu L}^{-1} \text{ h}^{-1}$), and >5 μm ($5.1 \pm 1.4 \text{ pmol Cu L}^{-1} \text{ h}^{-1}$) size fractions (Table 5.6). Carbon-normalized short-term Cu uptake rates ($\rho\text{Cu}_{\text{ST,C}}$) were more variable, and differed up to 130-fold across the size fractions (ranging from 0.7 ± 0.1 to $94.2 \pm 13 \text{ } \mu\text{mol Cu mol C}^{-1} \text{ h}^{-1}$). Total particulate $\rho\text{Cu}_{\text{ST,C}}$ varied ~9-fold, and ranged between 1.1 ± 0.1 and $9.8 \pm 1.4 \text{ } \mu\text{mol Cu mol C}^{-1} \text{ h}^{-1}$. Average $\rho\text{Cu}_{\text{ST,C}}$ were similar for the 1-5 μm ($17.3 \pm 24.2 \text{ } \mu\text{mol Cu mol C}^{-1} \text{ h}^{-1}$) and >5 μm ($14.3 \pm 16.4 \text{ } \mu\text{mol Cu mol C}^{-1} \text{ h}^{-1}$) size fractions, and were slowest for the 0.22-1 μm size fraction ($1.6 \pm 0.8 \text{ } \mu\text{mol Cu mol C}^{-1} \text{ h}^{-1}$).

Total particulate long-term volumetric uptake rates ($\rho\text{Cu}_{\text{LT,V}}$) varied 3.8-fold, and ranged between 32.9 ± 10.2 and $125.2 \pm 39.7 \text{ pmol Cu L}^{-1} \text{ d}^{-1}$. Similar to $\rho\text{Cu}_{\text{ST,V}}$, average $\rho\text{Cu}_{\text{LT,V}}$ were similar for the 0.22-1 μm ($22.7 \pm 16.5 \text{ pmol Cu L}^{-1} \text{ d}^{-1}$), 1-5 μm ($31.0 \pm 12.6 \text{ pmol Cu L}^{-1} \text{ d}^{-1}$), and >5 μm ($33.0 \pm 17.0 \text{ pmol Cu L}^{-1} \text{ d}^{-1}$) size fractions, and varied 187-fold among the size fractions (0.3 ± 0.1 to $125.2 \pm 19.9 \text{ pmol Cu L}^{-1} \text{ d}^{-1}$). Variation of carbon-normalized Cu uptake rates ($\rho\text{Cu}_{\text{LT,C}}$) in the total (5-fold), 1-5 μm (16-fold), and >5 μm (21-fold) size fractions was similar to variation in $\rho\text{Cu}_{\text{ST,C}}$. However, $\rho\text{Cu}_{\text{LT,C}}$ in the 0.22-1 μm size fraction was more variable (155-fold) than $\rho\text{Cu}_{\text{ST,C}}$ (5-fold). While there were no correlations between $\rho\text{Cu}_{\text{LT,C}}$ and any measure of Cu speciation along the transect for the eukaryotic size fractions, $\rho\text{Cu}_{\text{LT,C}}$ in the 0.22-1 μm size fraction was positively correlated with $\log K_{\text{CuL,Cu}^{2+}}^{\text{cond}}$ ($r^2 = 0.64$, $p = 0.0055$) (Table 5.7).

Short-term Cu uptake rates are in excess of long-term uptake rates due to either cellular efflux or remineralization by micrograzers (Chapter 2). The ratio of short-term:long-term uptake ratios (ST:LT) were calculated by first converting the hourly short-term rates ($\text{pmol Cu L}^{-1} \text{ h}^{-1}$) into daily rates ($\text{pmol Cu L}^{-1} \text{ d}^{-1}$). Average $\rho\text{Cu}_{\text{ST,V}}$ for all size fractions were ~11-times faster than $\rho\text{Cu}_{\text{LT,V}}$, and the total ST:LT ratios ranged between 2.7 and 11.2 across the transect (Table 5.6). The ST:LT ratios were more variable for the 0.22-1 μm size fraction (1.8-187) than the 1-5 μm or >5 μm size fractions (1.9-10.5). The two highest ST:LT values in the 0.22-1 μm size fraction (52 and 187) were outliers at P16. Without these outliers, the average ST:LT ratios for all size fractions were consistently lower at P26 (2.7 ± 1.0) and P16 (3.3 ± 1.1 ; without the two outliers) than P4 (6.9 ± 9.2) or P12 (6.5 ± 2.0).

5.3.2 P16 Incubation

5.3.2.1 Biomass and Net Primary Productivity

The average initial [chl *a*] for all treatments was relatively low ($0.11 \pm 0.01 \mu\text{g L}^{-1}$) (Figure 5.5ab). By the end of the incubation, [chl *a*] increased to $0.18 \pm 0.02 \mu\text{g L}^{-1}$ in the control. While [chl *a*] was 24 and 31% lower in the 5 and 30 nM Cyclam treatments, respectively, only the latter treatment was significantly lower than the control ($p = 0.029$; t-test). Copper additions had no significant effect on [chl *a*] during the incubation.

The average initial NPP_V and NPP_B for the incubation treatments were $7.50 \pm 1.38 \mu\text{g C L}^{-1} \text{ d}^{-1}$ and $73 \pm 24 \mu\text{g C } \mu\text{g chl } a^{-1} \text{ d}^{-1}$, respectively (Figure 5.5c-f). At the end of the incubation, NPP_V was fastest in the 30 nM Cyclam treatment ($18.65 \pm 2.63 \mu\text{g C L}^{-1} \text{ d}^{-1}$) and slowest in the 10 nM Cu treatment ($8.96 \pm 2.56 \mu\text{g C L}^{-1} \text{ d}^{-1}$). NPP_V was only significantly slower in the 10 nM Cu

treatment compared to the control ($14.07 \pm 1.29 \mu\text{g C L}^{-1} \text{d}^{-1}$) ($p = 0.037$; t-test). Similar to NPP_V , NPP_B was fastest in the 30 nM Cyclam treatment ($153.7 \pm 18.1 \mu\text{g C } \mu\text{g chl } a^{-1} \text{d}^{-1}$) and slowest in the 10 nM Cu treatment ($51.4 \pm 18.9 \mu\text{g C } \mu\text{g chl } a^{-1} \text{d}^{-1}$). Compared to the control treatment ($81.8 \pm 16.8 \mu\text{g C } \mu\text{g chl } a^{-1} \text{d}^{-1}$), NPP_B was only significantly different on day 4 in the 30 nM Cyclam treatment ($p = 0.007$; t-test).

The average initial cyanobacteria and picoeukaryote abundances were $5.72 \pm 1.50 \times 10^6$ and $8.28 \pm 1.23 \times 10^6 \text{ cells L}^{-1}$, respectively. Unfortunately, a number of the samples collected on day 4 were lost (Table 5.8), and so we were unable to statistically compare the control to the amended treatments via student's t-tests. Cyanobacteria and picoeukaryote abundances were highest in the 30 nM Cyclam treatment (6.12 ± 2.10 and $14.9 \pm 1.3 \times 10^6 \text{ cells L}^{-1}$, respectively), and lowest in the 10 nM Cu treatment (0.14 ± 0.04 and $10.6 \pm 2.0 \times 10^6 \text{ cells L}^{-1}$, respectively). Although the control and amended treatments cannot be compared via t-test, cyanobacteria abundances were inversely correlated with $[\text{Cu}']$, while picoeukaryote abundances responded to a smaller degree (Figure 5.6)

Dissolved macronutrients were measured at the beginning and end of the incubation. The initial $[\text{NO}_3^-]$, $[\text{PO}_4^{3-}]$, and $[\text{Si}(\text{OH})_4]$ were 7.00, 0.85, and 12.6 μM , respectively (Table 5.2). There were no significant differences in macronutrient drawdown over the course of the incubation (4 days) between the amended treatments and the control. Similarly, there were no differences in macronutrient drawdown ratios between treatments. On average, 0.03 ± 0.02 , 0.21 ± 0.11 , and $0.27 \pm 0.10 \mu\text{M}$ of NO_3^- , PO_4^{3-} , and $\text{Si}(\text{OH})_4$ were drawn down in all incubation bottles, respectively (data not shown).

5.3.2.2 >1 μm Cu:C Assimilation Ratios and Cu Uptake Rates

Cu:C assimilation ratios for the 1-5 μm and >5 μm size fractions in each treatment were indistinguishable (t-tests, $p > 0.05$), and so the values for the >1 μm size fraction are presented as representative of the eukaryotic marine phytoplankton in our incubation. The average initial Cu:C assimilation ratio measured in the cubitainers was $8.6 \pm 1.7 \mu\text{mol Cu mol C}^{-1}$, and varied little by the end of the incubation in the control ($10.9 \pm 1.4 \mu\text{mol Cu mol C}^{-1}$) (Figure 5.7ab). At the end of the incubation, Cu:C assimilation ratios varied 45-fold among treatments with significantly higher ratios in the 10 nM Cu treatment ($46.7 \pm 7.5 \mu\text{mol Cu mol C}^{-1}$) compared to the control ($p = 0.0012$; t-test), and significantly lower in the 5 nM Cyclam ($4.1 \pm 0.9 \mu\text{mol Cu mol C}^{-1}$) and 30 nM Cyclam ($1.0 \pm 0.7 \mu\text{mol Cu mol C}^{-1}$) treatments ($p = 0.0020$ and <0.0001 , respectively; t-test). The Cu:C assimilation ratio in the 1.5 nM Cu treatment was not significantly different than the control on day 4 (13.7 ± 6.0) due to variability among replicates.

Initial $\rho\text{Cu}_{\text{LT,V}}$ measured in all treatments was $19.0 \pm 5.5 \text{ pmol Cu L}^{-1} \text{ d}^{-1}$ for the >1 μm size fraction (Figure 5.7cd). During the incubation, volumetric uptake rates increased in the 1.5 nM (~2.5-fold) and 10 nM (~6-fold) Cu amended treatments during the incubation compared with the control. In contrast, $\rho\text{Cu}_{\text{LT,V}}$ were between 59-65%, and 89-93% slower in the 5 nM and 30 nM Cyclam amended treatments, respectively, during the incubation. Average initial $\rho\text{Cu}_{\text{LT,C}}$ in all treatments was $44.8 \pm 17.6 \mu\text{mol Cu mol C}^{-1} \text{ d}^{-1}$. By day 4, $\rho\text{Cu}_{\text{LT,C}}$ was 2.3 and 7.1-fold faster in the 1.5 nM and 10 nM Cu treatments, respectively, compared to the control ($36.7 \pm 10.5 \mu\text{mol Cu mol C}^{-1} \text{ d}^{-1}$) (Figure 5.7ef). Similar to $\rho\text{Cu}_{\text{LT,V}}$, by day 4 $\rho\text{Cu}_{\text{LT,C}}$ decreased 48 and 84% in the 5 nM Cyclam and 30 nM Cyclam treatments, respectively, compared to the control.

Carbon and volume-normalized rates in the four amended treatments were significantly different from the control on day 4 ($p < 0.05$; t-test).

There were statistically significant inverse logarithmic relationships between the $>1 \mu\text{m } \rho\text{Cu}_{\text{B,LT}}$ uptake rates (wherein particulate carbon was calculated from $>1 \mu\text{m } [\text{chl } a]$ and using a C:Chl a ratio of 50:1) and NPP_{B} on days 2 and 4 of the individual incubation (Figure 5.8). As $\rho\text{Cu}_{\text{B,LT}}$ decreased in the Cyclam-amended treatments, NPP_{B} nearly doubled. In contrast, NPP_{B} decreased only 40% as $\rho\text{Cu}_{\text{B,LT}}$ increased more than 7-fold in the Cu-amended treatments. Significant logarithmic fits were made for data collected on each sampling day and for the data set as a whole, and correlation coefficients ranged between 0.44 and 0.58.

5.4 Discussion

5.4.1 Distribution of Total Dissolved Cu in Line P Surface Waters

We present some of the first measurements of $[\text{Cu}]_{\text{d}}$ and Cu speciation in the northeast subarctic Pacific Ocean. Total dissolved Cu varied 1.9-fold across the transect (1.46 to 2.79 nM). These values are similar to surface water $[\text{Cu}]_{\text{d}}$ measured in the North Pacific (1.4 to 3.5 nmol kg^{-1}) (Boyle et al. 1977), NW Pacific and Bering Sea (1.2 to 2 nM) (Moffett and Dupont 2007), and in Washington coastal waters south of the Line P transect (1.86 to 5.25 nmol kg^{-1}) (Jones and Murray 1984).

Dissolved Cu was highest in less saline waters near the coast (salinity = 31.5 to 32) and decreased offshore. The elevated $[\text{Cu}]_{\text{d}}$ at P3 (7 and 12 m depth) and at 10 m depth at P4 is likely due to terrestrial sources of Cu. Downwelling is a prominent feature along the British

Columbia coast throughout the winter (Thomson 1981). Near station P3, the strength of downwelling reaches a maximum in December and begins to subside into spring. By March, upwelling begins to occur due to Ekman pumping as the California and Alaska currents bifurcate along the British Columbia coast (Foreman et al. 2011). Intermediate waters (250 to 500 m) off the coast of Washington are enriched in Cu (2 to 3 nM) relative to surface waters (Jones and Murray 1984). Upwelling of these waters could account for the observed enrichment of $[\text{Cu}]_d$ at P3 and P4.

Surface water $[\text{Cu}]_d$ at P26 (2.09 to 2.24 nM) was higher than previously measured at this station (1.44 to 1.54 nmol kg⁻¹) (Martin et al. 1989), and was higher than $[\text{Cu}]_d$ at P16 (1.70 to 1.94 nM). Dissolved Fe in the mixed layer was also significantly higher at P26 (0.13 to 0.21 nM) relative to P16 (0.03 to 0.07 nM) (J. Cullen, unpub. results). These data suggest that atmospheric deposition, or lateral transport of coastal waters via mesoscale eddies (Johnson et al. 2005) or isopycnal transport from continental margins (Lam et al. 2006) carried Cu and Fe to the P26 mixed layer. Satellite altimetry anomalies demonstrate that there was not an eddy at P26 during the time of sampling (Figure 5.9). It is not possible to distinguish between atmospheric and isopycnal transport of Cu to P26 with our data. Interestingly, $[\text{chl } a]$, F_v/F_m (a physiological indicator for Fe-limitation), and NPP_v were also elevated at P26 compared to P16. Thus, a recent Fe-input event may have occurred at P26.

5.4.2 Inorganic Cu along Line P

Inorganic Cu concentrations varied 5-fold (18.7 to 94.0 fM) with a corresponding pCu range of 15.11 to 14.51. While these values are higher than previous measurements of pCu in the north

Pacific (pCu 13 to 13.5; Coale and Bruland 1988), this is likely due to the lower analytical detection window used by Coale and Bruland (Bruland 2000; Buck et al. 2012). The pCu reported here are similar to more recent measurements in the northwest Pacific Ocean and Bering Sea (13.5 to 14; Moffett and Dupont 2007), the Southern Ocean (14 to 16.3; Buck et al. 2010; Bundy et al. 2013), and the eastern tropical south Pacific Ocean (13.5 to 14.5; Jacquot et al. 2013). Surface water [Cu'] was lower at the shallowest sampling depths across the entire transect, and is likely due to biological utilization and export of particulate Cu below the mixed layer. In support of this, we found biologically mediated drawdown of Cu' at P26, where NPP_v was highest, and corresponded with the lowest [Cu'] measured along the transect (18.7 fM). At P4, [Cu'] decreased from 65.9 fM at 20 m to 46.0 fM at 40 m. The lower [Cu'] at 40 m corresponds to the subsurface chlorophyll maximum, and is also likely due to biological uptake. The negative correlation between NPP_v and [Cu'] for all sampling depths (Figure 5.4) indicates that net primary productivity may influence [Cu'] along the Line P transect.

5.4.3 Source of Cu Ligands in Surface Waters along Line P

Strong Cu binding ligands were present across the transect at all sampling depths, and were always in excess of the total dissolved Cu concentrations, resulting in sparingly low inorganic Cu concentrations. Compared to previous studies (Buck et al. 2010; Bundy et al. 2013), a single, wider analytical window was employed, and so the ligand concentration range (6.30 to 17.36 nM) and strength ($\log K_{\text{CuL,Cu}^{2+}}^{\text{cond}} = 13.69$ to 14.53) represent both stronger ($\log K_{\text{CuL,Cu}^{2+}}^{\text{cond}} > 13.5$) and weaker ligands. As a result, the concentrations reported here are higher than those reported for the strong ligand class by other groups (2 to 4 nM) using a narrower analytical window (Moffett

and Dupont 2007; Buck et al. 2010; Jacquot et al. 2013). The ligand strengths ($\log K_{CuL,Cu^{2+}}^{cond}$) are similar to those previously reported for the northwest Pacific Ocean and Bering Sea (13.5 to 14; Moffett and Dupont 2007), the Southern Ocean (14 to 16.4; Buck et al. 2010; Bundy et al. 2013), and the eastern tropical south Pacific Ocean (13.5 to 14.5; Jacquot et al. 2013).

Although the provenance and nature of the strong Cu-binding ligands in seawater is unknown, there are a number of possible sources and candidate compounds. *Synechococcus* produces strong Cu-binding ligands when experiencing Cu-toxicity (Moffett and Brand 1996; Gordon et al. 2000). The concentration of these ligands is in excess (0 to 50%) of the total dissolved Cu present in the growth medium. Similarly, the heterotrophic bacterium *Vibrio alginolyticus* produces strong ligands in a 1:1 ratio with the total dissolved Cu concentration in the medium (Gordon et al. 2000).

There are three lines of evidence to suggest the Cu ligands along Line P are produced by microorganisms. Similar to the culture studies, [L] and [Cu]_d were positively correlated ($R^2 = 0.44$, $p = 0.0184$). The strengths of the ligands produced by prokaryotes ($\log K_{CuL,Cu^{2+}}^{cond} = 13$) (Moffett and Brand 1996; Croot et al. 2000; Gordon et al. 2000) are similar to the ligands measured along Line P. Indeed, the significant positive correlation between total bacterial cell densities and [L] ($R^2 = 0.65$, $p = 0.0016$) suggests that prokaryotes may be an important source of strong Cu ligands along Line P. Since [L] was not correlated with cyanobacteria abundance, heterotrophic bacteria may produce the majority of strong Cu binding ligands along Line P.

The high [L]:[Cu]_d ratio observed along Line P (~5) is significantly greater than the [L]:[Cu]_d ratio produced by laboratory cyanobacteria experiencing Cu toxicity (1.5:1), and so there may be other *in situ* sources of strong Cu binding ligands. Eukaryotic phytoplankton also release Cu-binding ligands that may be weaker than those produced by prokaryotes (Croot et al. 2000). The strength of the ligands produced depends on sensitivity of a species to Cu toxicity. For example, the dinoflagellate *Amphidinium carterae* releases stronger ligands than most eukaryotes ($\log K_{CuL,Cu^{2+}}^{cond} = 12$) and is more sensitive to Cu toxicity (Croot et al. 2000). Dinoflagellates are common along the Line P transect, and often comprise more than 20% of [chl *a*] during the late summer (Steinberg et al. 2012). Thus, eukaryotes may produce some strong ligands and this may account for the weak, but still significant, correlation between total [chl *a*] and >5 μm [chl *a*] with [L] along the transect.

Similar to [Cu]_d, [L] was highest near the fresher surface waters near the coast and decreased offshore. The higher [L]:[Cu]_d ratio at P3 compared to the average ratio across the transect suggests that there may be an additional source of strong Cu binding ligands along the shelf. Ligand concentrations in sediments can exceed 100 nM and can diffuse into the overlying bottom water (Skrabal et al. 2000; Shank et al. 2004). However, these ligands tend to be weaker than those in oceanic surface waters. As intermediate waters pass over the shelf sediments during upwelling, they may become enriched in weaker Cu binding ligands. The lowest $\log K_{CuL,Cu^{2+}}^{cond}$ measured along the transect were at P3 (12 m depth), and suggests that shelf waters might be a source of weaker Cu ligands in this region.

5.4.4 Environmental Controls of Cu Acquisition along Line P

While the metabolic Cu requirements of isolated marine phytoplankton species have been studied under varying Cu and Fe availability (Sunda and Huntsman 1996; Croot et al. 2003; Quigg et al. 2006; Annett et al. 2008; Guo et al. 2012), little is known about how *in situ* Cu physiology changes with shifts in environmental conditions. This study aimed to determine how Cu requirements responded to varying macronutrient, light, Fe, and Cu availability along a coastal-open oceanic transect.

5.4.4.1 Comparing Cu:C Assimilation Ratios with Previous Measurements

The Cu:C assimilation ratios presented here (0.4 to 80.2 $\mu\text{mol Cu mol C}^{-1}$) are within the range of Cu quotas reported in previous laboratory (0.04 to 156 $\mu\text{mol Cu mol C}^{-1}$) and field (0.98 to 23.6 $\mu\text{mol Cu mol C}^{-1}$) studies (Table 5.9). However, the Cu:C assimilation ratios may not estimate the true Cu quotas of the phytoplankton communities sampled since our incubations are not performed at steady-state (see section 5.2.6), and Cu uptake may proceed at night while C-fixation does not. The average Cu:C assimilation ratios for each size fraction (26.6 to 30.3 $\mu\text{mol Cu mol C}^{-1}$) are higher than those derived from the slope of $[\text{Cu}]_d$ and $[\text{PO}_4^{3-}]$ measured across the nutricline ($\Delta[\text{Cu}]_d:\Delta[\text{PO}_4^{3-}]$) in different ocean basins (and assuming a C:P ratio of 106) (0.98 to 23.6 $\mu\text{mol Cu mol C}^{-1}$; Table 5.9). This method assumes that both Cu and phosphate are supplied to the nutricline by the remineralization of exported phytoplankton in the overlying surface waters, and that both elements are primarily found within soft tissue in plankton. However, phosphate can adsorb to amorphous Fe-(oxy)hydroxide minerals that form on the outside of phytoplankton cells (Sañudo-Wilhelmy et al. 2004). This results in particulate C:P ratios that are ~ 2 times higher than the canonical Redfield ratio (106:1). Few studies have

measured particulate inorganic P concentrations in the North Pacific, but between 10 and 64% of the total particulate P pool is inorganic (Loh and Bauer 2000; Yoshimura et al. 2007).

Correcting the reported Cu:C ratios derived from $\Delta[\text{Cu}]_d:\Delta[\text{PO}_4^{3-}]$ for the range of excess extracellular PO_4^{3-} results in Cu:C ratios (1.1 to 39 $\mu\text{mol Cu mol C}^{-1}$) that are on par with those measured along the transect. Thus, the Cu:C assimilation ratios measured along Line P may represent true cellular Cu quotas.

The 200-fold variation of size fractionated Cu:C assimilation ratios measured along Line P is higher than the 22-fold variation in Cu quotas of various phytoplankton taxa grown in the same Cu concentration but using 100 μM EDTA to chelate the metals (0.40 to 9.01 $\mu\text{mol Cu mol C}^{-1}$; Ho et al. 2003). Thus, phytoplankton species composition may partially influence particulate Cu concentrations. Similarly, Cu quotas can increase 300-fold as Cu concentrations increase (from 1 nM to 40 μM) in the growth media also containing 100 μM EDTA (0.56 to 156 $\mu\text{mol Cu mol C}^{-1}$) (Sunda and Huntsman 1995b; Chang and Reinfelder 2000). Few studies have measured intracellular Cu during Cu toxicity, but quotas of 10 to 20 $\mu\text{mol Cu mol C}^{-1}$ may induce Cu toxicity in some marine phytoplankton (Sunda and Huntsman 1995b; Chang and Reinfelder 2000). The Cu:C assimilation ratios measured along Line P were often in excess of these values, and may indicate that phytoplankton communities along the transect may have been accumulating toxic levels of intracellular Cu. However, since Cu quotas vary considerably between species, we cannot determine whether the phytoplankton communities along Line P were experiencing toxicity at the time of sampling.

The Cu quotas of unialgal cultures grown in similar pCu's as those measured along the transect (pCu = 14.51 to 15.11) are much lower (0.04 to 6.20; Sunda and Huntsman 1995b; Annett et al. 2008; Guo et al. 2012) than the Cu:C assimilation ratios reported here. This would suggest that the Cu:C assimilation ratios overestimate the true Cu quotas of the phytoplankton sampled. However, the high concentrations of EDTA used in these culture studies cause Cu uptake rates to be artificially low, and is likely due to competition between EDTA and the phytoplankton transporters for Cu (Chapter 3). If the high EDTA concentration was not present, then Cu uptake rates may have been faster, resulting in higher intracellular Cu concentrations at lower Cu' concentrations. The higher Cu:C assimilation ratios measured along Line P compared to culture studies may reflect a laboratory measurement bias towards lower Cu quotas performed at equivalent pCu's.

5.4.4.2 Macronutrient and Light Availability

Compared to exponentially growing cells, the centric diatom *Thalassiosira weissflogii* has a 2 to 6-fold higher intracellular Cu quota during stationary phase (Chang and Reinfelder 2000). A light-limited natural phytoplankton assemblage accumulates 20-80% more intracellular Cu than when light-replete (Chapter 2). Thus, light or macronutrient limited phytoplankton may have higher Cu:C assimilation ratios. Although Cu:C assimilation ratios were high at low nitrate stations P4 and P12, they were also elevated at P16. Furthermore, Cu:C assimilation ratios showed no trend with depth. Thus, macronutrient and light availability were not primary determinants of intracellular Cu along Line P.

5.4.4.3 Iron-Copper Interactions

Some phytoplankton have higher Cu demands during Fe limitation. During Fe-limitation, diatoms acquire Fe through a Cu-dependent high-affinity Fe transport system (Peers et al. 2005; Maldonado et al. 2006). As a result, 4 out of 18 phytoplankton species surveyed increased their intracellular Cu demands in response to Fe limitation (Annett et al. 2008; Guo et al. 2012). Oceanic phytoplankton strains have higher basal metabolic Cu requirements compared to oceanic strains, and may reflect an increased reliance on Cu in waters with chronically low Fe (Peers and Price 2006; Annett et al. 2008). A recent incubation at station P20 confirmed that Cu drawdown by an Fe-replete phytoplankton community was lower than an Fe-limited control treatment, suggesting that Fe limitation may increase Cu demands in the Line P HNLC region (Chapter 4).

The suspected recent Fe-input event at P26 (see section 5.4.1) provides an opportunity to test whether natural Fe-enrichment events can influence the Cu physiology of marine phytoplankton compared to P16 where the community was clearly Fe-limited. The Cu:C assimilation ratios and $\rho_{\text{Cu}_{\text{LT,C}}}$ were consistently higher at P16 than at P26 for both 1-5 μm and $>5 \mu\text{m}$ size fractions. Furthermore, the differences between Cu:C assimilation ratios and $\rho_{\text{Cu}_{\text{LT,C}}}$ measured at P16 and P26 were greater for the $>5 \mu\text{m}$ (62 to 73%) than the 1-5 μm (0 to 47%) size fraction. Indeed, a previous incubation at P26 demonstrated that, in response to a 1 nM Cu addition, only phytoplankton in the $>5 \mu\text{m}$ size fraction increased F_v/F_m and Fe uptake by the Cu-dependent high-affinity Fe transport system (Chapter 4). These data indicate that there may be an interaction between Fe and Cu metabolism in indigenous phytoplankton communities, and that larger phytoplankton in HNLC regions may have a greater dependence on Cu availability.

5.4.4.4 Copper Acquisition and Speciation along Line P

Previous laboratory studies have hypothesized that Cu' concentrations determine Cu bioavailability to marine phytoplankton (Sunda and Guillard 1976; Anderson and Morel 1978; Sunda and Huntsman 1995b). Thus, we hypothesized that Cu:C assimilation ratios and Cu uptake rates might correlate with $[\text{Cu}]_d$ and/or $[\text{Cu}']$. There were no correlations between $\rho_{\text{Cu}_{\text{ST,C}}}$, $\rho_{\text{Cu}_{\text{LT,C}}}$, and Cu:C assimilation ratios with $[\text{Cu}']$ for the 1-5 μm or $>5 \mu\text{m}$ size fractions across the transect, and so $[\text{Cu}']$ does not determine Cu uptake rates or cellular quotas in natural marine phytoplankton communities. Laboratory studies of isolated marine phytoplankton strains have demonstrated that organically complexed Cu is bioavailable (Hudson 1998; Quigg et al. 2006; Annett et al. 2008; Guo et al. 2010; Chapter 3). *In situ* Cu ligand complexes were also bioavailable to marine phytoplankton surveyed at P26 in 2008 (Chapter 2). Despite this, Cu uptake rates or Cu:C assimilation ratios were not correlated with $[\text{Cu}]_d$. Since phytoplankton Cu quotas and steady-state Cu uptake rates can vary by an order of magnitude among taxa grown in identical Cu concentrations (Ho et al. 2003; Annett et al. 2008; Guo et al. 2012), phytoplankton species composition and Fe availability, and not $[\text{Cu}]_d$ or $[\text{Cu}']$, may primarily determine particulate biogenic Cu concentrations in surface waters.

Similar to our previous studies of Cu uptake rates at P26 (Semenuik et al. 2009; Chapter 2), short-term Cu uptake rates were faster than long-term uptake rates for all size classes along the Line P transect. The ST:LT ratios were highest at P4 and P12, and lowest at the open ocean stations (P16 and P26). Thus, either cellular Cu efflux or remineralization by micrograzers may have been occurring at faster rates near the coast. Further investigations of efflux rates and the effect of grazers on dissolved Cu concentrations are warranted.

5.4.4.5 Strong Ligands and Bacterial Cu Assimilation

While there were no relationships between Cu speciation and acquisition by the eukaryotic phytoplankton across the transect, $\rho\text{Cu}_{\text{LT,C}}$ in the 0.22-1 μm size fraction was positively correlated with the $\log K_{\text{CuL,Cu}^{2+}}^{\text{cond}}$ ($R^2 = 0.64$; $p = 0.0055$). This indicates that bacteria accumulated more Cu when stronger ligands were present. Although Cu uptake by marine heterotrophic bacteria isolates has yet to be examined, their Fe transport is enhanced in the presence of siderophores, strong Fe(III)-specific ligands produced to scavenge dissolved Fe in seawater (Granger and Price 1999). Similarly, chalkophores – strong Cu-binding ligands – are produced by the soil-dwelling methane oxidizer *Methylosinus trichosporium* OB3b to enhance Cu acquisition (Kim et al. 2004). Given bacterial abundance and [L] were positively correlated, marine bacteria may produce strong ligands to facilitate Cu acquisition.

The production of a strong Cu binding ligand by heterotrophic bacteria may serve to simultaneously facilitate Cu acquisition and detoxify Cu. Unfortunately, little is known about the substrate of Cu transport in prokaryotes. Copper(II) may enter bacteria through non-specific HmtA, ABC, or ZupT-like divalent metal transporters (reviewed by Rensing and McDevitt 2013). If Cu is not complexed by strong organic ligands, then it could enter the marine bacterial cell accidentally through a divalent metal transporter, accumulate, and potentially cause toxicity. Indeed, this has been demonstrated in eukaryote marine phytoplankton (Sunda and Huntsman 1998). However, if Cu is complexed by ligands produced by bacteria to prevent Cu from accidentally entering the cell, then bacteria could better regulate the acquisition of Cu through a ligand-mediated transport pathway. Given the inability of current analytical methods to

distinguish different types of Cu binding ligands in seawater, well-controlled laboratory studies should be carried out with marine bacteria isolates to verify this hypothesis.

5.4.4.6 Copper Uptake During the P16 Incubation

In the P16 incubation CuSO_4 amended treatments, Cu:C assimilation ratios and $\rho_{\text{Cu}_{\text{C,LT}}}$ increased with changes to $[\text{Cu}]_{\text{d}}$, and not $[\text{Cu}']$. The excess strong natural Cu ligands (7.75 nM) present in the incubation would have complexed all of the 1.5 nM CuSO_4 addition, and 78% of the 10 nM CuSO_4 addition. Thus, the presence of strong *in situ* ligands did not appear to prevent acquisition of the added Cu by the phytoplankton community at P16. These results indicate that organically complexed Cu was bioavailable to the phytoplankton community at P16, and support previous work that demonstrated organically complexed Cu was bioavailable to a natural phytoplankton community at P26 (Chapter 2). This relationship likely reflects the effect of short-term changes to Cu availability, whereby a single phytoplankton community may take up Cu when more Cu becomes available. Indeed, when dissolved Cu additions were made to an Fe-limited phytoplankton community at P20, Cu drawdown increased even though the added Cu was complexed by *in situ* organic ligands (Chapter 4). This provides further evidence that other factors (e.g. phytoplankton species composition), and not $[\text{Cu}]_{\text{d}}$ or $[\text{Cu}']$, may cause large variations in cellular Cu concentrations and uptake rates between stations.

In the Cyclam-amended treatments, the Cu:C assimilation was similar to Cu quotas in Cu-replete phytoplankton cultures despite incredibly low $[\text{Cu}']$ ($\ll 10$ fM) (Annett et al. 2008; Guo et al. 2012). In laboratory prymnesiophyte cultures isolated from Line P, Cu(II) bound to Cyclam was bioavailable (Chapter 3). However, Cyclam concentrations in excess of the total dissolved Cu

concentration can compete with the transporter active sites for Cu, thereby causing Cu uptake rates to decrease (Chapter 3). Similarly, the Cyclam additions in the P16 incubation would have competed with the phytoplankton transporters for Cu, resulting in slower cellular Cu uptake rates. On day 4, $\rho_{Cu_{LT,C}}$ was 1.9 and 6.4 times faster in the control than in the 5 nM and 30 nM Cyclam treatments, respectively. These correspond to the 1.5 and 4.9 times increases in excess strong ligand with the 5 nM and 30 nM Cyclam amendments, respectively. This provided additional evidence that the slower Cu uptake rates and lower Cu:C assimilation ratios in the Cyclam amended treatments was likely due to competition between the Cyclam and the phytoplankton transporters for the *in situ* dissolved Cu.

5.4.5 Copper Influences Rate Processes along Line P: Three Lines of Evidence

5.4.5.1 NPP_V Covaries with Cu Speciation along Line P

NPP_V was negatively correlated with [Cu'] and positively correlated with $\log K_{CuL,Cu^{2+}}^{cond}$ (Table 5.7). Thus, as inorganic Cu concentrations decreased and ligand strength increased, the bioavailability of *in situ* Cu decreased and carbon fixation increased. Furthermore, NPP_V in the 1-5 μm and >5 μm size fractions were similarly correlated with [Cu'] and $\log K_{CuL,Cu^{2+}}^{cond}$. These correlations are not solely driven by biomass (see section 5.3.1.4). Although the correlations between NPP_V and [Cu'], and $\log K_{CuL,Cu^{2+}}^{cond}$ could reflect increased drawdown of Cu' by phytoplankton as carbon-fixation rates increase, in light of the other lines of evidence (see below), we suggest these correlations reflect a response of the phytoplankton communities along Line P to changes in Cu bioavailability.

It should be noted that biomass-normalized NPP were not correlated with either $[Cu']$ or $\log K_{CuL,Cu^{2+}}^{cond}$. The C:Chl *a* ratio of autotrophs can vary more than 6-fold at P26 (Booth et al. 1993; Peña and Varela 2007), and by more than 10-fold between laboratory strains (MacIntyre et al. 2002). It is not surprising that variations in the C:Chl *a* ratio along the transect might preclude a significant correlation between NPP_B and either $[Cu']$ or $\log K_{CuL,Cu^{2+}}^{cond}$. As such, the effect of Cu speciation on NPP was only observed in volume-normalized rates.

5.4.5.2 Decreasing Cu Bioavailability Increased NPP_B at P16

The addition of the strong Cu(II)-binding ligand Cyclam to the community sampled at P16 significantly lowered $\rho_{Cu_{LT,C}}$ and Cu:C assimilation ratios in both the 5 nM and 30 nM Cyclam amended treatments. The Cu(II)-Cyclam complex is significantly less bioavailable than *in situ* Cu complexes (Chapter 2), and the addition of increasing amounts of Cyclam resulted in sequentially lower Cu bioavailability. Excess Cyclam also decreases Cu uptake by phytoplankton cultures (Chapter 3). The Cu:C assimilation ratios of the eukaryotes in the Cyclam amended treatments (1 to 4 $\mu\text{mol Cu mol C}^{-1}$) are similar to those of Cu-replete laboratory cultures (0.36 to 4.32 $\mu\text{mol Cu mol C}^{-1}$) (Sunda and Huntsman 1995b; Annett et al. 2008; Guo et al. 2012). In contrast, the initial Cu:C assimilation ratio was $8.6 \pm 1.7 \mu\text{mol Cu mol C}^{-1}$ in the on-deck incubations, and is near the value that can cause toxicity in *E. huxleyi* (10 $\mu\text{mol Cu mol C}^{-1}$), a particularly Cu sensitive marine phytoplankton (Sunda and Huntsman 1995b). In response to the decreased Cu bioavailability in the 30 nM Cyclam additions, NPP_B increased significantly compared to the control by day 4, and NPP_B on both sampling days increased as $\rho_{Cu_{LT,C}}$ decreased (Figure 5.7). These data indicate that specific growth rates

increased in response to decreased intracellular Cu, and suggest Cu bioavailability may have been controlling phytoplankton rate processes at P16.

The increase of NPP_B in the 30 nM Cyclam treatment was driven by both an increase in NPP_V and a decrease in [chl *a*]. Ciliates are particularly sensitive to Cu toxicity (Stoecker et al. 1986), and the decrease in [chl *a*] in the 30 nM Cyclam treatment may reflect a relief of Cu toxicity to micrograzers and subsequent enhanced grazing pressure. Since cyanobacteria and picoeukaryote abundance increased in the Cyclam amended treatments (Figure 6), the grazers were likely feeding on larger phytoplankton. The effect of reduced Cu bioavailability on micrograzing rates will be investigated during a future cruise.

Interestingly, while there was a significant decrease in NPP_V in the 10 nM $CuSO_4$ amended treatment by day 4, NPP_B did not respond to either $CuSO_4$ addition. This was also observed in two previous studies (Sunda et al. 1981; Chapter 4). A 10 nM Cu addition to surface waters at P20 in 2010 had no effect on [chl *a*] after 5 days (Chapter 4). In coastal waters of North Carolina, carbon-fixation underwent a 4 to 6 day lag period after the addition of 10 to 100 nM $CuSO_4$, and then proceeded to increase (Sunda et al. 1981). Given our very short incubation time (4 days), NPP_B might have not responded to the Cu amendment during the incubation.

5.4.5.3 Cyanobacteria Abundance Increased as Cu Bioavailability Decreased at P16

Cyanobacteria are more sensitive to Cu toxicity than any other phytoplankton group (Brand et al. 1986), and the production of strong Cu-binding ligands may be an adaptation to this sensitivity (Moffett and Brand 1996). Cyanobacteria abundance was positively correlated with NPP_B

during the P16 incubation ($r^2 = 0.67$, $p = 0.0039$), whereby cyanobacteria abundance nearly doubled in the Cyclam amended treatments compared to the control and the 1.5 nM Cu amended treatments. The response of the cyanobacterial community to decreased Cu availability supports the contention that Cu bioavailability at P16 was influencing phytoplankton growth at P16.

In laboratory studies, cyanobacteria growth rates decreased when $[Cu']$ exceeded 0.2 to 2 nM (Brand et al. 1986). The addition of 10 nM Cu saturated the strong Cu ligands, resulting in an initial $[Cu']$ of 2.2 nM. In response, cyanobacteria abundance decreased an order of magnitude in this treatment compared to the control. Given $[chl\ a]$ was indistinguishable from the control in this treatment, this confirms the greater sensitivity of cyanobacteria to Cu toxicity compared with eukaryotic phytoplankton. As Cu bioavailability decreased in the Cyclam-amended treatments, cyanobacteria that were experiencing Cu-induced stress were able to outgrow grazing pressure.

5.4.6 Reevaluating the Role Of Organic Complexation in Mediating Cu Bioavailability to *In Situ* Marine Microbial Communities

Early studies determined that dissolved Cu in coastal (van den Berg et al. 1979; van den Berg 1984ab) and oceanic (Coale and Bruland 1988; Moffett 1995) seawater was strongly bound to organic complexes. The subsequent discovery that cyanobacteria exuded strong Cu binding ligands during Cu toxicity indicated the organic ligands in seawater were of biogenic origin, and likely produced by cyanobacteria to detoxify Cu by lowering $[Cu']$ (Moffett and Brand 1996). In support of this, cyanobacteria cell abundances in polluted harbour waters were anticorrelated with $[Cu']$ (Moffett et al. 1997), and positively correlated with strong ligand concentrations in a

Swedish estuary (Croot 2003). Early work with eukaryotic marine phytoplankton also suggested that [Cu'] caused toxicity in marine phytoplankton, and decreasing [Cu'] resulted in lower intracellular Cu concentrations and faster growth rates (Sunda and Guillard 1976; Anderson and Morel 1978). Although not experimentally demonstrated, it was hypothesized that Cu' was the sole substrate for Cu transport in prokaryotic and eukaryotic marine phytoplankton.

Recent work casts doubt on these early assumptions. Laboratory studies have demonstrated that organically complexed Cu(II) and Cu(I) are bioavailable to eukaryotic marine phytoplankton (Hudson 1998; Quigg et al. 2006; Guo et al. 2010; Chapter 2; Chapter 3). A laboratory study of Cu uptake rates in *T. pseudonana* using Cu (1 nM) and ligand (3 nM) concentrations on par with those found in surface seawater demonstrated that organic complexation of either Cu(II) or Cu(I) did not significantly decrease Cu uptake rates (Chapter 3). This was likely due to acquisition of Cu from the ligand using a HACuTS that involves extracellular reduction of Cu(II) and uptake of Cu(I) (Guo et al. 2010; Guo et al. submitted; Chapter 3). Interestingly, natural phytoplankton communities acquired Cu from *in situ* Cu-ligand complexes (Semeniuk et al. 2009; Chapter 2), and cellular Cu uptake rates were similar to laboratory Cu uptake rates by two prymnesiophytes isolated along Line P (Chapter 3). Thus, although strong organic ligands may prevent toxicity in Cu-sensitive cyanobacteria by decreasing [Cu'], they may not prevent eukaryotic phytoplankton from accessing Cu.

In light of the evidence discussed in section 4.7, the negative correlation between NPP_V and [Cu'], and the positive correlation between NPP_V and $\log K_{CuL, Cu^{2+}}^{cond}$ may indicate that *in situ* ligands influence growth of marine phytoplankton. The positive correlations between total bacterial

abundance and [L], as well as $\rho\text{Cu}_{\text{C,LT}}$ in the 0.22-1 μm size fraction and $\log K_{\text{CuL,Cu}^{2+}}^{\text{cond}}$ may indicate that non-photosynthetic bacteria produce specific strong Cu binding ligands for Cu acquisition. Similarly, a soil methane oxidizing bacterium produces chalkophores, strong Cu binding ligands that facilitate Cu uptake (Kim et al. 2004). Given the positive correlation between NPP_{V} and $\log K_{\text{CuL,Cu}^{2+}}^{\text{cond}}$, the strong ligands that we propose are produced by bacteria and may decrease Cu uptake in eukaryotic phytoplankton and allow for higher NPP_{V} . As demonstrated for the P16 incubation, the small additions (5 to 30 nM) of a strong Cu(II) ligand caused Cu uptake rates to decrease and NPP_{V} and NPP_{B} to increase. The decrease in Cu bioavailability was not due to changes to *in situ* dissolved Cu speciation since Cu bound to Cyclam is bioavailable to laboratory and field marine phytoplankton (Chapter 2; Chapter 3). Instead, the ligands appear to decrease Cu acquisition by competing with the extracellular transporters for Cu (see section 5.4.6). Thus, we suggest that multiple strong Cu ligands exist in seawater, and they influence Cu uptake by either reducing its bioavailability (e.g. the strong ligands produced by cyanobacteria), or by slowing Cu uptake by chelating the transporter bound Cu.

5.5 Tables

Table 5.1. Locations, sampling dates, seafloor depths, mixed layer depths (MLD), and light extinction coefficient (k_D) of the stations sampled along Line P in August, 2011.

Station	Latitude	Longitude	Sampling Date	Seafloor Depth (m)	MLD (m)	k_D (m ⁻¹)
P3	48° 37.50'	126° 20.02'	Aug 17, 2011	815	15	0.211
P4	48° 39.00'	126° 40.00'	Aug 18, 2011	1320	23	0.093
P12	48° 58.91'	130° 39.91'	Aug 21, 2011	3230	15	0.093
P16	49° 14.93'	134° 13.87'	Aug 22-23, 2011	3620	31	0.093
P26	49° 59.95'	144° 59.99'	Aug 26, 2011	4225	29	0.096

Table 5.2. Light intensities, euphotic zone depth (Z_{eu}), and macronutrient concentrations at each sampling depth along Line P. Depths in bold are below the mixed layer.

Station	Z_{eu} (m)	Sampling Depth (m)	% Surface Irradiance (I_0) ^a	% I_0 of Incubation ^b	NO_3^- (μ M)	PO_4^{3-} (μ M)	$Si(OH)_4$ (μ M)
P3	22	7	22	26	BDL ^c	0.29	10.5
		12	10	11	BDL	0.27	10.2
P4	49	10	39	42	BDL	0.29	2.25
		20	16	18	BDL	0.29	2.30
		40	3	5	0.60	0.57	5.90
P12	49	10	39	42	BDL	0.38	6.70
		20	16	18	0.20	0.40	6.30
		40	3	5	5.30	0.76	11.1
P16	49	10	39	42	5.20	0.73	11.3
		37	3	5	7.00	0.85	12.6
P26	48	10	38	42	11.2	1.09	15.8
		35	4	5	13.1	1.24	ND ^d

^a% surface irradiance measured at each sampling depth

^b% surface irradiance experienced by the Cu uptake and primary productivity assay bottles in the on-deck incubators

^cBDL: below detection limit

^dND: not determined

Table 5.3. Total dissolved Cu ($[\text{Cu}]_d$), ligand concentrations ($[\text{L}] \pm 1\sigma$), conditional stability constants ($\log K_{\text{CuL.Cu}^{2+}}^{\text{cond}} \pm 1\sigma$), inorganic Cu concentration ($[\text{Cu}']$), and the dissolved $[\text{L}]:[\text{Cu}]_d$ ratio at each sampling depth along Line P. Depths in bold are below the mixed layer.

Station	Sampling Depth (m)	$[\text{Cu}]_d$ (nM)	$[\text{L}]$ (nM)	$\log K_{\text{CuL.Cu}^{2+}}^{\text{cond}}$	pCu ($-\log[\text{Cu}^{2+}]$)	$[\text{Cu}']$ (fM)	L: $[\text{Cu}]_d$
P3	7	2.42	14.74 ± 0.24	13.85 ± 0.19	14.56	66.7	6.1
	12	2.79	17.36 ± 0.25	13.69 ± 0.06	14.41	94.0	6.2
P4	10	2.43	10.96 ± 0.17	14.21 ± 0.28	14.75	44.1	4.5
	20	1.46	10.40 ± 0.61	13.83 ± 0.18	14.56	65.9	7.1
	40	1.82	7.60 ± 0.13	14.19 ± 0.21	14.72	46.0	4.2
P12	10	2.18	10.22 ± 0.27	14.33 ± 0.11	14.90	30.4	4.7
	20	2.22	8.77 ± 0.01	14.27 ± 0.10	14.74	43.6	4.0
	40	1.93	10.95 ± 0.61	13.99 ± 0.22	14.66	53.0	5.7
P16	10	1.70	6.30 ± 0.86	14.18 ± 0.40	14.61	58.8	3.7
	37	1.94	7.75 ± 0.18	14.02 ± 0.28	14.60	60.0	4.0
P26	10	2.09	10.15 ± 0.02	14.52 ± 0.01	15.11	18.7	4.9
	35	2.24	7.03 ± 0.05	14.53 ± 0.06	14.86	33.1	3.1

Table 5.4. Initial total dissolved Cu ($[Cu]_d$), Cu-binding ligands ($[L]$), free Cu^{2+} (pCu), and total inorganic Cu concentrations ($[Cu']$) in the P16 incubation treatments. The initial $[Cu]_d$ and $[L]$ in the amended treatments were determined by adding the initial $[Cu]_d$ and $[L]$ to the $CuSO_4$ and Cyclam additions, respectively.

Treatment	Initial $[Cu]_d$ (nM)	Initial $[L]$ (nM)	Initial pCu	Initial $[Cu']$ (M)
+10 nM $CuSO_4$	11.94	7.75	10.03	$10^{-8.65}$ •
+1.5 nM $CuSO_4$	3.44	7.75	14.28	$10^{-12.88}$ •
Control	1.94	7.75	14.60	$10^{-13.22}$
+5 nM Cyclam	1.94	12.75	<15.48	< $10^{-14.09}$ **
+30 nM Cyclam	1.94	37.75	<16.45	< $10^{-15.05}$ **

*The initial $[Cu']$ in the $CuSO_4$ amended treatments was calculated using the conditional stability constant and excess $[L]$ reported in Table 5.3.

**The initial pCu and $[Cu']$ in the Cyclam amended treatments was calculated using the conditional stability constant for Cyclam ($10^{15.29}$; Chapter 2) and assuming that the entire dissolved Cu pool would be complexed by the Cyclam addition. The actual $[Cu']$ in the Cyclam amended treatments would be lower than the calculated values due to chelation of Cu by the *in situ* strong ligands.

Table 5.5. Biomass and rate parameters measured at each sampling depth along Line P. Depths in bold are below the mixed layer. Volumetric (NPP) and chl-normalized (NPP_B) net primary productivity (NPP) was measured over 24 h. Volumetric (BP_V) and cell-normalized (BP_B) bacterial productivity was measured over 3-4 h.

Station	Sampling Depth (m)	Chl <i>a</i> (µg L ⁻¹)	F _v /F _m	Total Bacteria ^a	Cyanobacteria	Picoeukaryotes	NPP _V	NPP _B	BP _V	BP _B
P3	7	0.898	ND	32.0	200	16.3	ND ^b	ND	ND	ND
	12	0.958	ND	32.2	177	13.0	ND	ND	ND	ND
P4	10	0.044	0.64	1.08	1.73	0.55	25.2	583	1.88	1.74
	20	0.138	0.51	1.08	1.42	1.61	10.8	74.4	1.52	1.41
	40	0.549	0.23	2.11	38	5.08	46.8	85.2	3.96	1.87
P12	10	0.428	0.38	2.30	0.82	3.10	45.6	108	3.04	1.32
	20	0.202	0.29	3.66	1.23	3.86	40.8	202	1.49	0.41
	40	0.127	0.24	2.06	ND	ND	32.4	253	0.98	0.48
P16	10	0.262	0.19	1.25	0.77	2.63	40.8	157	2.33	1.86
	37	0.241	0.29	0.99	4.70	4.82	34.8	143	4.78	4.85
P26	10	0.418	0.29	1.10	4.79	7.97	110	264	1.97	1.80
	35	0.440	0.24	0.82	2.45	11.7	75.6	173	4.67	5.73

^aTotal bacterial abundance (heterotrophic and autotrophic bacteria)

Units: Total bacteria (10⁹ cells L⁻¹), cyanobacteria and picoeukaryotes (10⁶ cells L⁻¹), NPP_V (µg C L⁻¹ d⁻¹), NPP_B (µg C µg chl *a*⁻¹ d⁻¹), BP_V (µg C L⁻¹ d⁻¹), BP_B (fg C cell⁻¹ d⁻¹)

^bND: not determined

Table 5.6. Size-fractionated Cu:C assimilation ratios (24 h), short-term Cu uptake rates (2 h), long-term Cu uptake rates (24 h), and the short-term:long-term uptake rate ratio for each sampling depth along Line P in August 2011. Cu:C assimilation ratios were determined using ^{67}Cu and ^{14}C . Carbon-normalized uptake rates were measured using ^{67}Cu , and dividing by particulate C concentrations derived from bacterial abundance and chl *a* concentrations (section 5.2.6 for details). The ST:LT ratios were calculated by converting the hourly short-term Cu uptake rates to daily dates, and then dividing by the long-term Cu uptake rates. Values for half the range are reported for the average of duplicate measurements, and values in bold are for the total particulate size fraction. Errors reported are \pm half the range of two replicate measurements.

Station	Depth	Size (μm)	Chl <i>a</i>	Cu:C Assimilation		$\rho\text{Cu}_{\text{ST,V}}$	$\rho\text{Cu}_{\text{ST,C}}$	$\rho\text{Cu}_{\text{LT,V}}$	$\rho\text{Cu}_{\text{LT,C}}$	ST:LT Ratio
				Ratio						
P3	7m	0.22-1	0.08			7.7 ± 1.2	0.7 ± 0.1			
		1-5	0.48			3.3 ± 0.8	5.3 ± 1.2			
		>5	0.33			4.1 ± 0.1	1.9 ± 0.02			
		Total	0.90			15.1 ± 1.5	1.1 ± 0.1			
	12m	0.22-1	0.30			12.1 ± 0.9	1.1 ± 0.1			
		1-5	0.15			6.7 ± 0.6	3.4 ± 0.3			
		>5	0.51			6.5 ± 0.3	4.7 ± 0.2			
	Total	0.96			25.3 ± 1.7	1.8 ± 0.1				
P4	10m	0.22-1	0.004	68.7 ± 2.5		6.3 ± 0.9	3.5 ± 0.5	23 ± 0.5	12.8 ± 0.3	6.6
		1-5	0.02	52.5 ± 5.7		7.8 ± 1.1	94.2 ± 13.2	36.1 ± 2.6	433 ± 31.6	5.2
		>5	0.02	35.9 ± 5.0		5.2 ± 0.7	62 ± 8.3	39.3 ± 0.3	471 ± 4.1	3.2
		Total	0.044	46.4 ± 5.4		19.3 ± 2.7	9.8 ± 1.4	98.3 ± 3.5	50 ± 1.8	4.7
	20m	0.22-1	0.01	38.4 ± 0.4		4.3 ± 0.6	2.4 ± 0.3	4.8 ± 2.3	2.7 ± 1.3	21.3
		1-5	0.09	58.0 ± 9.6		6.6 ± 0.8	17.7 ± 2.1	15.1 ± 0.4	40.3 ± 1.0	10.5
		>5	0.04	27.8 ± 0.4		4.4 ± 0.4	26.4 ± 2.2	13 ± 2.4	77.9 ± 14.6	8.1
		Total	0.14	39.0 ± 3.3		15.3 ± 1.7	6.5 ± 0.7	32.9 ± 5.1	14 ± 2.2	11.2
	40m	0.22-1	0.04	42.5 ± 4.2		5.6 ± 0.8	1.6 ± 0.2	41.1 ± 5.7	11.7 ± 1.6	3.3
		1-5	0.30	28.2 ± 2.0		6.1 ± 0.1	4.9 ± 0.1	38.3 ± 2.1	30.6 ± 1.6	3.8
		>5	0.21	25.7 ± 3.5		3.5 ± 0.04	4.0 ± 0.1	39.3 ± 0.7	44.9 ± 0.8	2.1
		Total	0.55	30.6 ± 1.4		15.2 ± 1.0	2.7 ± 0.2	119 ± 8.5	21 ± 1.5	3.1

Table 5.6. continued

Station	Depth	Size (μm)	Chl <i>a</i>	Cu:C			$\rho\text{Cu}_{\text{LT,V}}$	$\rho\text{Cu}_{\text{LT,C}}$	ST:LT Ratio	
				Assimilation Ratio	$\rho\text{Cu}_{\text{ST,V}}$	$\rho\text{Cu}_{\text{ST,C}}$				
P12	10m	0.22-1	0.01	26.9 \pm 3.5	8.4 \pm 0.9	2.2 \pm 0.2	29.8 \pm 1.7	7.8 \pm 0.4	6.8	
		1-5	0.16	15.0 \pm 2.5	8.1 \pm 1.9	12.1 \pm 2.9	18.4 \pm 1.8	27.6 \pm 2.7	10.5	
		>5	0.26	15.0 \pm 1.0	5.7 \pm 0.5	5.3 \pm 0.5	22.2 \pm 0.7	20.5 \pm 0.6	6.2	
		Total	0.43	18.5 \pm 2.1	22.2 \pm 3.4	4.0 \pm 0.6	70.4 \pm 4.2	12.6 \pm 0.8	7.6	
	20m	0.22-1	0.003	35.4 \pm 3.8	6.4 \pm 1.4	1.1 \pm 0.2	46.5 \pm 3.0	7.6 \pm 0.5	3.3	
		1-5	0.07	21.6 \pm 1.0	6.3 \pm 0.5	21.5 \pm 1.8	24.8 \pm 2.0	85 \pm 6.7	6.1	
		>5	0.13	17.6 \pm 1.9	5 \pm 0.2	9.2 \pm 0.3	16.1 \pm 0.9	29.7 \pm 1.7	7.4	
		Total	0.20	25.7 \pm 1.4	17.7 \pm 2.1	2.5 \pm 0.3	87.4 \pm 5.9	12.6 \pm 0.8	4.9	
	40m	0.22-1	0.003	22.4 \pm 0.9	3.6 \pm 1.5	1.1 \pm 0.4	16.5 \pm 1.5	4.8 \pm 0.4	5.2	
		1-5	0.07	12.1 \pm 0.6	4.8 \pm 0.2	16.3 \pm 0.5	14.2 \pm 1.1	48.8 \pm 3.7	8.0	
		>5	0.05	14.3 \pm 1.5	2.7 \pm 0.2	12.8 \pm 0.8	10.9 \pm 0.8	52.1 \pm 4.1	5.9	
		Total	0.13	15.5 \pm 0.3	11 \pm 1.5	2.8 \pm 0.4	41.6 \pm 3.4	10.6 \pm 0.9	6.4	
P16	10m	0.22-1	0.007	0.4 \pm 0.1	2.5 \pm 0.02	1.2 \pm 0.01	0.3 \pm 0.1	0.3 \pm 0.1	187.4	
		1-5	0.14	18.4 \pm 1.4	6.1 \pm 0.9	10.4 \pm 1.5	29.7 \pm 2.4	51 \pm 4.2	4.9	
		>5	0.11	50.7 \pm 5.1	5.8 \pm 0.7	12.8 \pm 1.6	51.2 \pm 6.3	111.7 \pm 13.8	2.7	
		Total	0.26	24.0 \pm 1.6	14.5 \pm 0.2	4.6 \pm 0.1	81.3 \pm 8.9	26 \pm 2.8	4.3	
	37m	0.22-1	0.01	1.6 \pm 0.5	2.8 \pm 0.03	1.7 \pm 0.02	1.3 \pm 0.3	0.8 \pm 0.2	52.4	
		1-5	0.16	31.3 \pm 8.1	4.3 \pm 0.5	6.5 \pm 0.7	37.5 \pm 1.1	56.3 \pm 1.7	2.8	
		>5	0.08	80.2 \pm 23.2	4.9 \pm 0.4	14.8 \pm 1.3	61.1 \pm 23.6	183 \pm 70.9	1.9	
		Total	0.24	34.3 \pm 4.3	12.1 \pm 0.04	4.6 \pm 0.02	99.9 \pm 25	37.8 \pm 9.5	2.9	
	P26	10m	0.22-1	0.02	18.0 \pm 5.5	2.4 \pm 0.02	1.3 \pm 0.01	31.1 \pm 4.4	17 \pm 2.4	1.8
			1-5	0.16	11.9 \pm 2.8	4.2 \pm 0.1	6.4 \pm 0.1	45.8 \pm 2.6	68.6 \pm 3.8	2.2
			>5	0.24	13.9 \pm 6.1	5.9 \pm 0.03	5.9 \pm 0.03	34.4 \pm 5.9	34.4 \pm 5.9	4.2
			Total	0.42	13.7 \pm 4.5	12.6 \pm 0.01	3.6 \pm 0.01	111.2 \pm 4.0	31.8 \pm 1.2	2.7
35m		0.22-1	0.02	23.3 \pm 5.2	2.5 \pm 0.1	1.8 \pm 0.1	32.8 \pm 3.6	24.2 \pm 2.7	1.8	
		1-5	0.27	17.1 \pm 2.7	5.4 \pm 0.4	4.8 \pm 0.3	49.7 \pm 12.0	44.1 \pm 10.7	2.6	
		>5	0.15	21.8 \pm 5.0	7.8 \pm 0.6	12.5 \pm 1.0	42.7 \pm 4.2	68.3 \pm 6.7	4.4	
		Total	0.44	19.9 \pm 3.7	15.7 \pm 0.9	5.0 \pm 0.3	125 \pm 19.9	40.3 \pm 6.4	3.0	

Units: chl *a* ($\mu\text{g L}^{-1}$), Cu:C assimilation ratios ($\mu\text{mol Cu mol C}^{-1}$), $\rho\text{Cu}_{\text{ST,V}}$ ($\text{pmol Cu L}^{-1} \text{h}^{-1}$), $\rho\text{Cu}_{\text{ST,C}}$ ($\mu\text{mol Cu mol C}^{-1} \text{h}^{-1}$), $\rho\text{Cu}_{\text{LT,V}}$ ($\text{pmol Cu L}^{-1} \text{d}^{-1}$), $\rho\text{Cu}_{\text{LT,C}}$ ($\mu\text{mol Cu mol C}^{-1} \text{d}^{-1}$).

Table 5.7. Statistically significant Pearson correlations of biomass, productivity, Cu uptake, and chemical parameters measured along Line P in August 2011. Correlations with r^2 greater than 0.6 are in bold.

Size Fraction	Variable 1	Variable 1 Units	Variable 2	Variable 2 Units	r^2	p-value
Total	[Chl <i>a</i>]	$\mu\text{g L}^{-1}$	NPP _V	$\mu\text{g C L}^{-1} \text{d}^{-1}$	0.41	0.0460
	[Chl <i>a</i>]	$\mu\text{g L}^{-1}$	[L]	nM	0.39	0.0301
	[Chl <i>a</i>]	$\mu\text{g L}^{-1}$	Picoeukaryote	$10^6 \text{ cells L}^{-1}$	0.76	0.0005
	[Chl <i>a</i>]	$\mu\text{g L}^{-1}$	Total Bacteria	$10^9 \text{ cells L}^{-1}$	0.63	0.0021
	NPP _V	$\mu\text{g C L}^{-1} \text{d}^{-1}$	[Cu']	fM	-0.69	0.0010
	NPP _V	$\mu\text{g C L}^{-1} \text{d}^{-1}$	$\log K_{\text{CuL.Cu}^{2+}}^{\text{cond}}$	M^{-1}	0.74	0.0018
	NPP _V	$\mu\text{g C L}^{-1} \text{d}^{-1}$	[NO ₃ ⁻]	μM	0.54	0.0027
	NPP _V	$\mu\text{g C L}^{-1} \text{d}^{-1}$	[PO ₄ ³⁻]	μM	0.56	0.0123
	NPP _V	$\mu\text{g C L}^{-1} \text{d}^{-1}$	[Si(OH) ₄]	μM	0.54	0.0155
	F _v /F _m	unitless	[L]	nM	0.43	0.0383
>5 μm	[Chl <i>a</i>]	$\mu\text{g L}^{-1}$	NPP _V	$\mu\text{g C L}^{-1} \text{d}^{-1}$	0.51	0.0195
	[Chl <i>a</i>]	$\mu\text{g L}^{-1}$	[L]	nM	0.46	0.0154
	[Chl <i>a</i>]	$\mu\text{g L}^{-1}$	[Cu] _d	nM	0.42	0.0226
	NPP _V *	$\mu\text{g C L}^{-1} \text{d}^{-1}$	[Cu']	fM	-0.86	0.0001
	NPP _V *	$\mu\text{g C L}^{-1} \text{d}^{-1}$	$\log K_{\text{CuL.Cu}^{2+}}^{\text{cond}}$	M^{-1}	0.69	0.0029
1-5 μm	NPP _V *	$\mu\text{g C L}^{-1} \text{d}^{-1}$	[Cu']	fM	-0.63	0.0062
	NPP _V *	$\mu\text{g C L}^{-1} \text{d}^{-1}$	$\log K_{\text{CuL.Cu}^{2+}}^{\text{cond}}$	M^{-1}	0.63	0.0063
	NPP _V *	$\mu\text{g C L}^{-1} \text{d}^{-1}$	[NO ₃ ⁻]	μM	0.69	0.0028
	NPP _V *	$\mu\text{g C L}^{-1} \text{d}^{-1}$	[PO ₄ ³⁻]	μM	0.70	0.0026
	NPP _V *	$\mu\text{g C L}^{-1} \text{d}^{-1}$	[Si(OH) ₄]	μM	0.61	0.0127
s0.22-1 μm	Total Bacteria	$10^9 \text{ cells L}^{-1}$	[L]	nM	0.65	0.0016
	Total Bacteria	$10^9 \text{ cells L}^{-1}$	[Cu] _d	nM	0.42	0.0216
	BP _V	$\mu\text{g C L}^{-1} \text{d}^{-1}$	[L]	nM	-0.43	0.0417
	$\rho\text{Cu}_{\text{LT,C}}$	$\mu\text{mol Cu mol C}^{-1} \text{d}^{-1}$	$\log K_{\text{CuL.Cu}^{2+}}^{\text{cond}}$	M^{-1}	0.64	0.0055

*¹⁴C fixation data collected for each size fraction during the Cu:C assimilation ratio assays was used to calculate volumetric net primary productivity rates for the 1-5 μm and >5 μm size fractions (data not shown).

Table 5.8. Cyanobacteria and picoeukaryote abundance on Day 4 of the P16 incubation determined by flow cytometry. Values in parentheses are standard deviations (n=3) or half the range (n=2). For a description of the treatments, please see section 5.2.3.2.

Treatment	Replicate Cubitainers	Cyanobacteria (10 ⁶ cells L ⁻¹)	Picoeukaryotes (10 ⁶ cells L ⁻¹)
10 nM CuSO ₄	3	0.14 (0.04)	10.6 (2.0)
1.5 nM CuSO ₄	3	2.19 (0.20)	11.6 (0.5)
Control	1	2.41	13.9
5 nM Cyclam	1	4.74	15.1
30 nM Cyclam	2	6.12 (1.05)	14.9 (1.3)

Table 5.9. Literature particulate Cu:C ratios in laboratory grown phytoplankton species (20 species from 5 phyla) and in field samples.

Study Type	Cu:C Ratio ($\mu\text{mol Cu mol C}^{-1}$)	Method of Cu:C ratio determination	Study
Laboratory	0.56 – 150	^{14}C and GFAAS ^a	Sunda and Huntsman 1995b
	1.07 – 156	CHN Analyzer and GFAAS ^b	Chang and Reinfelder 2000
	0.40 – 9.01	HR-ICP-MS ^c	Ho et al. 2003
	0.32 – 6.32	^{14}C and ^{67}Cu ^d	Annett et al. 2008
	0.04 – 6.20	^{14}C and ^{67}Cu ^d	Guo et al. 2012
Field	4.6 – 5.1	GFAAS ^e	Sunda and Huntsman 1995b
	2.8 – 6.4	Nutricline $\Delta[\text{Cu}]_d:\Delta[\text{PO}_4^{3-}]^f$	Sunda and Huntsman 1995b
	0.98 – 23.6	Nutricline $\Delta[\text{Cu}]_d:\Delta[\text{PO}_4^{3-}]^f$	Annett et al. 2008
	1.35 – 4.21	^{14}C and ^{67}Cu ^g	Semeniuk et al. 2009
	4.6 – 81.8	^{14}C and ^{67}Cu ^g	This study

^aCells were filtered and rinsed with Gulf Stream seawater before undergoing acid-digestion. Particulate Cu and C concentrations were determined by graphite furnace atomic adsorption spectroscopy (GFAAS) and standard $\text{H}^{14}\text{CO}_3^-$ incubations, respectively.

^bCells were filtered and rinsed with experimental medium. Particulate Cu and C concentrations were determined by graphite furnace atomic adsorption spectroscopy (GFAAS) and standard CHN analysis, respectively.

^cCells were filtered and rinsed with chelexed synthetic ocean water before undergoing acid-digestion. Cellular Cu and P were measured using a HR-ICP-MS, and Cu:C ratios were calculated assuming a particulate C:P ratio of 106.

^dCells were incubated with ^{67}Cu and $\text{H}^{14}\text{CO}_3^-$ under steady-state conditions and continuous light for 24 h before harvested by filtration and washed with a 1 mM DTPA wash.

^eParticulate Cu and P reported by Martin et al. (1976) and Collier and Edmonds (1983) were converted to Cu:C using a particulate C:P ratio of 106.

^fCalculated from the linear slope of $[\text{Cu}]_d$ and $[\text{PO}_4^{3-}]$ in the nutricline, and assuming a particulate C:P ratio of 106.

^gSurface water samples were incubated at *in situ* light and temperature with ^{67}Cu and $\text{H}^{14}\text{CO}_3^-$ for 24 h before harvested by filtration and washed with a 1 mM DTPA wash.

5.6 Figures

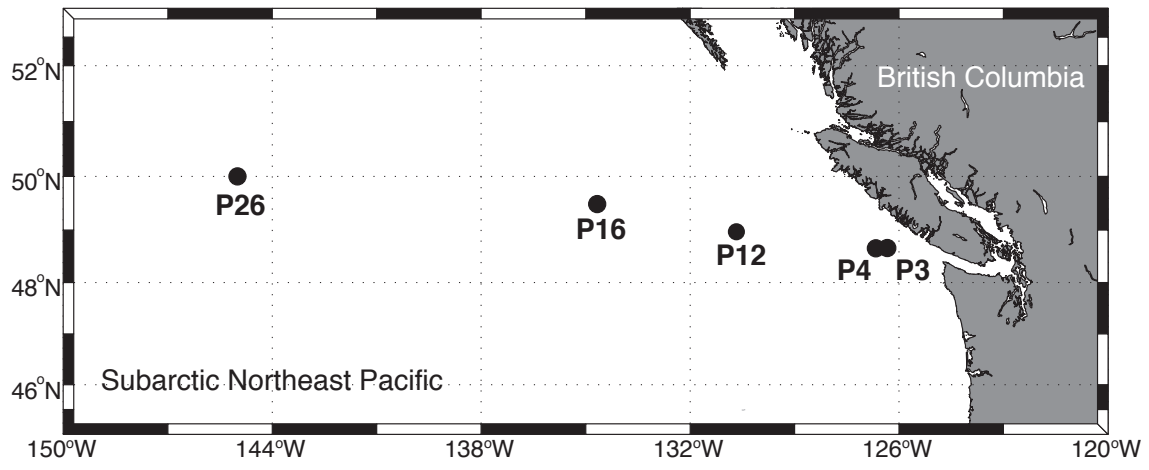


Figure 5.1. Stations sampled along the Line P transect in the northeast subarctic Pacific Ocean.

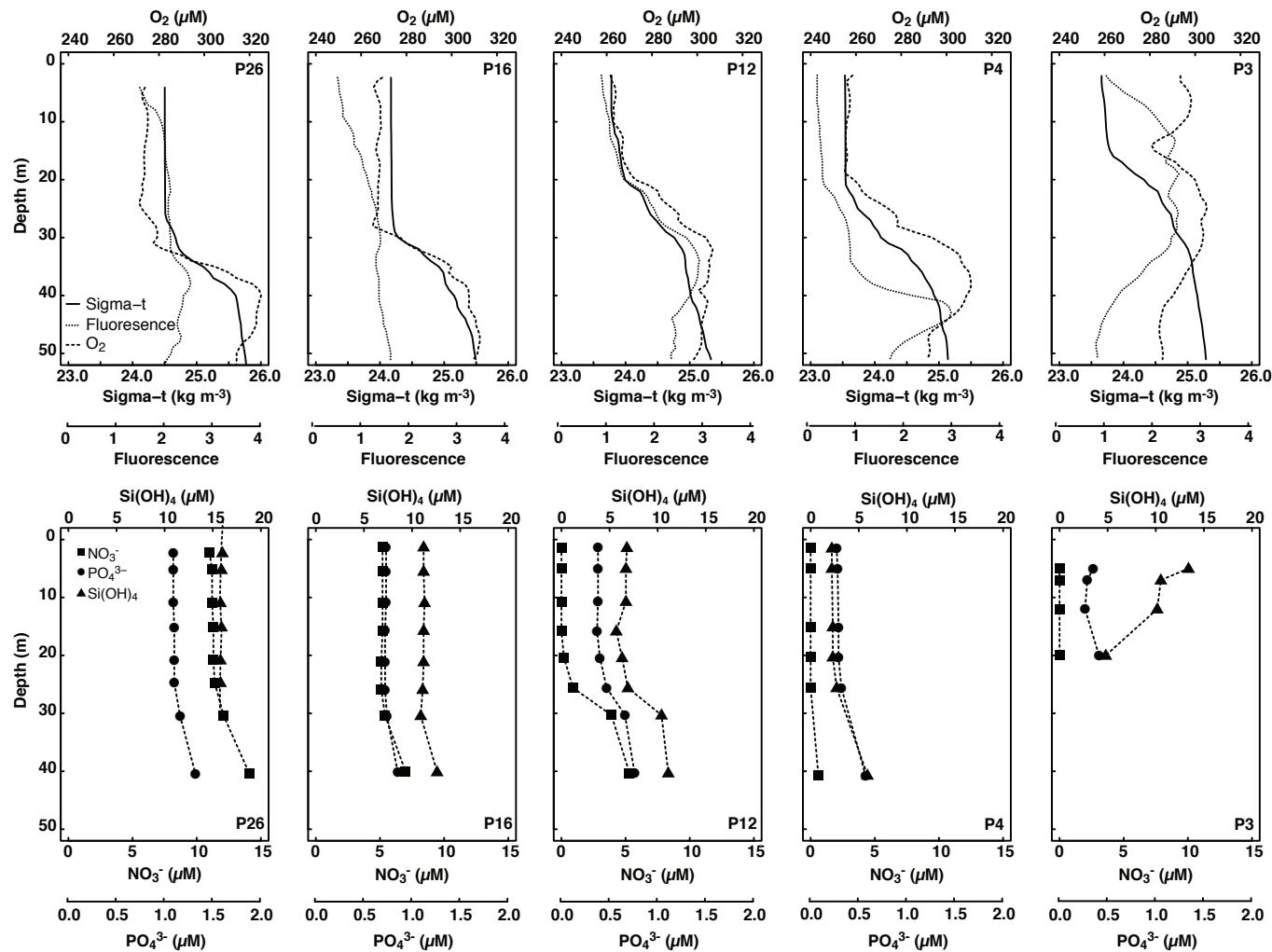


Figure 5.2. Depth profiles of sigma-t (kg m^{-3}), fluorescence (unitless), dissolved oxygen (μM), dissolved nitrate (μM), phosphate (μM), and silicic acid (μM) in surface waters (< 50 m) of stations sampled along the Line P transect. Only data collected during the same cast were plotted.

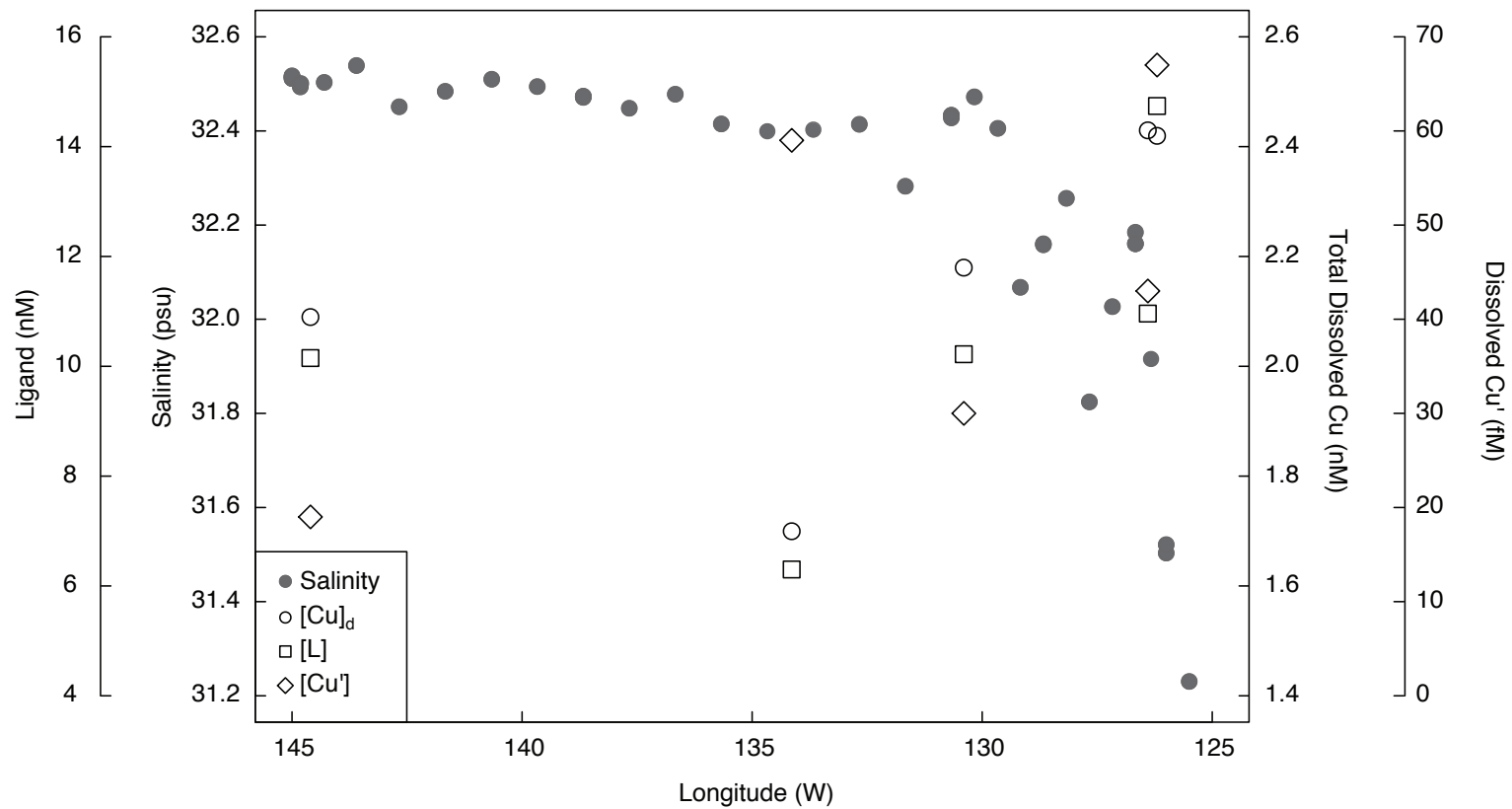


Figure 5.3. Surface salinity, total dissolved Cu (nM), Cu-binding ligands (nM), and inorganic Cu (nM) concentrations along the Line P transect. Salinity was sampled at 5 m using the ship’s internal seawater pumping system, while the Cu concentration and speciation samples were from the shallowest depths sampled along the transect (7 to 10 m; Table 2).

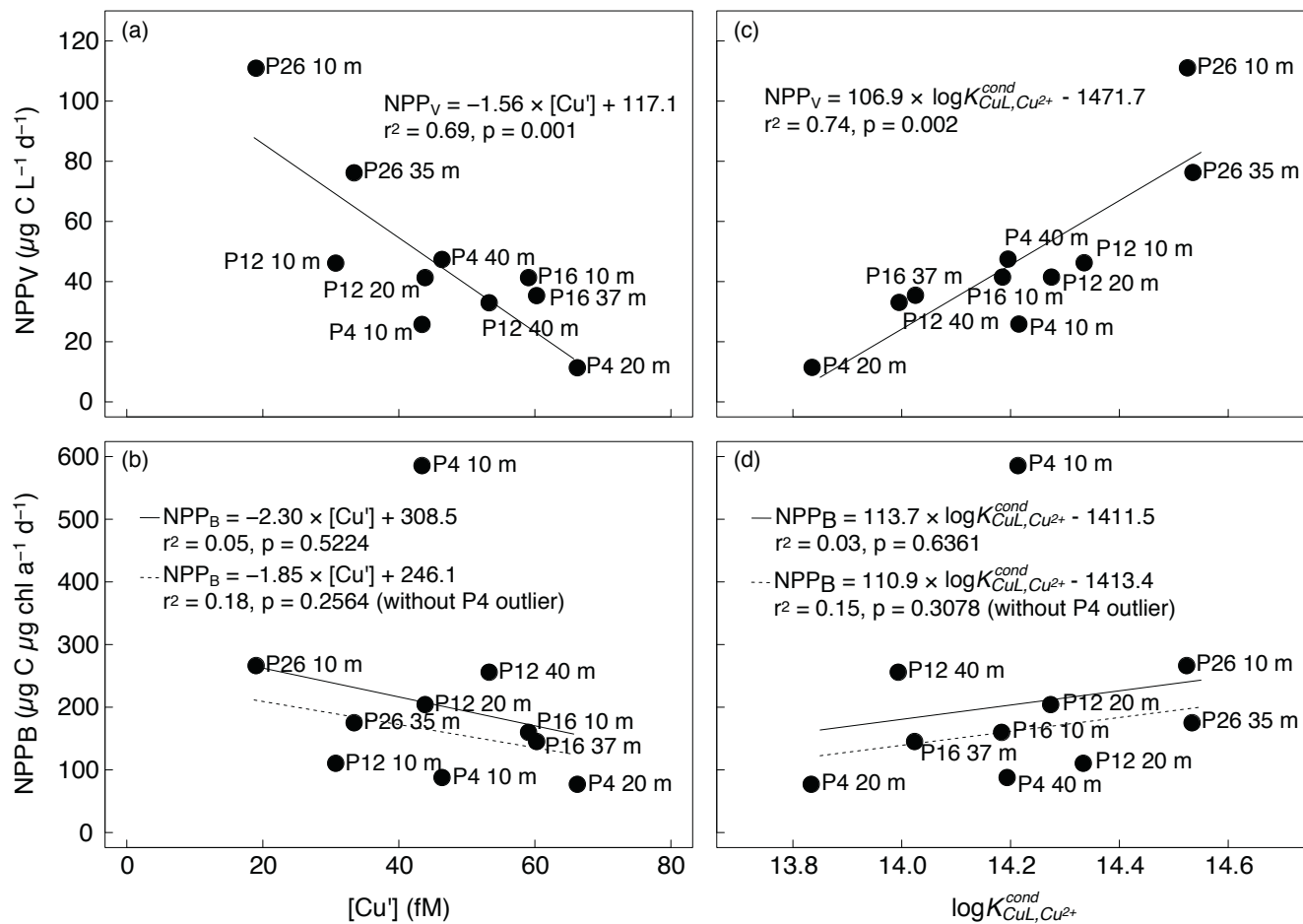


Figure 5.4. Volumetric net primary productivity ($\mu\text{g C L}^{-1} \text{d}^{-1}$) (a-c), and chl *a*-normalized net primary productivity ($\mu\text{g C } \mu\text{g chl } a^{-1} \text{d}^{-1}$) (b-d) versus $[Cu']$ (fM) and $\log K_{CuL,Cu^{2+}}^{cond}$ measured along Line P (2-3 depths per station) (see Tables 5.3 and 5.5).

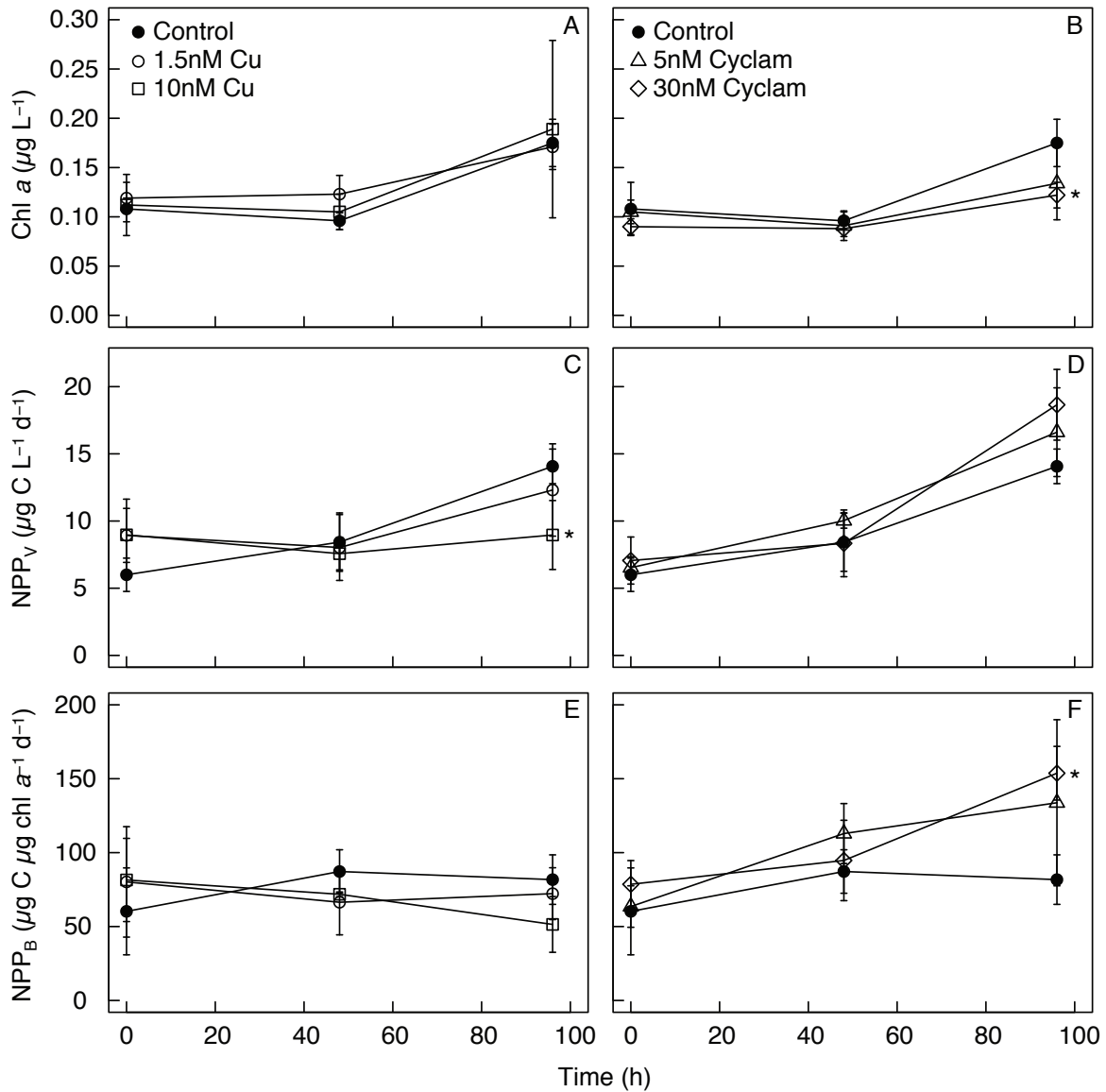


Figure 5.5. Chlorophyll *a* concentrations ($\mu\text{g L}^{-1}$) (a,b), volumetric net primary productivity ($\mu\text{g C L}^{-1} \text{d}^{-1}$) (c,d), and chl *a*-normalized net primary productivity ($\mu\text{g C } \mu\text{g chl } a^{-1} \text{d}^{-1}$) (e,f) measured during the P16 incubation. Error bars represent $\pm 1\sigma$ ($n=3$). Asterisks indicate a statistically significant difference compared to the control on the respective sampling day ($p < 0.05$; two-way t-test). For a description of the treatments, please see section 5.2.3.2.

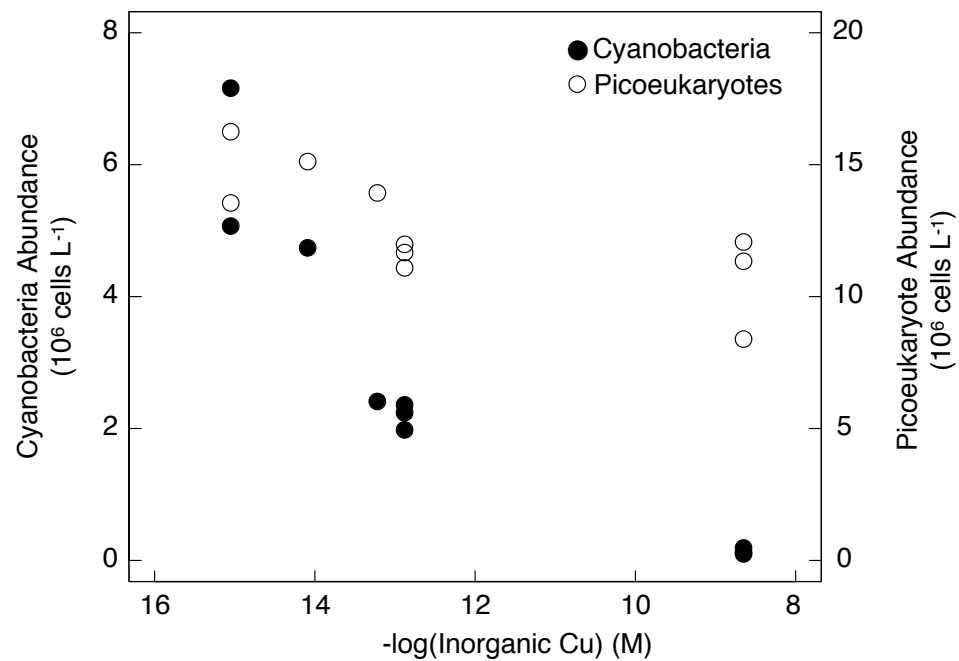


Figure 5.6. Cyanobacteria (closed symbols) and picoeukaryote (open symbols) cell abundance measured on day 4 of the P16 incubation (10^6 cells L^{-1}) with respect to the estimated inorganic Cu concentrations in the incubation treatments (Table 4).

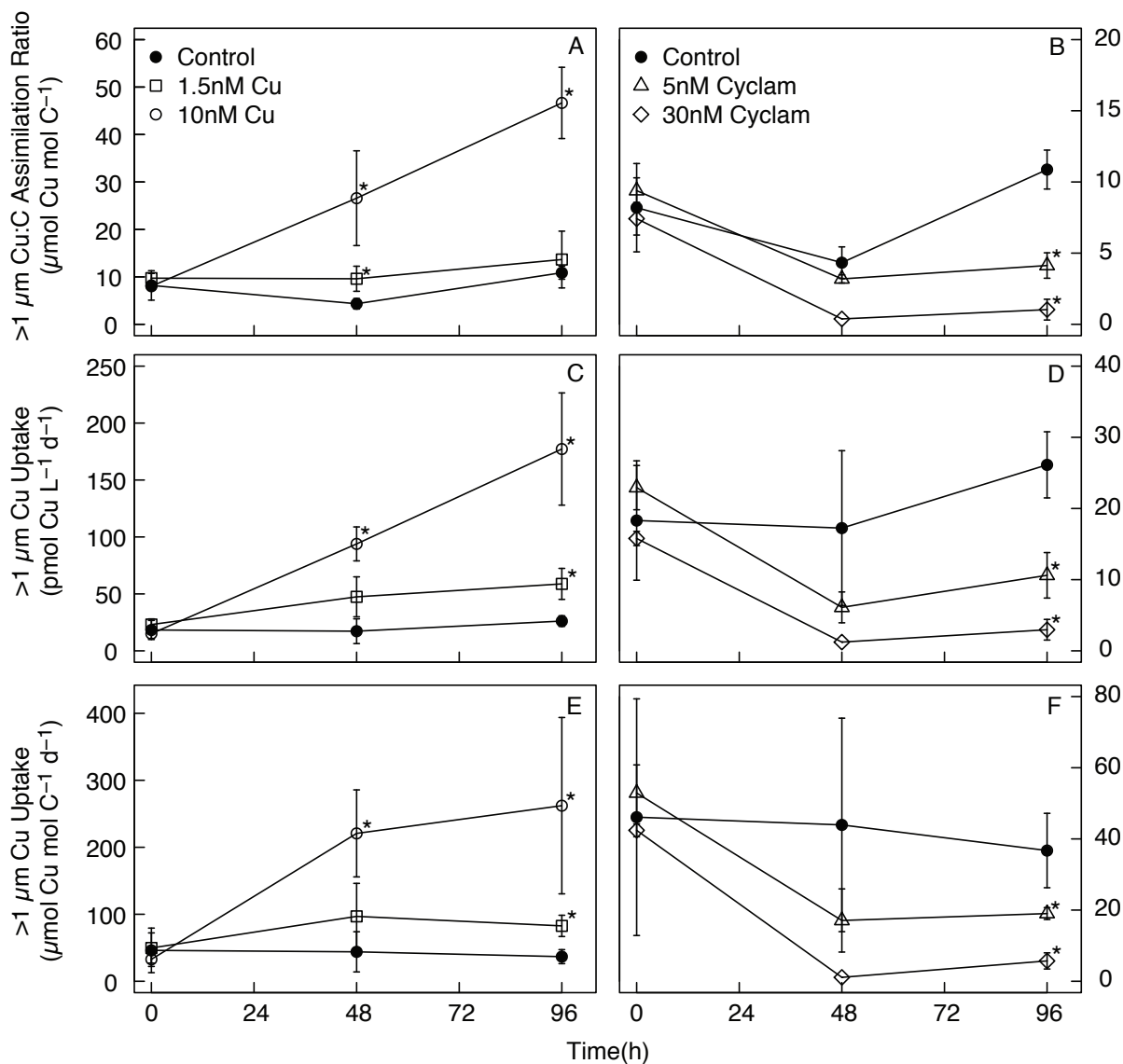


Figure 5.7. Cu:C assimilation ratios ($\mu\text{mol Cu mol C}^{-1}$) (ab), volumetric Cu uptake rates ($\text{pmol Cu L}^{-1} \text{d}^{-1}$) (cd), and long-term biomass normalized Cu uptake rates ($\mu\text{mol Cu mol C}^{-1} \text{d}^{-1}$) (ef) for the $>1 \mu\text{m}$ size fraction on each sampling day of the P16 incubation. Biomass-normalized Cu uptake rates were calculated by dividing volumetric rates by particulate carbon concentrations derived from total [chl *a*] and a C:Chl *a* ratio of $50 \text{ g C g chl } a^{-1}$. For a description of the treatments, please see section 5.2.3.2.

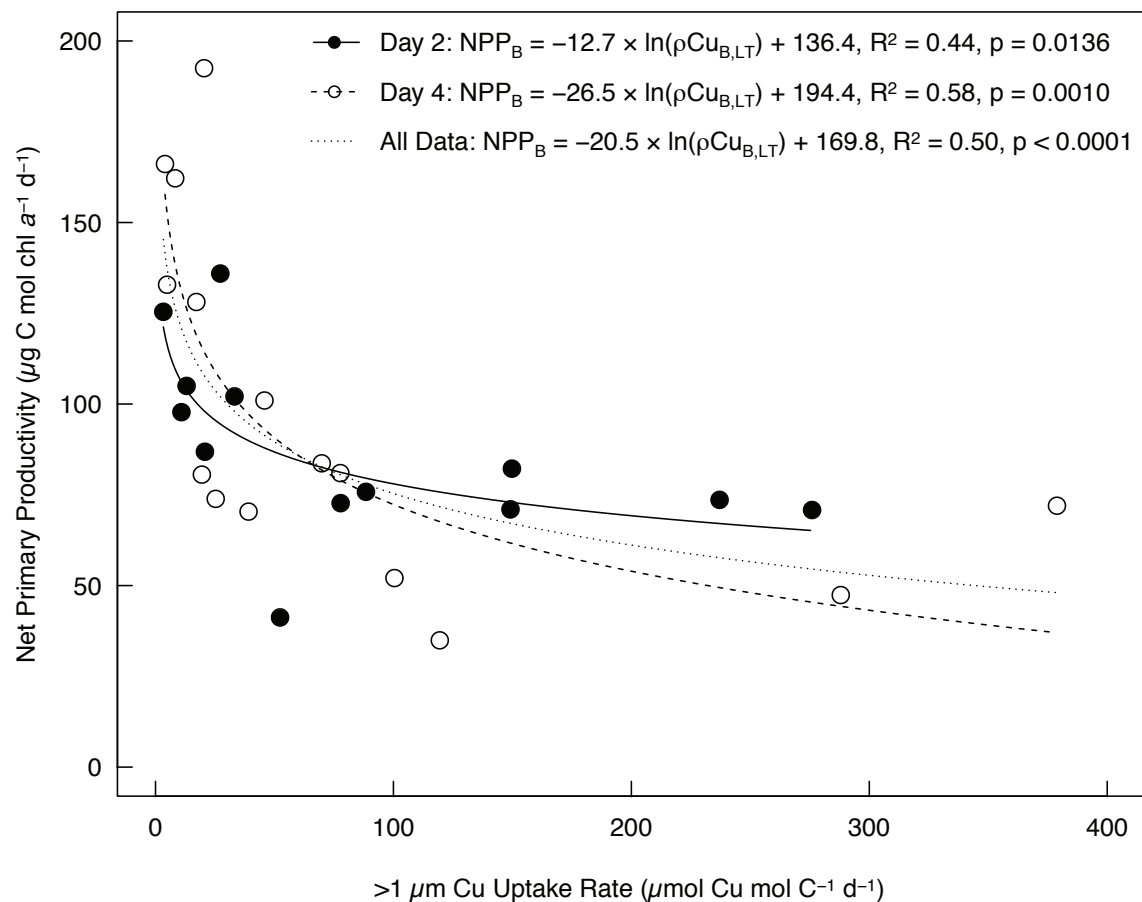


Figure 5.8. Biomass-normalized net primary productivity ($\mu\text{g C } \mu\text{g chl } a^{-1} \text{ d}^{-1}$) and biomass-normalized Cu uptake rates ($\mu\text{mol Cu } \mu\text{mol C}^{-1} \text{ d}^{-1}$) measured during the P16 incubation for the $>1 \mu\text{m}$ size fraction. Biomass-normalized Cu uptake rates were calculated by dividing volumetric rates by particulate carbon concentrations derived from total [chl *a*] and a C:Chl *a* ratio ($50 \text{ g C g chl } a^{-1}$). Data from each respective day and all the data were each fit to a logarithmic function ($p < 0.05$).

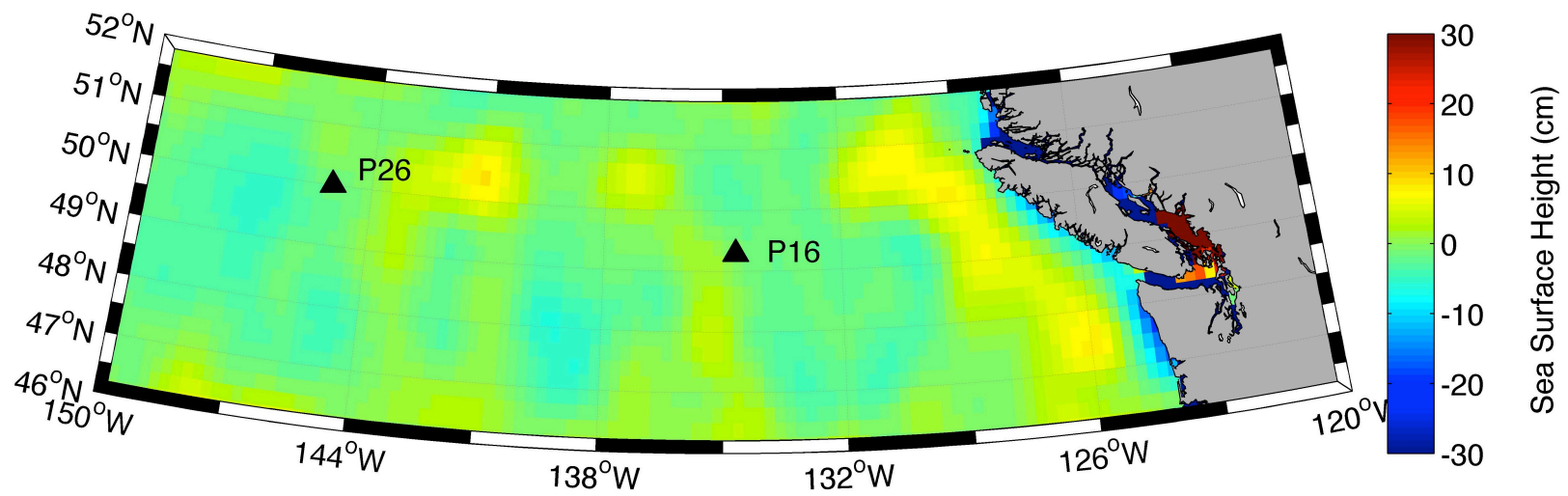


Figure 5.9. Satellite derived sea surface height anomalies (cm) along the Line P transect for August 8, 2011. Data were retrieved from the Colorado Centre for Astrodynamics Research (CCAR) online database.

Chapter 6: Conclusion

The goals of this thesis were to evaluate how Cu speciation influences Cu availability to marine phytoplankton – both in culture and in the field – and in turn determine how Cu bioavailability affects rate processes in the northeast subarctic Pacific Ocean. The primary questions of each chapter were: 1) what is the bioavailability of Cu bound to *in situ* ligands and different Cu-ligand complexes to a natural phytoplankton community?; 2) how is organically complexed Cu acquired by marine phytoplankton?; 3) are Fe limited and Fe-light co-limited phytoplankton also limited by Cu availability?; and 4) what environmental factors control phytoplankton Cu requirements?; and 5) how does Cu bioavailability influence primary productivity in the northeast subarctic Pacific Ocean?

The questions addressed in this thesis have important implications for advancing our understanding of how Cu may influence global marine primary. I present the first attempts to characterize the bioavailability of organically complexed Cu to natural phytoplankton communities in the open ocean, as well as to laboratory strains using environmentally relevant Cu concentrations and speciation. I also assessed how intracellular Cu levels in natural phytoplankton are controlled by different environmental variables, and how Cu speciation may influence primary productivity in the northeast subarctic Pacific Ocean. Thus, the data presented herein provide new insights into how Cu speciation and bioavailability may influence phytoplankton rate processes in marine ecosystems, and constitute the groundwork for future studies.

6.1 Major Findings And Contributions

Previous laboratory and limited field studies indicate that marine phytoplankton can acquire Cu from within organic complexes (e.g. Hudson 1998; Croot et al. 2003; Quigg et al. 2006; Guo et al. 2010; Semeniuk et al. 2009). Chapter 2 presents the most comprehensive field evidence that Cu(II) within strong ligand complexes and Cu bound to *in situ* ligands are bioavailable. Indeed, estimates of cellular Cu uptake rates for the phytoplankton community were significantly faster than the maximum supply of Cu' to the cell surface for two artificial Cu(II)L and Cu bound within the *in situ* ligands. In accordance with recent genetic evidence for a Cu(I)-specific high-affinity transport system in marine phytoplankton (Guo et al. submitted), we hypothesize that Cu(II) bound to the strong ligands was reduced prior to being internalized as Cu(I).

Furthermore, the addition of Cu with 10 nM weak ligands caused uptake rates to increase more than would be expected from changes to total dissolved Cu, suggesting that weak Cu binding ligands may increase *in situ* Cu bioavailability through a “weak ligand shuttle” (Aristilde et al. 2012). Thus, weak ligands may play an unreported, yet important role in determining *in situ* Cu bioavailability.

Given the findings of chapter 2, I performed a laboratory investigation of Cu uptake from a strong Cu(II)-ligand complex by four marine phytoplankton. Previous laboratory studies of Cu uptake by marine phytoplankton have used very high concentrations of Cu and ligands, so this was the first study to investigate Cu bioavailability of organically complexed Cu that mimicked *in situ* Cu speciation. Copper(II) within the complex was bioavailable, and cellular uptake rates were similar to those estimated for a phytoplankton community in Chapter 2. Thus, acquisition of organically complexed Cu(II) may be common among eukaryotic phytoplankton. To

elucidate how organically complexed Cu is acquired, I also investigated the substrate for the high-affinity Cu transport system in a marine diatom, *Thalassiosira pseudonana*. Competitive inhibition Cu uptake assays suggest that Cu(II)Cyclam is reduced prior to internalization of Cu(I). Similarly, uptake of inorganic Cu(II) likely involved reduction. The Cu uptake rates, in the presence of a strong Cu(II) chelator, are significantly faster than previously reported rates measured with more than 10,000 times more ligand present (EDTA). The slower rates measured previously may be due to competition for Cu between the excess ligand concentration and transporters. In previous growth rate studies, this competition would have artificially decreased Cu uptake rates, and lowered intracellular Cu concentrations. As such, the concentrations of Cu thought to cause limitation or toxicity would have been overestimated. The response of marine phytoplankton growth rates to varying inorganic Cu concentrations, in the presence of high excess Cu ligands, has formed the basis for predicting whether Cu will be limiting or toxic in natural phytoplankton communities. Given the results of chapter 2, one should use caution when applying the results of previous growth rate investigations to the study of natural marine phytoplankton.

Although previous laboratory and field incubation experiments have demonstrated that Fe-limited phytoplankton may become co-limited by Cu, chapter 4 presents the results of a more thorough examination of this possibility at two Fe-limited stations in the northeast subarctic Pacific Ocean. At one Fe-limited station (P20), Cu had no effect on the accumulation of chl *a*, Fe uptake by the high-affinity Fe transport system, or F_v/F_m . This indicated that *in situ* Cu availability was not limiting phytoplankton growth at this station. At station P26, light and Fe-light co-limited phytoplankton did not respond to Cu amendments. However, Fe uptake rates in

large phytoplankton and F_v/F_m increased temporarily in the Cu amended light-replete treatments. These data provide physiological evidence for a metabolic Fe-Cu interactions in an Fe-limited phytoplankton community. Since Fe limits phytoplankton in approximately one third of the global surface ocean, Cu bioavailability may modulate the degree of Fe limitation experienced by large phytoplankton.

In chapter 5, I performed an investigation of how Cu:C assimilation ratios and uptake rates of marine bacteria and phytoplankton vary with different environmental factors. I also undertook the an investigation of how Cu speciation may influence primary producers in the northeast subarctic Pacific Ocean. In eukaryotes, neither Cu uptake rates nor Cu:C assimilation ratios were correlated with inorganic Cu concentrations, total Cu concentrations, Cu-binding ligand concentrations, Cu-binding ligand strengths, or any other measured variable. These data indicate that phytoplankton species composition may play an important role in controlling particulate Cu concentrations. Volumetric rates of primary productivity for the 1-5 μm , 5 μm , and total particulate size fractions were negatively correlated with inorganic Cu concentrations, and positively correlated with the ligand strengths. These data provide evidence that Cu speciation may exert some influence on rate processes in natural phytoplankton communities. An incubation performed at an Fe-limited open ocean station revealed that reducing the *in situ* Cu bioavailability resulted in decreased Cu acquisition, increased specific carbon fixation rates, and increase cyanobacteria abundance. This is the first evidence that decreasing *in situ* Cu availability can increase phytoplankton growth, and indicates that Cu may influence rate processes in open ocean phytoplankton communities.

6.2 Future Directions

I hope that the results of this thesis will promote on-going investigations of the emerging role of Cu in influencing phytoplankton growth, and the seemingly complex roles that speciation may play in determining Cu bioavailability to different phytoplankton. As a result of this work, a number of questions have arisen and need to be addressed in order to better understand the influence Cu has on primary producers.

1. Do ligands produced by cyanobacteria and heterotrophic bacteria influence the bioavailability of Cu to different phytoplankton?

Cyanobacteria and heterotrophic bacteria produce strong Cu-binding ligands in response to Cu toxicity (Moffett and Brand 1996; Gordon et al. 2000). Previous growth rate studies in an artificial medium by Brand et al. (1986) led to the hypothesis that strong Cu-binding ligands found in seawater were produced by prokaryotes in order to detoxify Cu via extracellular complexation. However, the bioavailability of Cu bound to these ligands has not been demonstrated experimentally. The structure and binding groups of Cu binding ligands remains largely unresolved. There is evidence that these ligands have sulfur-containing functional groups, and may bind Cu(I) (Ross et al. 2003; Wiramanaden et al. 2008). The results presented in chapters 2 and 3 indicate that organically complexed Cu is bioavailable to eukaryotic phytoplankton, so it is possible that the complexes produced by prokaryotes may not make Cu unavailable to all phytoplankton. To test this, cyanobacteria could be induced to produce the strong ligands while suspended in ^{67}Cu labeled seawater (following the protocols of Moffett and Brand 1996), thereby producing ^{67}Cu -ligand complexes. The cyanobacteria could be filtered out,

and the ^{67}Cu -ligand labeled seawater used to perform short-term Cu uptake experiments with phytoplankton of ecological importance (e.g. *Synechococcus*, *Prochlorococcus*, *E. huxleyi*, *Micromonas*, *Phaeocystis antarctica*, *Fragilariopsis*, etc.). Rates of uptake from the ^{67}Cu -ligand complex would be compared to a control treatment with equivalent concentrations of inorganic ^{67}Cu . This would prove whether the strong ligands hypothesized to detoxify Cu for cyanobacteria actually do so by making it less available for acquisition. It would also demonstrate whether these ligands prevent other phytoplankton from acquiring Cu.

2. Do all phytoplankton groups acquire Cu at similar rates in a natural community?

Copper uptake rates measured in chapter 3 were nearly 10 times faster for diatoms than prymnesiophytes. It is likely that individual species or phyla in a natural phytoplankton community will acquire Cu at different rates, and so the phytoplankton community structure could control *in situ* phytoplankton Cu uptake rates. Changes in species composition could result in drawdown of Cu in surface waters to low concentrations (e.g. < 0.5 nM; Jacquot et al. 2013; Thompson et al. 2014) that may limit growth rates of some phytoplankton (e.g. diatoms), but not others (e.g. prymnesiophytes) (Annett et al. 2008; Guo et al. 2012). Future field investigations of Cu uptake rates by individual phytoplankton could be performed using ^{67}Cu complexed to *in situ* ligands, a sea-going gamma counter, and a sorting flow cytometer. Given the high specific activity of ^{67}Cu and relatively high total dissolved Cu concentrations compared to other metals (e.g. Fe, Zn), this could feasibly be done (unlike other radioisotopes with lower specific activities; e.g. ^{55}Fe or ^{59}Fe). Uptake rates of individual cell populations (including heterotrophic and cyanobacteria) could be measured and compared to 16s and 18s ssRNA

analysis to identify the microbes present. This work could produce the first *in situ* metal uptake rates for an individual phytoplankton species. Similarly, the effect of altering the *in situ* Cu speciation with small additions of competing ligands (e.g. Cyclam) on Cu uptake rates could be assessed for individual phytoplankton groups.

3. What is the nature of strong Cu binding ligands in seawater?

Little is known about the strong ligands that bind Cu in seawater due to their low concentrations in seawater and the likely varied structures of a mixture of strong and weak ligands. Laboratory evidence suggests that prokaryotic and eukaryotic plankton may produce some of the strong ligands found in seawater in response to Cu toxicity (Moffett and Brand 1996; Croot et al. 2000; Gordon et al. 2000). Other candidate strong ligands include thiols produced by phytoplankton to detoxify Cu (e.g. phytochelatins), and their derivatives (e.g. cysteine, glutathione) (Ahner et al. 1997; 2002; Dupont et al. 2004; 2006). Weaker Cu binding ligands may be humic and fulvic acids (Yang and van den Berg 2009). The speciation of dissolved Cu is further complicated by Cu redox cycling in surface waters, and a significant portion of the dissolved Cu pool could be inorganic Cu(I) or Cu(II) bound to thiols (e.g. Moffett and Zika 1988; Leal and van den Berg 1998; Beurge-Weirich and Sulzberger 2004). Given the reactive nature of thiols with metals, the development of analytical capabilities for isolating Cu ligands – e.g. immobilized metal-ion chromatography or high performance liquid chromatography, either couple with electrospray ionization mass spectrometry (Ross et al. 2003; McCormack et al. 2003) – that maintained their *in situ* chemical properties would significantly advance this field.

4. Does Cu bioavailability control rate processes in surface waters elsewhere?

Data from chapters 4 and 5 indicate that Cu bioavailability may influence phytoplankton rate processes in the northeast subarctic Pacific Ocean. It would be prudent to investigate whether Cu influences phytoplankton in other oceanic regions. In chapter 4, I observed two lines of evidence for a metabolic interaction between Fe and Cu in Fe-limited phytoplankton: greater drawdown of Cu by Fe-limited phytoplankton, and a physiological response to Cu amendments (increased F_v/F_m and increased Fe uptake by large phytoplankton). Recent measurements of total dissolved Cu concentrations in surface waters in the eastern South Pacific Ocean and Tasman Sea indicate that Cu can become low enough to potentially cause Cu-limitation (e.g. < 0.5 nM) (Jacquot et al. 2013; Thompson et al. 2014). Thus, Fe-Cu interactions may be important in other oceanic waters. Decreased pH in surface waters resulting from ocean acidification may also cause *in situ* Fe bioavailability to decrease (Shi et al. 2010), and could result in a greater metabolic dependence on Cu by large (>5 μm) Fe-limited phytoplankton (see Chapter 4). Approximately 30% of surface ocean waters are Fe-limited, so additional work is warranted to identify variables (e.g. species composition, cell size, light availability) that may determine whether Cu will limit Fe-limited phytoplankton populations. In chapter 6, Cu also appeared to influence rate processes along Line P, whereby decreasing Cu availability at P16 resulted in increased primary productivity. It would be warranted to investigate whether decreasing Cu availability in other regions also stimulates phytoplankton growth, and how different environmental variables (e.g. nutrient and light availability) affect Cu nutrition in marine phytoplankton.

Climate change and its impacts will become a chief driving force of change to marine ecosystems over the next century. Increasing sea surface temperatures and decreasing mixed layer depths over the past century have resulted in ~1% decrease in chl *a* per year relative to the global median chl *a* (Boyce et al. 2010). Model projections indicate that future surface waters in different regions may experience differential combinations of stressors, such as changes in temperature, pH, light and trace metal bioavailability (e.g. Boyd and Hutchins 2012; Gao et al. 2012; Hoffmann et al. 2012). Decreasing seawater pH will cause Cu(I) oxidation rates to decrease slightly (~10 %) in oxic surface waters (González-Dávila et al. 2009). This will result in longer lived pools of dissolved Cu(I), and may alter *in situ* Cu bioavailability to marine microbes. Decreased pH may also cause Cu-ligand complexes to weaken (Louis et al. 2009), thereby affecting the potential detoxifying role of some strong Cu binding ligands. Given the results presented in this thesis, it will become urgent to better characterize the putative role Cu may play in influencing marine primary production and the potential synergistic and antagonistic relationships Cu may have with other environmental stressors (e.g. Pörtner 2012).

References

- Achterberg, E.P., Braungardt, C.B., Sandford, R.C., Worsfold, P.J., 2001. UV digestion of seawater samples prior to the determination of copper using flow injection with chemiluminescence detection. *Anal. Chim. Act.* 440, 27-36.
- Achterberg, E.P., van den Berg, C.M.G., 1997. Chemical speciation of chromium and nickel in the western Mediterranean. *Deep-Sea Res. II* 44, 693-720.
- Ahner, B.A., Kong, S., Morel, F.M.M., 1995. Phytochelatin production in marine algae. 1. An interspecies comparison. *Limnol. Oceanogr.* 40, 649-657.
- Ahner, B.A., Morel, F.M.M., Moffett, J.W., 1997. Trace metal control of phytochelatin production in coastal waters. *Limnol. Oceanogr.* 42, 601-608.
- Ahner, B.A., Wei, L., Oleson, J.R., Ogura, N., 2002. Glutathione and other low molecular weight thiols in marine phytoplankton under metal stress. *Mar. Ecol. Prog. Ser.* 232, 93-103.
- Albrecht-Gary A-M, Crumbliss AL., 1998. The coordination chemistry of siderophores: Thermodynamics and kinetics of iron chelation and release. In: Sigel A, Sigel H, eds. *Metal Ions in Biological Systems*. New York: Marcel Dekker, pp. 239-327.
- Anderson, D.M., Morel, F.M.M., 1978. Copper sensitivity of *Gonyaulax tamarensis*. *Limnol. Oceanogr.* 23, 283-295
- Anderson, M.A., Morel, F.M.M., 1982. The influence of aqueous iron chemistry on the uptake of iron by the coastal diatom *Thalassiosira weissflogii*. *Limnol. Oceanogr.* 27, 789-813.
- Annett, A.L., Lapi, S., Ruth, T.J., Maldonado, M.T., 2008. The effects of Cu and Fe availability on the growth and Cu:C ratios of marine diatoms. *Limnol. Oceanogr.* 53, 2451-2461.
- Aristilde, L., Xu, Y., Morel, F.M.M., 2012. Weak organic ligands enhance zinc uptake in marine phytoplankton. *Environ. Sci. Technol.* 36, 5438-5445.
- Barber, R.T., Ryther, J.H., 1969. Organic chelators: factors affecting primary production in the Cromwell Current upwelling. *J. Exp. Mar. Biol. Ecol.* 3, 191-199.
- Barber, R.T., 1973. Organic ligands and phytoplankton growth in nutrient-rich seawater. In: P.S. Singer (ed.) *Trace Metals and Metal-Organic Interactions in Natural Waters*. Ann Arbor Science, Michigan, pp 321-338.
- Barwell-Clarke, J., Whitney, F.A., 1996. Institute of Ocean Sciences nutrient methods and analysis. Canadian Technical Report of Hydrography and Ocean Sciences 182, 43pp.

- Bertinato, J., Cheung, L., Hoque, R., & Plouffe, L. J. (2010). Ctr1 transports silver into mammalian cells. *Journal of Trace Elements in Medicine and Biology*, 24(3), 178–184.
- Booth, B.C., 1988. Size classes and major taxonomic groups of phytoplankton at two locations in the subarctic Pacific Ocean in May and August, 1984. *Mar. Bio.* 97, 275-286.
- Booth, B.C., Lewin, J., Postel, J.R., 1993. Temporal variation in the structure of autotrophic and heterotrophic communities in the subarctic Pacific. *Prog. Oceanog.* 32, 57-99.
- Bowler, C., Van Camp, W., Montagu, M.V., Inzé, D., Asada, K., 1994. Superoxide dismutase in plants. *Crit Rev. Plant Sci.* 13, 199-218.
- Boyce, D.G., Lewis, M.R., Worm, B., 2010. Global phytoplankton decline over the past century. *Nature* 466, 591-596.
- Boyd, P.W., Abraham, E.R., 2001. Iron-mediated changes in phytoplankton photosynthetic competence during SOIREE. *Deep Sea Res. II* 48, 2529 – 2550.
- Boyd, P.W., Harrison, P.J., 1999. Phytoplankton dynamics in the NE subarctic Pacific. *Deep-Sea. Res. II* 46, 2405-2432.
- Boyd, P.W., Hutchins, D.A., 2012. Understanding the responses of ocean biota to a complex matrix of cumulative anthropogenic change. *Mar. Ecol. Progr. Ser.* 470, 125-135.
- Boyd, P.W., Jickells, T., Law, C.S., Blain, S., Boyle, E.A., Buesseler, K.O., Coale, K.H., Cullen, J.J., de Baar, J.W., Follows, M., Harvey, M., Lancelot, C., Levasseur, M., Owens, N.P.J., Pollard, R., Rivkin, B., Sarmiento, J., Schoemann, V., Smetacek, V., Takeda, S., Tsuda, A., Turner, S., Watson, A.J., 2007. Mesoscale iron enrichment experiments 1993-2005: synthesis and future directions. *Science* 315, 612-617.
- Boyle, E.A., Husteded, S.S., Jones, S.P., 1981. On the distribution of copper, nickel, and cadmium in the surface waters of the North Atlantic and North Pacific Ocean. *J. Geophys. Res.* 86, 8048-8066.
- Boyle, E.A., Selater, F.R., Edmond, J.M., 1977. The distribution of dissolved copper in the Pacific. *Earth Planet. Sci. Lett.* 37, 38-54.
- Brand, L.E., 1991. Minimum iron requirements of marine phytoplankton and the implications for the biogeochemical control of new production. *Limnol. Oceanogr.* 36, 1756-1771.
- Brand, L.E., Sunda, W.G., Guillard, R.R.L., 1986. Reduction of marine phytoplankton reproduction rates by copper and cadmium. *J. Exp. Mar. Biol. Ecol.* 96, 225-250.
- Bruland, K.W., 1989. Complexation of zinc by natural organic ligands in the central North Pacific. *Limnol. Oceanogr.* 34, 269-285.

- Bruland, K.W., Lohan, M.C., 2003. Controls of trace metals in seawater. *Treatise Geochem.* (1st Edition) Vol. 6, 23-47.
- Bruland, K.W., Rue, E.L., Donat, J.R., Skrabal, S.A., Moffett, J.W., 2000. Intercomparison of voltammetric techniques to determine the chemical speciation of dissolved copper in a coastal seawater sample. *Anal. Chim. Acta* 405, 99–113.
- Buck, K.N., Bruland, K.W., 2005. Copper speciation in San Francisco Bay: a novel approach using multiple analytical windows. *Mar. Chem.* 96 (1–2), 185–198.
- Buck, K.N., Selph, K.E., Barbeau, K.A., 2010. Iron-binding ligand production and copper speciation in an incubation experiment of Antarctic Peninsula shelf waters from the Bransfield Strait, Southern Ocean. *Mar. Chem.* 122, 148-159.
- Buerge-Weirich, D., Sulzberger, B., 2004. Formation of Cu(I) in estuarine and marine waters: application of a new solid-phase extraction method to measure Cu(I). *Environ. Sci. Technol.* 38, 1843-1848.
- Buesseler, K.O., Lamborg, C.H., Boyd, P.W., Lam, P.J., Trull, T.W., Bidigare, R.R., Bishop, J.K., Casciotti, K.L., Behairs, F., Elskens, M., Honda, M., Karl, D.M., Siegel, D.A., Silver, M.W., Steinberg, D.K., Valdes, J., Van Mooy, B., Wilson, S., 2007. Revisiting carbon flux through the ocean's twilight zone. *Science* 316, 567-570.
- Bundy, R.M., Barbeau, K.A., Buck, K.N., 2013. Sources of strong copper-binding ligands in Antarctic Peninsula surface waters. *Deep Sea Res. II* 90, 134-146.
- Chadd, H.E., Newman, J., Mann, N.H., Carr, N.G., 1996. Identification of iron superoxide dismutase and a copper/zinc superoxide dismutase enzyme activity within the marine cyanobacterium *Synechococcus* sp. WH 7803. *FEMS Microbiol. Lett.* 138, 161-165.
- Chang, S.I., Reinfelder, J.R., 2000. Bioaccumulation, subcellular distribution, and trophic transfer of copper in a coastal marine diatom. *Environ. Sci. Technol.* 34, 4931-4935.
- Cheah, S.-F., Kraemer, S.M., Cervini-Silva, J., Sposito, G., 2003. Steady-state dissolution kinetics of goethite in the presence of desferrioxamine B and oxalate ligands: implications for the microbial acquisition of iron. *Chem. Geol.* 198, 63-75.
- Ciriolo, M.R., Desideri, A., Paci, M., Rotilio, G., 1990. Reconstitution of Cu, Zn-superoxide dismutase by the Cu(I)-glutathione complex. *J. Biol. Chem.* 265, 11030-11034.
- Coale, K.H., 1991. Effects of iron, manganese, copper, and zinc enrichments on productivity and biomass in the Subarctic Pacific. *Limnol. Oceanogr.* 36, 1851-1864.
- Coale, K.H., Bruland, K.W., 1988. Copper complexation in the Northeast Pacific. *Limnol. Oceanogr.* 33, 1084–1101.

- Croot, P.L., 2003. Cycle of Copper Speciation in Gullmar Fjord, Sweden. *Limnol. Oceanogr.* 48, 764-776.
- Croot, P.L., Karlson, B., van Elteren, J.T., Kroon, J.J., 2003. Uptake and efflux of ^{64}Cu by the marine cyanobacterium *Synechococcus* (WH7803). *Limnol. Oceanogr.* 48, 179-188.
- Croot, P.L., Moffett, J.W., Luther, G.W., 1999. Polarographic determination of half-wave potentials for copper-organic complexes in seawater. *Mar. Chem.* 67, 219-232.
- Cullen, J.T., Chase, Z., Coale, K.H., Fitzwater, S.E., Sherrell, R.M., 2003. Effect of Iron Limitation on the Cadmium to Phosphorus Ratio of Natural Phytoplankton Assemblages from the Southern Ocean. *Limnol. Oceanogr.* 48, 1079-1087.
- Cummins, P.F. Freeland, H.J., 2007. Variability of the North Pacific current and its bifurcation. *Progr. Oceanogr.* 75, 253-265.
- Cutter, G., Andersson, P., Codispoti, L., Croot, P., Francois, R., Lohan, M., Obata, H., van der Loeff, M.R., 2010. Sampling and sample-handling protocols for GEOTRACES cruises.
- Dancis, A., Haile, D., Yuan, D.S., Klausner, R.D., 1994. The *Saccharomyces cerevisiae* copper transport protein (Ctr1p). *J. Biol. Chem.* 41, 25860-25667.
- De La Rocha, C.L., Passow, U., 2007. Factors influencing the sinking of POC and the efficiency of the biological carbon pump. *Deep Sea Res. II* 54, 639-658.
- Debelius, B., Forja, J.M., Lubián, L.M., 2011. Toxicity of copper, nickel and zinc to *Synechococcus* populations from the Strait of Gibraltar. *J. Mar. Systems* 88, 113-119.
- Donat, J.R., Lao, K.A., Bruland, K.W., 1994. Speciation of dissolved copper and nickel in south San-Francisco bay - a multimethod approach. *Anal. Chim. Act.* 284, 547-571.
- Dryden, C.L., Gordon, A.S., Donat, J.R., 2004. Interactive regulation of dissolved copper toxicity by an estuarine microbial community. *Limnol. Oceanogr.* 49 (4), 1115-1122.
- Dupont, C.L., Ahner, B.A., 2005. Effects of copper, cadmium, and zinc on the production and exudation of thiols by *Emiliana huxleyi*. *Limnol. Oceanogr.* 50, 508-515.
- Dupont, C.L., Moffett, J.W., Bidigare, R.R., Ahner, B.A., 2006. Distributions of dissolved and particulate biogenic thiols in the subarctic Pacific Ocean. *Deep Sea Res. I* 53, 1961-1974.
- Dupont, C.L., Nelson, R.K., Bashir, S., Moffett, J.W., Ahner, B.A., 2004. Novel copper-binding and nitrogen-rich thiols produced and exuded by *Emiliana huxleyi*. *Limnol. Oceanogr.* 49, 1754-1762.

- Eckhardt, U., Buckhout, T.J., 1998. Iron assimilation in *Chlamydomonas reinhardtii* involves ferric reduction and is similar to Strategy I higher plants. *J. Exp. Botany* 49, 1219-1226.
- Eide, D., Davis-Kaplan, S., Jordan, I., Sipe, D., Kaplan, J., 1992. Regulation of iron uptake in *Saccharomyces cerevisiae*. *J. Biol. Chem.* 267, 20774-20781.
- Egleston, E.S., Morel, F.M.M., 2008. Nickel limitation and zinc toxicity in a urea-grown diatom. *Limnol. Oceanogr.* 53, 2462-2471.
- Eldridge, M. L., Trick, C.G., Alm, M. B., DiTullio, G. R., Rue, E. L., Bruland, K. W., Hutchins, D. A., Wilhelm, S.W., 2004. The response of the marine phytoplankton community to a manipulation of bioavailable iron in HNLC waters of the subtropical Pacific Ocean. *Aquat. Microb. Ecol.*, 35, 79–91.
- Elrod, V.A., Berelson, W.M.N., Coale, K.H., Johnson, K.S., 2004. The flux of iron from continental shelf sediments: A missing source for global budgets. *Geophys. Res. Lett.* 31, L12307, doi:10.1029/2004GL020216.
- Falkowski, P.G., Owens, T.G., Ley, A.C., Mauzerall, D.C., 1981. Effects of growth irradiance levels on the ratio of reaction centers in two species of marine phytoplankton. *Plant Physiol.* 68, 969-973.
- Field, C., Behrenfeld, M., Randerson, J., Falkowski, P., 1998. Primary production of the biosphere: integrating terrestrial and oceanic components. *Science* 281, 237-40.
- Flegal, R., Smith, G.J., Gill, G.A., Sañudo-Wilhelmy, S., Anderson, L.C.D., 1991. Dissolved trace element cycles in the San Francisco Bay estuary. *Mar. Chem.* 36, 329-363.
- Foreman, M.G.G., Pal, B., Merryfield, W.J., 2011. Trends in upwelling and downwelling winds along the British Columbia shelf. *J. Geophys. Res.* 116, C10023, doi:10.1029/2011JC006995.
- Foster, P.L., 1977. Copper exclusion as a mechanism of heavy metal tolerance in a green alga. *Nature* 269, 322-323.
- Gaillardet, J., Viers, J., Dupré, B., 2003. Trace elements in river waters. *Treatise Geochem.* (1st Edition) Vol. 6, 225-72.
- Gargett, A.E., 1991. Physical processes and the maintenance of nutrient-rich euphotic zones. *Limnol. Oceanogr.* 36, 1527-1545.
- Gao, K., Helbling, E.W., Häder, D.-P., Hutchins, D.A., 2012. Responses of marine primary producers to interactions between ocean acidification, solar radiation, and warming. *Mar. Ecol. Progr. Ser.* 470, 167-189.

- Georgatsou, E., Mavrogiannis, L.A., Fragiadakis, G.S., Alexandraki, D., 1997. The yeast Fre1p/Fre2p cuprix reductases facilitate copper uptake and are regulated by the copper-modulated Mac1p activator. *J. Biol. Chem.* 272, 13786-13792.
- Gledhill, M., Buck, K. N., 2012. The organic complexation of iron in the marine environment: a review. *Front. Microbiol.* doi: 10.3389/fmicb.2012.00069.
- Gledhill, M., McCormack, P., Ussher, S., Achterberg, E.P., Mantoura, R.F.C., Worsfold, P.J., 2004. Production of siderophore type chelates by mixed bacterioplankton populations in nutrient enriched seawater incubations. *Mar. Chem.* 88, 75-83.
- Gledhill, M., van den Berg, C.M.M., 1994. Determination of complexation of iron (III) with natural organic complexing ligands in seawater using cathodic stripping voltammetry. *Mar. Chem.* 47, 41-54.
- González-Dávila, M., Santana-Casiano, J.M., González, A.G., Pérez, N., Millero, F.J., 2009. Oxidation of copper(I) in seawater at nanomolar levels. *Mar. Chem.* 115, 118-124.
- Gordon, A.S., Donat, J.R., Kango, R.A., Dyer, B.J., Stuart, L.M., 2000. Dissolved copper-complexing ligands in cultures of marine bacteria and estuarine water. *Mar. Chem.* 70, 149-160.
- Greene, R.M., Geider, R.J., Falkowski, P.G., 1991. Effect of iron limitation on photosynthesis in a marine diatom. *Limnol. Oceanogr.* 36,1772–82
- Guo, J., Annett, A. L., Taylor, R. L., Lapi, S., Ruth, T. J., Maldonado, M. T. 2010. Copper uptake kinetics of coastal and oceanic diatoms. *J. Phycol.* 46, 1218–28.
- Guo, J., Green, B.R., Maldonado, M.T., 2014. Sequence Analysis and Gene Expression of Potential Components of Copper Transport and Homeostasis in *Thalassiosira pseudonana*. *Submitted to Protist*.
- Guo, J., Lapi, S., Ruth, T.J., Maldonado, M.T., 2012. The effects of iron and copper availability on the copper stoichiometry of marine phytoplankton. *J. Phycol.* 48, 312-325.
- Hain, M.P., Sigman, D.M., Haug, G.H., 2014. The biological pump in the past. *Treatise Geochem.* (2nd Edition)), Vol. 8, 485-517.
- Hall, A., Fielding, A.H., Butler, M., 1979. Mechanisms of copper tolerance in the marine fouling alga *Ectocarpus siliculosus* – evidence for an exclusion mechanism. *Mar. Biol.* 54, 195-199.
- Hamme, R.C., Webley, P.W., Crawford, W.R., Whitney, F.A., DeGrandpre, M.D., Emerson,

- S.R., Eriksen, C.C., Giesbrecht, K.E., Gower, J.F.R., Kavanaugh, M.T., Peña, M.A., Sabine, C.L., Batten, S.D., Coogan, .A., Grundle, D.S., Lockwood, D., 2010. Volcanic ash fuels anomalous plankton bloom in subarctic northeast Pacific. *Geophys. Res. Lett.* 37, L19604, doi:10.1029/2010GL044629.
- Harrison, P.J., Whitney, F.A., Tsuda, A., Saito, H., Tadokoro, K., 2004. Nutrient and plankton dynamics in the ne and NW gyres of the subarctic Pacific Ocean. *J. Oceanogr.* 60, 93-117.
- Hassett, R., Kosman, D.J., 1995. Evidence for Cu(II) reduction as a component of copper uptake by *Saccharomyces cerevisiae*. *J. Biol. Chem.* 270, 128-134.
- Hassler, C.S., Schoemann, V., Nichols, C.M., Nutler, E.C.V., Boyd, P.W., 2011. Saccharides enhance iron bioavailability to Southern Ocean phytoplankton. *Proc. Nat. Acad. Sci.* 108, 1076-1081.
- Heller, M.I., Croot, P.L., 2010. Superoxide decay kinetics in the Southern Ocean. *Environ. Sci.* 44, 191-196.
- Heller, M.I., Croot, P.L., 2011. Superoxide decay as a probe for speciation changes during dust dissolution in Tropical Atlantic surface waters near Cape Verde. *Mar. Chem.* 126, 37-55.
- Hering, J.G., Morel, F.M.M., 1988. Kinetics of trace metal complexation: role of alkaline-earth metals. *Environ. Sci. Technol.* 22, 1469-1478.
- Hill, K.L., Hassett, R., Kosmon, D., Merchant, S., 1996. Regulated copper uptake in *Chlamydomonas reinhardtii* in response to copper availability. *Plant Physiol.* 112, 697-704.
- Ho, T.Y., Quigg, A., Finkel, Z.V., Milligan, A.J., Wyman, K., Falkowski, P.G., Morel, F.M.M., 2003. The elemental composition of some marine phytoplankton. *J. Phycol.* 39, 1145-1159.
- Hoffmann, L.J., Breitbarth, E., Boyd, P.W., Hunter, K.A., 2012. Influence of ocean warming and acidification on trace metal biogeochemistry. *Mar. Ecol. Progr. Ser.* 470, 191-205.
- Hsieh, W. W., D. M. Ware, Thomson, R.E., 1995. Wind-induced upwelling along the West Coast of North America, 1899–1988, *Can. J. Fish. Aquat. Sci.*, 52, 325–334.
- Hudson, R.J.M., 1998. Which aqueous species control the rates of trace metal uptake by aquatic biota? Observations and predictions of non-equilibrium effects. *Sci. Tot. Environ.* 219, 95-115.
- Hudson, R.J., Covault, D.T., Morel, F.M.M., 1992. Investigations of iron coordination and redox

reactions in seawater using ^{59}Fe radiometry and ion-pair solvent extraction of amphiphilic iron complexes. *Mar. Chem.* 38, 209-235.

Hudson, R.J.M., Morel, F.M.M., 1989. Distinguishing between extra- and intracellular iron in marine phytoplankton. *Limnol. Oceanogr.* 34, 1113–1120.

Hudson, R.J.M., Morel, F.M.M., 1990. Iron transport in marine phytoplankton: kinetics of cellular and medium coordination reactions. *Limnol. Oceanogr.* 35, 1002-1020.

Hudson, R.J.M., Rue, E.L., Bruland, K.W., 2003. Modeling complexometric titrations of natural waters samples. *Environ. Sci. Technol.* 37, 1553-1562.

Hutchins, D.A., DiTullio, G.R., Zhang, Y., Bruland, K.W., 1998. An iron limitation mosaic in the California upwelling regime. *Limnol. Oceanogr.* 43, 1037-1054.

Iwade, S., Kuma, K., Isoda, Y., Yoshida, M., Kudo, I., Nishioka, J., Suzuki, K., 2006. Effect of high iron concentrations on iron uptake and growth of a coastal diatom *Chaetoceros sociale*. *Aquat. Microb. Ecol.* 43, 177-191.

Jackson, G.A., Morgan, J.J., 1978. Trace metal-chelator interactions and phytoplankton growth in seawater media: theoretical analysis and comparison with reported observations. *Limnol. Oceanogr.* 23, 268-282.

Jacquot, J.E., Kondo, Y., Knapp, A.N., Moffett, J.W., 2013. The speciation of copper across active gradients in nitrogen-cycle processes in the eastern tropical South Pacific. *Limnol. Oceanogr.* 58, 1387-1394.

Janssen, D.J., Conway, T.M., John, S.G., Christian, J.R., Kramer, D.I., Pedersen, T.F., Cullen, J.T., 2014. Undocumented water column sink for cadmium in open ocean oxygen-deficient zones. *Proc. Nat. Acad. Sci.* 111, 6888–6893.

Johnson, K.S., Gordon, R.M., Coale, K.H., 1997. What controls dissolved iron concentrations in the world ocean? *Mar. Chem.* 57, 137–161.

Johnson, W.K., Miller, L.A., Sutherland, N.E., Wong, C.S., 2005. Iron transport by mesoscale Haida eddies in the Gulf of Alaska. *Deep-Sea Res. II* 52, 933–953.

Jones, G.J., Palenik, B.P., Morel, F.M.M., 1987. Trace metal reduction by phytoplankton: the role of plasmalemma redox enzymes. *J. Phycol.* 23, 237-244.

Jones, C.J., Murray, J.W., 1984. Nickel, cadmium, and copper in the northeast Pacific off the coast of Washington. *Limnol. Oceanogr.* 29, 711-720.

Jordi, A., Basterretxea, G., Tovar-Sánchez, A., Alastuey, A., Querol, X., 2012. Copper aerosols

inhibit phytoplankton growth in the Mediterranean Sea. *Proc. Nat. Acad. Sci.* 109, 21246–21249.

- Kanamaru, K., Kashiwagi, S., Mizuno, T., 1994. A copper-transporting P-type ATPase found in the thylakoid membrane of the cyanobacteria *Synechococcus* species PCC7942. *Molec. Microbiol.* 13, 369-377.
- Kawakami, S.K., Gledhill, M., Achterberg, E.P., 2006. Production of phytochelatins and glutathione by marine phytoplankton in response to metal stress. *J. Phycol.* 42, 975-989.
- Kieber, R.J., Skrabal, S.A., Smith, C., Willey, J.D., 2004. Redox speciation of copper in rainwater: temporal variability and atmospheric deposition. *Environ. Sci. Technol.* 38, 3587-3594.
- Kustka, A.B., Allen, A.E., Morel, F.M.M., 2007. Sequence analysis and transcriptional regulation of iron acquisition genes in two marine diatoms. *J. Phycol.* 43, 715–729
- Lage, O.M., Parente, A.M., Soares, H.M.V.M., Vasconcelos, M.T.S.D., Salema, R., 1994. Some effects of copper on the dinoflagellates *Amphidinium carterae* and *Prococentrum micans* in batch culture. *Europ. J. Phycol.* 29. 253-260.
- Laglera, L.M., van den Berg, C.M.G., 2003. Copper complexation by thiol compounds in estuarine waters. *Mar. Chem.* 82, 71-89.
- Laglera, L.M., van den Berg, C.M.G., 2006. Photochemical oxidation of thiols and copper complexing ligands in estuarine waters. *Mar. Chem.* 101, 130-140.
- Lam, P.J., Bishop, J.K.B., Henning, C.C., Marcus, M.A., Waychunas, G.A., Fung, I.Y., 2006. Wintertime phytoplankton bloom in the subarctic Pacific supported by continental margin iron. *Glob. Biogeochem. Cyc.* 20, Gb1006, doi:10.29/2005GB002557.
- Lane, E.S., Jang, K., Cullen, J.T., Maldonado, M.T., 2008. The interaction between inorganic iron and cadmium uptake in the marine diatom *Thalassiosira oceanica*. *Limnol. Oceanogr.* 53, 1784-1789.
- LaRoche, J., Boyd, P.W., McKay, R.M.L., Geider, R.J., 1996. Flavodoxin as an in situ marker for iron stress in phytoplankton. *Nature* 382, 802–805.
- Leal, M.F.C., Vasconcelos, T.S.D., van den Berg, C.M.G., 1999. Copper-induced release of complexing ligands similar to thiols by *Emiliania huxleyi* in seawater cultures. *Limnol. Oceanogr.* 44, 1750-1762.
- Leal, M.F.C., van den Berg, C.M.G., 1998. Evidence for strong copper(I) complexation by organic ligands in seawater. *Aquat. Geochem.* 4, 49–75.

- Lee, S., Fuhrman, J.A., 1987. Relationships between biovolume and biomass of naturally derived marine bacterioplankton. *App. Environ. Microb.* 53, 129-1303.
- Lee, J., Peña, M.M.O., Nose, Y., Thiele, D.J., 2002. Biochemical characterization of the human copper transporter Ctr1. *J. Biol. Chem.* 277, 4380-4387.
- Levitus, S., 1982. Climatological atlas of the world ocean, Prof. Pap. 13, Natl. Oceanic Atmos. Admin., Rockville, Md.
- Levy, J.L., Stauber, J.L., Jolley, D.F., 2007. Sensitivity of marine microalgae to copper: the effect of biotic factors on copper adsorption and toxicity. *Sci. Tot. Environ.* 387, 141-154.
- Li, Y.-H., Gregory, A., 1974. Diffusion of ions in sea water and in deep-sea sediments. *Gecochim. Cosmochim. Act.* 38, 708-714.
- Lindsay, W.L., Schwab, A.P., 1982. The chemistry of iron in soils and its availability to plants. *J. Plant Nut.* 5, 821-840.
- Liu, X., Millero, J.F., 2002. The solubility of iron in seawater. *Mar. Chem.* 77, 43-54.
- Liu, Z.D., Hider, R.C., 2002. Iron chelator chemistry. In D.M. Templeton (Ed.), *Molecular and cellular iron transport*, Chapter 12. New York, NY: Marcel Dekker.
- Lohan, M.C., Crawford, D.W., Purdie, D.A., Statham, P.J., 2005. Iron and zinc enrichments in the northeastern subarctic Pacific: ligand production and zinc availability in response to phytoplankton growth. *Limnol. Oceanogr.* 50, 1427-1437.
- Louis, Y., Garnier, C., Lenoble, V., Omanović, D., Mounier, S., Pižeta, I., 2009. Characterisation and modelling of marine dissolved organic matter interactions with major and trace cations. *Mar. Environ. Res.* 67, 100-107.
- Mahowald, N.M., Baker, A.R., Bergametti, G., Brooks, N., Duce, R.A., Jickells, T.D., Kubilay, N., Prospero, J.M., Tegen, I., 2005. Atmospheric global dust cycle and iron inputs to the ocean. *Glob. Biogeochem. Cyc.* 19, GB4025, doi:10.1029/2004GB002402
- Maldonado, M.T., Allen, A.E., Chong, J.S., Lin, K., Leus, D., Karpenko, N., Harris, S., 2006. Copper-dependent iron transport in coastal and oceanic diatoms. *Limnol. Oceanogr.* 51, 1729-1743.
- Maldonado, M.T., Boyd, P.W., Harrison, P.J., Price, N.M., 1999. Co-limitation of phytoplankton growth by light and Fe during winter in the NE subarctic Pacific Ocean. *Deep Sea Res. II* 46, 2475-2485.
- Maldonado, M.T., Boyd, P.W., LaRoche, R., Strzepek, R., Waite, A., Bowie, A.R., Croot, P.L.,

- Frew, R.D., Price, N.M., 2001. Iron Uptake and Physiological Response of Phytoplankton during a Mesoscale Southern Ocean Iron Enrichment. *Limnol. Oceanogr.* 46, 1802-1808.
- Maldonado, M.T., Hughes, M.P., Rue, E.L., Wells, M.L., 2002. The effect of Fe and Cu on growth and domoic acid production by *Pseudo-nitzschia*. *Limnol. Oceanogr.* 47, 515-526.
- Maldonado, M.T., Price, N.M., 1996. Influence of N substrate on Fe requirements of marine centric diatoms. *Mar. Ecol. Prog. Ser.* 141, 161-172.
- Maldonado, M.T., Price, N.M., 2000. Nitrate regulation of Fe reduction and transport by Fe-limited *Thalassiosira oceanica*. *Limnol. Oceanogr.* 45, 814-826.
- Maldonado, M.T., Price, N.M., 2001. Reduction and transport of organically bound iron by *Thalassiosira oceanica* (Bacillariophyceae). *J. Phycol.* 37, 298-309.
- Mann, E.L., Ahlgren, N., Moffett, J.W., Chrisholm, S.W., 2002. Copper toxicity and cyanobacterial ecology in the Sargasso Sea. *Limnol. Oceanogr.* 47, 976-988.
- Marchetti, A., Sherry, N.D., Kiyosama, H., Tsuda, A., Harrison, P.J., 2006a. Phytoplankton processes during a mesoscale iron environment in the NE subarctic Pacific: Part I – biomass and assemblage. *Deep-Sea Res. II* 53, 2095-2113.
- Marchetti, A., Maldonado, M.T., Lane, E.S., Harrison, P.J., 2006b. Iron requirements of the pennate diatom *Pseudo-nitzschia*: comparison of oceanic (high-nitrate, low-chlorophyll waters) and coastal species. *Limnol. Oceanogr.* 51, 2092-2101.
- Marchetti, A., Parker, M.S., Moccia, L.P., Lin, E.O., Arrieta, A.L., Ribalet, F., Murphy, M.E.P., Maldonado, M.T., Armbrust, E.V., 2009. Ferritin is used for iron storage in bloom-forming marine pennate diatoms. *Nature* 457, 467-470.
- Martell, A.E., Smith, R.M., 2004. NIST Critically Selected Stability Constants of Metal Complexes Database. National Institute of Standards and Technology, USA.
- Martin, J.H., Fitzwater, S.E., 1988. Iron deficiency limits phytoplankton growth in the north-east Pacific subarctic. *Nature* 331, 341-343.
- Martin, J.H., Gordon, R.M., Fitzwater, S., Broenkow, W.W., 1989. Vertex: phytoplankton/iron studies in the Gulf of Alaska. *Deep Sea Res.* 36, 649-680.
- McCormack, P., Worsfold, P.J., Gledhill, M., 2003. Separation and detection of siderophores produced by marine bacterioplankton using high-performance liquid chromatography with electrospray ionization mass spectrometry. *Anal. Chem.* 75, 2647-2652.

- Merchant, S.S., Allen, M.D., Kropat, J., Moseley, J.L., Long, J.C., Tottey, S., Terauchi, A.M., 2006. Between a rock and a hard place: trace element nutrition in *Chlamydomonas*. *Biochim. Biophys. Act.* 1763, 578-594.
- Mies, K.A., Wirgau, J.I., Crumbliss, A.L., 2006. Ternary complex formation facilitates a redox mechanism for iron release from a siderophore. *BioMetals* 19, 115-126.
- Moffett, J.W., 1995. Temporal and spatial variability of copper complexation by strong chelators in the Sargasso Sea. *Deep Sea Res. I* 41, 1273-1295.
- Moffett, J.W., Brand, L.E., Croot, P.L., Barbeau, K.A., 1997. Cu speciation and cyanobacterial distribution in harbors subject to anthropogenic Cu inputs. *Limnol. Oceanogr.* 42, 789-799.
- Moffett, J.W., Brand, L.E., 1996. Production of strong, extracellular Cu chelators by marine cyanobacteria in response to Cu stress. *Limnol. Oceanogr.* 41 (3), 388-395.
- Moffett, J.W., Dupont, C., 2007. Cu complexation by organic ligands in the sub-arctic NW Pacific and Bering Sea. *Deep-Sea Res. I* 54, 586-595.
- Moffett, J.W., Zika, R.G., 1983. Oxidation kinetics of Cu(I) in seawater: implications for its existence in the marine environment. *Mar. Chem.* 13, 239-251.
- Moffett, J.W., Zika, R.G., 1987. Reaction kinetics of hydrogen peroxide with copper and iron in seawater. *Environ. Sci. Technol.* 21, 804-810.
- Moffett, J.W., Zika, R.G., 1988. Measurement of copper(I) in surface waters of the sub-tropical Atlantic and Gulf of Mexico. *Geochim. Cosmochim. Acta.* 52, 1849-1857.
- Monzyk, B., Crumbliss, A. L. 1982. Kinetics of mechanism of the stepwise dissociation of Fe(III) from ferrioxamine B in aqueous acid. *J. Am. Chem. Soc.* 104, 4921-4929.
- Moore, C.M., Suggett, D.J., Hickman, A.E., Kim, Y.-N., Tweddle, J.F., Sharples, J., Geider, R.J., Holligan, P.M., 2006. Phytoplankton photoacclimation and photoadaptation in response to environmental gradients in a shelf sea. *Limnol. Oceanogr.* 51, 936-949.
- Moore, C.M., Mills, M.M., Arrigo, K.R., Berman-Frank, I., Bopp, L., Boyd, P.W., Galbraith, E.D., Geider, R.J., Guieu, C., Jaccard, S.L., Jickells, T.D., La Roche, J., Lenton, T.M., Mahowald, N.M., Marañón, E., Marinov, I., Moore, J.K., Nakatsuka, T., Oschlies, A., Saito, M.A., Thingstad, T.F., Tsuda, a., Ulloa, O., 2013. *Nature Geosci.* 6, 701-710.
- Moore, J.K., Doney, S.C., Lindsay, K., 2004. Upper ocean ecosystem dynamics and iron cycling in a global three-dimensional model. *Glob. Biogeochem. Cyc.* 18, GB4028, doi:10.1029/2004GB002220.

- Morel, F.M.M., Hering, J.G. Principles and applications of aquatic chemistry. New York Wiley, 1993, 588.
- Morel, F.M.M., Hudson, R.J.M., Price, N.M., 1991. Limitation of productivity by trace metals in the sea. *Limnol. Oceanogr.* 36, 1742-1755.
- Morel, F.M.M., Price, N.M., 2003. The biogeochemical cycles of trace metals in the oceans. *Science* 300, 944-947.
- Nimmo, M., van den Berg, C. M. G., Brown, J., 1989. The chemical speciation of dissolved nickel, copper, vanadium and iron in Liverpool Bay, Irish Sea. *Estuarine and Coastal Shelf Science*, 29, 57-74.
- Noctor, G., Foyer, C.H., 1998. Ascorbate and glutathione: keeping active oxygen under control. *Annu. Rev. Plant Physiol. Plant Mol. Biol.* 49, 249-279.
- Okamoto, O.K., Pinto, E., Latorre, L.R., Bechara, E.J.H., Colepicolo, P., 2001. Antioxidate modulation in response to metal-induced oxidative stress in algal chloroplasts. *Arch. Environ. Contam. Toxicol.* 40, 18-24.
- Page, M.D., Kropat, J., Hamel, P.P., Merchant, S.S., 2009. Two *Chlamydomonas* CTR copper transporters with a novel Cys-Met motif are localized to the plasma membrane and function in copper assimilation. *The Plant Cell* 21, 928-943.
- Palenik, B., Brahamsha, B., Larimer, F.W., Land, M., Hauser, L., Chain, P., Lamerdin, J., Regala, W., Allen, E.E., McCarren, J., Paulsen, I., Dufresne, A., Partensky, F., Webb, E.A., Waterbury, J., 2003. The genome of a motile marine *Synechococcus*. *Nature* 424, 1037-1042.
- Palenik, B., Morel, F.M.M., 1991. Amine oxidases of marine phytoplankton. *Appl. Environ. Microbiol.* 57, 2440-2443.
- Paytan, A., Mackey, K.R.M., Chen, Y., Lima, I.D., Doney, S.C., Mahowald, N., Labiosa, R., Postf, A.F., 2009. Toxicity of atmospheric aerosols on marine phytoplankton. *Proc. Nat. Acad. Sci.* 106, 4601-4605.
- Peers, G., Price, N.M., 2006. Copper-containing plastocyanin used for electron transport by an oceanic diatom. *Nature* 441, 341-344.
- Peers, G., Quesnel, S.A., Price, N.M., 2005. Copper requirements for iron acquisition and growth of coastal and oceanic diatoms. *Limnol. Oceanogr.* 50, 1149-1158.
- Peña, M.A., Bograd, S.J., 2007. Time series of the northeast Pacific. *Prog. Oceanogr.* 75, 115-119.

- Peña, M.A., Varela, D.E., 2007. Seasonal and interannual variability in phytoplankton and nutrient dynamics along Line P in the NE subarctic Pacific. *Prog. Oceanogr.* 75, 200-222.
- Pérez-Almeida, M. G.-D., Santana-Casiano, J.M., González, A.G., Suárez de Tangil, M., 2013. Oxidation of Cu(I) in Seawater at Low Oxygen Concentrations. *Environ. Sci. Technol.* 47, 1239-1247.
- Pinto, E., Sigaud-Kutner, T.C.S., Leitão, M.A.S., Okamoto, O.K., Morse, D., Colepicolo, P., 2003. Heavy-metal induced oxidative stress in algae. *J. Phycol.* 39, 1009-1018.
- Pommier, T., Cånback, B., Riemann, L., Boström, K.H., Simo, K., Lunberg, P., Tunlid, A., Hagström, Å., 2007. Global patterns of diversity and community structure in marine bacterioplankton. *Mol. Ecol.* 16, 867-880.
- Pope, C.R., Flores, A.G., Kaplan, J.H., Unfer, V.M., 2012. Structure and function of copper uptake transporters. *Curr. Topics Membranes* 69, 97-112.
- Pörtner, H.-O., 2012. Integrating climate-related stressor effects on marine organisms: unifying principles linking molecule to ecosystem-level changes. *Mar. Ecol. Progr. Ser.* 470, 273-290.
- Price, N.M., Harrison, G.I., Hering, J.G., Hudson, R.J., Nirel, P.M.V., Palenik, B., Morel, F.M.M., 1989. Preparation and chemistry of the artificial algal culture medium Aquil. *Biol Oceanogr* 6, 443-461.
- Price, N.M., Morel, F.M.M., 1991. Colimitation of phytoplankton growth by nickel and nitrogen. *Limnol. Oceanogr.* 36, 1071-1077.
- Quigg, A., Reinfelder, J.R., Fisher, N.S., 2006. Copper uptake kinetics in diverse marine phytoplankton. *Limnol. Oceanogr.* 51, 893-899
- Rae, T.D., Schmidt, P.J., Pufahl, R.A., Culotta, V.C., O'Halloran, T.V., 1999. Undetectable intracellular free Cu: the requirement of a copper chaperone for superoxide dismutase. *Science* 284, 805-808.
- Raven, J., 1988. The iron and molybdenum use efficiencies of plant growth with different energy, carbon and nitrogen sources. *New Phytol.* 109, 279-287.
- Raven, J.A., 1990. Predictions of Mn and Fe use efficiencies of phototrophic growth as a function of light availability for growth and of C assimilation pathway. *New Phytol.* 116, 1-18.
- Raven, J.A., Evans, M.C., Korb, R.E., 1999. The role of trace metals in photosynthetic electron transport of O₂-evolving organisms. *Photosynthesis Res.* 60, 111-149.

- Rensing, C., McDevitt, S.F., 2013. The copper metallome in prokaryotic cells, in: L. Banci (Ed.), *Metallomics and the Cell, Metal Ions in Life Sciences 12*. Springer Science+Business Media, Dordrecht, pp. 417-450.
- Ridge, P.G., Zhang, Y., Gladyshev, V.N., 2008. Comparative genomic analyses of copper transporters and cuproproteomes reveal evolutionary dynamics of copper utilization and its link to oxygen. *PLoS ONE* 3(1): e1378. doi:10.1371/journal.pone.0001378.
- Ross, A.R.S., Ikonomou, M.G., Orians, K.J., 2003. Characterization of copper-complexing ligands in seawater using immobilized copper(II)-ion affinity chromatography and electrospray ionization mass spectrometry. *Mar. Chem.* 83, 47-58.
- Rozan, T.F., Benoit, G., 1999. Geochemical factors controlling free ion concentrations in river water. *Geochim. Cosmochim. Acta.* 63, 3311-3319.
- Rozan, T.F., Lassman, M.E., Ridge, D.P., Luther III, G.W., 2000. Evidence for iron, copper and zinc complexation as multinuclear sulphide clusters in oxic rivers. *Nature* 406, 879-882.
- Rubino, J.T., Chenkin, M.P., Keller, M., Riggs-Gelasco, P., Franz, K.J., 2011. A comparison of methionine, histidine and cysteine in copper (I)-binding peptides reveals differences relevant to copper uptake by organisms in diverse environments. *Metallomics* 3, 61-73.
- Rubino, J.T., Riggs-Gelasco, P., Franz, K.J., 2010. Methionine motifs of copper transport proteins provide general and flexible thioether-only binding sites for Cu(I) and Ag(I). *J. Biol. Inorg. Chem.* 15, 1033-1049.
- Rue, E.L., Bruland, K.W., 1995. Complexation of Fe(III) by natural organic ligands in the central North Pacific as determined by a new competitive ligand equilibration/adsorption cathodic stripping voltammetric technique. *Mar. Chem.* 50, 117-138.
- Semeniuk, D.M., Cullen, J.T., Johnson, W.K., Gagnon, K., Ruth, T.J., Maldonado, M.T., 2009. Plankton copper requirements and uptake in the subarctic Northeast Pacific Ocean. *Deep Sea Res. I* 56, 130-1142.
- Shaked, Y., Kustka, A.B., Morel, F.M.M., 2005. A general kinetic model for iron acquisition by eukaryotic phytoplankton. *Limnol. Oceanogr.* 50, 872-882
- Shank, G.C., Skrabal, S.A., Whitehead, R.F., Kieber, R.J., 2004. Fluxes of strong Cu-complexing ligands from sediments of an organic-rich estuary. *Est. Coast. Sci.* 60, 349-358.
- Shank, G.C., Whitehead, R.F., Smith, M.L., Skrabal, S.A., Kieber, R.J., 2006. Photodegradation of strong copper-complexing ligands in organic-rich estuarine waters. *Limnol. Oceanogr.* 51, 884-892.

- Shatwell, K.P., Dancis, A., Cross, A.R., Klausner, R.D., Seal, A.W., 1996. The FRE1 ferric reductase of *Saccharomyces cerevisiae* is a cytochrome *b* similar to that of NADPH oxidase. *J. Biol. Chem.* 271, 14240-14244.
- Sherry, N.D., Boyd, P.W., Sugimoto, K., Harrison, P.J., 1999. Seasonal and spatial patterns of heterotrophic bacterial production, respiration, and biomass in the subarctic NE Pacific. *Deep-Sea Res. II* 46, 2557-2578.
- Shi, D., Hopkinson, B.M., Morel, F.M.M., 2010. Effect of ocean acidification on iron availability to marine phytoplankton. *Science* 327, 676-679.
- Sigman, D.M., Boyle, E.A., 2000. Glacial/interglacial variations in atmospheric carbon dioxide. *Nature* 407, 859-869.
- Speisky, H., Gómez, M., Carrasco-Pozo, C., Pastene, E., Lopez-Alarcón, C., Olea-Azar, C., 2008. Cu(I)-glutathione complex: a potential source of superoxide radicals generation. *Bioorg. Med. Chem.* 16, 6568-6574.
- Spokes, L.J., Campos, M.L.A.M., Jickells, T.D., 1996. The role of organic matter in controlling copper speciation in precipitation. *Atmos. Environ.* 30, 3959-3966.
- Steiner, N.S., Robert, M., Arychuk, M., Levasseur, M.L., Merzouk, A., Peña, M.A., Richardson, W.A., Tortell, P.D., 2012. Evaluating DMS measurements and model results in the Northeast subarctic Pacific from 1996-2010. *Biogeochem.* 110, 269-285.
- Stoecker, D.K., Sunda, W.G., Davis, L.H., 1986. Effects of copper and zinc on two planktonic ciliates. *Mar. Biol.* 92, 21-29.
- Strzepek, R.F., Harrison, P.J., 2004. Photosynthetic architecture differs in coastal and oceanic diatoms. *Nature* 431, 689-692.
- Sunda, W.G., 2012. Feedback interactions between trace metal nutrients and phytoplankton in the ocean. *Front. Microbiol.* 3, 1-22.
- Sunda, W.G., Barber, R.T., Huntsman, S.A., 1981. Phytoplankton growth in nutrient rich seawater: important of copper-manganese cellular interactions. *J. Mar. Res.* 39, 567-587.
- Sunda, W.G., Guillard, R.R.L., 1976. Relationship between cupric ion activity and toxicity of copper to phytoplankton. *Mar. Res.* 34, 511-529.
- Sunda, W.G., Huntsman, S.A., 1983. Effect of competitive interactions between manganese and copper on cellular manganese and growth in estuarine and oceanic species of the diatom *Thalassiosira*. *Limnol. Oceanogr.* 28, 924-934.
- Sunda, W.G., Huntsman, S.A., 1992. Feedback interactions between zinc and phytoplankton in

seawater. *Limnol. Oceanogr.* 37, 25-40.

- Sunda, W.G., Huntsman, S.A., 1995a. Iron uptake and growth limitation in oceanic and coastal phytoplankton. *Mar. Chem.* 50, 189-206.
- Sunda, W.G., Huntsman, S.A., 1995b. Regulation of copper concentration in the oceanic nutricline by phytoplankton uptake and regeneration cycles. *Limnol. Oceanogr.* 40, 132-137.
- Sunda, W.G., Huntsman, S.A., 1997. Interrelated influence of iron, light and cell size on marine phytoplankton growth. *Nature* 390, 389-392.
- Sunda, W.G., Huntsman, S.A., 1998. Processes regulating cellular metal accumulation and physiological effects: phytoplankton as model systems. *Sci. Tot. Environ.* 219, 165-181.
- Sunda, W.G., Huntsman, S.A., 1991. The use of chemiluminescence and ligand competition with EDTA to measure copper concentration and speciation in seawater. *Mar. Chem.* 36, 137-163.
- Sunda, W.G., Lewis, J.A.M., 1978. Effect of complexation by natural organic ligands on the toxicity of copper to a unicellular alga, *Monochrysis lutheri*. *Limnol. Oceanogr.* 23, 870-876.
- Tang, D., Shafer, M.M., Karner, D.A., Overdier, J., Armstrong, D.E., 2004. Factors affecting the presence of dissolved glutathione in estuarine waters. *Environ. Sci. Technol.* 38, 4247-4253.
- Tang, D., Shafer, M.M., Karner, D.A., Armstrong, D.E., 2005. Response of nonprotein thiols to copper stress and extracellular release of glutathione in the diatom *Thalassiosira weissflogii*. *Limnol. Oceanogr.* 50, 516-525.
- Taylor, R.L., Semeniuk, D.M., Payne, C.D., Zhou, J., Tremblay, J.-É., Cullen, J.T., Maldonado, M.T., 2013. Colimitation by light, nitrate, and iron in the Beaufort Sea in late summer. *J. Geophys. Res. Oceans* 118, 1-17.
- Thompson, C.M., Ellwood, M.J., Sander, S.G., 2014. Dissolved copper speciation in the Tasman Sea, SW Pacific Ocean. *Mar. Chem.* doi: 10.1016/j.marchem.2014.06.003.
- Thomson, R. E., 1981. Oceanography of the British Columbia coast. *Can. Spec. Publ. of Fish. and Aquat. Sci.* 56, 291 pp., Dept. of Fish. and Oceans, Ottawa, Ont., Canada.
- Tripathi, B.N., Mehta, S.K., Amar, A., Gaur, J.P., 2006. Oxidative stress in *Scenedesmus sp.* during short- and long-term exposure to Cu²⁺ and Zn²⁺. *Chemosphere* 62, 538-544.
- Turner, D.R., Whitfield, M., Dickson, A.G., 1981. The equilibrium speciation of dissolved

components in freshwater and seawater at 25°C and 1 atm pressure. *Geochim. Cosmochim. Acta.* 45, 855-881.

- van den Berg, D.M.G., 1984. Determination of the complexing capacity and conditional stability constants of complexed of copper(II) with natural organic ligands in seawater by cathodic stripping voltammetry of copper-catechol complex ons. *Mar. Chem.* 15, 1-18.
- van den Berg, C.M.G., Househam, B.C., Riley, J.P., 1988. Determination of cystine and cysteine in seawater using cathodic stripping voltammetry in the presence of Cu(II). *J. Electroanaly. Chem.* 239, 137-148.
- Van Ho, A., Ward, D.M., Kaplan, J., 2002. Transition metal transport in yeast. *Annu. Rev. Microbiol.* 56, 237-261.
- Varela, D.E., Harrison, P.J., 1999. Seasonal variability in nitrogenous nutrition of phytoplankton assemblages in the northeastern subarctic Pacific Ocean. *Deep Sea Res. II* 46, 2505-2538.
- Vasconcelos, M.T.S.D., Leal, M.F.C., 2008. Exudates of different marine algae promote growth and mediate trace metal binding in *Phaeodactylum tricorutum*. *Mar. Environ. Res.* 66, 499-507.
- Vaulot, D., 1989. CYTOPC: Processing software for flow cytometric data. *Signal Noise*, 2, 8.
- Verma, S.K., Singh, H.N., 1991. Evidence for energy-dependent copper efflux as a mechanism of Cu²⁺ resistance in the cyanobacterium *Nostoc calcicola*. *FEMS Microbiol. Lett.* 84, 291-294.
- Voelker, B.M., Sedlak, D.L., Zafirov, O.C., 2000. Chemistry of superoxide radical in seawater: reactions with organic Cu complexes. *Environ. Sci. Technol.* 34, 1036-1042.
- Walsh, M.J., Ahner, B.A., 2013. Determination of stability constants of Cu(I), Cd(II) & Zn(II) c complexes with thiols using fluorescent probes. *J. Inorg. Biochem.* 128, 1120123.
- Walsh, M.J., Ahner, B.A., 2014. Copper export contributes to low copper levels and copper tolerance in *Emiliana huxleyi*. *Limnol. Oceanogr.* 59, 827-839.
- Wells, M.L., Trick, C.G., Cochlan, W.P., Hughes, M.P., Trainer, V.L., 2005. Domoic Acid: The Synergy of Iron, Copper, and the Toxicity of Diatoms. *Limnol. Oceanogr.* 50, 1908-1917.
- Whitney, F.A., Freeland, H.J., 1999. Variability in upper-ocean water properties in the NE Pacific Ocean. *Deep Sea Res. II* 46, 2351-2370.
- Wiramanaden, C.I.E., 2006. Characterization of copper binding ligands from marine

cyanobacterial cultures using voltammetry and mass spectrometry. Ph.D. Thesis, University of British Columbia.

Wiramanaden, C.I.E, Cullen, J.T., Ross, A.R.S., Orians, K.J., 2008. Cyanobacterial copper-binding ligands isolated from artificial seawater cultures. *Mar. Chem.* 28-41.

Witt, M. Jickells, T., 2005. Copper complexation in marine and terrestrial rain water. *Atmos. Environ.* 39, 7657-7666.

Wolf-Gladrow, D., Riebesell, U., 1997. Diffusion and reactions in the vicinity of plankton: A refined model for inorganic carbon transport. *Mar. Chem.* 59, 17-34.

Xiao, Z., Wedd, A.G., 2002. A c-terminal domain of the membrane copper pump Ctr1 exchanges copper(I) with the copper chaperone Atx1. *Chem. Commun.* 588-589
10.1039/B111180A

Yang, R.J., van den Berg, C.M.G., 2009. Metal complexation by humic substances in seawater. *Environ. Sci. Technol.* 43, 7192-7197.

Yuan, M., Li, X., Xiao, J., Wang, S., 2011. Molecular and functional analyses of COPT/Ctr-type copper transporter-like gene family in rice. *BMC Plant Biol.* 11, 69-80.

Zafiriou, O.C., Voelkner, B.M., Sedlak, D.L., 1998. Chemistry of superoxide radical (O_2^-) in seawater: reactions with inorganic copper complexes. *J. Phys. Chem. A* 102, 5693-5700.

Zamzow, H., Coale, K.H., Johnson, K.S., Sakamoto, C.M., 1998. Determination of copper complexation in seawater using flow injection analysis with chemiluminescence detection. *Anal. Chim. Acta* 377, 133-144.

Zanello, P., Seeber, R., Cinquantini, A., Mazzocchin, G.-A., Fabbrizzi, L., 1982. Electrochemical behaviour of complexes of copper(II) with 14-membered saturated tetra-aza macrocycles. *J. Chem. Soc. Dal. Trans.* 5, 893-897.

Zhou, H., Cadigan, K.M., Thiele, D.J., 2003. A copper-regulated transporter required for copper acquisition, pigmentation, and specific stages of development in *Drosophila melanogaster*. *J. Biol. Chem.* 278, 48210-48218.

Zhou, B., Gitschier, J., 1997. hCTR1: a human gene for copper uptake identified by complementation in yeast. *Proc. Nat. Acad. Sci.* 94, 7481-7486.

Appendices

Appendix A

Table A.1. Previously published short-term and steady-state Cu uptake rates (ρCu) measured for a suite of phytoplankton, inorganic Cu (Cu') in the uptake media, the ligand used to complex Cu, calculated maximum diffusive supply of Cu' to the cell surface (J_D), and the ratio of $\rho\text{Cu}:J_D$. Italicized values indicate the study measured short-term uptake rates; the other rates are steady-state rates calculated from the cellular Cu quotas (zmol Cu cell^{-1}) and growth rates (h^{-1}).

Species	$-\log([\text{Cu}'])$ (M) ^a	Ligand	Cellular Uptake Rate ($\text{amol Cu cell}^{-1} \text{h}^{-1}$)	Diffusive Cu' Supply ($\text{amol Cu cell}^{-1} \text{h}^{-1}$) ^a	$\rho\text{Cu}:J_D$	Publication ^b
<i>T. pseudonana</i> 3H	13.74	EDTA	0.028	0.011	25.4	SH1995
<i>T. pseudonana</i> 3H	13.74	EDTA	0.030	0.011	27.1	SH1995
<i>T. pseudonana</i> 3H	12.61	EDTA	0.135	0.15	9.2	SH1995
<i>T. pseudonana</i> 3H	12.13	EDTA	0.202	0.44	4.6	SH1995
<i>T. pseudonana</i> 3H	11.64	EDTA	0.224	1.4	1.6	SH1995
<i>T. pseudonana</i> 3H	11.14	EDTA	0.280	4.3	0.6	SH1995
<i>T. pseudonana</i> 3H	11.14	EDTA	0.307	4.4	0.7	SH1995
<i>T. pseudonana</i> 3H	11.14	EDTA	0.330	4.3	0.8	SH1995
<i>T. pseudonana</i> 3H	10.64	EDTA	0.406	13.7	0.3	SH1995
<i>T. pseudonana</i> 3H	10.14	EDTA	0.545	43.7	0.1	SH1995
<i>T. pseudonana</i> 3H	9.64	EDTA	0.794	136	0.06	SH1995
<i>T. oceanica</i>	13.04	EDTA	0.099	0.070	14.2	SH1995
<i>T. oceanica</i>	12.61	EDTA	0.118	0.19	6.2	SH1995
<i>T. oceanica</i>	12.12	EDTA	0.200	0.59	3.4	SH1995
<i>T. oceanica</i>	12.13	EDTA	0.225	0.58	3.9	SH1995
<i>T. oceanica</i>	12.12	EDTA	0.263	0.59	4.5	SH1995
<i>T. oceanica</i>	11.66	EDTA	0.343	1.7	2.0	SH1995
<i>T. oceanica</i>	11.13	EDTA	0.398	5.7	0.7	SH1995
<i>T. oceanica</i>	10.65	EDTA	0.496	17.4	0.3	SH1995
<i>T. oceanica</i>	10.13	EDTA	0.569	57.6	0.1	SH1995

Species	$-\log([\text{Cu}'])$ (M) ^a	Ligand	Cellular Uptake Rate (amol Cu cell ⁻¹ h ⁻¹)	Diffusive Cu' Supply (amol Cu cell ⁻¹ h ⁻¹) ^a	$\rho\text{Cu}:J_D$	Publication ^b
<i>T. oceanica</i>	9.65	EDTA	0.890	179	0.05	SH1995
<i>T. oceanica</i>	9.13	EDTA	1.575	594	0.03	SH1995
<i>Emiliana huxleyi</i>	13.74	EDTA	0.004	0.008	4.8	SH1995
<i>E. huxleyi</i>	13.41	EDTA	0.019	0.42	0.5	SH1995
<i>E. huxleyi</i>	13.06	EDTA	0.029	0.92	0.3	SH1995
<i>E. huxleyi</i>	12.64	EDTA	0.031	2.3	0.1	SH1995
<i>E. huxleyi</i>	12.15	EDTA	0.049	7.5	0.06	SH1995
<i>E. huxleyi</i>	12.15	EDTA	0.043	7.5	0.06	SH1995
<i>E. huxleyi</i>	11.67	EDTA	0.064	22.5	0.03	SH1995
<i>E. huxleyi</i>	11.16	EDTA	0.076	74.6	0.01	SH1995
<i>E. huxleyi</i>	10.68	EDTA	0.159	218	0.01	SH1995
<i>E. huxleyi</i>	10.16	EDTA	0.222	755	0.003	SH1995
<i>E. huxleyi</i>	9.68	EDTA	0.267	2299	0.001	SH1995
<i>E. huxleyi</i>	9.16	EDTA	3.568	9834	0.004	SH1995
<i>Synechococcus</i> sp. DC2	11.24	NTA	0.001	0.007	1.2	Croot2003
<i>Synechococcus</i> sp. DC2	10.54	NTA	0.009	0.033	2.7	Croot2003
<i>Synechococcus</i> sp. DC2	9.94	NTA	0.039	0.13	3.0	Croot2003
<i>Synechococcus</i> sp. DC2	9.24	NTA	0.157	0.65	2.4	Croot2003
<i>Synechococcus</i> sp. DC2	8.20	NTA	0.217	7.1	0.3	Croot2003
<i>Synechococcus</i> sp. DC2	9.33	None	0.004	0.53	0.08	Croot2003
<i>Synechococcus</i> sp. DC2	7.94	None	0.007	12.9	0.01	Croot2003
<i>Synechococcus</i> sp.	10.55	EDTA	366.000	6.0	610	Quigg2006
<i>Pyramimonas parkeae</i>	10.55	EDTA	30.000	39.6	7.6	Quigg2006
<i>Tetraselmis levis</i>	10.55	EDTA	28.800	30.6	9.4	Quigg2006
<i>Amphidinium carterae</i>	10.55	EDTA	120.000	37.8	31.7	Quigg2006
<i>Emiliana huxleyi</i>	10.55	EDTA	25.200	24.6	10.2	Quigg2006
<i>E. huxleyi</i>	10.55	EDTA	48.000	20.4	23.5	Quigg2006
<i>T. weissflogii</i>	10.55	EDTA	19.800	46.2	4.3	Quigg2006
<i>T. weissflogii</i>	12.62	EDTA	0.222	0.31	7.2	Annett2008
<i>T. pseudonana</i> 3H	12.62	EDTA	0.058	0.13	4.6	Annett2008

Species	$-\log([\text{Cu}'])$ (M) ^a	Ligand	Cellular Uptake Rate (amol Cu cell ⁻¹ h ⁻¹)	Diffusive Cu' Supply (amol Cu cell ⁻¹ h ⁻¹) ^a	$\rho\text{Cu}:J_D$	Publication ^b
<i>Skeletonema costatum</i>	12.62	EDTA	0.199	0.25	8.0	Annett2008
<i>T. pseudonana</i> (1014)	12.62	EDTA	0.044	0.091	4.8	Annett2008
<i>T. oceanica</i> (610)	12.62	EDTA	0.080	0.16	5.1	Annett2008
<i>T. oceanica</i> (1003)	12.62	EDTA	0.146	0.16	9.1	Annett2008
<i>Skeletonema menzellii</i>	12.62	EDTA	0.311	0.21	14.7	Annett2008
<i>T. weissflogii</i>	13.62	EDTA	0.089	0.031	28.9	Annett2008
<i>T. pseudonana</i> 3H	13.62	EDTA	0.069	0.013	54.6	Annett2008
<i>Skeletonema costatum</i>	13.62	EDTA	0.113	0.025	45.5	Annett2008
<i>T. pseudonana</i> (1014)	13.62	EDTA	0.022	0.009	24.0	Annett2008
<i>T. oceanica</i> (610)	13.62	EDTA	0.058	0.016	37.5	Annett2008
<i>T. oceanica</i> (1003)	13.62	EDTA	0.040	0.016	25.0	Annett2008
<i>Skeletonema menzellii</i>	13.62	EDTA	0.032	0.021	15.0	Annett2008
<i>T. pseudonana</i> 3H	13.70	EDTA	0.026	0.017	15.3	Guo2010
<i>T. pseudonana</i> 3H	12.40	EDTA	0.291	0.26	11.2	Guo2010
<i>T. pseudonana</i> 3H	12.15	EDTA	0.482	0.52	9.3	Guo2010
<i>T. pseudonana</i> 3H	11.82	EDTA	1.224	1.1	11.7	Guo2010
<i>T. pseudonana</i> 3H	11.54	EDTA	0.820	2.1	3.9	Guo2010
<i>T. pseudonana</i> 3H	11.21	EDTA	1.220	4.4	2.8	Guo2010
<i>T. pseudonana</i> 3H	10.92	EDTA	1.965	8.7	2.3	Guo2010
<i>T. pseudonana</i> 3H	10.60	EDTA	2.256	17.4	1.3	Guo2010
<i>T. oceanica</i>	13.70	EDTA	0.011	0.016	6.9	Guo2010
<i>T. oceanica</i>	12.40	EDTA	0.130	0.23	5.7	Guo2010
<i>T. oceanica</i>	12.15	EDTA	0.235	0.47	5.0	Guo2010
<i>T. oceanica</i>	11.82	EDTA	0.225	0.94	2.4	Guo2010
<i>T. oceanica</i>	11.54	EDTA	0.518	1.9	2.8	Guo2010
<i>T. oceanica</i>	11.21	EDTA	0.587	3.9	1.5	Guo2010
<i>T. oceanica</i>	10.92	EDTA	0.681	7.8	0.9	Guo2010
<i>T. oceanica</i>	10.60	EDTA	0.939	15.6	0.6	Guo2010
<i>Phaeocystis pouchetii</i>	12.62	EDTA	0.045	0.094	4.8	Guo2012
<i>Emiliania huxleyi</i> (732a)	12.62	EDTA	0.029	0.22	1.3	Guo2012

Species	$-\log([\text{Cu}'])$ (M) ^a	Ligand	Cellular Uptake Rate (amol Cu cell ⁻¹ h ⁻¹)	Diffusive Cu' Supply (amol Cu cell ⁻¹ h ⁻¹) ^a	$\rho\text{Cu}:J_D$	Publication ^b
<i>Chrysochromulina polylepsis</i>	12.62	EDTA	0.028	0.096	3.0	Guo2012
<i>Prorocentrum dentatum</i>	12.62	EDTA	0.038	0.23	1.6	Guo2012
<i>Phaeocystis cordata</i>	12.62	EDTA	0.009	0.076	1.1	Guo2012
<i>Emiliania huxleyi</i> (646)	12.62	EDTA	0.020	0.098	2.0	Guo2012
<i>Chrysochromulina kappa</i>	12.62	EDTA	0.044	0.096	4.5	Guo2012
<i>Prorocentrum minimum</i>	12.62	EDTA	0.101	0.23	4.5	Guo2012
<i>P. pouchetii</i>	13.62	EDTA	0.029	0.009	32.0	Guo2012
<i>E. huxleyi</i> (732a)	13.62	EDTA	0.001	0.023	0.6	Guo2012
<i>C. polylepsis</i>	13.62	EDTA	0.020	0.009	20.9	Guo2012
<i>P. dentatum</i>	13.62	EDTA	0.010	0.024	4.0	Guo2012
<i>P. cordata</i>	13.62	EDTA	0.002	0.008	2.1	Guo2012
<i>E. huxleyi</i> (646)	13.62	EDTA	0.002	0.010	1.6	Guo2012
<i>C. kappa</i>	13.62	EDTA	0.015	0.010	15.8	Guo2012
<i>P. minimum</i>	13.62	EDTA	0.031	0.023	13.7	Guo2012
<i>T. pseudonana</i> 3H	9.00	None	0.786	705	0.01	This thesis
<i>T. pseudonana</i> 3H	13.78	Cyclam	0.536	0.012	459	This thesis
<i>T. pseudonana</i> 3H	15.48	Cyclam	0.168	0.0002	7189	This thesis
<i>T. pseudonana</i> 3H	16.48	Cyclam	0.038	0.00002	16261	This thesis
<i>T. oceanica</i>	13.78	Cyclam	0.437	0.015	292	This thesis
<i>Chrysochromulina polylepsis</i>	13.78	Cyclam	0.057	0.012	49	This thesis
<i>Phaeocystis pouchetii</i>	13.78	Cyclam	0.028	0.010	28	This thesis

^aThe maximum diffusive inorganic Cu supply to the cell surfaces were calculated as described in Table 3.4.

^bSH1995 (Sunda and Huntsman 1995b), Croot2003 (Croot et al. 2003); Quigg2006 (Quigg et al. 2006); Annett2008 (Annett et al. 2008); Guo2010 (Guo et al. 2010); Guo2012 (Guo et al. 2012)